NASA SP-164

THERMAL RADIATION HEAT TRANSFER

NATIONAL AERONAUTICS AND SPACE ADMINISTRATION U.S.A.

NASA SP-164

THERMAL RADIATION HEAT TRANSFER

Volume I

The Blackbody, Electromagnetic Theory, and Material Properties

Robert Siegel and John R. Howell
Lewis Research Center
Cleveland, Ohio

Scientific and Technical Information Division
OFFICE OF TECHNOLOGY UTILIZATION 1968
NATIONAL AERONAUTICS AND SPACE ADMINISTRATION
Washington, D.C.

PREFACE

Several years ago it was realized that thermal radiation was becoming of increasing importance in aerospace research and design. This importance arose from several areas: high temperatures associated with increased engine efficiencies, high-velocity flight which is accompanied by elevated temperatures from frictional heating, and the operation of devices beyond the Earth's atmosphere where convection vanishes and radiation becomes the only external mode of heat transfer. As a result, a course in thermal radiation was initiated at the NASA Lewis Research Center as part of an internal advanced study program.

The course was divided into three main sections. The first dealt with the radiation properties of opaque materials including a discussion of the blackbody, electromagnetic theory, and measured properties. The second discussed radiation exchange in enclosures both with and without convection and conduction. The third section treated radiation in partially transmitting materials—chiefly gases.

When the course was originated, there was not available any single radiation textbook that covered the desired span of material. As a result the authors began writing a set of notes; the present publication is an outgrowth of the notes dealing with the first of the three main sections.

During the past few years, a few radiation textbooks have appeared in the literature; hence, the need for a single reference has been partially satisfied. The objectives here are more extensive than the content of a standard textbook intended for a one-semester course. Many parts of the present discussion have been made quite detailed so that they will serve as a source of reference for some of the more subtle points in radiation theory. The detailed treatment has resulted in some of the sections being rather long, but the intent was to be thorough rather than to try to conserve space. The sections have been subdivided so that specific portions can be located for easy reference.

This volume is divided into five chapters. The introduction discusses the conditions where thermal radiation is of importance and indicates some of the inherent differences and complexities of radiation problems as compared with convection and conduction.

Chapter 2 deals with the blackbody, which is defined as a perfect absorber. It is important to understand the behavior of a blackbody before considering real materials, as the blackbody provides an ideal performance with which real material performance can be compared. First the blackbody is discussed qualitatively with its properties being deduced from the original definition of a perfect absorber. A quantitative elaboration, including a numerical tabulation, then provides the blackbody emission as a function of wavelength and temperature.

The third chapter is completely devoted to the definitions of emissivity, absorptivity, and reflectivity. These properties are used to compare the radiative performance of real materials with the ideal (blackbody) behavior. A functional notation has been introduced that includes prime superscripts to denote directional quantities and by which ambiguities in the various hemispherical and directional quantities are avoided. An extensive examination of the property definitions is made in order to demonstrate when it is valid to use various reciprocity relations and equalities, such as Kirchhoff's laws relating emissivity and absorptivity. The restrictions on these relations are summarized in tables for convenient reference.

The use of classical electromagnetic theory for the prediction of radiative properties is the subject of chapter 4. The electromagnetic theory discussed deals with ideal surfaces and hence does not account for the many factors (e.g., contamination and roughness) that influence the behavior of real surfaces. In spite of this shortcoming, the theory does provide a valuable basis for many observed trends and serves to relate optical and electrical properties to radiative properties.

The final chapter illustrates the radiative performance of real materials by showing a number of examples of property variations with wavelength and temperature.

Each chapter contains numerical examples to acquaint the reader with the use of the analytical relations. It is hoped that these examples will help bridge the gap between theory and practical application.

CONTENTS

CONTENTS

Chapter 1. Introduction

All substances continuously emit electromagnetic radiation by virtue of the molecular and atomic agitation associated with the internal energy of the material. In the equilibrium state, this internal energy is in direct proportion to the temperature of the substance. The emitted radiant energy can range from radio waves, which can have wavelengths of miles, to cosmic rays with wavelengths of less than 10^{-10} centimeter (cm). In this volume, only radiation that is detected as heat or light will be considered; this is termed *thermal radiation*, and it occupies an intermediate wavelength range. This range is defined explicitly in section 1.5.

Although radiant energy constantly surrounds us, we are not very aware of it because our bodies are able to detect only portions of it directly. Other portions require detection by use of some intermediate instrumentation. Our eyes are sensitive direct detectors of light, being able to form images of objects, but are relatively insensitive to heat (infrared) radiation. Our skin is a direct detector for heat radiation but not a good one. The skin is not aware of images of warm or cool surfaces around us unless the heat radiation is large. We require indirect means such as infrared-sensitive film in a camera to form images using heat radiation.

Before discussing the nature of thermal radiation in detail, it is well to consider why thermal radiation is so important in our modern technology.

1.1 IMPORTANCE OF THERMAL RADIATION

One of the factors that causes some of the important applications of thermal radiation to arise is the dependence of radiant emission on temperature. For conduction and convection the transfer of energy between two locations depends on the temperature difference of the locations to approximately the first power.[1] The transfer of energy by thermal radiation, however, depends on the differences of the individual absolute temperatures of the bodies each raised to a power in the range of about 4 or 5.

From this basic difference between radiation and the convection and conduction energy exchange mechanisms, it is evident that the importance of radiation becomes intensified at high absolute temperature levels. Consequently, radiation contributes substantially to the heat

[1] For free convection or when variable property effects are included, the power of the temperature difference may become larger than unity but usually in convection and conduction does not approach 2.

transfer in furnaces and combustion chambers and in the energy emission from a nuclear explosion. The laws of radiation govern the temperature distribution within the Sun and the radiant emission from the Sun or from a source duplicating the Sun in a solar simulator. Some devices for space applications are designed to operate at high temperature levels in order to achieve high thermal efficiency. Hence, radiation must often be considered when calculating thermal effects in devices such as a rocket nozzle, a nuclear powerplant, or a gaseous core nuclear rocket.

A second distinguishing feature of radiative transfer is that *no* medium need be present between two locations in order for radiant interchange to occur. The radiative energy will pass perfectly through a vacuum. This is in contrast to convection and conduction where a physical medium must be present to carry the energy with the convective flow or to transport it by means of thermal conduction. When no medium is present, radiation becomes the only significant mode of heat transfer. Some common instances are the heat leakage through the evacuated walls of a Dewar flask or thermos bottle, or the heat dissipation from the filament of a vacuum tube. A more recent application is the radiation used to reject waste heat from a powerplant operating in space.

Radiation can be of importance in some instances even though the temperature levels are not elevated and other modes of heat transfer are present. The following example is quoted from a Cleveland newspaper published in the spring of 1964. A florist "noted the recurrence of a phenomenon he has observed for two seasons since using plastic coverings over [flower] flats. Water collecting in the plastic has formed ice a quarter-inch thick [at night] when the official [temperature] reading was well above freezing. 'I'd like an answer to that, I supposed you couldn't get ice without freezing temperatures.' " The florist's oversight was in considering only the convection to the air and omitting the nighttime radiation loss occurring between the water covered surface and the very cold heat sink of outer space.

Another similar illustration is the discomfort that a person experiences in a room where cold surfaces are present. Cold window surfaces, for example, have a chilling effect as the body radiates directly to them without receiving compensating energy from them. Covering the windows with a shade or drape will greatly decrease the bodily discomfort.

Finally, we note that the thermal radiation that we shall examine is in the wavelength region that gives mankind heat, light, photosynthesis, and all their attendant benefits. This in itself is strong justification for studying thermal radiation. Our existence depends on the solar radiant energy incident upon the Earth. Understanding the interaction of this radiation with the atmosphere and surface of the Earth can provide additional benefits in its utilization.

1.2 SYMBOLS

c	speed of electromagnetic radiation propagation in medium
c_0	speed of electromagnetic radiation propagation in vacuum
k	thermal conductivity
n	index of refraction, c_0/c
q_c	energy per unit area per unit time resulting from heat conduction
q_r	radiant energy per unit area per unit time arriving at surface element
q_s	radiant energy per unit area per unit time arriving from unit surface element
q_v	radiant energy per unit area per unit time arriving from unit volume element
S	surface area
T	temperature
V	volume
x, y, z	coordinates in Cartesian system
ζ	arbitrary direction
λ	wavelength in vacuum
ν	frequency

1.3 COMPLEXITIES INHERENT IN RADIATION PROBLEMS

First let us discuss some of the mathematical complexities that arise from the basic nature of radiation exchange. In conduction and convection heat transfer, energy is transported through a physical medium. The energy transferred into and from an infinitesimal volume element of solid or fluid depends on the temperature gradients and physical properties in the *immediate vicinity* of the element. For example, for the relatively simple case of heat conduction in a material (no convection) with temperature distribution $T(x, y, z)$ and constant thermal conductivity k, the heat conduction is obtained by locally applying the following Fourier conduction law:

$$q_c\Big|_{\substack{\text{In } \zeta \\ \text{direction}}} = -k\frac{\partial T}{\partial \zeta} \qquad (1\text{-}1)$$

For an elemental cube within a solid as shown in figure 1–1(a), a consideration of the net heat flow in and out of all the faces using the terms in the figure yields the Laplace equation governing the heat conduction within the material

$$\frac{\partial^2 T}{\partial x^2}+\frac{\partial^2 T}{\partial y^2}+\frac{\partial^2 T}{\partial z^2}=0 \tag{1-2}$$

The terms in this equation depend only on local temperature derivatives in the material.

A similar although more complex analysis can be made for the convection process, again demonstrating that the heat balance depends only on the conditions in the immediate vicinity of the location being considered.

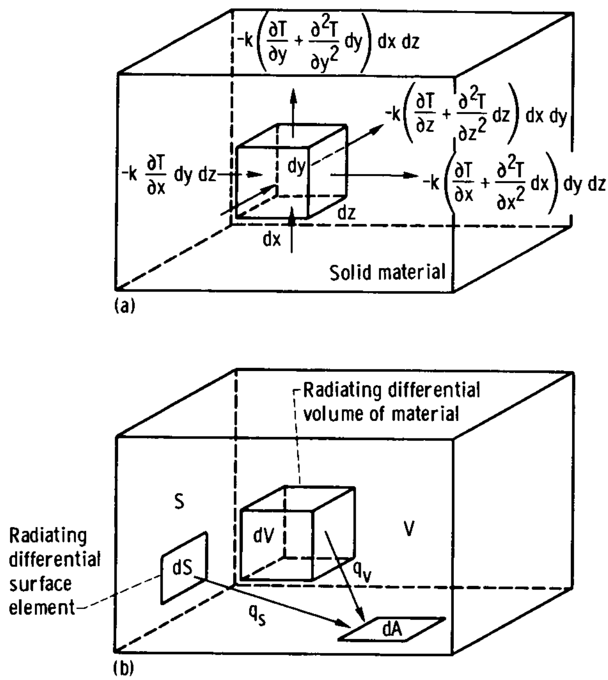

(a) Heat conduction terms for volume element in solid.
(b) Radiation terms for enclosure filled with radiating material.

FIGURE 1–1.—Comparison of types of terms for conduction and radiation heat balances.

In radiation, energy is transmitted between separated elements *without* the need of a medium between the elements. Consider a heated enclosure of surface S and volume V filled with radiating material (such as gas or glass) as shown in figure 1–1(b). If q_s is the radiant energy flux (energy per unit area and per unit time) arriving at dA from an element on the surface dS of the enclosure and q_v arrives at dA from an element of the medium dV, then the total radiation arriving per unit area at dA is

$$q_r = \int_S q_s \, dS + \int_V q_v \, dV \tag{1-3}$$

These types of terms lead to heat balances in the form of integral equations which are generally not as familiar to the engineer as differential equations. When radiation is combined with conduction and/or convection, the presence of both integral and differential terms having different powers of temperature leads to nonlinear integrodifferential equations. These are, in general, extremely difficult to solve.

In addition to the mathematical difficulties, there is a second complexity inherent in radiation problems. This is in accurately specifying the physical property values to be inserted into the equations. The difficulty in specifying accurate property values arises because the properties for solids depend on many variables such as: surface roughness and degree of polish, purity of material, thickness of a coating such as paint on a surface (for a thin coating the underlying material may have an effect), temperature, wavelength of radiation, and angle at which radiation leaves the surface. Unfortunately, many measurements have been reported where all the pertinent surface conditions have not been precisely defined.

1.4 WAVE AGAINST QUANTUM MODEL

The theory of radiant energy propagation can be considered from two viewpoints—classical electromagnetic wave theory and quantum mechanics. The quantum-mechanical view of the interaction of radiation and matter yields, in most cases, equations that are remarkably similar to the classical results. With a few exceptions, thermal radiation may therefore be viewed as a phenomenon based on the classical concept of the transport of energy by electromagnetic waves. These exceptions, however, include some of the most important effects common to radiative transfer studies, such as the spectral distribution of the energy emitted from a body and the radiative properties of gases. These can only be explained and derived on the basis of quantum effects in which the energy is assumed to be carried by discrete particles (photons). The "true" nature of electromagnetic energy (i.e., waves or quanta) is not known, nor is it generally important to the engineer. Throughout the present work, the wave theory will generally be adhered to because it has the greatest utility in engineering calculations and also generally produces the same formal equations as the quantum theory. Occasional reference will be made to phenomena where quantum arguments must be invoked.

1.5 ELECTROMAGNETIC SPECTRUM

Within the framework of the wave theory, electromagnetic radiation follows the laws governing transverse waves that oscillate in a direction perpendicular to the direction of travel. The speed of propagation for electromagnetic radiation is the same as for light; light after all is simply

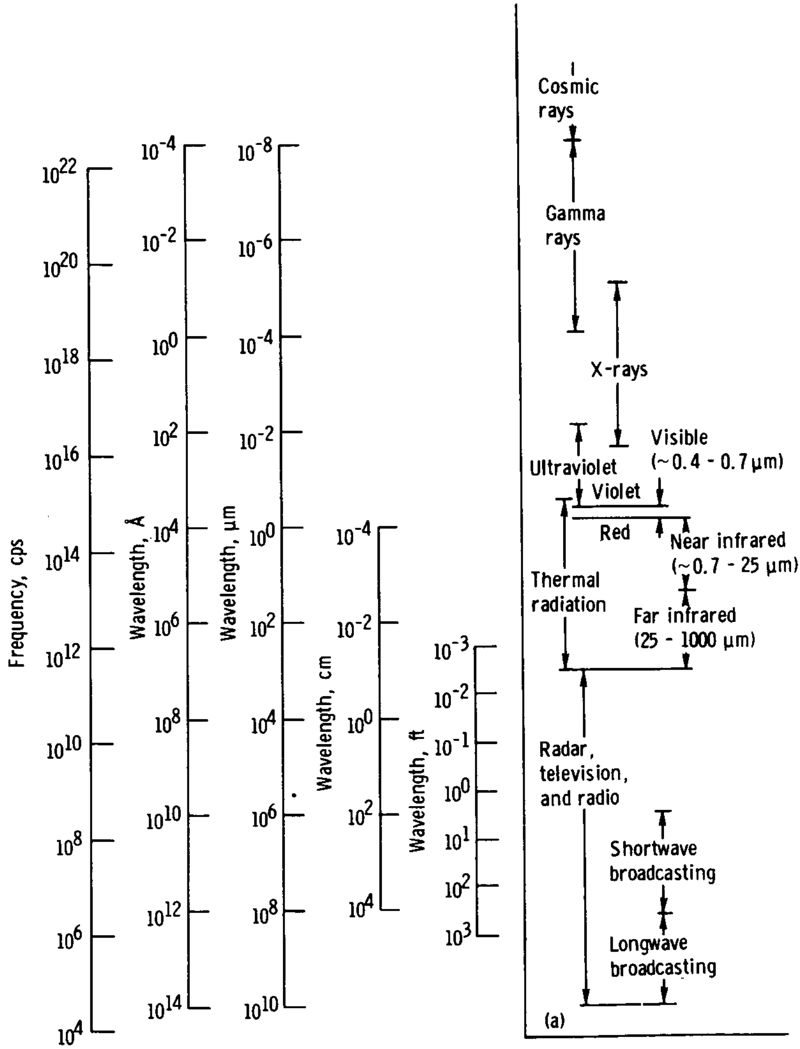

(a) Type of radiation.

FIGURE 1-2.—Spectrum of

the special case of electromagnetic radiation in a small region of the spectrum. In vacuum the speed of propagation is $c_0 = 2.998 \times 10^{10}$ centimeters per second (cm/sec) or 186 000 miles per second (mi/sec). The speed c in a medium is less than c_0 and for dielectrics is commonly given in terms of the index of refraction $n = c_0/c$, where n is greater than unity.[2] For glass n is about 1.5, while for gases n is very close to 1.

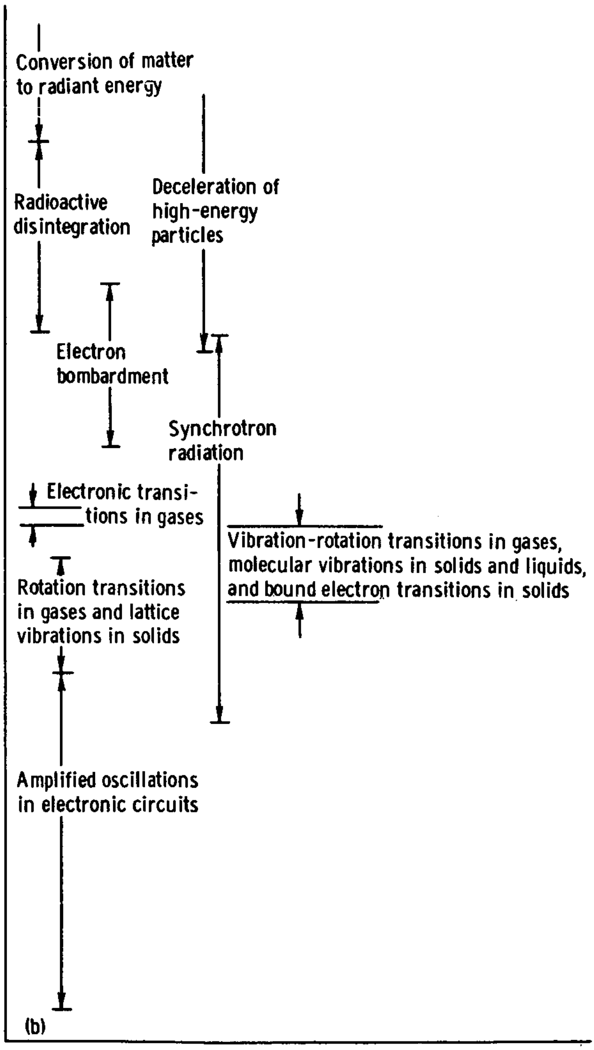

(b) Production mechanism.

electromagnetic radiation.

The types of electromagnetic radiation can be classified according to their wavelength λ (or frequency ν where $c=\lambda\nu$). Common units for wavelength measurement are the micron (μm) where 1 μm $=10^{-4}$ cm or 10^{-6} meter (m) and the angstrom (Å) where 1 Å $=10^{-10}$ m. Hence, 10^4 Å $=1$ μm. A chart of the radiation spectrum is shown in figure 1–2. A set of conversion factors for basic units in radiative transfer is given in tables I to III in the appendix.

The region of interest here includes a portion of the long wave fringe of the ultraviolet, the visible light region which extends from wavelengths of approximately 0.4 to 0.7 μm, and the infrared region which extends from beyond the red end of the visible spectrum to about $\lambda=1000$ μm. The infrared region is sometimes divided into the near infrared, extending from the visible region to about $\lambda=25$ μm, and the far infrared composed of the longer wavelength portion of the infrared spectrum.

The column at the far right in figure 1–2 indicates the various mechanisms by which electromagnetic radiation is produced. Some of the descriptions are from a quantum-mechanical viewpoint in which electrons or molecules in a state of agitation undergo transitions from one energy state to another. These transitions result in a radiative energy release. The transitions may occur spontaneously, or they may be initiated by the presence of a radiation field.

In this chapter we have discussed the importance of thermal radiation, the difficulties inherent in radiation problems, and the wavelength region occupied by thermal radiation within the electromagnetic spectrum. In the next chapter, the radiative behavior of the *ideal* radiating surface, termed a black surface, will be examined. Using the behavior of this ideal as a standard for comparison, the behavior of radiative energy for conditions of interest to the engineer will be discussed in succeeding chapters.

---

[2] For metals the index of refraction is a complex quantity of which n is only the real part. In this case n can be less than unity which at first glance might convey the impression that the propagation speed in metals is greater than c_o. This is not the case; the imaginary part of the complex index must also be considered and this part is greater than unity. A detailed discussion is given in chapter 4.

Chapter 2. Radiation from a Blackbody

Before discussing the idealized concept of the blackbody, let us examine a few aspects of the interaction of incident radiant energy with matter. The idea we are concerned with is that the interaction at the surface of a body is not the result of only a surface property but depends as well on the bulk material beneath the surface.

When radiation is incident on a homogeneous body, some of the radiation is reflected and the remainder penetrates into the body. The radiation may then be absorbed as it travels through the medium. If the material thickness required to substantially absorb the radiation is large compared with the thickness dimension of the body or if the material is transparent, then most of the radiation will be transmitted entirely through the body and will emerge with its nature unchanged. If, on the other hand, the material is a strong internal absorber the radiation that is not reflected from the body will be converted into internal energy within a very thin layer adjacent to the surface. A very careful distinction must be made between the ability of a material to let radiation pass through its surface and its ability to internally absorb the radiation after it has passed into the body. For example, a highly polished metal will generally reflect all but a small portion of the incident radiation, but the radiation passing into the body will be strongly absorbed and converted to internal energy within a very short distance within the material. Thus the metal has strong *internal* absorption ability, although it is a poor absorber for the incident beam since most of the incident beam is reflected. Nonmetals may exhibit the opposite tendency. Nonmetals may allow a substantial portion of the incident beam to pass into the material, but a larger thickness will be required than in the case of a metal to internally absorb the radiation and convert it into internal energy. When *all* the radiation that passes into the body is absorbed internally, the body is called *opaque*.

If metals in the form of very fine particles are deposited on a subsurface, the result is a surface of low reflectivity. This combined with the high internal absorption of the metal causes this type of surface to be a good absorber. This is the basis for formation of the metallic "blacks" such as platinum or gold black.

295-763 OL-68—2

2.1 SYMBOLS

A	surface area
C_1, C_2	constants in Planck's spectral energy distribution (see table IV of the appendix)
C_3	constant in Wien's displacement law (see table IV of the appendix)
c	speed of light in medium other than a vacuum
c_o	speed of light in vacuum
E	energy emitted per unit time
e	emissive power
$F_{0-\lambda}$	fraction of total blackbody intensity or emissive power lying in spectral region $0-\lambda$
h	Planck's constant
i	radiant intensity
k	Boltzmann constant
n	refractive index
Q	rate of energy
r	radius
T	absolute temperature
β	azimuthal, or cone angle (measured from normal of surface)
ζ	the quantity $C_2/\lambda T$
η	wave number
θ	circumferential angle
κ	extinction coefficient for electromagnetic radiation
λ	wavelength in vacuum
λ_m	wavelength in medium other than a vacuum
ν	frequency
σ	Stefan-Boltzmann constant (eq. (2–22))
ω	solid angle

Superscript:

$'$	directional heat flow quantity

Subscripts:

b	blackbody
max	corresponding to maximum energy
n	normal direction
p	projected
s	sphere
η	wave number dependent
λ	spectrally (wavelength) dependent
$\lambda_1-\lambda_2$	in wavelength span λ_1 to λ_2
λT	evaluated at λT
ν	frequency dependent

2.2 DEFINITION OF A BLACKBODY

A *blackbody* is defined as an ideal body that allows *all* the incident radiation to pass into it (no reflected energy) and absorbs internally *all* the incident radiation (no transmitted energy). This is true of radiation for all wavelengths and for all angles of incidence. Hence *the blackbody is a perfect absorber of incident radiation.* All other qualitative aspects of blackbody behavior can be derived from this definition.

The concept of a blackbody is basic to the study of radiative energy transfer. As a perfect absorber, it serves as a standard with which real absorbers can be compared. As will be seen, the blackbody also emits a maximum energy and hence serves as an ideal standard of comparison for a body emitting radiation. The radiative properties of the ideal blackbody have been well established by use of quantum theory, and have been verified by experiment.

Only a few surfaces such as carbon black, carborundum, platinum black, and gold black approach the blackbody in their ability to absorb radiant energy. The blackbody derives its name from the observation that good absorbers of incident visible light do indeed appear black to the eye. However, except for the visible region the eye is not a good indicator of absorbing ability in the wavelength range of thermal radiation. For example, a surface coated with white oil paint is a very good absorber for infrared radiation emitted at room temperature, although it is a poor absorber for the shorter wavelength region characteristic of visible light.

2.3 PROPERTIES OF A BLACKBODY

Aside from being a perfect absorber of radiation, the blackbody has other important properties, which will now be discussed.

2.3.1 Perfect Emitter

Consider a blackbody at a uniform temperature placed within a perfectly insulated enclosure of arbitrary shape whose walls are also composed of blackbodies at some uniform temperature initially different from that of the enclosed blackbody (fig. 2–1). After a period of time, the blackbody and the enclosure will attain a common uniform equilibrium temperature. In this equilibrium condition, the blackbody must radiate exactly as much energy as it absorbs. To prove this, consider what would happen if the incoming and outgoing amounts of radiation were not equal. Then the enclosed blackbody would either increase or decrease in temperature. This would involve a net amount of heat transferred from a cooler to a warmer body which is in violation of the second law of thermodynamics. It follows then that because the blackbody is by definition absorbing the maximum possible radiation from the enclosure at each wavelength and from each direction, it must also be emitting the maximum total amount of radiation. This is made clear by considering any less-than-perfect absorber, which must emit less energy than the blackbody to remain in equilibrium.

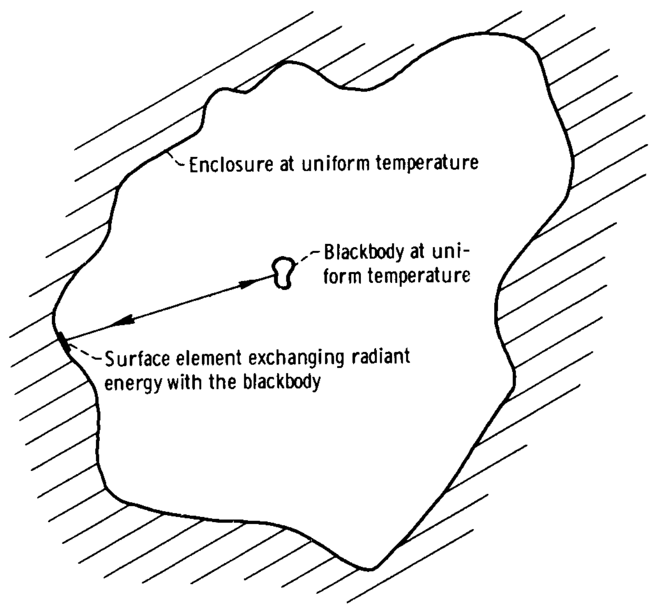

FIGURE 2–1.—Enclosure geometry for derivation of blackbody properties.

2.3.2 Radiation Isotropy in a Black Enclosure

Now consider the isothermal enclosure with black walls and arbitrary shape shown in figure 2–1, and move the blackbody to another position and rotate it to another orientation. The blackbody must still be at the same temperature because the whole enclosure remains isothermal. Consequently, the blackbody must be emitting the same amount of radiation as before. To be in equilibrium, the body must still be receiving the same amount of radiation from the enclosure walls. Thus, the total radiation received by the blackbody is independent of body orientation or position throughout the enclosure; therefore, the radiation traveling through any point within the enclosure is independent of position or direction. This means that the black radiation filling the enclosure is *isotropic*.

In addition to emitting the maximum possible total radiation, the blackbody emits the maximum possible energy at each wavelength and in each direction. This is shown by the following arguments:

2.3.3 Perfect Emitter in Each Direction

Consider an area element on the surface of the black isothermal enclosure and an elemental blackbody within the enclosure. Some of the radiation from the surface element strikes the elemental body and is at an angle to the body surface. All this radiation, by definition, is absorbed. In order to maintain thermal equilibrium and isotropic radiation throughout the enclosure, the radiation emitted back into the incident direction must equal that received. Since the body is absorbing the maximum radiation from any direction, it must be emitting the maximum in any direction. Furthermore since the black radiation filling the enclosure is isotropic, the radiation received or emitted in *any* direction by the enclosed black surface, per unit projected area normal to that direction, must be the same.

2.3.4 Perfect Emitter at Every Wavelength

Consider a blackbody inside an enclosure with the whole system in thermal equilibrium. The enclosure boundary is specified as being of a very special type—it emits and absorbs radiation only in the small wavelength interval $d\lambda_1$ around λ_1. The blackbody, being a perfect absorber, absorbs all the incident radiation in this wavelength interval. To maintain the thermal equilibrium of the enclosure, the blackbody must reemit radiation in this same wavelength interval; the radiation can then be absorbed by the enclosure boundary which only absorbs in this particular wavelength interval. Since the blackbody is absorbing a maximum of the radiation in $d\lambda_1$, it must be emitting a maximum in $d\lambda_1$. A second enclosure can now be specified that only emits and absorbs in the interval $d\lambda_2$ around λ_2. The blackbody must then emit a maximum at the wavelength λ_2. In this manner the blackbody is shown to be a perfect emitter at each wavelength. The special nature of the enclosure assumed in this discussion is of no significance relative to the blackbody, because the emissive properties of a body depend only on the nature of the body and are independent of the enclosure.

2.3.5 Total Radiation a Function Only of Temperature

If the enclosure temperature is altered, the enclosed blackbody temperature must adjust and become equal to the new enclosure temperature (i.e., the complete isolated system must tend toward thermal equilibrium). The system will again be isothermal, and the absorbed and emitted energy of the blackbody will again be equal to each other although the magnitude differs from the value for the previous enclosure temperature. Since by definition the body absorbs (and hence emits) the maximum amount corresponding to this temperature, the characteristics of the surroundings do not affect the emissive behavior of the blackbody. Hence, *the total radiant energy emitted by a blackbody is a function only of its temperature.*

Further, the second law of thermodynamics forbids net energy transfer from a cooler to a hotter surface without doing work on the system. If the radiant energy emitted by a blackbody increased with decreasing temperature, we could easily build a device to violate this law. Consider, for example, the infinite parallel black plates shown in figure 2–2. The upper plate is held at temperature T_1, which is higher than the temperature T_2 of the lower plate.

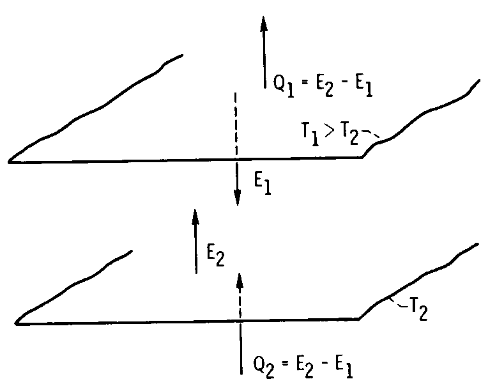

FIGURE 2–2.—Device violating second law of thermodynamics.

If the emission of energy decreased with increasing temperature, then the energy emitted per unit time by plate 2, E_2, is larger than that emitted by plate 1, E_1. Because the plates are black, each absorbs all energy emitted by the other. To maintain the temperature of the plates, an amount of energy $Q_1 = E_2 - E_1$ must be extracted from plate 1 per unit time and an equal amount added to plate 2. Thus, we are transferring net energy from the colder to the warmer plate without doing external work. Experience as embodied in the second law of thermodynamics says that this cannot be done. Therefore, the radiant energy emitted by a blackbody must *increase* with temperature.

From these arguments, the total radiant energy emitted by a blackbody is expected to be proportional only to a monotonically increasing function of temperature.

2.4 EMISSIVE CHARACTERISTICS OF A BLACKBODY

2.4.1 Definition of Blackbody Radiation Intensity [3]

Consider an elemental surface area dA surrounded by a hemisphere of radius r as shown in figure 2–3. A hemisphere has a surface area of $2\pi r^2$ and subtends a solid angle of 2π steradians (sr) about a point at

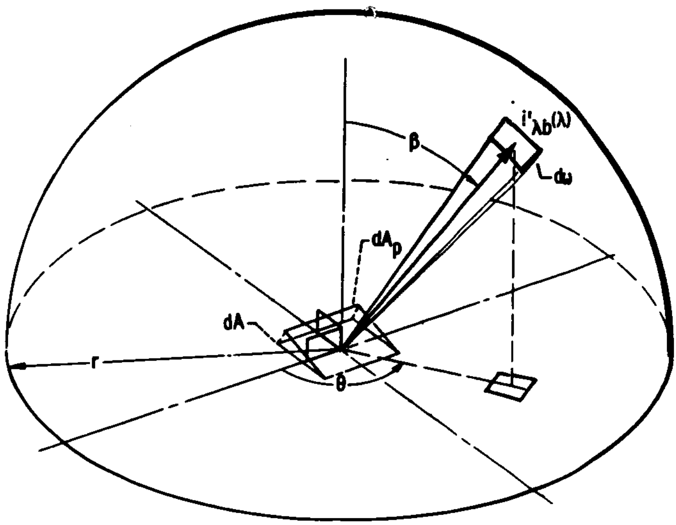

FIGURE 2–3.—Spectral emission intensity from black surface.

the center of its base. Hence, by considering a hemisphere of unit radius, the solid angle about the center of the base can be regarded directly as the area on the unit hemisphere. Direction is measured by the angles θ and β as shown in figure 2–3, where the angle β is measured from the direction *normal* to the surface. The angular position for $\theta=0$ is arbitrary.

The radiation emitted in any direction will be defined in terms of the *intensity*. There are two types of intensities: the *spectral intensity* refers to radiation in an interval $d\lambda$ around a single wavelength, while

[3] The system of units and definition of terms used here have been made as self-consistent as possible to avoid confusion. This is not true for all areas of radiation, where separate interests and needs have caused a great variety of inconsistent systems of units and definitions to be used. A good example of this was provided to the authors by Dr. Fred Nicodemus, who sent a data sheet used in the field of ophthalmology to define units of luminance. Enough comment is probably provided by the following equality taken from the data sheet:

$$1 \text{ nit} = 3.14 \text{ apostilb} = 10^4 \text{ Bougie-Hectomètre-Carré} = 2.919 \text{ foot-lambert}.$$

the *total intensity* refers to the combined radiation including all wavelengths. The spectral intensity of a blackbody will be given by $i'_{\lambda b}(\lambda)$. The subscripts denote, respectively, that one wavelength is being considered and that the properties are for a blackbody. The prime denotes that radiation in a single direction is being considered. The notation is explained in detail in chapter 3, section 3.1.2. The spectral intensity is the energy emitted per unit time per unit small wavelength interval around the wavelength λ, per unit elemental *projected surface area* normal to the (β, θ) direction and into a unit elemental solid angle centered around the direction (β, θ). As will be shown in section 2.4.2 the blackbody intensity defined in this way (i.e., on the basis of projected area) is independent of direction; hence, the symbol for blackbody intensity is not modified by any (β, θ) designation. The total intensity i'_b is defined analogously to $i'_{\lambda b}$, except that it includes the radiation for all wavelengths; hence, the subscript λ and the functional dependence (λ) do not appear. The spectral and total intensities are related by the integral over all wavelengths

$$i'_b = \int_{\lambda=0}^{\infty} i'_{\lambda b}(\lambda)d\lambda \tag{2-1}$$

2.4.2 Angular Independence of Intensity

The angular independence of the blackbody intensity can be shown by considering a spherical isothermal blackbody enclosure of radius r with a blackbody element dA at its center, as shown in figure 2-4(a). Once again, the enclosure and the central elemental body are in thermal equilibrium. Thus, all radiation in transit throughout the enclosure must be isotropic. Consider radiation in a wavelength interval $d\lambda$ about λ that is emitted by an element dA_s on the enclosure surface and travels toward the central element dA (fig. 2-4(b)). The emitted energy in this direction per unit solid angle and time is $i'_{\lambda b,n}(\lambda)dA_s d\lambda$. The normal spectral intensity of a blackbody is used because the energy is emitted normal to the black wall element dA_s of the spherical enclosure. The amount of energy per unit time that impinges upon dA depends on the solid angle that dA occupies when viewed from the location of dA_s. This solid angle is the projected area of dA normal to the (β, θ) direction divided by r^2. The projected area of dA is

$$dA_p = dA \cos\beta \tag{2-2}$$

Then the energy absorbed by dA is

$$Q'_{\lambda b}(\lambda, \beta, \theta) = i'_{\lambda b, n}(\lambda)dA_s d\lambda \frac{dA \cos\beta}{r^2} \tag{2-3}$$

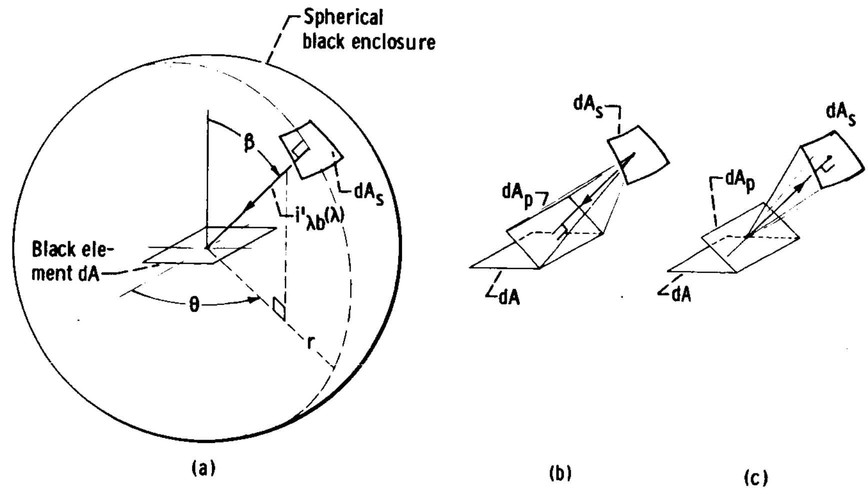

(a) Black element dA within black spherical enclosure.

(b) Energy transfer from dA_s to dA_p.

(c) Energy transfer from dA_p to dA_s.

FIGURE 2–4.—Energy exchange between element of enclosure surface and element within enclosure.

The energy emitted by dA in the (β, θ) direction and incident on dA_s (fig. 2–4(c)) must be equal to that absorbed from dA_s, or equilibrium would be disturbed; hence,

$$i'_{\lambda b}(\lambda, \beta, \theta) dA_p \frac{dA_s}{r^2} d\lambda = Q'_{\lambda b}(\lambda, \beta, \theta) = i'_{\lambda b, n}(\lambda) dA_s \frac{dA \cos \beta}{r^2} d\lambda \qquad (2\text{–}4)$$

Then, by virtue of equation (2–2),

$$i'_{\lambda b}(\lambda, \beta, \theta) = i'_{\lambda b, n}(\lambda) \neq \text{function of } \beta, \theta \qquad (2\text{–}5)$$

Equation (2–5) shows that the *intensity of radiation from a blackbody,* as defined here on the basis of projected area, *is independent of the direction of emission.* Neither the subscript n nor the (β, θ) notation is really needed for complete description of the black intensity. Since the blackbody is always a perfect absorber and emitter, these properties of the blackbody are independent of its surroundings. Hence, these results are independent of both the assumptions used in the derivation of a spherical enclosure and thermodynamic equilibrium with the surroundings.[4]

2.4.3 Blackbody Emissive Power—Definition and Cosine Law Dependence

The intensity has been defined on the basis of projected area. It is useful also to define a quantity which gives the energy emitted in a given direction per unit of actual (unprojected) surface area. This is defined as $e'_{\lambda b}(\lambda, \beta, \theta)$ which is the energy emitted by a black surface per unit time within a unit small wavelength interval centered around the wavelength λ, per unit elemental surface area and into a unit elemental solid angle $d\omega$ centered around the direction (β, θ). The energy in the wavelength interval $d\lambda$ centered about λ emitted per unit time in any direction $Q'_{\lambda b}(\lambda, \beta, \theta)$ can then be expressed in the two forms

$$Q'_{\lambda b}(\lambda, \beta, \theta) = e'_{\lambda b}(\lambda, \beta, \theta)\, dA\, d\omega\, d\lambda = i'_{\lambda b}(\lambda)\, dA \cos\beta\, d\omega\, d\lambda$$

Consequently, there exists the relation

$$e'_{\lambda b}(\lambda, \beta, \theta) = i'_{\lambda b}(\lambda) \cos\beta = e'_{\lambda b}(\lambda, \beta) \tag{2–6}$$

It is evident from the $i'_{\lambda b}(\lambda) \cos\beta$ term in equation (2–6) that $e'_{\lambda b}(\lambda, \beta, \theta)$ does not depend on θ and hence can be expressed as $e'_{\lambda b}(\lambda, \beta)$. The quantity $e'_{\lambda b}(\lambda, \beta)$ is called the *directional spectral emissive power* for a black surface. In the case of some nonblack surfaces, there will be a dependence of e'_{λ} on angle θ.

Equation (2–6) is known as *Lambert's cosine law*, and surfaces having a directional emissive power that follows this relation are known as "diffuse" or "cosine law" surfaces. A blackbody, because it is always a diffuse surface, serves as a standard for comparison with the directional properties of real surfaces that do not, in general, follow the cosine law.

[4] It should be noted that some exceptions do exist for most of the blackbody "laws" presented in this chapter. The exceptions are of minor importance in almost any practical engineering situation but need to be considered when extremely rapid transients are present in a radiative transfer process. If the transient period is of the order of the time scale of whatever process is governing the emission of radiation from the body in question, then the emission properties of the body may lag the absorption properties. In such a case, the concepts of temperature used in the derivations of the blackbody laws no longer hold rigorously. The treatment of such problems is outside the scope of this work.

2.4.4 Hemispherical Spectral Emissive Power of a Blackbody

In calculations of total radiant energy rejection by a surface, there is needed the spectral emissive power integrated over all solid angles of a hemispherical envelope placed over a black surface. This quantity is called the *hemispherical spectral emissive power* of a black surface $e_{\lambda b}(\lambda)$. It is the energy leaving a black surface per unit time per unit area and per unit wavelength interval around λ. Figure 2–5 shows the elemental area dA at the center of the base of a unit hemisphere. By definition, a solid

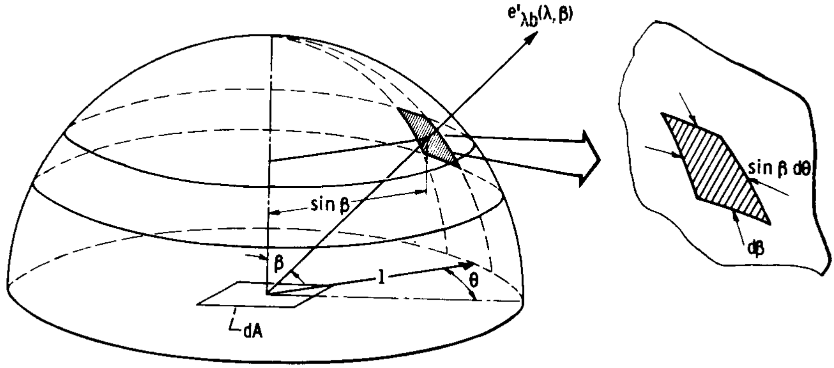

FIGURE 2–5.—Unit hemisphere used to obtain relation between blackbody intensity and hemispherical emissive power.

angle anywhere above dA is equal to the intercepted area on the unit hemisphere. An element of this hemispherical area is given by

$$d\omega = \sin\beta\, d\beta d\theta$$

Hence, the spectral emission from dA per unit time and unit surface area passing through the element on the hemispherical area is given by

$$e'_{\lambda b}(\lambda, \beta) \sin\beta\, d\beta d\theta$$

By virtue of equation (2–6), this is equal to

$$e'_{\lambda b}(\lambda, \beta) d\omega = i'_{\lambda b}(\lambda) \cos\beta \sin\beta\, d\beta d\theta \qquad (2\text{–}7)$$

To obtain the blackbody emission passing through the entire hemisphere, equation (2–7) is integrated over all solid angles to give

$$e_{\lambda b}(\lambda)=i'_{\lambda b}(\lambda)\int_{\theta=0}^{2\pi}\int_{\beta=0}^{\pi/2}\cos\beta\sin\beta\,d\beta d\theta \tag{2–8a}$$

or

$$e_{\lambda b}(\lambda)=2\pi i'_{\lambda b}(\lambda)\int_{0}^{1}\sin\beta\,d(\sin\beta)=\pi i'_{\lambda b}(\lambda) \tag{2–8b}$$

where the prime notation is absent in the designation of the hemispherical quantity. Also from equation (2–6), when the emission is normal to the surface ($\beta=0$) so that $\cos\beta=1$,

$$e'_{\lambda b,\,n}(\lambda)=i'_{\lambda b}(\lambda)$$

and, from equation (2–8b),

$$e_{\lambda b}(\lambda)=\pi e'_{\lambda b,\,n}(\lambda) \tag{2–9}$$

Hence, purely from the geometry involved, this simple relation is found: *The blackbody hemispherical emissive power is π times the directional emissive power normal to the surface or π times the intensity.* This relation will prove to be very useful in relating directional and hemispherical quantities in following chapters.

2.4.5 Spectral Emissive Power Through a Finite Solid Angle

Sometimes the emission through only part of the hemispherical solid angle enclosing an area element may be desired. The emission through the solid angle extending from β_1 to β_2 and θ_1 to θ_2 is found by modifying the limits of integration in equation (2–8a)

$$e_{\lambda b}(\lambda,\beta_1-\beta_2,\theta_1-\theta_2)=i'_{\lambda b}(\lambda)\int_{\theta_1}^{\theta_2}\int_{\beta_1}^{\beta_2}\cos\beta\sin\beta\,d\beta d\theta$$

$$=i'_{\lambda b}(\lambda)\,\frac{(\sin^2\beta_2-\sin^2\beta_1)}{2}\,(\theta_2-\theta_1) \tag{2–10}$$

2.4.6 Spectral Distribution of Emissive Power

Some of the blackbody characteristics that have been discussed are: The blackbody is defined as a perfect absorber and is also a perfect emitter. Its spectral intensity and therefore its spectral emissive power are only functions of the temperature of the blackbody. The emitted blackbody spectral energy follows Lambert's cosine law.

All these blackbody properties have been demonstrated by thermodynamic arguments. However, a very important fundamental property of the blackbody remains to be presented. This is the formula that gives the magnitude of the emitted energy at each of the wavelengths that comprise the radiation spectrum. This relation cannot be obtained from purely thermodynamic arguments. Indeed, the search for this formula led Planck to investigation and hypothesis that became the foundation of quantum theory. The derivation of the spectral distribution is beyond the scope of interest of the present discussion. Therefore the results will be presented here without derivation. The interested reader may consult various standard physics texts (refs. 1 to 3) for the complete development.

It has been shown by the quantum arguments of Planck (ref. 4) and verified experimentally that for a blackbody the spectral distributions of hemispherical emissive power and radiant intensity in a *vacuum* are given as a function of absolute temperature and wavelength by

$$e_{\lambda b}(\lambda) = \pi i'_{\lambda b}(\lambda) = \frac{2\pi C_1}{\lambda^5 (e^{C_2/\lambda T} - 1)} \qquad \text{(2-11a)}$$

This is known as *Planck's spectral distribution of emissive power.* As will be shown later, for radiation into a medium where the speed of light is not close to c_o, equation (2-11a) must be modified by including index of refraction multiplying factors (see section 2.4.12). For most engineering work, the radiant emission is into air or other gases with an index of refraction so close to unity that equation (2-11a) is applicable. The values of the constants C_1 and C_2 are given in table IV of the appendix in two common systems of units. These constants are equal to $C_1 = hc_o^2$ and $C_2 = hc_o/k$ where h is Planck's constant and k is the Boltzmann constant.[5, 6] Equation (2-11a) is of great importance as it provides quantitative results for the radiation from a blackbody.

EXAMPLE 2-1: A plane black surface is radiating at a temperature of 1500° F. What is the directional spectral emissive power of the blackbody at an angle of 60° from the normal and at a wavelength of 6 μm?

---

[5] $h = 6.625 \times 10^{-27}$ (erg) (sec) and $k = 1.380 \times 10^{-16}$ erg/°K.

[6] In some literature, the constant C_1 is defined as $2\pi hc_o^2$.

From equation (2–11a),

$$i'_{\lambda b}(6\ \mu\text{m})=\frac{2\times 0.1889\times 10^{8}\,(\text{Btu})(\mu\text{m})^{4}/(\text{hr})(\text{sq ft})}{6^{5}(\mu\text{m})^{5}\,(e^{25898/6\times 1960}-1)\,(\text{sr})}$$

$$=606\,\frac{\text{Btu}}{(\text{hr})(\text{sq ft})(\mu\text{m})(\text{sr})}.$$

From equation (2–6) the directional emissive power is

$$e'_{\lambda b}(6\ \mu\text{m}, 60°)=606\cos 60°=303\,\frac{\text{Btu}}{(\text{hr})(\text{sq ft})(\mu\text{m})(\text{sr})}$$

Alternate forms of equation (2–11a) are sometimes employed where frequency or wave number is used rather than wavelength. The use of frequency has an advantage when radiation travels from one medium into another, as in this instance the frequency remains constant while the wavelength changes because of the change in propagation velocity. To make the transformation of equation (2–11a) to frequency, note that in vacuum $\lambda=c_0/\nu$, and hence $d\lambda=-(c_0/\nu^2)d\nu$. Then the hemispherical emissive power in the wavelength interval $d\lambda$ becomes

$$e_{\lambda b}(\lambda)d\lambda=\frac{2\pi C_1 d\lambda}{\lambda^5(e^{C_2/\lambda T}-1)}=\frac{-2\pi C_1\nu^3 d\nu}{c_0^4(e^{C_2\nu/c_0 T}-1)}=-e_{\nu b}(\nu)d\nu \qquad \text{(2–11b)}$$

The quantity $e_{\nu b}(\nu)$ is the emissive power *per unit frequency* about ν.

The wave number $\eta=1/\lambda$ is the number of waves per unit length. Then

$$d\lambda=-\frac{1}{\eta^2}d\eta$$

and

$$e_{\lambda b}(\lambda)d\lambda=-\frac{2\pi C_1\eta^3 d\eta}{(e^{C_2\eta/T}-1)}=-e_{\eta b}(\eta)d\eta \qquad \text{(2–11c)}$$

The quantity $e_{\eta b}(\eta)$ is the emissive power *per unit wave number* about η.

To understand better the implications of equation (2–11a), it has been plotted in figure 2–6. Here the hemispherical spectral emissive power is given as a function of wavelength for several different values of the

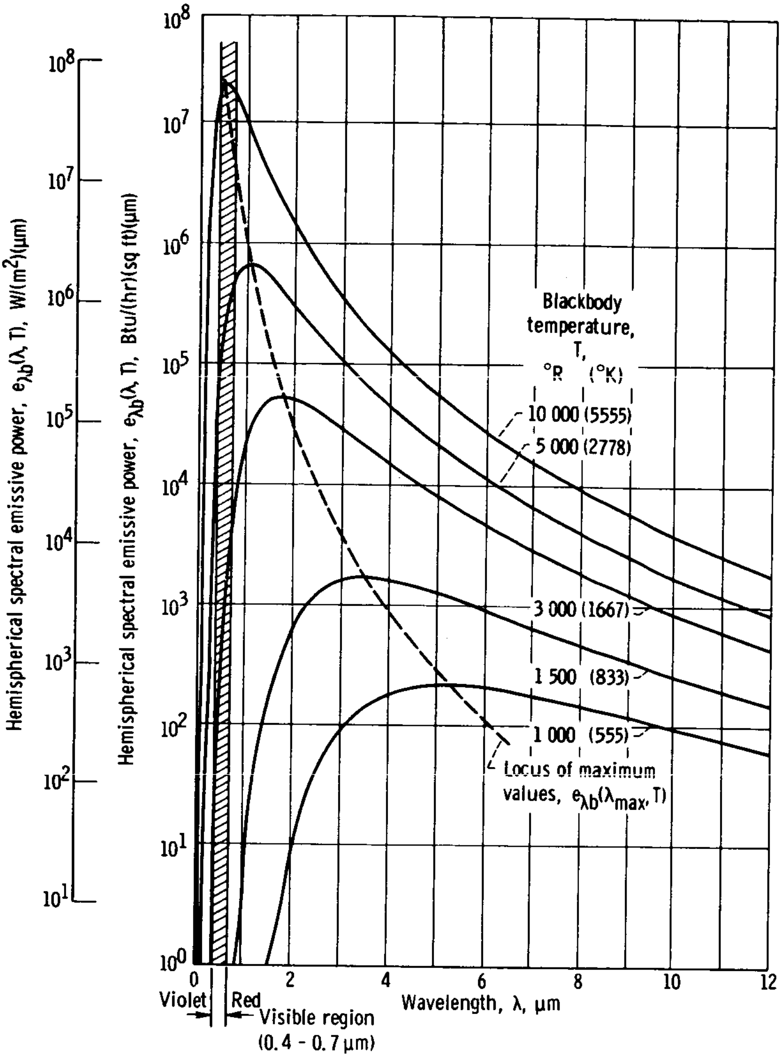

FIGURE 2–6.—Hemispherical spectral emissive power of blackbody for several different temperatures.

absolute temperature. One characteristic that is quite evident is that the energy emitted at all wavelengths increases as the temperature increases. It was shown in section 2.3.5, and it is known from common experience that the total (including all wavelengths) radiated energy must increase with temperature; the curves show that this is also true for the energy at each wavelength. Another characteristic is that the peak spectral emissive power shifts toward a smaller wavelength as the temperature is increased. A cross plot of figure 2–6 giving energy as a function of temperature for fixed wavelengths shows that the energy emitted at the shorter wavelength end of the spectrum increases more rapidly with temperature than the energy at the long wavelengths.

The position of the range of wavelengths included in the visible spectrum is included in figure 2–6. For a body at 1000° R only a very small amount of energy would be in the visible region and would not be sufficient to be detected by eye. Since the curves at the lower temperatures slope downward from the red toward the violet end of the spectrum, as the temperature is raised the red light becomes visible first.[7] Higher temperatures make visible additional wavelengths of the visible light range, and at a sufficiently high temperature the light emitted becomes white, representing radiation composed of a mixture of all the visible wavelengths.

For the filament of an incandescent lamp to operate efficiently, the temperature must be high, otherwise too much of the electrical energy would be dissipated as radiation in the infrared region rather than in the visible range. Most tungsten filament lamps operate at about 5400° R, and thus do give off a large fraction of their energy in the infrared, but their filament vaporization rate limits the temperature to near this value. The Sun emits a spectrum quite similar to that of a blackbody at a temperature of about 10 000° R, and an appreciable amount of energy release is in what we sense as the visible region. This may be because evolution has caused the eye to be most sensitive in the spectral region of greatest energy. If the eye were sensitive in other regions (for example, the infrared so that we could see thermal images in the "dark"), our definition of the "visible region of the spectrum" would change. If man finds life in other solar systems, where the Sun has an effective temperature different from ours, it will be interesting to discover what wavelength range encompasses the "visible spectrum" if the beings there possess sight.

Equation (2–11a) can be placed in a more convenient form that eliminates the need for providing a separate curve for each value of T. This is done by dividing by the fifth power of temperature to give

$$\frac{e_{\lambda b}(\lambda, T)}{T^5}=\frac{\pi i'_{\lambda b}(\lambda, T)}{T^5}=\frac{2\pi C_1}{(\lambda T)^5(e^{C_2/\lambda T}-1)} \qquad (2\text{–}12)$$

This equation gives the quantity $e_{\lambda b}(\lambda, T)/T^5$ in terms of the single vari-

[7] This occurs at the so-called Draper point of 977° F (ref. 5), at which red light first becomes visible from a heated object in darkened surroundings.

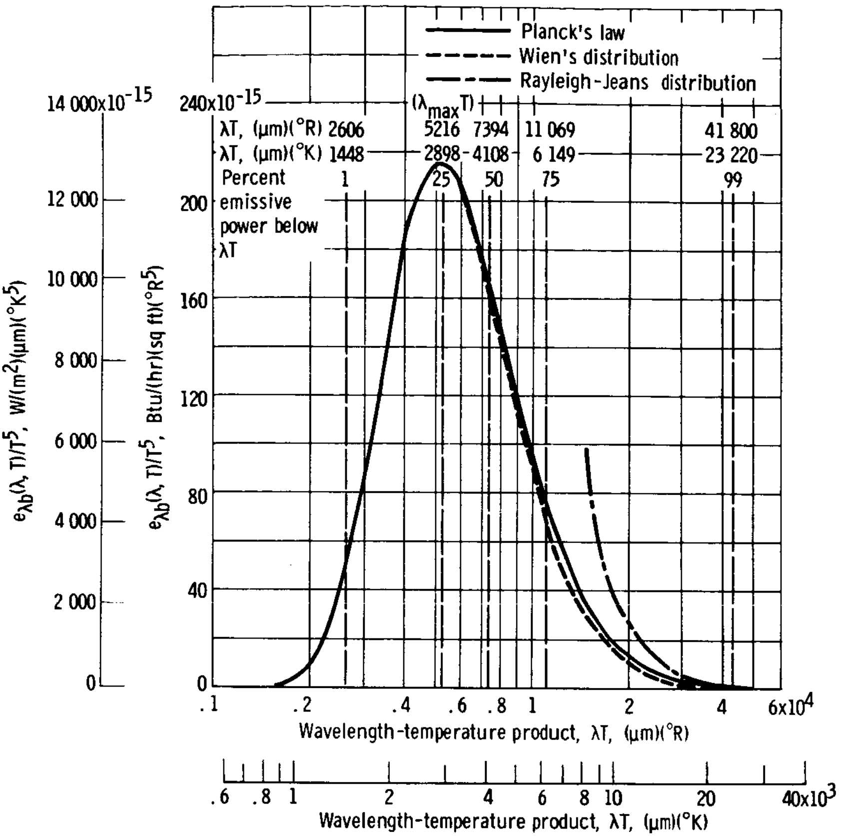

FIGURE 2–7.—Spectral distribution of blackbody hemispherical emissive power.

able λT. A plot of this relation is given in figure 2–7 and replaces the multiple curves in figure 2–6. A compilation of values is presented in table V of the appendix.

EXAMPLE 2–2: For a blackbody at 1500° R what is the spectral hemispherical emissive power at a wavelength of 2 μm? Use table V of the appendix.

The value of λT is 3000 (μm)(°R). From table V, at this λT, $e_{\lambda b}/T^5 = 87.047 \times 10^{-15}$ Btu/(hr)(sq ft)(μm)(°R)^5. Then $e_{\lambda b}(2\ \mu\text{m}) = 87.047 \times 10^{-15} (1500)^5 = 661$ Btu/(hr)(sq ft)(μm).

2.4.7 Approximations for Spectral Distribution

Planck's spectral distribution gives the maximum (blackbody) intensity of radiation which any body can emit at a given wavelength for a given temperature. This intensity serves as an optimum standard with which real surface performance can be compared. In chapter 3, the methods of comparison will be defined. Planck's distribution also provides a means to evaluate the maximum radiative performance that can be attained for any radiating device.

Some approximate forms of Planck's distribution are occasionally useful because of their simplicity. Care must be taken to use them only in the range where their accuracy is acceptable.

2.4.7.1 *Wien's formula.*—If the term $e^{C_2/\lambda T}$ is much larger than 1, equation (2–12) reduces to

$$\frac{i'_{\lambda b}(\lambda, T)}{T^5}=\frac{2C_1}{(\lambda T)^5 e^{C_2/\lambda T}} \tag{2–13}$$

which is known as *Wien's formula.* It is accurate to within 1 percent for λT less than 5400(μm)(°R).

2.4.7.2 *Rayleigh-Jeans formula.*—Another approximation is found by taking the denominator of equation (2–12) and expanding it in a series to give

$$e^{C_2/\lambda T}-1=1+\frac{C_2}{\lambda T}+\frac{1}{2!}\left(\frac{C_2}{\lambda T}\right)^2+\frac{1}{3!}\left(\frac{C_2}{\lambda T}\right)^3+\ldots-1 \tag{2–14}$$

For λT much larger than C_2, this series can be approximated by the single term $C_2/\lambda T$, and equation (2–12) becomes

$$\frac{i'_{\lambda b}(\lambda, T)}{T^5}=\frac{2C_1}{C_2}\frac{1}{(\lambda T)^4} \tag{2–15}$$

This is known as the *Rayleigh-Jeans formula* and is accurate to within 1 percent for λT greater than 14×10^5 (μm)(°R). This is well outside the range generally encountered in thermal radiation problems, since a blackbody emits over 99.9 percent of its energy at λT values below this. The formula has utility for long-wave radiation of other classifications, such as radio waves.

A comparison of these approximate formulae with the Planck distribution is shown in figure 2–7.

2.4.8 Wien's Displacement Law

Another quantity of interest with regard to the blackbody emissive spectrum is the wavelength λ_{max} at which the emitted energy is a maximum for a given temperature. This maximum shifts toward shorter wavelengths as the temperature is increased, as shown by the dotted line in figure 2–6. The value of $\lambda_{max}T$ can be found at the peak of the distribution curve given in figure 2–7. Alternately it can be found analytically by differentiating Planck's distribution from equation (2–12) and setting the left side equal to zero. This gives the transcendental equation

$$\lambda_{max}T=\frac{C_2}{5}\left(\frac{1}{1-e^{-C_2/\lambda_{max}T}}\right) \tag{2–16}$$

The solution to this equation is of the form

$$\lambda_{max}T=C_3 \tag{2–17}$$

which is one form of *Wien's displacement law*. Values of the constant C_3 are given in table IV of the appendix. Equation (2–17) indicates that the peak emissive power and intensity shift to a shorter wavelength at a higher temperature in inverse proportion to T.

EXAMPLE 2–3: For a blackbody to radiate its maximum energy at the center of the visible spectrum what would its temperature have to be?

Figure 1–2 shows the visible spectrum spans the range 0.4 to 0.7 μm, and the center of the range is at 0.55 μm. From equation (2–17)

$$T=\frac{C_3}{\lambda_{max}}=\frac{5216\ (\mu\text{m})(°\text{R})}{0.55\ \mu\text{m}}=9480°\ \text{R}$$

This is close to the effective surface temperature of the Sun.

2.4.9 Total Intensity and Emissive Power

The previous discussion has provided the energy per unit wavelength interval that a blackbody radiates at each wavelength. It will now be shown how the total intensity of radiation, which includes the radiation for all wavelengths, can be determined. The result is a surprisingly simple relation.

The energy emitted over the small wavelength interval $d\lambda$ is given by $i'_{\lambda b}(\lambda)d\lambda$. Integrating the spectral intensity over all wavelengths from $\lambda=0$ to $\lambda=\infty$ gives the *total intensity*

$$i'_b=\int_0^\infty i'_{\lambda b}(\lambda)\,d\lambda \tag{2–18}$$

This integral may be evaluated by substitution of Planck's distribution from equation (2–12) and a transformation of variables in terms of $\zeta = C_2/\lambda T$. Equation (2–18) then becomes

$$i_b' = \int_0^\infty \frac{2C_1}{\lambda^5 (e^{C_2/\lambda T} - 1)} \, d\lambda$$

$$= \int_\infty^0 \left(\frac{C_2}{\lambda T}\right)^5 \left(\frac{T}{C_2}\right)^5 \frac{2C_1}{(e^{C_2/\lambda T} - 1)} \left(\frac{\lambda T}{C_2}\right)^2 \left(\frac{-C_2}{T}\right) d\left(\frac{C_2}{\lambda T}\right)$$

$$= \frac{2C_1 T^4}{C_2^4} \int_0^\infty \frac{\zeta^3}{(e^\zeta - 1)} \, d\zeta \qquad (2\text{–}19)$$

From a table of integrals (ref. 6), this can be evaluated as

$$i_b' = \frac{2C_1 T^4}{C_2^4} \frac{\pi^4}{15} \qquad (2\text{–}20)$$

Defining a new constant results in

$$i_b' = \frac{\sigma}{\pi} T^4 \qquad (2\text{–}21)$$

where the constant is

$$\sigma = \frac{2C_1 \pi^5}{15 C_2^4} = 0.1712 \times 10^{-8} \, \frac{\text{Btu}}{(\text{hr})(\text{sq ft})(^\circ\text{R}^4)} \qquad (2\text{–}22)$$

The *hemispherical total emissive power* of a surface is then

$$e_b = \int_0^\infty e_{\lambda b}(\lambda) \, d\lambda = \int_0^\infty \pi i_{\lambda b}'(\lambda) \, d\lambda = \sigma T^4 \qquad (2\text{–}23)$$

which is known as the *Stefan-Boltzmann law*, where σ is the *Stefan-Boltzmann constant*. The value of σ as determined experimentally differs slightly from that calculated by equation (2–22). This is indicated in table IV of the appendix.

EXAMPLE 2–4: The beam emitted normal to a blackbody surface is found to have a total radiation per unit solid angle and per unit surface area of 3000 Btu/(hr)(sq ft)(sr). What is the surface temperature?

The hemispherical total emissive power is related to the total emissive power in the normal direction by $e_b = \pi e_{b,n}'$. Hence, from equation

(2–23) $T=(\pi e'_{b,n}/\sigma)^{1/4}=(3000\pi/0.173\times10^{-8})^{1/4}=1528°$ R. The experimental value of the Stefan-Boltzmann constant has been used.

EXAMPLE 2–5: A black surface is radiating with a hemispherical total emissive power of 2000 Btu/(hr)(sq ft). What is the surface temperature? At what wavelength is its maximum spectral emissive power?

From the Stefan-Boltzmann law, the temperature of the blackbody is $T=(e_b/\sigma)^{1/2}=(2000/0.173\times10^{-8})^{1/4}=1037°$ R. Then from Wien's displacement law, $\lambda_{max}=C_3/T=5216/1037=5.04\ \mu m$.

2.4.10 Behavior of Maximum Intensity with Temperature

The spectral intensity of a black surface $i'_{\lambda b}(\lambda)$ was shown in equation (2–5) to be independent of the angle of emission. Integrating over all wavelengths of course did not change this angular independence.

The intensity of a surface is what the eye interprets as "brightness." The Sun, which radiates with a spectral distribution of intensity similar to that of a blackbody at 10 000° R, appears equally bright across its surface to the unaided eye. The Sun thus gives qualitative experimental verification that the intensity is indeed invariant with direction of emission, because the radiation reaching us from the center of the solar disk was emitted normal to the surface, while that from the edge was emitted at nearly 90° to the normal.

The intensity at a given wavelength is found from Planck's spectral distribution. It is interesting to note that substitution of Wien's displacement law (eq. (2–17)) into equation (2–12) gives

$$i'_{\lambda_{max} b}=T^5\left[\frac{2C_1}{C_3^5(e^{C_2/C_3}-1)}\right] \tag{2–24}$$

This shows that the maximum intensity increases as temperature to the fifth power. Indeed, because $i_{\lambda b}/T^5$ is a function only of λT as shown by equation (2–12), it is evident that if the blackbody temperature is changed from T_1 to T_2 and at the same time the wavelengths λ_1 and λ_2 are chosen such that $\lambda_1 T_1=\lambda_2 T_2$, the value of $i'_{\lambda b}/T^5$ remains unchanged. Therefore, the intensity at λ_2 for temperature T_2 increases as temperature to the fifth power from the value at λ_1 for temperature T_1. This is the general statement of Wien's law.

2.4.11 Blackbody Radiation in a Wavelength Interval

The Stefan-Boltzmann law shows that the hemispherical total emissive power of a blackbody is given by

$$e_b = \int_0^\infty e_{\lambda b}(\lambda)\, d\lambda = \sigma T^4$$

It is often desirable in calculations of radiative exchange to determine the fraction of the total emissive power that is emitted in a given wave-

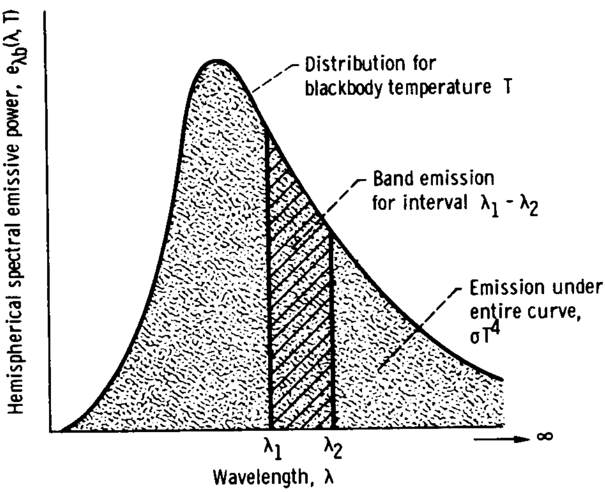

FIGURE 2-8.—Emitted energy in wavelength band.

length band as illustrated by figure 2-8. This fraction is designated by $F_{\lambda_1-\lambda_2}$ and is given by the ratio

$$F_{\lambda_1-\lambda_2} = \frac{\int_{\lambda_1}^{\lambda_2} e_{\lambda b}(\lambda)\, d\lambda}{\int_0^\infty e_{\lambda b}(\lambda)\, d\lambda} = \frac{1}{\sigma T^4} \int_{\lambda_1}^{\lambda_2} e_{\lambda b}(\lambda)\, d\lambda \tag{2-25}$$

The last integral in equation (2-25) can be expressed by two integrals each beginning at $\lambda = 0$

$$F_{\lambda_1-\lambda_2} = \frac{1}{\sigma T^4} \left[\int_0^{\lambda_2} e_{\lambda b}(\lambda)\, d\lambda - \int_0^{\lambda_1} e_{\lambda b}(\lambda)\, d\lambda \right] = F_{0-\lambda_2} - F_{0-\lambda_1} \tag{2-26}$$

The fraction of the emissive power for any wavelength band can therefore be found by having available the values of $F_{0-\lambda}$ as a function λ. The $F_{0-\lambda_1}$ function is illustrated by figure 2-9(a) where it would equal the crosshatched area divided by the total area (shaded) under the curve.

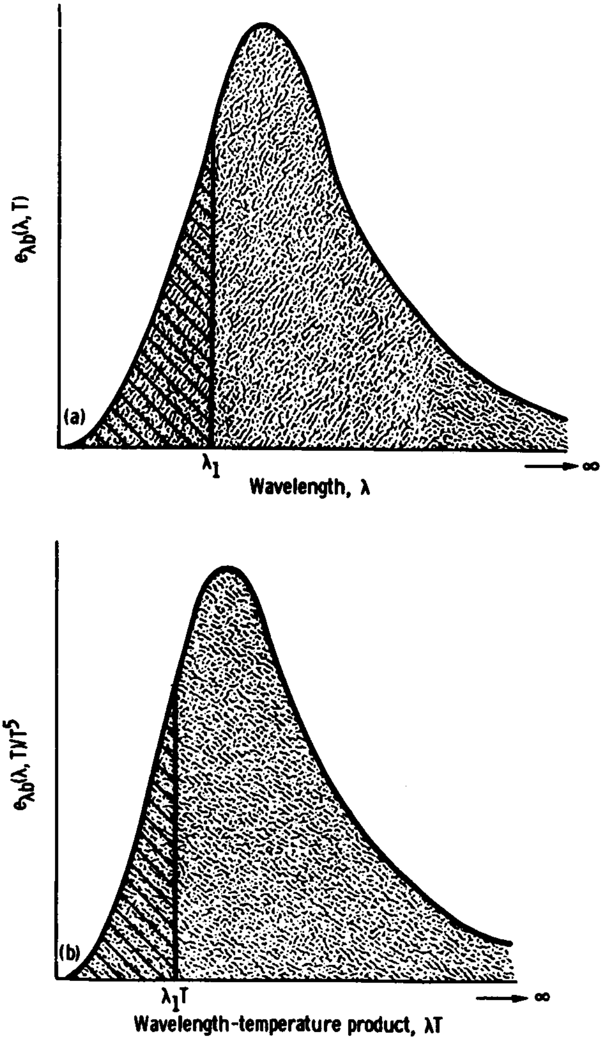

(a) In terms of curve for specific temperature. Entire area under curve, σT^4.
(b) In terms of universal curve. Entire area under curve, σ.

FIGURE 2–9.—Physical representation of F factor, where $F_{0-\lambda_1}$ or $F_{0-\lambda_1 T}$ is ratio of cross-hatched to shaded area.

For a blackbody, because of the simple manner in which the hemispherical emissive power is related to the intensity (eq. (2–8b)) the $F_{\lambda_1-\lambda_2}$ function also gives the fraction of the intensity which lies in the wavelength interval $\lambda_1 - \lambda_2$. Since $e_{\lambda b}$ depends on T, the application of equation (2–26) would require that $F_{0-\lambda}$ be tabulated for each T. There is no need to have this complexity, however, as it is possible to arrange the F function in terms of only the single variable λT, figure 2–9(b). In this way a universal set of F values is obtained that can apply for all temperatures and wavelengths. The universal form is found by rewriting equation (2–26) as

$$F_{\lambda_1 T-\lambda_2 T}=\frac{1}{\sigma}\left[\int_0^{\lambda_2 T}\frac{e_{\lambda b}(\lambda)}{T^5}\,d(\lambda T)-\int_0^{\lambda_1 T}\frac{e_{\lambda b}(\lambda)}{T^5}\,d(\lambda T)\right]=F_{0-\lambda_2 T}-F_{0-\lambda_1 T} \tag{2–27}$$

As shown by equation (2–12), $e_{\lambda b}/T^5$ is only a function of λT so that the integrands in equation (2–27) are only dependent on the λT variable. The $F_{0-\lambda T}$ values are given in table V of the appendix and a plot of $F_{0-\lambda T}$ as a function of λT is shown in figure 2–10.

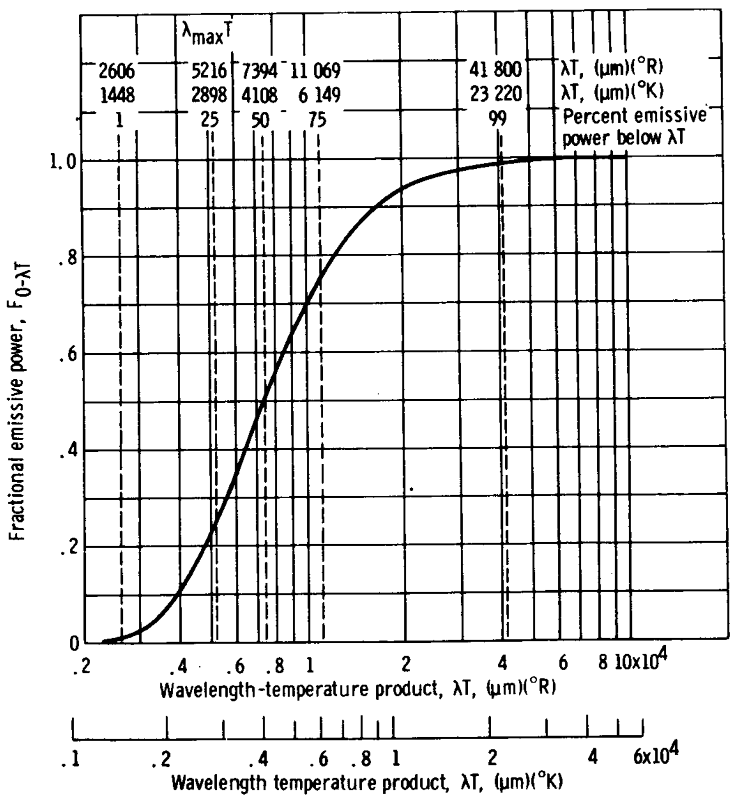

FIGURE 2–10. —Fractional blackbody emissive power in range 0 to λT.

For calculations involving desired accuracy of greater than 1 percent, it should be noted that the values of $F_{0-\lambda T}$ in table V were computed using the constants C_1 and C_2 of table IV of the appendix. The value of σ, the Stefan-Boltzmann constant, which corresponds to these C_1 and C_2 values is the *calculated* value shown in table IV. This calculated σ should be used to determine the total energy quantities that are to be multiplied by the F factors to obtain the energy in a wavelength interval. Use of the experimental value for σ introduces an error of slightly less than 1 percent because of the inconsistency of the experimental σ with the one used in equation (2–27) to obtain table V.

The tabulated $F_{0-\lambda T}$ values are also available in expanded form for use where even greater accuracy is required. The tables of Pivovonsky and Nagel (ref. 7), for example, tabulate values for every λT interval of 10 (μm)(°K) over a very wide range of λT.

Polynomial approximation expressions for $F_{0-\lambda T}$ are also available and are included in the appendix.

The compilation of values of $F_{0-\lambda T}$ has a number of uses as illustrated in the following examples.

EXAMPLE 2–6: A blackbody is radiating at a temperature of 5000° R. An experimenter wishes to measure the total radiant emission by use of a radiation detector. This detector absorbs all radiation in the λ range 0.8 to 5 μm, but detects no energy outside that range. What percentage correction will the experimenter have to apply to his energy measurement? If the sensitivity of the detector could be extended in range by 0.5 μm at only one end of the sensitive range, which end should be extended?

Taking $\lambda_1 T = 0.8 \times 5000 = 4000$ (μm)(°R) and $\lambda_2 T = 5 \times 5000 = 25\,000$ (μm)(°R) results in the fraction of energy outside the sensitive range being

$$F_{0-\lambda_1 T} + F_{\lambda_2 T-\infty} = F_{0-\lambda_1 T} + (1 - F_{0-\lambda_2 T}) = (0.1050 + 1 - 0.9621) = 0.1429$$

or a correction of 14.3 percent of the total incident energy. Extending the sensitive range to the longer wavelength side of the measurement interval adds little accuracy because of the small slope of the curve of F against λT in that region, so extending to shorter wavelengths would provide the greatest increase in detected energy.

EXAMPLE 2–7: The experimenter of the previous example has designed a radiant energy detector which can only be made sensitive over any 1-μm range of wavelength. He wants to measure the total emissive power of two blackbodies, one at 5000° and the other at 10 000° R. He plans to adjust his 1-μm interval to give a 0.5-μm sensitive band on each side of the peak blackbody emissive power. For which blackbody should he expect to detect the greatest percentage of the total emissive power? What will the percentage be in each case?

Wien's displacement law tells us that the peak emissive power will occur at $\lambda_{max} = (5216/T)$ μm in each case. Because for the higher temperature a wavelength interval of 1 μm will give a wider spread of λT values around the peak of $\lambda_{max}T$ on the normalized blackbody curve (fig. 2–7), the measurement should be more accurate for the 10 000° R case. For the 10 000° R blackbody, $\lambda_{max} = 0.5216$ μm, and $\lambda_1 T = (0.5216 - 0.5000) \times 10\,000 = 216$ (μm)(°R). Similarly, $\lambda_2 T = 1.0216 \times 10\,000 = 10\,216$ (μm)(°R). The percentage of detected emissive power is then

$$100(F_{0-10\,216} - F_{0-216}) = 100 \times (0.708 - 0) = 70.8 \text{ percent}$$

A similar calculation for the 5000° R blackbody shows that 51.7 percent of the emissive power is detected.

Some commonly used values of $F_{0-\lambda T}$ are given in table 2–I. It is interesting to note that exactly one-fourth of the total emissive power

TABLE 2–I.—FRACTION OF BLACKBODY EMISSION CONTAINED IN THE RANGE $0-\lambda T$

λT		$F_{0-\lambda T}$
(μm) (°R)	(μm) (°K)	
2 606	1 448	0.01
5 216 = $\lambda_{max}T$	2 898	.25
7 394	4 108	.50
11 069	6 149	.75
41 800	23 220	.99

lies in the wavelength range below the peak of the Planck spectral distribution at any temperature. This relation appears to have no simple physical explanation and must be put down alongside those other phenomena such as gravitational attraction and the Stefan-Boltzmann fourth power law in which nature provides us with a simple law to describe an apparently complex event.

2.4.12 Blackbody Emission in a Medium Other Than a Vacuum

The previous expressions for blackbody emission have been for emission into a vacuum. When emission is considered from a location within a large volume of medium other than a vacuum, the quantities C_1 and C_2 appearing in Planck's energy distribution equation (eq. (2–11a)) should be replaced by the quantities

$$C_1' = hc^2 \tag{2–28a}$$

$$C_2' = hc/k \tag{2–28b}$$

so that

$$e_{\lambda_m b}(\lambda_m)\,d\lambda_m = \frac{2\pi C_1'}{\lambda_m^5(e^{C_2'/\lambda_m T}-1)}\,d\lambda_m \tag{2–29}$$

where k is the Boltzmann constant, h is Planck's constant, c is the speed of propagation of light *in the medium considered*, and λ_m is the wavelength *in the medium.*

Since the speed c depends on the medium under consideration, it is better to define C_1 and C_2 in terms of c_o, the speed of light in vacuum, so that C_1 and C_2 are then truly constants. For a *dielectric*, the speed in the medium is given by $c = c_o/n$ where n is the index of refraction. Planck's distribution for the energy in a wavelength interval $d\lambda_m$ becomes (note that λ_m is the wavelength in the *medium*)

$$e_{\lambda_m b}(\lambda_m) = \frac{2\pi c^2 h}{\lambda_m^5(e^{ch/k\lambda_m T}-1)}\,d\lambda_m = \frac{2\pi c_0^2 h}{n^2\lambda_m^5(e^{c_o h/nk\lambda_m T}-1)}\,d\lambda_m$$

$$= \frac{2\pi C_1}{n^2\lambda_m^5(e^{C_2/n\lambda_m T}-1)}\,d\lambda_m \tag{2–30}$$

If n can be considered independent of wavelength, then $d\lambda_m = d\left(\frac{\lambda}{n}\right) = \frac{1}{n}\,d\lambda$ and

$$e_{\lambda_m b}(\lambda)\,d\lambda_m = \frac{2\pi C_1 n^2}{\lambda^5(e^{C_2/\lambda T}-1)}\,d\lambda \tag{2–31}$$

In equations (2–30) and (2–31), $C_1 = hc_0^2$ and $C_2 = hc_o/k$ which are the values of C_1 and C_2 presented in table IV of the appendix. The λ is the wavelength in a *vacuum*, while λ_m is the wavelength in the *medium*. Note that the refractive index cancels out of the exponential term when λ is used. Equation (2–31) gives the emissive power for a wavelength interval in the medium in terms of the corresponding wavelength interval in vacuum where $\lambda = n\lambda_m$.

The integration of equation (2–31) over all wavelengths follows directly from equation (2–19) when n is constant. This yields the Stefan-Boltzmann law for hemispherical total emissive power in a medium of refractive index n

$$e_{b,m} = n^2\sigma T^4 \tag{2–32}$$

The emission within glass ($n \sim 1.5$) can thus be 2.25 times that from a surface into air.

Finally, Wien's displacement law by similar arguments becomes

$$\lambda_{\max}T = n\lambda_{\max,m}T = C_3 \tag{2–33}$$

where $\lambda_{\max}$ is the wavelength at peak emission *into a vacuum* and $\lambda_{\max,m}$ is the wavelength at peak emission *into a medium*.

For metals, it is shown in chapter 4 that the simple index of refraction must be replaced by the complex index of refraction $n - i\kappa$. In determining the speed of propagation c in terms of c_0 in metals, the simple refractive index n in equations (2–30) to (2–33) must be replaced by the modulus of the complex refractive index, $|n - i\kappa| = (n^2 + \kappa^2)^{1/2}$, remembering that the restriction of wavelength independence has been imposed.

These refinements will not be carried in succeeding sections because their applicability to engineering radiation problems is small. A notable exception is the work of Gardon and others (refs. 8 to 10) dealing with radiation effects in molten glass.

2.5 EXPERIMENTAL PRODUCTION OF A BLACKBODY

When making experimental measurements of the radiative properties of real materials, it is desirable to have a black surface for reference so that a direct comparison can be made between the real surface and the ideal (black) surface. Since perfectly black surfaces do not exist in nature, a special technique is utilized to provide a very close approximation to a black area. Figure 2–11 shows a metal cylinder that has been hollowed out to form a cavity with a small opening. If an incident beam passes into the cavity as shown, it strikes the cavity wall and part is absorbed with the remainder being reflected. The reflected portion

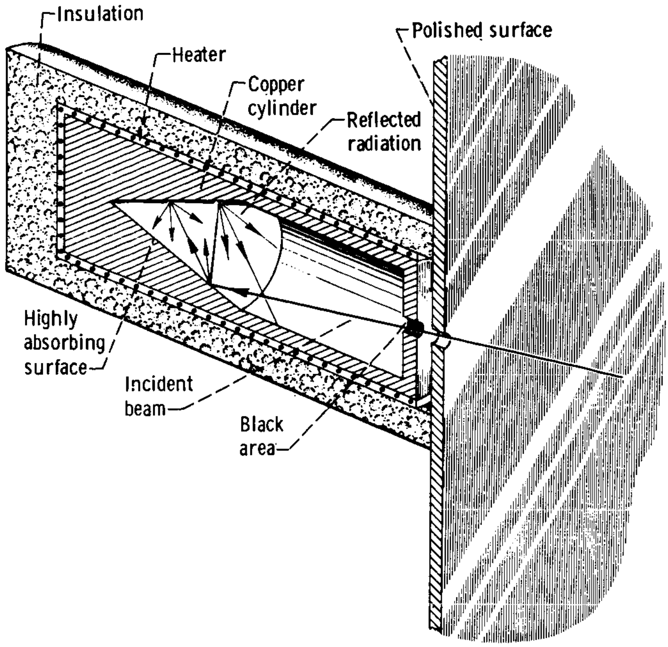

FIGURE 2–11.—Cavity used to produce blackbody area.

strikes other parts of the wall and is again partially absorbed. It is evident that, if the opening to the cavity is very small, very little of the original incident beam will manage to escape back out through the opening. Thus by making the opening sufficiently small, the opening area approaches the behavior of a black surface because essentially all the radiation passing in through it is absorbed. To help keep the cavity at a uniform temperature so that the internal radiation will all be in thermal equilibrium, the cavity shown in figure 2–11 is machined from a copper cylinder and surrounded by insulation. By heating the cavity, a source of black radiation is obtained at the opening since, as previously discussed in section 2.3.1, a perfectly absorbing surface is also perfectly emitting. The polished surface at the front of the cavity aids in shielding the opening from stray radiation from the surroundings.

The attainment of isothermal conditions in such a cavity (often referred to as a "hohlraum") is a difficult but necessary condition in the accurate experimental determination of radiative properties.

2.6 SUMMARY OF BLACKBODY PROPERTIES

It has been shown in this chapter that the ideal blackbody possesses

TABLE 2–II. — BLACKBODY

Symbol	Name	Definition
$i'_{\lambda b}(\lambda, T)$	Spectral intensity	Emission in any direction per unit of projected area normal to that direction, and per unit time, wavelength interval about λ, and solid angle
$i'_b(T)$	Total intensity	Emission, including all wavelengths, in any direction per unit of projected area normal to that direction, and per unit time and solid angle
$e'_{\lambda b}(\lambda, \beta, T)$	Directional spectral emissive power	Emission per unit solid angle in direction β per unit surface area, wavelength interval, and time
$e'_b(\beta, T)$	Directional total emissive power	Emission, including all wavelengths, in direction β per unit surface area, solid angle, and time

Radiation Quantities

<table>
<tr><th>Geometry</th><th>Formula</th></tr>
<tr><td>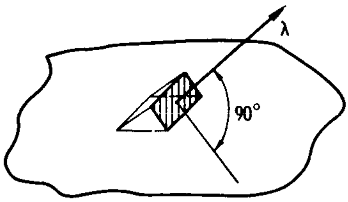
</td><td>$\frac{2C_1}{\lambda^5\left(e^{C_2/\lambda T} - 1\right)}$</td></tr>
<tr><td>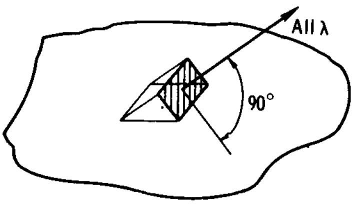
</td><td>$\frac{\sigma T^4}{\pi}$</td></tr>
<tr><td>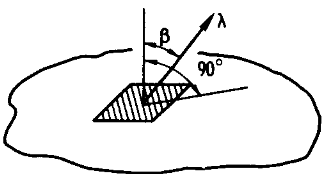
</td><td>$i'_{\lambda b} \cos \beta$</td></tr>
<tr><td>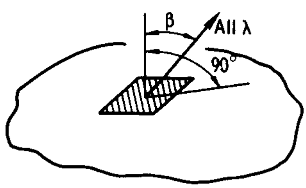
</td><td>$\frac{\sigma T^4}{\pi} \cos \beta$</td></tr>
</table>

TABLE 2-II.—BLACKBODY

Symbol	Name	Definition
$e_{\lambda b}(\lambda, \beta_1 - \beta_2, \theta_1 - \theta_2, T)$	Finite solid angle spectral emissive power	Emission in solid angle $\beta_1 \leq \beta \leq \beta_2$, $\theta_1 \leq \theta \leq \theta_2$ per unit surface area, wavelength interval, and time
$e_b(\beta_1 - \beta_2, \theta_1 - \theta_2, T)$	Finite solid angle total emissive power	Emission, including all wavelengths, in solid angle $\beta_1 \leq \beta \leq \beta_2$, $\theta_1 \leq \theta \leq \theta_2$ per unit surface area and time
$e_{\lambda b}(\lambda_1 - \lambda_2, \beta_1 - \beta_2, \theta_1 - \theta_2, T)$	Finite solid angle band emissive power	Emission in solid angle $\beta_1 \leq \beta \leq \beta_2$, $\theta_1 \leq \theta \leq \theta_2$ and wavelength band $\lambda_1 - \lambda_2$ per unit surface area and time
$e_{\lambda b}(\lambda, T)$	Hemispherical spectral emissive power	Emission into hemispherical solid angle per unit surface area, wavelength interval, and time

RADIATION QUANTITIES – Continued

<table>
<tr><th>Geometry</th><th>Formula</th></tr>
<tr><td>
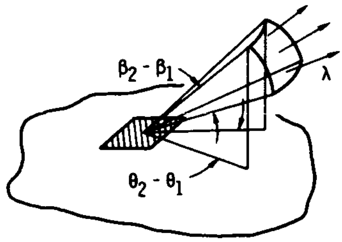

</td><td>

$i'_{\lambda b}(\theta_2 - \theta_1)\dfrac{(\sin^2\beta_2 - \sin^2\beta_1)}{2}$

</td></tr>
<tr><td>
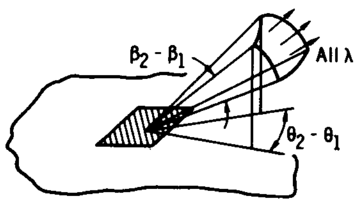

</td><td>

$\dfrac{\sigma T^4}{\pi}(\theta_2 - \theta_1)\dfrac{(\sin^2\beta_2 - \sin^2\beta_1)}{2}$

</td></tr>
<tr><td>
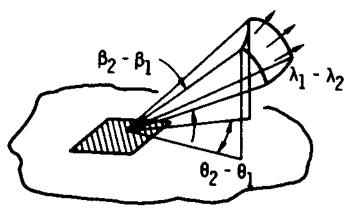

</td><td>

$\dfrac{\sigma T^4}{\pi}(\theta_2 - \theta_1)\dfrac{(\sin^2\beta_2 - \sin^2\beta_1)}{2}\left(F_{0-\lambda_2} - F_{0-\lambda_1}\right)$

</td></tr>
<tr><td>
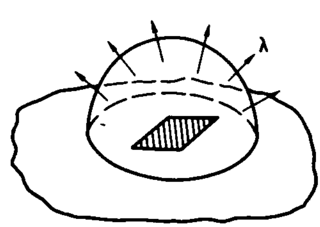

</td><td>

$\pi i'_{\lambda b}$

</td></tr>
</table>

295-763 OL-68—4

TABLE 2-II.—BLACKBODY

Symbol	Name	Definition
$e_{\lambda b}(\lambda_1 - \lambda_2, T)$	Hemispherical band emissive power	Emission in wavelength band $\lambda_1 - \lambda_2$ into hemispherical solid angle per unit surface area and time
$e_b(T)$	Hemispherical total emissive power	Emission, including all wavelengths, into hemispherical solid angle per unit surface area and time

certain fundamental properties that make it a standard with which real radiating bodies can be compared. These properties, listed here for convenience, are the following:

(1) The blackbody is the best possible absorber and emitter of radiant energy at any wavelength and in any direction.

(2) The total radiant intensity and hemispherical total emissive power of a blackbody are given by the Stefan-Boltzmann law:

$$\pi i_b' = e_b = \sigma T^4$$

(3) The blackbody directional spectral and total emissive power follow Lambert's cosine law:

$$e_{\lambda b}'(\lambda, \beta) = e_{\lambda b, n}(\lambda) \cos \beta$$

$$e_b'(\beta) = e_{b, n} \cos \beta$$

(4) The spectral distribution of intensity of a blackbody is given by Planck's distribution:

RADIATION QUANTITIES – Continued

Geometry	Formula
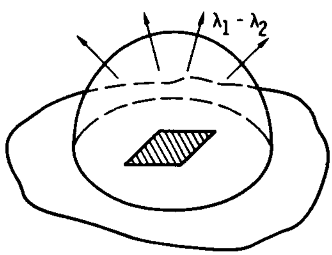	$\sigma T^4(F_{0-\lambda_2} - F_{0-\lambda_1})$
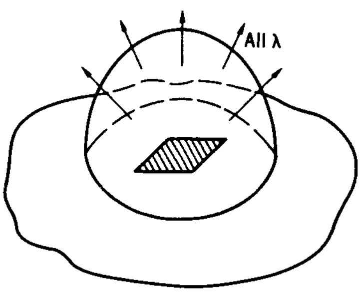	σT^4

$$i'_{\lambda b}(\lambda) = \frac{2C_1}{\lambda^5(e^{C_2/\lambda T} - 1)}$$

(5) The wavelength at which the maximum spectral intensity of radiation for a blackbody occurs is given by Wien's displacement law:

$$\lambda_{max} = \frac{C_3}{T}$$

Because of the many definitions introduced in this chapter, it is convenient to summarize the quantities in tabular form. This has been done in table 2–II. The formulas for the quantities are given in terms of either the spectral intensity $i'_{\lambda b}(\lambda)$, which is computed from Planck's law, or the surface temperature T.

2.7 HISTORICAL DEVELOPMENT

The derivation of the approximate spectral distributions of Wien and of Rayleigh and Jeans, the Stefan-Boltzmann law, and Wien's displacement law are all seen to be logical consequences of the spectral distribution of intensity as derived by Max Planck. However, it is interesting to note that all of these relations were formulated *prior* to publication of Planck's work in 1901 and were originally derived through fairly complex thermodynamic arguments.

Joseph Stefan (ref. 11) proposed in 1879, after study of some experimental results, that emissive power was related to the fourth power of the absolute temperature of a radiating body. Ludwig Edward Boltzmann (ref. 12) was able to derive the same relation in 1884 by analyzing a Carnot cycle in which radiation pressure was assumed to act as the pressure of the working fluid.

Wilhelm Carl Werner Otto Fritz Franz (Willy) Wien (ref. 13) derived the displacement law in 1891 by consideration of a piston moving within a mirrored cylinder. He found that the spectral energy density in an isothermal enclosure and the spectral emissive power of a blackbody are both directly proportional to the fifth power of the absolute temperature when "corresponding wavelengths" are chosen. The relation presented in section 2.4.8 (eq. (2–17)) is more often cited as Wien's displacement law, but is actually a consequence of the previous sentence.

Wien (ref. 14) also derived his spectral distribution of intensity through thermodynamic argument plus assumptions concerning the absorption and emission processes.

Lord Rayleigh (1900) and Sir James Jeans (1905) based their spectral distribution on the assumption that the classical idea of equipartition of energy was valid (refs. 15 and 16).

The fact that measurements and some theoretical considerations [8] indicated Wien's expression for the spectral distribution to be invalid at high temperatures and/or large wavelengths led Planck to an investigation of harmonic oscillators which were assumed to be the emitters and absorbers of radiant energy. Various further assumptions as to the average energy of the oscillators led Planck to derive both the Wien and the Rayleigh-Jeans distributions. Planck finally found an empirical equation which fit the measured energy distributions over the entire spectrum. In determining what modifications to the theory would allow derivation of this empirical equation, he was led to the assumptions which form the basis of the quantum theory. As we have seen, his equation leads directly to all the results derived previously by Wien, Stefan, Boltzmann, Rayleigh, and Jeans.

For an interesting and informative comprehensive review of the history of the field of thermal radiation, the article by Barr (ref. 17) is recommended.

---

[8] It was felt that as temperature approaches large values, the intensity of a blackbody should not approach a finite limit. Examination of Wien's formula (eq. (2–13)) shows that this condition is not met. Planck's distribution law (eq. (2–11)), however, does satisfy the condition.

REFERENCES

1. RICHTMYER, F. K.; AND KENNARD, E. H.: Introduction to Modern Physics. Fourth ed., McGraw-Hill Book Co., Inc., 1947.
2. TER HAAR, D.: Elements of Statistical Mechanics. Second ed., Holt, Rinehart and Winston, Inc., 1960.
3. TRIBUS, MYRON: Thermostatics and Thermodynamics; an Introduction to Energy, Information and States of Matter, with Engineering Applications. D. Van Nostrand Co., Inc., 1961.
4. PLANCK, MAX: Distribution of Energy in the Spectrum. Ann. d. Physik, vol. 4, no. 3, Mar. 1901, pp. 553–563.
5. DRAPER, JOHN W.: On the Production of Light by Heat. Phil. Mag., Ser. 3, vol. 30, 1847, pp. 345–360.
6. DWIGHT, HERBERT B.: Tables of Integrals and Other Mathematical Data. Fourth ed., Macmillan Book Co., 1961, p. 231.
7. PIVOVONSKY, MARK; AND NAGEL, MAX R.: Tables of Blackbody Radiation Functions. Macmillan Book Co., 1961.
8. GARDON, ROBERT: The Emissivity of Transparent Materials. Am. Ceramic Soc. J., vol. 39, no. 8, Aug. 1956, pp. 278–287.
9. GARDON, ROBERT: A Review of Radiant Heat Transfer in Glass. Am. Ceramic Soc. J., vol. 44, no. 7, July 1961, pp. 305–312.
0. KELLETT, B. S.: The Steady Flow of Heat Through Hot Glass. Opt. Soc. Am. J., vol. 42, no. 5, May 1952, pp. 339–343.
11. STEFAN, JOSEPH: Ueber die Beziehung zwischen der Wärmestrahlung und der Temperatur. Sitz. ber. Akad. Wiss. Wien., vol. 79, pt. II, 1879, pp. 391–428.
12. BOLTZMANN, LUDWIG: Ableitung des Stefan'schen Gesetzes, Betreffend die Abhängigkeit der Wärmestrahlung von der Temperatur aus der Electromagnetischen Lichttheorie. Ann. d. Physik, Ser. 2, vol. 22, 1884, pp. 291–294.
13. WIEN, WILLY: Temperatur und Entropie der Strahlung. Ann. d. Physik, Ser. 2, vol. 52, 1894, pp. 132–165.
14. WIEN, WILLY: Ueber die Energievertheilung im Emissionsspectrum eines Schwarzen Körpers. Ann. d. Physik, Ser. 3, vol. 58, 1896, pp. 662–669.
15. LORD RAYLEIGH: The Law of Complete Radiation. Phil. Mag., vol. 49, June 1900, pp. 539–540.
16. JEANS, SIR JAMES: On the Partition of Energy Between Matter and the Ether. Phil. Mag., vol. 10, 1905, pp. 91–97.
17. BARR, E. SCOTT: Historical Survey of the Early Development of the Infrared Spectral Region. Am. J. Phys., vol. 28, no. 1, Jan. 1960, pp. 42–54.

Chapter 3. Definitions of Properties for Nonblack Surfaces

3.1 INTRODUCTION

In chapter 2 the radiative behavior of a blackbody was presented in detail. The ideal behavior of the blackbody serves as a standard with which the performance of real radiating bodies can be compared. The radiative behavior of a real body depends on many factors such as composition, surface finish, temperature, wavelength of the radiation, angle at which radiation is either being emitted or intercepted by the surface, and the spectral distribution of the radiation incident on the surface. Various emissive, absorptive, and reflective properties, both unaveraged and averaged, are used to describe the radiative behavior of real materials relative to blackbody behavior.

The definitions of radiative properties of opaque materials are given in this chapter. To make them of greatest value, the definitions are presented rigorously and in detail. Since the definitions are numerous, the reader should not expect to read the present chapter in as complete detail as the discussion on the blackbody in chapter 2. Rather, some of the alternate forms of defining the same quantity can be briefly scanned to obtain an overall view of what information is available, and the chapter then used as a reference source. The sections have been subdivided and made fairly independent to facilitate use for reference purposes.

The rigorous examination of radiative property definitions arises from the need to properly interpret available property data for use in heat-transfer computations. A limited amount of data in the literature provides detailed directional and spectral measurements. Because of the difficulties in making these detailed measurements, most of the tabulated property values are *averaged* quantities. An averaged radiative performance has been measured for all directions, all wavelengths, or both. A clear understanding of the averages involved can be obtained from the definitions of this chapter. The definitions also reveal relations between various averaged properties in the form of equalities or reciprocity relations. This enables the researcher or engineer to make maximum use of the available property information. Thus, for example, absorptivity data can be obtained from measured emissivity data *if certain restrictions are observed.* These restrictions have often been misunderstood, resulting in confusion or inaccuracy in applying measured properties.

By detailed examination of the derivation of property definitions, the restrictions on the property relations are demonstrated. As an aid to understanding these definitions, figure 3–1 provides a schematic representation of the types of directional properties. The various parts of this figure will be referred to as each definition is introduced to help provide a physical interpretation of the quantities being discussed. Further,

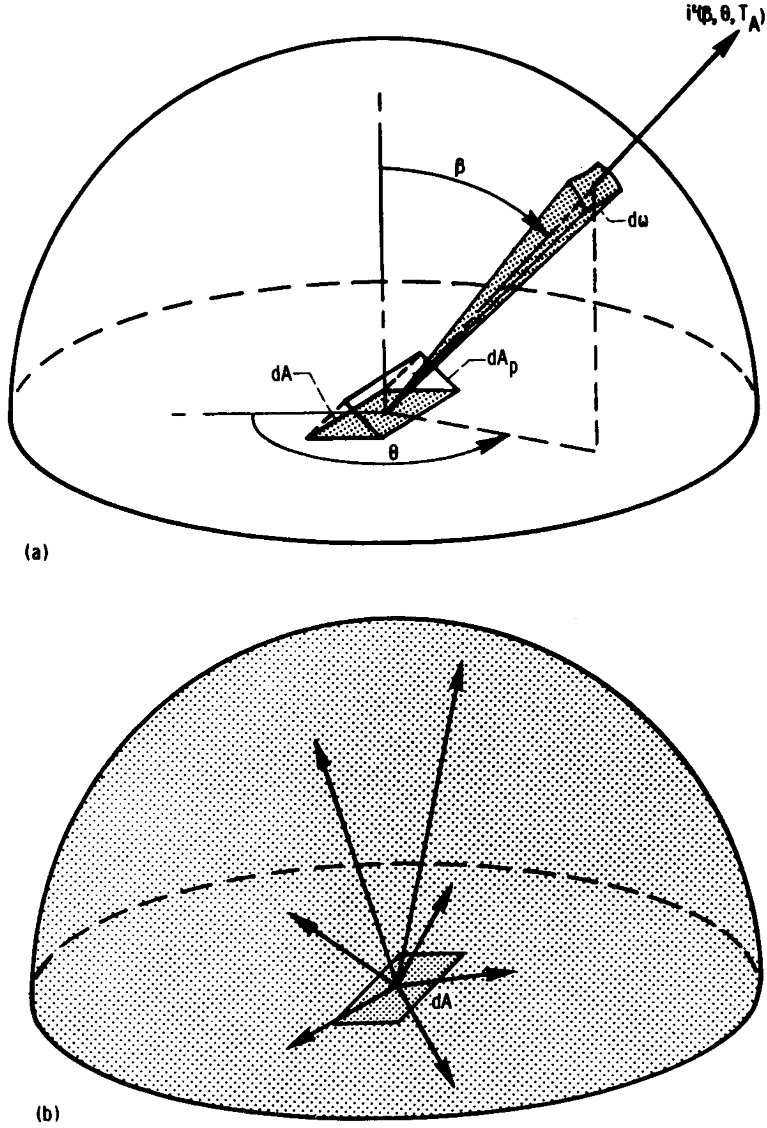

(a) Directional emissivity $\epsilon'(\beta, \theta, T_A)$.
(b) Hemispherical emissivity $\epsilon(T_A)$.

FIGURE 3–1.—Pictorial description of directional and hemispherical radiation properties.

table 3–I lists each of the properties, its symbolic notation, and the equation number of its definition. The notation is described in section 3.1.2.

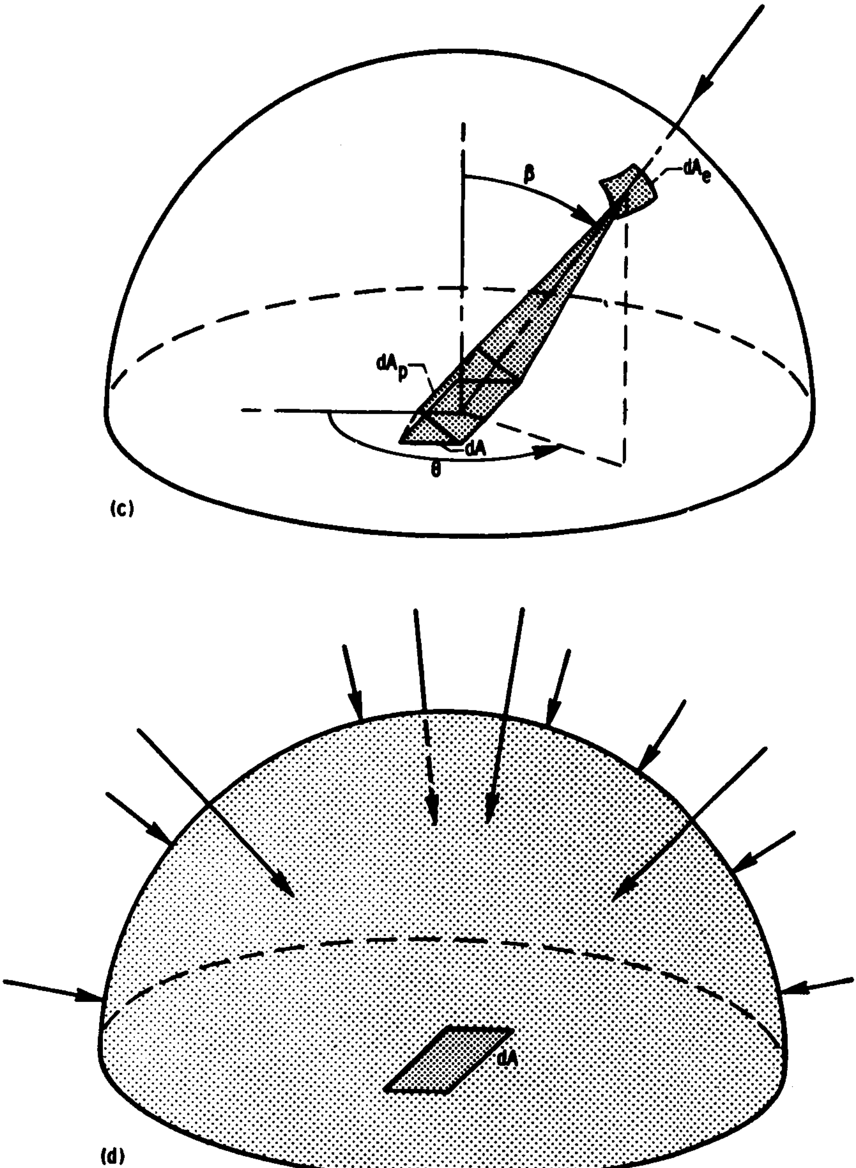

(c) Directional absorptivity $\alpha'(\beta, \theta, T_A)$.
(d) Hemispherical absorptivity $\alpha(T_A)$.

FIGURE 3–1. – Continued.

Measured properties of real materials are given in chapter 5 to demonstrate the practical use of the relations derived here.

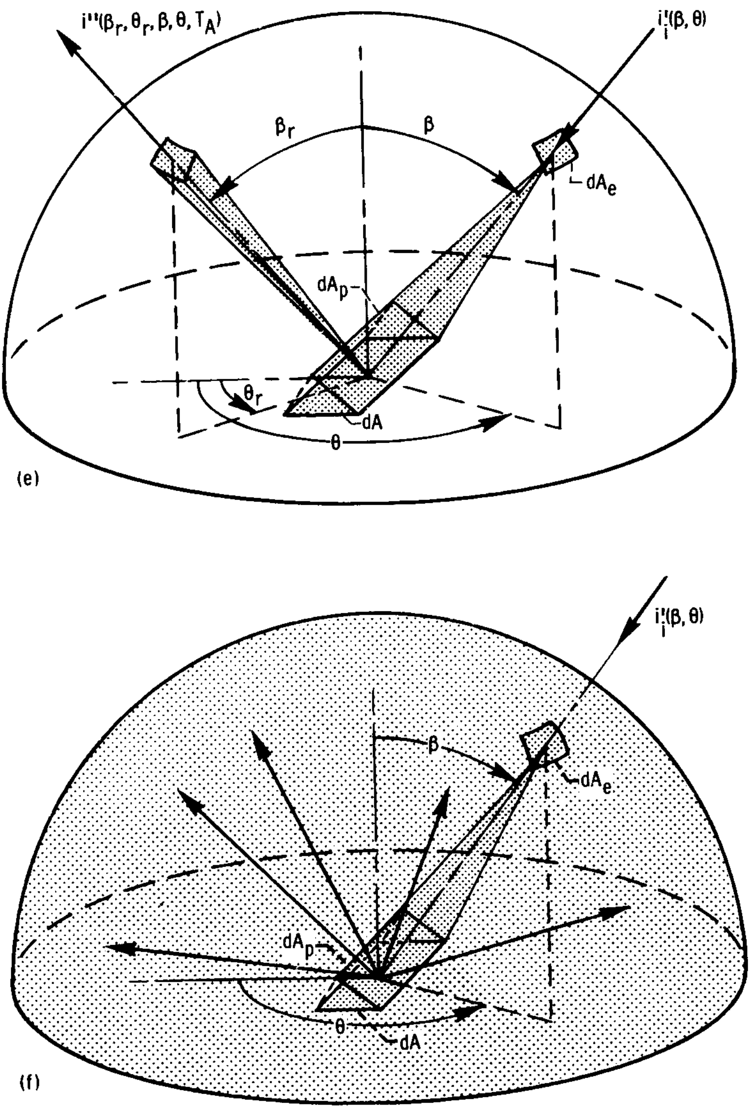

(e) Bidirectional reflectivity $\rho''(\beta_r, \theta_r, \beta, \theta, T_A)$.
(f) Directional-hemispherical reflectivity $\rho'(\beta, \theta, T_A)$.

FIGURE 3–1.—Continued.

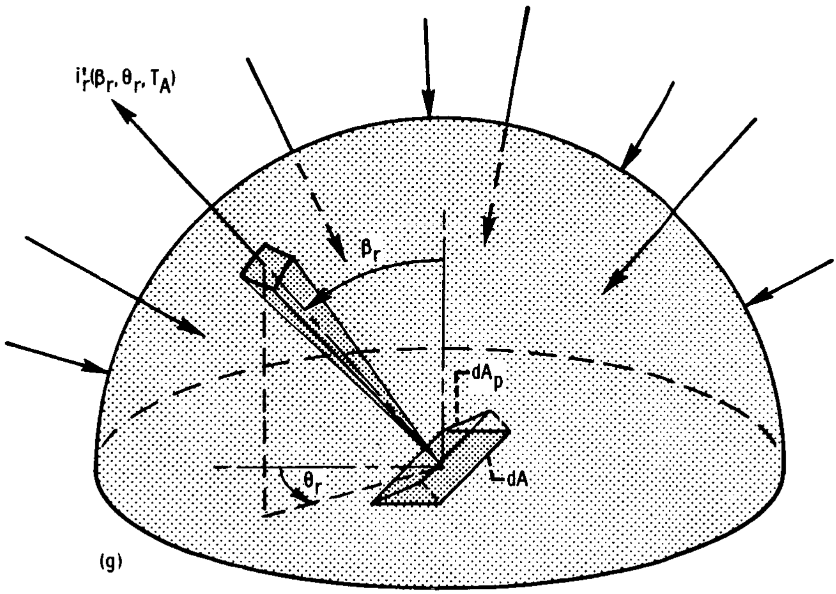

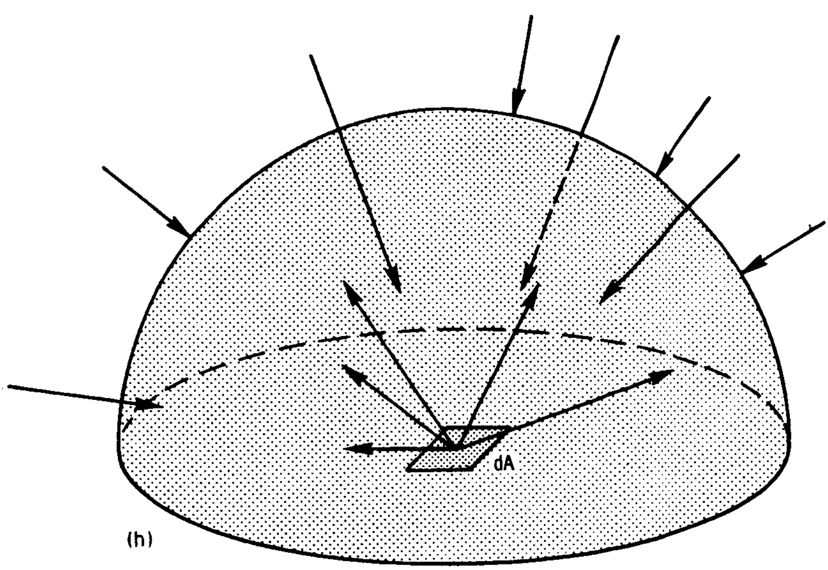

(g) Hemispherical-directional reflectivity $\rho'(\beta_r, \theta_r, T_A)$.
(h) Hemispherical reflectivity $\rho(T_A)$.

FIGURE 3-1.—Concluded.

TABLE 3-I.—SUMMARY OF SURFACE PROPERTY DEFINITIONS

Quantity	Symbol	Defining equation	Descriptive figure
Emissivity			
Directional spectral	ϵ'_λ	3-2	3-1(a)
Directional total	ϵ'	3-3	3-1(a)
Hemispherical spectral	ϵ_λ	3-5	3-1(b)
Hemispherical total	ϵ	3-6	3-1(b)
Absorptivity			
Directional spectral	α'_λ	3-10a	3-1(c)
Directional total	α'	3-14	3-1(c)
Hemispherical spectral	α_λ	3-16	3-1(d)
Hemispherical total	α	3-18	3-1(d)
Reflectivity			
Bidirectional spectral	ρ''_λ	3-20	3-1(e)
Directional-hemispherical spectral	$\rho'_\lambda(\beta, \theta)$	3-24	3-1(f)
Hemispherical-directional spectral	$\rho'_\lambda(\beta_r, \theta_r)$	3-26	3-1(g)
Hemispherical spectral	ρ_λ	3-29	3-1(h)
Bidirectional total	ρ''	3-39	3-1(e)
Directional-hemispherical total	$\rho'(\beta, \theta)$	3-41a	3-1(f)
Hemispherical-directional total	$\rho'(\beta_r, \theta_r)$	3-41b	3-1(g)
Hemispherical total	ρ	3-43	3-1(h)

3.1.1 Nomenclature

A number of suggestions have been made in an effort to standardize the nomenclature of radiation. One controversy centers around the ending "ivity" for the various radiative properties of materials. The National Bureau of Standards is attempting to standardize nomenclature, and in their publications reserve this ending for the properties of an optically smooth substance with an uncontaminated surface (emissivity, reflectivity, etc.), while assigning the "ance" ending (i.e., emittance, reflectance, etc.), to measured properties where there is a need to specify surface conditions.

It is the practice in most fields of science to assign the "ivity" ending to intensive properties of materials, such as in the cases of electrical resistivity, thermal conductivity, or diffusivity. The "ance" ending is reserved, however, for extensive properties of materials as in electrical resistance or conductance. Use of the term "emittance" as defined in the previous paragraph does not follow this convention, since "emittance" would still be an intensive property as long as opaque materials are considered. Further, it seems cumbersome to define two terms for the same concept, using one term to differentiate the one very special case of the perfectly prepared pure substance.

For these reasons, the "ivity" ending will be used throughout this book for the radiative properties of opaque materials whether for ideal uncontaminated surfaces or for properties with some given surface condition. The "ance" ending can then be reserved for an extensive property such as the emittance of a layer of water where the emittance would vary with thickness. The derived relations of course apply regardless of the nomenclature adopted.

It must be noted that the "ance" ending is often found in the literature dealing with the experimental determination of surface properties. The term "emittance" is also used in some references to describe what we have called emissive power.

3.1.2 Notation

Because of the many independent variables that must be specified for radiative properties, a concise but accurate notation is necessary. The notation to be used here is an extension of that introduced in the preceding chapter. A functional notation is used to explicitly give the variables upon which a quantity depends. For example $\epsilon_\lambda'(\lambda, \beta, \theta, T_A)$ shows that ϵ_λ' depends on the four variables noted. The prime denotes a directional quantity, and the λ subscript specifies that the quantity is spectral. Certain quantities depend upon *two* directions (four angles); these will be given a double prime. A hemispherical quantity will not have a prime, and a total quantity will not have a λ subscript. A quantity that is directional in nature, that is, it is evaluated on a "per unit solid angle" basis, will always have a prime even if in a specific case its numerical value is independent of direction; the independence of direction is denoted by the absence of (β, θ) in the functional notation. Similarly a spectral quantity will always have a λ subscript even when in specific cases the numerical value does not vary with wavelength; such a specific case would not have a λ in the functional notation.

Additional notation is needed for the energy rate Q for a finite area in order to keep consistent mathematical forms for energy balances.

Thus, $d^2Q'_\lambda$ denotes as before a directional-spectral quantity, but the second differential is needed to denote that the energy is of differential order in both wavelength and solid angle. Thus, dQ' and dQ_λ are differential quantities with respect to solid angle and wavelength, respectively. If a differential area is involved, the order of the derivative is correspondingly increased.

This notation may appear somewhat redundant, but the usefulness will become clear in dealing with certain special cases, such as gray and diffuse bodies. In addition, the shorthand value of referring to ϵ'_λ in the text rather than writing out the term "directional spectral emissivity" should be apparent. A study of table 3–I will help clarify the notation system being used.

The three main sections of the chapter each deal with a different property, that is, emissivity, absorptivity, and reflectivity. In each of these sections the most basic unaveraged property is presented first; for example, in the first section, the directional spectral emissivity is presented. Then the averaged quantities are obtained by integration. The section on absorptivity also contains forms of Kirchhoff's law relating absorptivity to emissivity. The section on reflectivity includes the reciprocity relations.

3.2 SYMBOLS

A	surface area
C	a coefficient
e	radiative emissive power
F	fraction of blackbody total emissive power
i	radiation intensity
Q	energy rate; energy per unit time
q	energy flux; energy per unit area per unit time
r	distance between emitting and absorbing elements
T	absolute temperature
α	absorptivity
β	cone angle measured from normal of surface
θ	circumferential angle
ϵ	emissivity
λ	wavelength
ρ	reflectivity
σ	Stefan-Boltzmann constant, table IV of the appendix
ω	solid angle
$\int_\Delta$	integration over solid angle of entire enclosing hemisphere

Subscripts:

A	of surface A
a	absorbed
b	blackbody
d	diffuse
e	emitted or emitting
i	incident
p	projected
r	reflected
s	specular
λ	spectrally dependent

Superscripts:

$'$	directional
$''$	bidirectional

3.3 EMISSIVITY

The *emissivity* is a measure of how well a body can radiate energy as compared with a blackbody. The emitting ability can depend on factors such as body temperature, the particular wavelength being considered for the emitted energy, and angle at which the energy is being emitted. The emissivity is usually measured experimentally at a direction normal to the surface and as a function of wavelength. In calculating energy loss by a body, the emission into all directions is required, and for such a calculation an emissivity is needed that is averaged over all directions and wavelengths. For radiant interchange between surfaces, emissivities averaged over wavelength but not direction might be needed; in other cases, when spectral effects become large, spectral values averaged only over direction are used. Thus, various averaged emissivities may be required by the analyst, and they must often be obtained from available measured values.

In this section, the basic derivation of the directional spectral emissivity is given. This emissivity is then averaged in turn with respect to wavelength, direction, and then wavelength and direction simultaneously.

Values averaged with respect to wavelength are termed "total" quantities; averages with respect to direction are termed "hemispherical" quantities. This convention will be adhered to throughout this publication.

3.3.1 Directional Spectral Emissivity $\epsilon'_\lambda(\lambda, \beta, \theta, T_A)$

Consider the geometry for emitted radiation shown in figure 3–1(a). As discussed in chapter 2 the radiation intensity is the energy per unit time emitted in direction (β, θ) per unit of the *projected* area dA_p *normal* to this direction, per unit solid angle and per unit wavelength band. In some texts the intensity has been defined relative to the actual surface area rather than the projected value. By basing the intensity on the projected area as is done here, there is the advantage that for a black surface the intensity has the same value for all directions. Unlike the intensity from a blackbody, the emission from a real body *does* depend on direction and hence the (β, θ) designation is included in the notation for intensity. The *energy* leaving a real surface dA of temperature T_A, per unit time in the wavelength interval $d\lambda$ and within the solid angle $d\omega$, is then given by

$$d^3Q'_\lambda(\lambda, \beta, \theta, T_A) = i'_\lambda(\lambda, \beta, \theta, T_A)dA \cos\beta \, d\lambda d\omega = e'_\lambda(\lambda, \beta, \theta, T_A)dA d\lambda d\omega \tag{3-1a}$$

For a blackbody the intensity is independent of direction and was designated in chapter 2 by $i'_{\lambda b}(\lambda)$. The T_A notation is introduced here to clarify when properties are temperature dependent so that the blackbody intensity is designated as $i'_{\lambda b}(\lambda, T_A)$. The energy leaving a black area element per unit time within $d\lambda$ and $d\omega$ is

$$d^3Q'_{\lambda b}(\lambda, \beta, T_A) = i'_{\lambda b}(\lambda, T_A)dA \cos\beta \, d\lambda d\omega = e'_{\lambda b}(\lambda, \beta, T_A)dA d\lambda d\omega \tag{3-1b}$$

The emissivity is then defined as the ratio of the emissive ability of the real surface to that of a blackbody; this provides the definition

$$\textit{Directional spectral emissivity} \equiv \epsilon'_\lambda(\lambda, \beta, \theta, T_A) = \frac{d^3Q'_\lambda(\lambda, \beta, \theta, T_A)}{d^3Q'_{\lambda b}(\lambda, \beta, T_A)}$$

$$= \frac{i'_\lambda(\lambda, \beta, \theta, T_A)}{i'_{\lambda b}(\lambda, T_A)} = \frac{e'_\lambda(\lambda, \beta, \theta, T_A)}{e'_{\lambda b}(\lambda, \beta, T_A)} \tag{3-2}$$

This is the most fundamental emissivity, because it includes the dependence on wavelength, direction, and surface temperature.

EXAMPLE 3–1: At 60° from the normal, a surface heated to 1500° R has a directional spectral emissivity of 0.70 at a wavelength of 5 μm. The emissivity is isotropic with respect to the angle θ. What is the spectral intensity in this direction?

From table V of the appendix, for a blackbody at λT_A of 7500 (μm)(°R),

$e_{\lambda b}(\lambda, T_A)/T_A^5 = 163.5 \times 10^{-15}$ Btu/(hr)(sq ft)(μm)(°R). Then

$$i'_\lambda(5\ \mu\text{m}, 60°, 1500°\ \text{R}) = \epsilon'_\lambda(5\ \mu\text{m}, 60°, 1500°\ \text{R})\, i'_{\lambda b}(5\ \mu\text{m}, 1500°\ \text{R})$$

$$= \epsilon'_\lambda(5\ \mu\text{m}, 60°, 1500°\ \text{R})\, \frac{e_{\lambda b}}{\pi}(5\ \mu\text{m}, 1500°\ \text{R})$$

$$= 0.70 \times \frac{163.5 \times 10^{-15}}{\pi}(1500)^5 = 276\ \text{Btu/(hr)(sq ft)}(\mu\text{m})(\text{sr})$$

3.3.2 Averaged Emissivities

From the directional spectral emissivity as given in equation (3–2), an averaged emissivity can now be derived by proceeding along one of two approaches: averaging over all wavelengths or averaging over all directions.

3.3.2.1 *Directional total emissivity* $\epsilon'(\beta, \theta, T_A)$.—Looking first at an average over all wavelengths, the radiation emitted into direction (β, θ), including the contributions from all wavelengths, is found by integrating the directional spectral emissive power to give the *directional total emissive power* (as in chapter 2 the term "total" denotes that radiation from all wavelengths is included)

$$e'(\beta, \theta, T_A) = \int_0^\infty e'_\lambda(\lambda, \beta, \theta, T_A)\, d\lambda$$

Similarly from table 2–II the directional total emissive power for a *blackbody* is given by

$$e'_b(\beta, T_A) = \int_0^\infty e_{\lambda b}(\lambda, \beta, T_A)\, d\lambda = \frac{\sigma T_A^4 \cos\beta}{\pi}$$

The directional total emissivity is the ratio of $e'(\beta, \theta, T_A)$ for the real surface to $e'_b(\beta, T_A)$ emitted by a blackbody at the same temperature; that is,

$$\textit{Directional total emissivity} \equiv \epsilon'(\beta, \theta, T_A) = \frac{e'(\beta, \theta, T_A)}{e'_b(\beta, T_A)}$$

$$= \frac{\int_0^\infty e'_\lambda(\lambda, \beta, \theta, T_A)\, d\lambda}{\frac{\sigma T_A^4}{\pi}\cos\beta} \tag{3–3a}$$

The $e'_\lambda(\lambda, \beta, \theta, T_A)$ in the numerator can be replaced in terms of $\epsilon'_\lambda(\lambda, \beta, \theta, T_A)$ by using equation (3–2) to give

Directional total emissivity (in terms of directional spectral emissivity) $\equiv \epsilon'(\beta, \theta, T_A)$

$$= \frac{\int_0^\infty \epsilon'_\lambda(\lambda, \beta, \theta, T_A) e'_{\lambda b}(\lambda, \beta, T_A) d\lambda}{\frac{\sigma T_A^4}{\pi} \cos \beta}$$

$$= \frac{\pi \int_0^\infty \epsilon'_\lambda(\lambda, \beta, \theta, T_A) i'_{\lambda b}(\lambda, T_A) d\lambda}{\sigma T_A^4} \tag{3-3b}$$

Thus if the wavelength dependence of $\epsilon'_\lambda(\lambda, \beta, \theta, T_A)$ is known, the $\epsilon'(\beta, \theta, T_A)$ is obtained as an integrated average weighted by the blackbody emissive power. The $\epsilon'_\lambda(\lambda, \beta, \theta, T_A)$ must be known with good accuracy in the region where $e'_{\lambda b}(\lambda, \beta, T_A)$ is large, so that the integrand of equation (3–3b) will be accurate where it has large values.

EXAMPLE 3–2: At 1000° R the $\epsilon'_\lambda(\lambda, \beta, \theta, T_A)$ can be approximated by 0.8 in the range $\lambda = 0$ to 5 μm and 0.4 for $\lambda > 5$ μm. What is the value of $\epsilon'(\beta, \theta, T_A)$?

From equation (3–3b),

$$\epsilon'(\beta, \theta, T_A) = \frac{\int_0^\infty \epsilon'_\lambda(\lambda, \beta, \theta, T_A) e'_{\lambda b}(\lambda, \beta, T_A) d\lambda}{\frac{\sigma T_A^4}{\pi} \cos \beta}$$

Apply the following relation obtained from table 2–II:

$$e'_{\lambda b}(\lambda, \beta, T_A) = \frac{e_{\lambda b}(\lambda, T_A) \cos \beta}{\pi}$$

This yields

$$\epsilon'(\beta, \theta, T_A) = \int_0^{5T_A} \frac{0.8}{\sigma} \left[\frac{e_{\lambda b}(\lambda, T_A)}{T_A^5}\right] d(\lambda T_A) + \int_{5T_A}^\infty \left[\frac{0.4}{\sigma} \frac{e_{\lambda b}(\lambda, T_A)}{T_A^5}\right] d(\lambda T_A)$$

From equation (2–27),

$$\epsilon'(\beta, \theta, T_A) = 0.8\ F_{0-5000} + 0.4\ F_{5000-\infty} = 0.8(0.223) + 0.4(0.777) = 0.490$$

Since 77.7 percent of the emitted blackbody energy at 1000° R is in the region for $\lambda > 5\ \mu m$, the result is weighted heavily toward the 0.4 emissivity value.

3.3.2.2 *Hemispherical spectral emissivity* $\epsilon_\lambda(\lambda, T_A)$.—Now return to equation (3–2) and consider the average obtained by integrating the directional spectral quantities over all directions of a hemispherical envelope covering the surface (fig. 3–1(b)). The spectral radiation emitted by a unit surface area into all directions of the hemisphere is termed the *hemispherical spectral emissive power* and is found by integrating the spectral energy per unit solid angle over all solid angles. This is analogous to equation (2–8a) for a blackbody and is given by

$$e_\lambda(\lambda, T_A) = \int_{\frown} i'_\lambda(\lambda, \beta, \theta, T_A) \cos \beta\, d\omega$$

The notation $\int_{\frown} d\omega$ signifies integration over the hemispherical solid angle. Here, $i'_\lambda(\lambda, \beta, \theta, T_A)$ cannot in general be removed from under the integral sign as was done for a blackbody. By using equation (3–2) this can be written as

$$e_\lambda(\lambda, T_A) = i'_{\lambda b}(\lambda, T_A) \int_{\frown} \epsilon'_\lambda(\lambda, \beta, \theta, T_A) \cos \beta\, d\omega \qquad (3\text{–}4a)$$

For a blackbody the hemispherical spectral emissive power is from equation (2–8b)

$$e_{\lambda b}(\lambda, T_A) = \pi i'_{\lambda b}(\lambda, T_A) \qquad (3\text{–}4b)$$

The ratio of actual to blackbody emission from the surface (eq. (3–4a) divided by eq. (3–4b)) provides the following definition:

Hemispherical spectral emissivity (in terms of directional spectral emissivity $\equiv \epsilon_\lambda(\lambda, T_A)$

$$= \frac{e_\lambda(\lambda, T_A)}{e_{\lambda b}(\lambda, T_A)} = \frac{1}{\pi} \int_{\frown} \epsilon'_\lambda(\lambda, \beta, \theta, T_A) \cos \beta\, d\omega \qquad (3\text{–}5)$$

3.3.2.3 *Hemispherical total emissivity* $\epsilon(T_A)$.—To derive the hemispherical total emissivity, consider that from a unit area the spectral emissive power in any direction is derived from equation (3–2) as $\epsilon'_\lambda(\lambda, \beta, \theta, T_A)i'_{\lambda b}(\lambda, T_A) \cos \beta$. This is integrated over all λ and ω to give the *hemispherical total emissive power.* Dividing by σT_A^4, which is the hemispherical total emissive power for a blackbody, results in the following emissivity:

Hemispherical total emissivity (in terms of directional spectral emissivity $\equiv \epsilon(T_A)$

$$= \frac{e(T_A)}{e_b(T_A)} = \frac{\int_\cap \left[\int_0^\infty e'_\lambda(\lambda, \beta, \theta, T_A)\, d\lambda\right] d\omega}{\sigma T_A^4}$$

$$= \frac{\int_\cap \left[\int_0^\infty \epsilon'_\lambda(\lambda, \beta, \theta, T_A) i'_{\lambda b}(\lambda, T_A)\, d\lambda\right] \cos \beta \, d\omega}{\sigma T_A^4} \qquad \text{(3–6a)}$$

By using equation (3–3b) this can be placed in a second form

Hemispherical total emissivity (in terms of directional total emissivity) $\equiv \epsilon(T_A)$

$$= \frac{1}{\pi} \int_\cap \epsilon'(\beta, \theta, T_A) \cos \beta \, d\omega \qquad \text{(3–6b)}$$

If the order of the integrations is interchanged in equation (3–6a), there results

$$\epsilon(T_A) = \frac{\int_0^\infty i'_{\lambda b}(\lambda, T_A) \left[\int_\cap \epsilon'_\lambda(\lambda, \beta, \theta, T_A) \cos \beta \, d\omega\right] d\lambda}{\sigma T_A^4}$$

Equation (3–5) is then utilized to obtain a third form

Hemispherical total emissivity (in terms of hemispherical spectral emissivity) $\equiv \epsilon(T_A)$

$$= \frac{\pi \int_0^\infty \epsilon_\lambda(\lambda, T_A) i'_{\lambda b}(\lambda, T_A)\, d\lambda}{\sigma T_A^4} \qquad \text{(3–6c)}$$

Substituting equation (3–4b) gives

$$\epsilon(T_A)=\frac{\int_0^\infty \epsilon_\lambda(\lambda, T_A)e_{\lambda b}(\lambda, T_A)\,d\lambda}{\sigma T_A^4} \tag{3-6d}$$

To interpret equation (3–6d) physically, look at figure 3–2. In figure 3–2(a) is shown the emissivity ϵ_λ for a surface temperature T_A. The solid curve in figure 3–2(b) is the hemispherical spectral emissive power for a blackbody at T_A. The area under the solid curve is σT_A^4 which is the denominator of equation (3–6d) and is equal to the radiation emitted per unit area by a black surface including all wavelengths and directions.

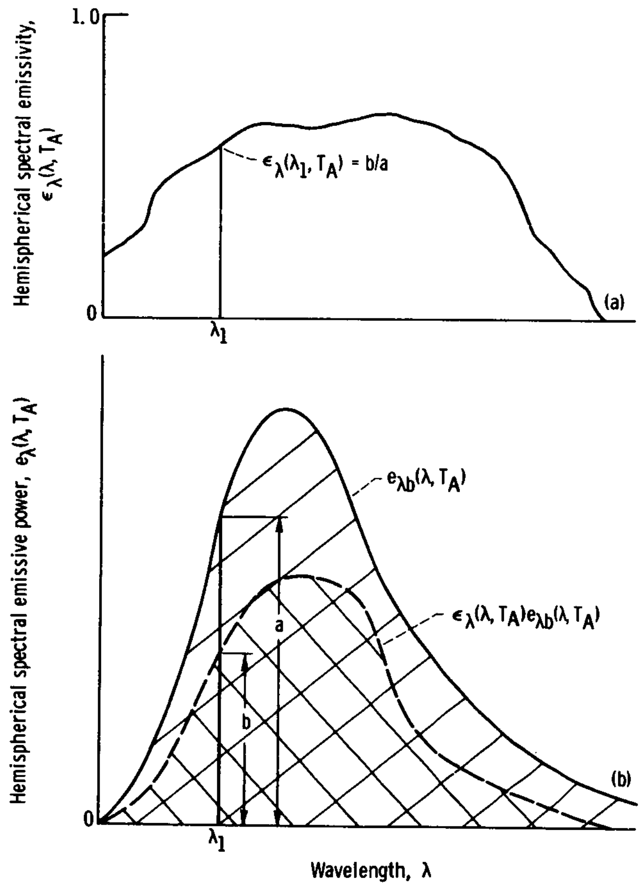

(a) Measured emissivity values.
(b) Interpretation of emissivity as ratio of actual emissive power to blackbody emissive power.

FIGURE 3–2.—Physical interpretation of hemispherical spectral and total emissivities.

The dashed curve in figure 3–2(b) is the product $\epsilon_\lambda(\lambda, T_A)e_{\lambda b}(\lambda, T_A)$ and the area under this curve is the integral in the numerator of equation (3–6d) which is the emission from the real surface. Hence $\epsilon(T_A)$ is the ratio of the area under the dashed curve to that under the solid curve. From a slightly different viewpoint, at each λ the quantity ϵ_λ is the ordinate of the dashed curve divided by the ordinate of the solid curve. As shown in figure 3–2, for λ_1 the hemispherical spectral emissivity is $\epsilon_\lambda(\lambda_1, T_A) = b/a$.

EXAMPLE 3–3: A surface at 1800° R is isotropic in the sense that ϵ' is independent of θ, but depends on β as shown in figure 3–3. What is the hemispherical total emissivity and the hemispherical total emissive power?

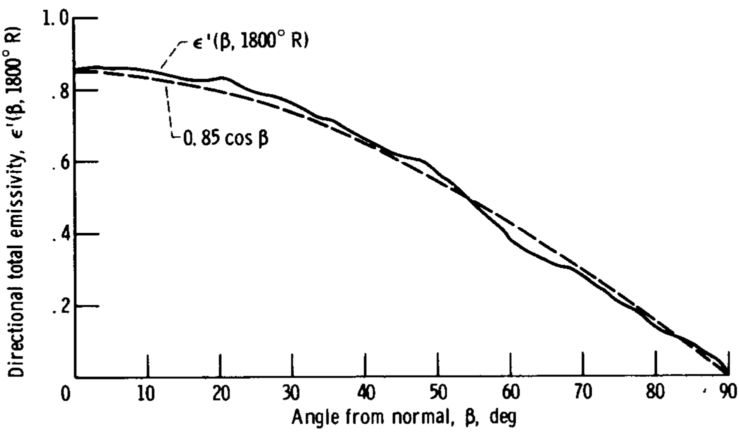

FIGURE 3–3.—Directional total emissivity at 1800° R for example 3–3.

The $\epsilon'(\beta, 1800° \text{ R})$ can be approximated in this case quite well by the function 0.85 cos β (dashed line). Then from equation (3–6b) the hemispherical total emissivity is

$$\epsilon(T_A) = \frac{1}{\pi}\int_{\theta=0}^{2\pi}\int_{\beta=0}^{\pi/2} 0.85 \sin\beta\cos^2\beta\, d\beta d\theta = -1.70\left(\frac{\cos^3\beta}{3}\right)\Bigg|_0^{\pi/2} = 0.57$$

The hemispherical total emissive power is then

$$e(T_A) = \epsilon(T_A)\sigma T_A^4 = 0.57 \times 0.173 \times 10^{-8} \times 1800^4 = 10\,300 \text{ Btu/(hr)(sq ft)}$$

Generally the $\epsilon'(\beta, T_A)$ will not be well approximated by a convenient analytical function, and the integration must be carried out numerically.

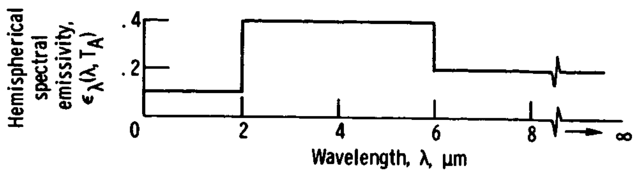

FIGURE 3–4. – Hemispherical spectral emissivity for example 3–4. Surface temperature T_A, 2000° R.

EXAMPLE 3–4: The $\epsilon_\lambda(\lambda, T_A)$ for a surface at $T_A = 2000°$ R can be approximated as shown in figure 3–4. What is the hemispherical total emissivity and the hemispherical total emissive power of the surface?

From equation (3–6d)

$$\epsilon(T_A) = \frac{1}{\sigma T_A^4}\int_0^\infty \epsilon_\lambda(\lambda, T_A) e_{\lambda b}(\lambda, T_A)\, d\lambda = \frac{1}{\sigma}\int_0^2 0.1\frac{e_{\lambda b}(\lambda, T_A)}{T_A^5} T_A\, d\lambda$$
$$+\frac{1}{\sigma}\int_2^6 0.4\frac{e_{\lambda b}(\lambda, T_A)}{T_A^5} T_A\, d\lambda + \frac{1}{\sigma}\int_6^\infty 0.2\frac{e_{\lambda b}(\lambda, T_A)}{T_A^5} T_A\, d\lambda$$

This yields

$$\epsilon(T_A) = \frac{0.1}{\sigma}\int_0^{4000}\frac{e_{\lambda b}}{T_A^5}\, d(\lambda T_A) + \frac{0.4}{\sigma}\int_{4000}^{12\,000}\frac{e_{\lambda b}}{T_A^5}\, d(\lambda T_A)$$
$$+\frac{0.2}{\sigma}\int_{12\,000}^\infty \frac{e_{\lambda b}}{T_A^5}\, d(\lambda T_A)$$

where the quantity $e_{\lambda b}/T_A^5$ is a function of λT_A. From equation (2–27) this can be written as

$$\epsilon(T_A) = 0.1F_{0-4000} + 0.4(F_{0-12\,000} - F_{0-4000}) + 0.2(1 - F_{0-12\,000})$$

$$= -0.3F_{0-4000} + 0.2F_{0-12\,000} + 0.2$$

$$= -0.3(0.1051) + 0.2(0.7877) + 0.2 = 0.3260$$

The hemispherical total emissive power is

$$e(T_A) = \epsilon(T_A)\sigma T_A^4 = 0.326 \times 0.173 \times 10^{-8}(2000)^4 = 9020 \text{ Btu/(hr)(sq ft)}.$$

3.4 ABSORPTIVITY

The absorptivity is defined as the fraction of the energy incident on a body that is absorbed by the body. The incident radiation is the result of the radiative conditions at the *source* of the incident energy. The spectral distribution of the incident radiation is independent of the temperature or physical nature of the absorbing element (unless the radiation emitted from the surface is partially reflected back to the surface). Compared with emissivity, additional complexities are introduced into the absorptivity because the directional and spectral characteristics of the incident radiation must now be accounted for.

Experimentally it is often easier to measure the emissivity than the absorptivity; hence, it is desirable to have relations between these two quantities so that measured values of one will allow the other to be calculated. Such relations are developed in this section along with the definitions of the absorptivity quantities.

3.4.1 Directional Spectral Absorptivity $\alpha'_\lambda(\lambda, \beta, \theta, T_A)$

Figure 3–1(c) illustrates the energy incident on a surface element dA from the (β, θ) direction. The line from dA in direction (β, θ) passes normally through an area element dA_e on the surface of a hemisphere of radius r placed over dA. The incident spectral intensity passing through dA_e is $i'_{\lambda,i}(\lambda, \beta, \theta)$. This is the energy per unit area of the hemisphere, per unit incident solid angle (the shaded solid angle in fig. 3–1(c)), per unit time, and per unit wavelength interval. The energy within the incident solid angle strikes the area dA of the absorbing surface. The fraction of this incident energy that is absorbed is defined as the *directional spectral absorptivity* $\alpha'_\lambda(\lambda, \beta, \theta, T_A)$. In addition to depending on the wavelength and direction of the incident radiation, the spectral absorptivity is a function of the absorbing surface temperature. The energy per unit time incident from direction (β, θ) in the wavelength interval $d\lambda$ is

$$d^3Q'_{\lambda,i}(\lambda, \beta, \theta) = i'_{\lambda,i}(\lambda, \beta, \theta)\, dA_e \frac{dA \cos\beta}{r^2}\, d\lambda \qquad (3\text{–}7)$$

where $dA \cos \beta/r^2$ is the solid angle subtended by dA when viewed from dA_e. Note that

$$\frac{dA \cos\beta}{r^2} dA_e = \frac{dA_e}{r^2} \cos\beta\, dA = d\omega \cos\beta\, dA \qquad (3\text{–}8)$$

where $d\omega$ is the solid angle subtended by dA_e when viewed from dA located at the center of the base of the hemisphere (fig. 3-1(c)). Equation (3-8) will be used in many of the derivations that follow. Equation (3-7) can then be written as

$$d^3Q'_{\lambda,i}(\lambda,\beta,\theta)=i'_{\lambda,i}(\lambda,\beta,\theta)\,d\omega\cos\beta\,dA\,d\lambda \tag{3-9}$$

The amount of the incident energy $d^3Q'_{\lambda,i}$ that is absorbed is designated as $d^3Q'_{\lambda,a}$. Then the ratio is formed

$$\textit{Directional spectral absorptivity} \equiv \alpha'_\lambda(\lambda,\beta,\theta,T_A)=\frac{d^3Q'_{\lambda,a}(\lambda,\beta,\theta,T_A)}{d^3Q'_{\lambda,i}(\lambda,\beta,\theta)}$$

$$=\frac{d^3Q'_{\lambda,a}(\lambda,\beta,\theta,T_A)}{i'_{\lambda,i}(\lambda,\beta,\theta)\,dA\cos\beta\,d\omega d\lambda} \tag{3-10a}$$

If the incident energy is from black surroundings at uniform temperature T_b, then there is the special case

$$\alpha'_\lambda(\lambda,\beta,\theta,T_A)=\frac{d^3Q'_{\lambda,a}(\lambda,\beta,\theta,T_A)}{i'_{\lambda b,i}(\lambda,T_b)\,dA\cos\beta\,d\omega d\lambda} \tag{3-10b}$$

3.4.2 Kirchhoff's Law

This law is concerned with the relation between the emitting and absorbing abilities of a body. The law can have various conditions imposed on it depending on whether spectral, total, directional, or hemispherical quantities are being considered. From equations (3-1) and (3-2) the energy emitted per unit time by an element dA in a wavelength interval $d\lambda$ and solid angle $d\omega$ is

$$d^3Q'_{\lambda,e}=i'_\lambda(\lambda,\beta,\theta,T_A)\,dA\cos\beta\,d\omega d\lambda$$

$$=\epsilon'_\lambda(\lambda,\beta,\theta,T_A)i'_{\lambda b}(\lambda,T_A)\,dA\cos\beta\,d\omega d\lambda \tag{3-11}$$

If the element dA at temperature T_A is assumed to be placed in an isothermal black enclosure also at temperature T_A, then the intensity of the energy incident on dA from the direction (β,θ) (recalling the isotropy of intensity in a black enclosure) will be $i'_{\lambda b}(\lambda, T_A)$. To maintain the isotropy of the radiation within the black enclosure, the absorbed and emitted energies given by equations (3-10b) and (3-11) must be equal.

Equating these gives

$$\epsilon'_\lambda(\lambda, \beta, \theta, T_A) = \alpha'_\lambda(\lambda, \beta, \theta, T_A) \tag{3-12}$$

This equality is a fixed relation between the properties of the material and holds without restriction. This is the most *general form of Kirchhoff's law.*[9]

3.4.3 Directional Total Absorptivity $\alpha'(\beta, \theta, T_A)$

The directional total absorptivity is the ratio of the energy including all wavelengths that is absorbed from a given direction to the energy incident from that direction. The total energy incident from the given direction is obtained by integrating the spectral incident energy (eq. (3–9)) over all wavelengths to obtain

$$d^2Q'_i(\beta, \theta) = \cos\beta \, dA d\omega \int_0^\infty i'_{\lambda, i}(\lambda, \beta, \theta) d\lambda \tag{3-13a}$$

The radiation absorbed is determined by integrating equation (3–10a) over all wavelengths, that is,

$$d^2Q'_a(\beta, \theta, T_A) = \cos\beta \, dA d\omega \int_0^\infty \alpha'_\lambda(\lambda, \beta, \theta, T_A) i'_{\lambda, i}(\lambda, \beta, \theta) d\lambda \tag{3-13b}$$

The following ratio is then formed:

$$\textit{Directional total absorptivity} \equiv \alpha'(\beta, \theta, T_A) = \frac{d^2Q'_a(\beta, \theta, T_A)}{d^2Q'_i(\beta, \theta)}$$

$$= \frac{\int_0^\infty \alpha'_\lambda(\lambda, \beta, \theta, T_A) i'_{\lambda, i}(\lambda, \beta, \theta) d\lambda}{\int_0^\infty i'_{\lambda, i}(\lambda, \beta, \theta) d\lambda} \tag{3-14a}$$

By use of Kirchhoff's law (eq. (3–12)) an alternate form of equation (3–14a) is

[9] As will be discussed in chapter 4 in connection with radiation properties of electrical conductors, radiation is polarized in the sense of having two wave components vibrating at right angles to each other and to the propagation direction. For the special case of black radiation the two components of polarization are equal. To be strictly accurate, equation (3–12) holds only for each component of polarization; and for equation (3–12) to be valid as written for all incident energy, the incident radiation must be polarized into equal components.

$$\alpha'(\beta, \theta, T_A) = \frac{\int_0^\infty \epsilon'_\lambda(\lambda, \beta, \theta, T_A) i'_{\lambda, i}(\lambda, \beta, \theta) d\lambda}{\int_0^\infty i'_{\lambda, i}(\lambda, \beta, \theta) d\lambda} \tag{3–14b}$$

3.4.4 Kirchhoff's Law for Directional Total Properties

The general form of Kirchhoff's law (eq. 3–12) shows that ϵ'_λ and α'_λ are equal. It is now of interest to examine this equality for the directional total quantities. This can be accomplished by comparing a special case of equation (3–14b) with equation (3–3b). If in equation (3–14b) the incident radiation has a spectral distribution proportional to that of a blackbody at T_A, then $i'_{\lambda, i}(\lambda, \beta, \theta) = C(\beta, \theta) i'_{\lambda b}(\lambda, T_A)$ and equation (3–14b) becomes

$$\alpha'(\beta, \theta, T_A) = \frac{\int_0^\infty \epsilon'_\lambda(\lambda, \beta, \theta, T_A) i'_{\lambda b}(\lambda, T_A) d\lambda}{\int_0^\infty i'_{\lambda b}(\lambda, T_A) d\lambda \left(= \frac{\sigma T_A^4}{\pi} \right)} = \epsilon'(\beta, \theta, T_A)$$

Hence when ϵ'_λ *and* α'_λ *are dependent on wavelength,* $\alpha'(\beta, \theta, T_A) = \epsilon'(\beta, \theta, T_A)$ *only when the incident radiation meets the restriction* $i'_{\lambda, i}(\lambda, \beta, \theta) = C(\beta, \theta) i'_{\lambda b}(\lambda, T_A)$ *where* C *is independent of wavelength.*

There is another important case when the relation $\alpha'(\beta, \theta, T_A) = \epsilon'(\beta, \theta, T_A)$ is valid. If the directional emission from a surface has the same wavelength dependence as a blackbody, $i'_\lambda(\lambda, \beta, \theta, T_A) = C(\beta, \theta) i'_{\lambda b}(\lambda, T_A)$, then the ϵ'_λ is independent of λ. From equations (3–3b) and (3–14b) if $\epsilon'_\lambda(\beta, \theta, T_A)$ and hence $\alpha'_\lambda(\beta, \theta, T_A)$ do not depend on λ, then, for the direction (β, θ), ϵ'_λ, α'_λ, ϵ', and α' are all equal. A surface exhibiting such behavior is termed a *directional gray* surface.

3.4.5 Hemispherical Spectral Absorptivity $\alpha_\lambda(\lambda, T_A)$

The hemispherical spectral absorptivity is the fraction of the spectral energy that is absorbed from the spectral energy incident from all directions over a surrounding hemisphere (fig. 3–1(d)). The spectral energy from an element dA_e on the hemisphere that is intercepted by a surface element dA is given by equation (3–9). The incident energy on dA from all directions of the hemisphere is then given by the integral

$$d^2Q_{\lambda, i} = dA d\lambda \int_\Omega i'_{\lambda, i}(\lambda, \beta, \theta) \cos\beta \, d\omega \tag{3–15a}$$

The amount absorbed is found by integrating equation (3–10a) over the hemisphere

$$d^2Q_{\lambda,a} = dA\,d\lambda \int_\Omega \alpha'_\lambda(\lambda, \beta, \theta, T_A)\, i'_{\lambda,i}(\lambda, \beta, \theta) \cos\beta\, d\omega \tag{3–15b}$$

The ratio of these quantities gives

Hemispherical spectral absorptivity $\equiv \alpha_\lambda(\lambda, T_A)$

$$= \frac{d^2Q_{\lambda,a}}{d^2Q_{\lambda,i}} = \frac{\int_\Omega \alpha'_\lambda(\lambda, \beta, \theta, T_A)\, i'_{\lambda,i}(\lambda, \beta, \theta) \cos\beta\, d\omega}{\int_\Omega i'_{\lambda,i}(\lambda, \beta, \theta) \cos\beta\, d\omega} \tag{3–16a}$$

or by using Kirchhoff's law

$$\alpha_\lambda(\lambda, T_A) = \frac{\int_\Omega \epsilon'_\lambda(\lambda, \beta, \theta, T_A)\, i'_{\lambda,i}(\lambda, \beta, \theta) \cos\beta\, d\omega}{\int_\Omega i'_{\lambda,i}(\lambda, \beta, \theta) \cos\beta\, d\omega} \tag{3–16b}$$

The hemispherical spectral absorptivity and emissivity can now be compared by looking at equations (3–16b) and (3–5). It is found that for the general case, where α'_λ and ϵ'_λ are functions of λ, β, θ, and T_A, $\alpha_\lambda(\lambda, T_A) = \epsilon_\lambda(\lambda, T_A)$ *only if* $i'_{\lambda,i}(\lambda)$ *is independent of* β *and* θ, *that is, if the incident spectral intensity is uniform over all directions.* If this is so, the $i'_{\lambda,i}$ can be canceled in equation (3–16b) and the denominator becomes π which then compares with equation (3–5).

For the case $\alpha'_\lambda(\lambda, T_A) = \epsilon'_\lambda(\lambda, T_A)$, that is, the directional spectral properties are independent of angle, then the hemispherical spectral properties are related by $\alpha_\lambda(\lambda, T_A) = \epsilon_\lambda(\lambda, T_A)$ for any angular variation of incident intensity. Such a surface is termed a *diffuse spectral* surface.

3.4.6 Hemispherical Total Absorptivity $\alpha(T_A)$

The hemispherical total absorptivity represents the fraction of energy absorbed that is incident from all directions of the enclosing hemisphere and for all wavelengths as shown in figure 3–1(d). The total incident energy that is intercepted by a surface element dA is determined by integrating equation (3–9) over all λ and all (β, θ) of the hemisphere which results in

$$dQ_i = dA \int_{\frown} \left[\int_0^\infty i'_{\lambda,i}(\lambda, \beta, \theta)\, d\lambda \right] \cos\beta\, d\omega \tag{3-17a}$$

Similarly by integrating equation (3–10a), the total amount of energy absorbed is equal to

$$dQ_a(T_A) = dA \int_{\frown} \left[\int_0^\infty \alpha'_\lambda(\lambda, \beta, \theta, T_A)\, i'_{\lambda,i}(\lambda, \beta, \theta)\, d\lambda \right] \cos\beta\, d\omega \tag{3-17b}$$

The ratio of absorbed to incident energy provides the definition

Hemispherical total absorptivity (in terms of directional spectral absorptivity or emissivity) $\equiv \alpha(T_A)$

$$= \frac{dQ_a(T_A)}{dQ_i} = \frac{\int_{\frown} \left[\int_0^\infty \alpha'_\lambda(\lambda, \beta, \theta, T_A)\, i'_{\lambda,i}(\lambda, \beta, \theta)\, d\lambda \right] \cos\beta\, d\omega}{\int_{\frown} \left[\int_0^\infty i'_{\lambda,i}(\lambda, \beta, \theta)\, d\lambda \right] \cos\beta\, d\omega} \tag{3-18a}$$

or from Kirchhoff's law

$$\alpha(T_A) = \frac{\int_{\frown} \left[\int_0^\infty \epsilon'_\lambda(\lambda, \beta, \theta, T_A)\, i'_{\lambda,i}(\lambda, \beta, \theta)\, d\lambda \right] \cos\beta\, d\omega}{\int_{\frown} \left[\int_0^\infty i'_{\lambda,i}(\lambda, \beta, \theta)\, d\lambda \right] \cos\beta\, d\omega} \tag{3-18b}$$

Equation (3–18b) can be compared with equation (3–6a) to determine under what conditions the hemispherical total absorptivity and emissivity are equal. It is recalled in equation (3–6a) that

$$\sigma T_A^4 = \int_{\frown} \left[\int_0^\infty i'_{\lambda b}(\lambda, T_A)\, d\lambda \right] \cos\beta\, d\omega$$

The comparison reveals that for the general case when ϵ'_λ and α'_λ vary with both wavelength and angle, then $\alpha(T_A) = \epsilon(T_A)$ *only when the incident intensity is independent of the incident angle and has the same spectral form as that emitted by a blackbody with temperature equal to the surface temperature* T_A, that is, only when

$$i'_{\lambda,i}(\lambda, \beta, \theta) = Ci'_{\lambda b}(\lambda, T_A)$$

where C is a constant. Some more restrictive cases are listed in table 3–II.

TABLE 3–II.—SUMMARY OF KIRCHHOFF'S LAW RELATIONS BETWEEN ABSORPTIVITY AND EMISSIVITY

Type of quantity	Equality	Restrictions
Directional spectral........	$\alpha'_\lambda(\lambda, \beta, \theta, T_A)$ $=\epsilon'_\lambda(\lambda, \beta, \theta, T_A)$	None
Directional total.............	$\alpha'(\beta, \theta, T_A)$ $=\epsilon'(\beta, \theta, T_A)$	Incident radiation must have a spectral distribution proportional to that of a blackbody at T_A $i'_{\lambda,i}(\lambda, \beta, \theta)=C(\beta, \theta)i'_{\lambda b}(\lambda, T_A)$; *or* $\alpha'_\lambda(\beta, \theta, T_A)=\epsilon'_\lambda(\beta, \theta, T_A)$ are independent of wavelength (directional-gray surface)
Hemispherical spectral....	$\alpha_\lambda(\lambda, T_A)$ $=\epsilon_\lambda(\lambda, T_A)$	Incident radiation must be independent of angle $i'_{\lambda,i}(\lambda)=C(\lambda)$; *or* $\alpha'_\lambda(\lambda, T_A)=\epsilon'_\lambda(\lambda, T_A)$ do not depend on angle (diffuse-spectral surface)
Hemispherical total........	$\alpha(T_A)=\epsilon(T_A)$	Incident radiation must be independent of angle and have a spectral distribution proportional to that of a blackbody at T_A $i'_{\lambda,i}(\lambda)=Ci'_{\lambda b}(\lambda, T_A)$; *or* incident radiation independent of angle and $\alpha'_\lambda(\beta, \theta, T_A)=\epsilon'_\lambda(\beta, \theta, T_A)$ are independent of λ (directional-gray surface); *or* incident radiation from each direction has spectral distribution proportional to that of a blackbody at T_A and $\alpha'_\lambda(\lambda, T_A)=\epsilon'_\lambda(\lambda, T_A)$ are independent of angle (diffuse-spectral surface); *or* $\alpha'_\lambda(T_A)=\epsilon'_\lambda(T_A)$ are independent of wavelength and angle (diffuse-gray surface)

Substituting equation (3–14a) into equation (3–18a) gives the following alternate forms:

Hemispherical total absorptivity (in terms of directional total absorptivity) $\equiv \alpha(T_A)$

$$= \frac{\int_{\cap} \left[\int_0^{\infty} i'_{\lambda,i}(\lambda, \beta, \theta) d\lambda\right] \alpha'(\beta, \theta, T_A) \cos \beta \, d\omega}{\int_{\cap} \left[\int_0^{\infty} i'_{\lambda,i}(\lambda, \beta, \theta) d\lambda\right] \cos \beta \, d\omega} \tag{3–18c}$$

or

$$\alpha(T_A) = \frac{\int_{\cap} \alpha'(\beta, \theta, T_A) i'_i(\beta, \theta) \cos \beta \, d\omega}{\int_{\cap} i'_i(\beta, \theta) \cos \beta \, d\omega} \tag{3–18d}$$

where $i'_i(\beta, \theta)$ is the incident total intensity from direction (β, θ).

Changing the order of integration in equation (3–18a) and then substituting equation (3–16a) give

Hemispherical total absorptivity (in terms of hemispherical spectral absorptivity) $\equiv \alpha(T_A)$

$$= \frac{\int_0^{\infty} \left[\alpha_\lambda(\lambda, T_A) \cdot \int_{\cap} i'_{\lambda,i}(\lambda, \beta, \theta) \cos \beta \, d\omega\right] d\lambda}{\int_0^{\infty} \left[\int_{\cap} i'_{\lambda,i}(\lambda, \beta, \theta) \cos \beta \, d\omega\right] d\lambda} \tag{3–18e}$$

or

$$\alpha(T_A) = \frac{\int_0^{\infty} \alpha_\lambda(\lambda, T_A) d^2Q_{\lambda,i}}{\int_0^{\infty} d^2Q_{\lambda,i}} \tag{3–18f}$$

where $d^2Q_{\lambda,i}$ is the spectral energy incident from all directions that is intercepted by the surface element dA.

3.4.7 Summary of Kirchhoff's Law Relations

The restrictions on application of Kirchhoff's law are summarized in table 3–II.

3.5 REFLECTIVITY

The reflective properties of a surface are more complicated to specify than either the emissivity or absorptivity. This is because the reflected energy depends not only on the angle at which the incident energy impinges on the surface, but additionally on the direction being considered for the reflected energy. Some of the pertinent reflectivity quantities will now be defined.

3.5.1 Spectral Reflectivities

3.5.1.1 *Bidirectional spectral reflectivity* $\rho''_\lambda(\lambda, \beta_r, \theta_r, \beta, \theta)$.—Consider incident spectral radiation on a surface from direction (β, θ) as shown in figure 3–1(e). Part of this energy is reflected into the (β_r, θ_r) direction and provides a part of the reflected intensity in the (β_r, θ_r) direction. The subscript r will always denote quantities evaluated after reflection. The entire magnitude of the $i'_{\lambda,r}(\lambda, \beta_r, \theta_r)$ is the result of summing the reflected intensities produced by the incident intensities $i'_{\lambda,i}(\lambda, \beta, \theta)$ from all incident directions (β, θ) of the hemisphere surrounding the surface element. The contribution to $i'_{\lambda,r}(\lambda, \beta_r, \theta_r)$ produced by the incident energy from only one (β, θ) will be designated as $i''_{\lambda,r}(\lambda, \beta_r, \theta_r, \beta, \theta)$ and it depends on both the incidence and reflection angles.

The energy from direction (β, θ) intercepted by dA per unit area and wavelength is from equation (3–9),

$$\frac{d^3Q'_{\lambda,i}(\lambda, \beta, \theta)}{dA\, d\lambda} = i'_{\lambda,i}(\lambda, \beta, \theta) \cos \beta \, d\omega \tag{3–19}$$

The *bidirectional spectral reflectivity* is a ratio expressing the contribution that $i'_{\lambda,i}(\lambda, \beta, \theta) \cos \beta \, d\omega$ makes to the reflected spectral intensity in the (β_r, θ_r) direction.

Bidirectional spectral reflectivity $\equiv \rho''_\lambda(\lambda, \beta_r, \theta_r, \beta, \theta)$

$$= \frac{i''_{\lambda,r}(\lambda, \beta_r, \theta_r, \beta, \theta)}{i'_{\lambda,i}(\lambda, \beta, \theta) \cos \beta \, d\omega} \tag{3–20}$$

Although the reflectivity is a function of surface temperature, the T_A notation modifying ρ will be omitted at present for simplicity. The ratio in equation (3–20) is a reflected intensity divided by the intercepted intensity arriving within solid angle $d\omega$. Having $\cos \beta \, d\omega$ in the denominator means that when $\rho''_\lambda(\lambda, \beta_r, \theta_r, \beta, \theta) i'_{\lambda,i}(\lambda, \beta, \theta) \cos \beta \, d\omega$ is integrated over all incidence angles to provide the reflected intensity $i'_{\lambda,r}(\lambda, \beta_r, \theta_r)$, this reflected intensity will be properly weighted by the amount of energy intercepted from each direction. Since i'' is one differential order smaller than i', the $d\omega$ in the denominator prevents $\rho''_\lambda(\lambda, \beta_r, \theta_r, \beta, \theta)$ from being a differential quantity. For a diffuse reflection the incident energy from (β, θ) contributes equally to the reflected intensity for all (β_r, θ_r). It will be shown that the form of equation (3–20) leads to some convenient reciprocity relations.

3.5.1.2 *Reciprocity for bidirectional spectral reflectivity.*—It is generally true that $\rho''_\lambda(\lambda, \beta_r, \theta_r, \beta, \theta)$ is symmetric with regard to reflection and incidence angles, that is, ρ''_λ for energy incident at (β, θ) and reflected at (β_r, θ_r) is equal to ρ''_λ for energy incident at (β_r, θ_r) and reflected at (β, θ).

This is demonstrated by considering a nonblack element dA_2 located within an isothermal black enclosure as shown in figure 3–5. For the isothermal condition, the net energy exchange between black elements

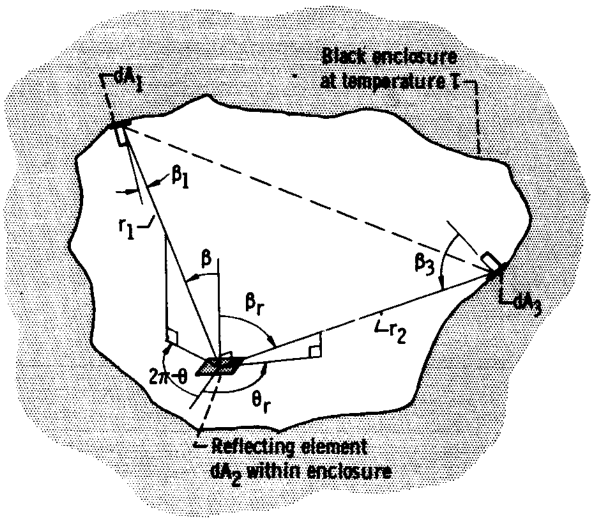

FIGURE 3–5.—Enclosure used to prove reciprocity of bidirectional spectral reflectivity.

dA_1 and dA_3 must be zero. This energy exchange is by two possible paths. The first is the direct exchange along the dashed line. This direct exchange between black elements is uninfluenced by the presence of dA_2 and hence is zero as it would be in a black isothermal enclosure without dA_2. If the net exchange along this path is zero and net exchange including all paths between dA_1 and dA_3 is zero, then net exchange along the remaining path having reflection from dA_2 must also be zero.

295-763 OL-68—6

We can now write the following for the energy traveling along the reflected path:

$$d^4Q''_{\lambda,\,1-2-3}=d^4Q''_{\lambda,\,3-2-1} \tag{3-21a}$$

The energy reflected from dA_2 that reaches dA_3 is

$$d^4Q''_{\lambda,\,1-2-3}=i''_{\lambda,\,r}(\lambda,\,\beta_r,\,\theta_r,\,\beta,\,\theta)\cos\beta_r\,dA_2\frac{dA_3\cos\beta_3}{r_2^2}\,d\lambda$$

or, using equation (3–19),

$$d^4Q''_{\lambda,\,1-2-3}=\rho''_\lambda(\lambda,\,\beta_r,\,\theta_r,\,\beta,\,\theta)\,i'_{\lambda,\,1}(\lambda,\,T)\cos\beta\,\frac{dA_1\cos\beta_1}{r_1^2}\cos\beta_r$$

$$\times\,dA_2\,\frac{dA_3\cos\beta_3}{r_2^2}\,d\lambda \tag{3-21b}$$

Similarly,

$$d^4Q''_{\lambda,\,3-2-1}=\rho''_\lambda(\lambda,\,\beta,\,\theta,\,\beta_r,\,\theta_r)\,i'_{\lambda,\,3}(\lambda,\,T)\cos\beta_r\,\frac{dA_3\cos\beta_3}{r_1^2}\cos\beta$$

$$\times\,dA_2\,\frac{dA_1\cos\beta_1}{r_2^2}\,d\lambda \tag{3-21c}$$

Substituting equations (3–21b) and (3–21c) into equation (3–21a) gives

$$\rho''_\lambda(\lambda,\,\beta_r,\,\theta_r,\,\beta,\,\theta)\,i'_{\lambda,\,1}(\lambda,\,T)=\rho''_\lambda(\lambda,\,\beta,\,\theta,\,\beta_r,\,\theta_r)\,i'_{\lambda,\,3}(\lambda,\,T)$$

or, because $i'_{\lambda,\,1}(\lambda,\;T)=i'_{\lambda,\,3}(\lambda,\;T)=i'_{\lambda b}(\lambda,\;T)$, we find the following *reciprocity relation for* ρ''_λ:

$$\rho''_\lambda(\lambda,\,\beta_r,\,\theta_r,\,\beta,\,\theta)=\rho''_\lambda(\lambda,\,\beta,\,\theta,\,\beta_r,\,\theta_r) \tag{3-22}$$

3.5.1.3 *Directional spectral reflectivities.*—If $i''_{\lambda,\,r}$ is multiplied by $d\lambda\cos\beta_r\,dA\,d\omega_r$ and integrated over the hemisphere for all β_r and θ_r, the energy per unit time is obtained that is reflected into the entire hemisphere as the result of an incident intensity from one direction

$$d^3Q'_{\lambda,\,r}(\lambda,\,\beta,\,\theta)=d\lambda\,dA\int_{\bigcirc} i''_{\lambda,\,r}(\lambda,\,\beta_r,\,\theta_r,\,\beta,\,\theta)\cos\beta_r\,d\omega_r$$

By use of equation (3–20) this is equal to

$$d^3Q'_{\lambda,r}(\lambda,\beta,\theta)=i'_{\lambda,i}(\lambda,\beta,\theta)\cos\beta\,d\omega\,d\lambda\,dA\int_{\cap}\rho''_{\lambda}(\lambda,\beta_r,\theta_r,\beta,\theta)\cos\beta_r\,d\omega_r \tag{3-23}$$

The directional-hemispherical spectral reflectivity is then defined as the energy reflected into all solid angles divided by the incident energy from one direction (fig. 3–1(f)). This gives equation (3–23) divided by the incident energy from equation (3–19)

Directional-hemispherical spectral reflectivity (in terms of bidirectional spectral reflectivity) $\equiv\rho'_{\lambda}(\lambda,\beta,\theta)$

$$=\frac{d^3Q'_{\lambda,r}(\lambda,\beta,\theta)}{d^3Q'_{\lambda,i}(\lambda,\beta,\theta)}=\int_{\cap}\rho''_{\lambda}(\lambda,\beta_r,\theta_r,\beta,\theta)\cos\beta_r\,d\omega_r \tag{3-24}$$

Equation (3–24) defines how much of the radiant energy incident from one direction will be reflected into all directions. Another directional reflectivity is useful when one is concerned with the reflected intensity into one direction resulting from incident radiation coming from all directions. It is called the *hemispherical-directional spectral reflectivity* (fig. 3–1(g)). The reflected intensity into the $(\beta_r,\ \theta_r)$ direction is found by integrating equation (3–20) over all incident directions

$$i'_{\lambda,r}(\lambda,\beta_r,\theta_r)=\int_{\cap}\rho''_{\lambda}(\lambda,\beta_r,\theta_r,\beta,\theta)\,i'_{\lambda,i}(\lambda,\beta,\theta)\cos\beta\,d\omega \tag{3-25}$$

The hemispherical-directional spectral reflectivity is then defined as the reflected intensity in the $(\beta_r,\ \theta_r)$ direction divided by the integrated average incident intensity

Hemispherical-directional spectral reflectivity (in terms of bidirectional spectral reflectivity) $\equiv\rho'_{\lambda}(\lambda,\beta_r,\theta_r)$

$$=\frac{\int_{\cap}\rho''_{\lambda}(\lambda,\beta_r,\theta_r,\beta,\theta)\,i'_{\lambda,i}(\lambda,\beta,\theta)\cos\beta\,d\omega}{\frac{1}{\pi}\int_{\cap}i'_{\lambda,i}(\lambda,\beta,\theta)\cos\beta\,d\omega} \tag{3-26}$$

3.5.1.4 *Reciprocity for directional spectral reflectivity.*—A reciprocity relation can also be found for ρ'_{λ} in the following manner. When the incident intensity is uniform over all incident directions, equation (3–26) reduces to

Hemispherical-directional spectral reflectivity (for uniform incident intensity) $\equiv \rho'_\lambda(\lambda, \beta_r, \theta_r)$

$$= \int_{\cap} \rho''_\lambda(\lambda, \beta_r, \theta_r, \beta, \theta) \cos\beta \, d\omega \tag{3–27}$$

By comparing equations (3–24) and (3–27) and noting equation (3–22), the *reciprocal relation for* ρ'_λ results (restricted to uniform incident intensity)

$$\rho'_\lambda(\lambda, \beta, \theta) = \rho'_\lambda(\lambda, \beta_r, \theta_r) \tag{3–28}$$

where (β_r, θ_r) and (β, θ) are the same angles. This means that the reflectivity of a material irradiated at a given angle of incidence (β, θ) as measured by the energy collected over the entire hemisphere of reflection is equal to the reflectivity for *uniform* irradiation from the hemisphere as measured by collecting the energy at a single angle of reflection (β_r, θ_r) when (β_r, θ_r) is the same angle as (β, θ). This relation is employed in the design of "hemispherical reflectometers" for measuring radiative properties (ref. 1).

3.5.1.5 *Hemispherical spectral reflectivity* $\rho_\lambda(\lambda)$.—If the incident spectral radiation arrives from all angles over the hemisphere (fig. 3–1(h)), then all the radiation intercepted by the area element dA of the surface $d^2Q_{\lambda,i}$ is given by equation (3–15a) as

$$d^2Q_{\lambda,i}(\lambda) = d\lambda dA \int_{\cap} i'_{\lambda,i}(\lambda, \beta, \theta) \cos\beta \, d\omega$$

The amount of $d^2Q_{\lambda,i}$ that is reflected is, by integration of equation (3–24),

$$d^2Q_{\lambda,r}(\lambda) = \int_{\cap} \rho'_\lambda(\lambda, \beta, \theta) \, d^3Q'_{\lambda,i}(\lambda, \beta, \theta)$$

$$= d\lambda dA \int_{\cap} \rho'_\lambda(\lambda, \beta, \theta) i'_{\lambda,i}(\lambda, \beta, \theta) \cos\beta \, d\omega$$

The fraction of $d^2Q_{\lambda,i}(\lambda)$ that is reflected provides the definition

Hemispherical spectral reflectivity (in terms of directional-hemispherical spectral reflectivity) $\equiv \rho_\lambda(\lambda)$

$$=\frac{d^2Q_{\lambda,r}(\lambda)}{d^2Q_{\lambda,i}(\lambda)}=\frac{d\lambda\, dA}{d^2Q_{\lambda,i}(\lambda)}\int_{\cap}\rho_\lambda'(\lambda,\beta,\theta)i_{\lambda,i}'(\lambda,\beta,\theta)\cos\beta\, d\omega \quad (3\text{–}29)$$

3.5.1.6 *Limiting cases for spectral surfaces.*—Two important limiting cases of spectrally reflecting surfaces will be discussed in this section.

3.5.1.6.1 Diffusely reflecting surfaces: For a *diffuse surface* the incident energy from direction (β, θ) that is reflected produces a reflected intensity that is uniform over all (β_r, θ_r) directions, but the amount of energy reflected may vary as a function of *incident* angle.[10] When viewing a diffuse surface element irradiated by an incident beam, the element will appear equally bright from all viewing directions. The bidirectional spectral reflectivity is then independent of (β_r, θ_r), and equation (3–24) simplifies to

$$\rho_{\lambda,d}'(\lambda,\beta,\theta)=\rho_\lambda''(\lambda,\beta,\theta)\int_{\cap}\cos\beta_r\, d\omega_r$$

Carrying out the integration gives for a *diffuse* surface

$$\rho_{\lambda,d}'(\lambda,\beta,\theta)=\pi\rho_\lambda''(\lambda,\beta,\theta) \quad (3\text{–}30)$$

so that for any incidence angle the directional-hemispherical spectral reflectivity is equal to π times the bidirectional spectral reflectivity. This is because $\rho_{\lambda,d}'$ accounts for the reflected energy into all (β_r, θ_r) directions, while ρ_λ'' accounts for the reflected intensity into only one direction. This is analogous to the relation between blackbody hemispherical emissive power and intensity, $e_{\lambda b}(\lambda)=\pi i_{\lambda b}'(\lambda)$.

Equation (3–25) provides the intensity in the (β_r, θ_r) direction when the incident radiation is distributed over (β, θ) values. If the surface is *diffuse*, and if the *bidirectional reflectivity is independent of incidence angle, and if the incident intensity is uniform for all incident angles*, equation (3–25) reduces to

$$i_{\lambda,r}'(\lambda)=\rho_\lambda''(\lambda)i_{\lambda,i}'(\lambda)\int_{\cap}\cos\beta\, d\omega=\pi\rho_\lambda''(\lambda)i_{\lambda,i}'(\lambda) \quad (3\text{–}31a)$$

By using equation (3–30), which applies for the diffuse surface,

$$i_{\lambda,r}'(\lambda)=\rho_{\lambda,d}'(\lambda)i_{\lambda,i}'(\lambda) \quad (3\text{–}31b)$$

[10] It is often tacitly assumed that diffuse reflectivities are independent of angle of incidence (β, θ), but this is not a necessary condition for the diffuse definition.

so that the reflected intensity in any direction for this case is simply the hemispherical-directional reflectivity (which has been assumed independent of incidence angle) times the incident intensity. For the assumed uniform irradiation, the spectral energy per unit time intercepted by the surface element dA from all angular directions in the hemisphere is

$$d^2Q_{\lambda,i}(\lambda) = \pi i'_{\lambda,i}(\lambda)\, dA\, d\lambda$$

so that

$$i'_{\lambda,r}(\lambda) = \rho'_{\lambda,d}(\lambda) \frac{d^2Q_{\lambda,i}(\lambda)}{\pi\, dA\, d\lambda} \tag{3-31c}$$

3.5.1.6.2 Specularly reflecting surfaces: Mirror-like, or specular, surfaces obey well-known laws of reflection. The perfect specular reflector and the perfect diffuse surface provide two relatively simple special cases that can be used for the calculation of heat exchange in enclosures. For an incident beam from a single direction, a specular reflector, by definition, obeys a definite relation between incident and reflected angles. The reflected beam is at the same angle from the surface normal as the incident beam and is in the same plane as that formed by the incident beam and normal. Hence,

$$\beta_r = \beta, \qquad \theta_r = \theta + \pi \tag{3-32}$$

and at all other angles, the bidirectional spectral reflectivity of a specular surface is zero. We can write

$$\rho''_{\lambda}(\lambda, \beta, \theta, \beta_r, \theta_r)_{\text{specular}} = \rho''_{\lambda}(\lambda, \beta, \theta, \beta_r = \beta,\ \theta_r = \theta + \pi) \equiv \rho''_{\lambda,s}(\lambda, \beta, \theta) \tag{3-33}$$

and the bidirectional spectral reflectivity of a specular surface is considered to be only a function of the incident direction.

For the intensity of radiation reflected from a specular surface into the solid angle around (β_r, θ_r), equation (3–25) gives, for an *arbitrary* directional distribution of incident intensity,

$$i'_{\lambda,r}(\lambda, \beta_r, \theta_r) = \int_{\Omega} \rho''_{\lambda,s}(\lambda, \beta, \theta) i'_{\lambda,i}(\lambda, \beta, \theta) \cos\beta\, d\omega \tag{3-34a}$$

The integrand of equation (3–34a) has a nonzero value only in the small solid angle around the direction (β, θ) because of the properties of $\rho'_{\lambda,s}(\lambda, \beta, \theta)$. Equation (3–34a) can then be written as

$$i'_{\lambda,r}(\lambda, \beta_r, \theta_r) = \rho''_{\lambda,s}(\lambda, \beta, \theta) i'_{\lambda,i}(\lambda, \beta, \theta) \cos \beta \, d\omega \qquad (3\text{–}34b)$$

Let us now consider for a moment the general equation for bidirectional spectral reflectivity (eq. (3–20)). When written for a specular surface, it becomes

$$i''_{\lambda,r}(\lambda, \beta_r = \beta, \theta_r = \theta + \pi) = \rho''_{\lambda,s}(\lambda, \beta, \theta) i'_{\lambda,i}(\lambda, \beta, \theta) \cos \beta \, d\omega \qquad (3\text{–}35)$$

This result is the intensity reflected into a solid angle around (β_r, θ_r) from a single beam incident at $(\beta = \beta_r, \theta = \theta_r - \pi)$. The right side of equation (3–35) is seen to be identical to the right side of equation (3–34b), which gives the intensity reflected into the solid angle around (β_r, θ_r) from distributed incident radiation. The point of this line of reasoning is to demonstrate the following rather obvious fact: In examining the radiation reflected from a specular surface into a given direction, only that radiation incident at the (β, θ) defined by equation (3–32) need be considered as contributing to the reflected intensity *regardless* of the directional distribution of incident energy.

From equations (3–26) and (3–34a), the hemispherical-directional spectral reflectivity for *uniform irradiation* of a specular surface is given by

$$\rho'_{\lambda,s}(\lambda, \beta_r, \theta_r) = \frac{\int_{\Omega} \rho''_{\lambda,s}(\lambda, \beta, \theta) i'_{\lambda,i}(\lambda) \cos \beta \, d\omega}{\frac{1}{\pi} \int_{\Omega} i'_{\lambda,i}(\lambda) \cos \beta \, d\omega} = \frac{i'_{\lambda,r}(\lambda, \beta_r, \theta_r)}{i'_{\lambda,i}(\lambda)} \qquad (3\text{–}36a)$$

Comparison with equation (3–34b) gives the relation between bidirectional and hemispherical-directional spectral reflectivities for a *specular surface* with uniform incident intensity as

$$\rho'_{\lambda,s}(\lambda, \beta_r, \theta_r) = \rho''_{\lambda,s}(\lambda, \beta, \theta) \cos \beta \, d\omega \qquad (3\text{–}36b)$$

Use of the reciprocity relation (eq. 3–28) shows that the directional-hemispherical reflectivity $\rho'_{\lambda,s}(\lambda, \beta, \theta)$ for a single incident beam is

$$\rho'_{\lambda,s}(\lambda, \beta, \theta) = \rho'_{\lambda,s}(\lambda, \beta_r, \theta_r) = \rho''_{\lambda,s}(\lambda, \beta, \theta) \cos \beta_r \, d\omega_r \qquad (3\text{–}36c)$$

where the restrictions of equation (3–32) still apply and the incident intensity is uniform.

The hemispherical spectral reflectivity of a uniformly irradiated specular reflector is, from equation (3–29),

$$\rho_{\lambda,s}(\lambda)=\frac{1}{\pi}\int_{\cap}\rho'_{\lambda,s}(\lambda,\beta,\theta)\cos\beta\,d\omega \tag{3–37}$$

If $\rho'_{\lambda,s}$ is independent of incident angle, evaluation of the integral in equation (3–37) gives

$$\rho_{\lambda,s}(\lambda)=\rho'_{\lambda,s}(\lambda) \tag{3–38}$$

3.5.2 **Total Reflectivities**

The previous reflectivity definitions have dealt only with spectral radiation; the definitions are now considered that include the contributions from all wavelengths.

3.5.2.1 *Bidirectional total reflectivity* $\rho''(\beta_r, \theta_r, \beta, \theta)$.—The bidirectional total reflectivity gives the contribution made by the total energy incident from direction (β, θ) to the reflected total intensity into the direction (β_r, θ_r). By analogy with equation (3–20),

Bidirectional total reflectivity $\equiv \rho''(\beta_r, \theta_r, \beta, \theta)$

$$=\frac{\int_0^\infty i''_{\lambda,r}(\lambda,\beta_r,\theta_r,\beta,\theta)\,d\lambda}{\cos\beta\,d\omega\int_0^\infty i'_{\lambda,i}(\lambda,\beta,\theta)\,d\lambda}$$

$$=\frac{i''_r(\beta_r,\theta_r,\beta,\theta)}{i'_i(\beta,\theta)\cos\beta\,d\omega} \tag{3–39a}$$

As an alternate form, the reflected energy is given by integrating equation (3–20) over all wavelengths

$$i''_r(\beta_r,\theta_r,\beta,\theta)=\cos\beta\,d\omega\int_0^\infty\rho''_\lambda(\lambda,\beta_r,\theta_r,\beta,\theta)\,i'_{\lambda,i}(\lambda,\beta,\theta)\,d\lambda$$

so that equation (3–39a) can also be written as

Bidirectional total reflectivity (in terms of bidirectional spectral reflectivity) $\equiv \rho''(\beta_r, \theta_r, \beta, \theta)$

$$= \frac{\int_0^\infty \rho''_\lambda(\lambda, \beta_r, \theta_r, \beta, \theta) i'_{\lambda,i}(\lambda, \beta, \theta) d\lambda}{i'_i(\beta, \theta)} \tag{3-39b}$$

where $i'_i(\beta, \theta) = \int_0^\infty i'_{\lambda,i}(\lambda, \beta, \theta) d\lambda$.

3.5.2.2 *Reciprocity.*—Rewriting equation (3–39b) for the case of energy incident from direction (β_r, θ_r) and reflected into direction (β, θ) gives

$$\rho''(\beta, \theta, \beta_r, \theta_r) = \frac{\int_0^\infty \rho''_\lambda(\lambda, \beta, \theta, \beta_r, \theta_r) i'_{\lambda,i}(\lambda, \beta_r, \theta_r) d\lambda}{i'_i(\beta_r, \theta_r)} \tag{3-39c}$$

Comparison of equations (3–39b) and (3–39c) shows that

$$\rho''(\beta, \theta, \beta_r, \theta_r) = \rho''(\beta_r, \theta_r, \beta, \theta) \tag{3-40}$$

if the *spectral distribution of incident intensity is the same for all directions or in a less restrictive sense if* $i'_{\lambda,i}(\lambda, \beta, \theta) = C i'_{\lambda,i}(\lambda, \beta_r, \theta_r)$.

3.5.2.3 *Directional total reflectivity* ρ'.—The *directional-hemispherical total reflectivity* is the fraction of the total energy incident from a single direction that is reflected into all angular directions. The spectral energy from a given direction that is intercepted by the surface is $i'_{\lambda,i}(\lambda, \beta, \theta) \cos \beta \, d\omega d\lambda dA$. The portion of this energy that is reflected is $\rho'_\lambda(\lambda, \beta, \theta) i'_{\lambda,i}(\lambda, \beta, \theta) \cos \beta \, d\omega d\lambda dA$. If these quantities are integrated over all wavelengths to provide total values, the following definition is formed:

Directional-hemispherical total reflectivity (in terms of directional-hemispherical spectral reflectivity) $\equiv \rho'(\beta, \theta)$

$$= \frac{d^2Q'_r(\beta, \theta)}{d^2Q'_i(\beta, \theta)}$$

$$= \frac{\int_0^\infty \rho'_\lambda(\lambda, \beta, \theta) i'_{\lambda,i}(\lambda, \beta, \theta) d\lambda}{\int_0^\infty i'_{\lambda,i}(\lambda, \beta, \theta) d\lambda} \tag{3-41a}$$

Another directional total reflectivity specifies the fraction of radiation reflected into a given (β_r, θ_r) direction when there is uniform irradiation. The total radiation intensity reflected into the (β_r, θ_r) direction when the incident intensity is uniform for all directions is

$$i_r'(\beta_r, \theta_r) = \int_0^\infty i_{\lambda, r}'(\lambda, \beta_r, \theta_r)\, d\lambda = \int_0^\infty i_{\lambda, i}'(\lambda) \rho_\lambda'(\lambda, \beta_r, \theta_r)\, d\lambda$$

where $\rho_\lambda'(\lambda, \beta_r, \theta_r)$ was discussed in connection with equation (3–27). Then the reflectivity can be defined as the reflected intensity divided by the incident intensity:

Hemispherical-directional total reflectivity (for uniform irradiation) $\equiv \rho'(\beta_r, \theta_r)$

$$= \frac{\int_0^\infty \rho_\lambda'(\lambda, \beta_r, \theta_r)\, i_{\lambda, i}'(\lambda)\, d\lambda}{\int_0^\infty i_{\lambda, i}'(\lambda)\, d\lambda} \tag{3–41b}$$

3.5.2.4 *Reciprocity.*—Equations (3–41a) and (3–41b) are now compared, bearing in mind that the latter is restricted to uniform incident intensity. With this restriction, from equation (3–28) $\rho_\lambda'(\lambda, \beta, \theta) = \rho_\lambda'(\lambda, \beta_r, \theta_r)$, it is also found that

$$\rho'(\beta_r, \theta_r) = \rho'(\beta, \theta) \tag{3–42}$$

where (β_r, θ_r) and (β, θ) are the same angles *when there is a fixed spectral distribution of the incident radiation such that*

$$i_{\lambda, i}'(\lambda, \beta, \theta) = C i_{\lambda, i}'(\lambda)$$

3.5.2.5 *Hemispherical total reflectivity* ρ.—If the incident total radiation arrives from all angles over the hemisphere, the total radiation intercepted by a unit area at the surface is given by equation (3–17a). The amount of this radiation that is reflected is

$$dQ_r = dA \int_\Omega \rho'(\beta, \theta) i_i'(\beta, \theta) \cos\beta\, d\omega$$

The ratio of these two quantities is then the hemispherical total reflectivity, which is the fraction of all the incident energy that is reflected including all directions of reflection; that is, *Hemispherical total reflectivity* (in terms of directional-hemispherical total reflectivity) $\equiv \rho$

$$=\frac{dQ_r}{dQ_i}=\frac{dA}{dQ_i}\int_{\frown} \rho'(\beta, \theta) i_i'(\beta, \theta) \cos \beta \, d\omega \qquad (3\text{–}43\text{a})$$

Another form is found by using $d^2Q_{\lambda,i}(\lambda)$ which is the incident hemispherical spectral energy intercepted by the surface. The amount of this that is reflected is $\rho_\lambda(\lambda) d^2Q_{\lambda,i}$ where $\rho_\lambda(\lambda)$ is the hemispherical spectral reflectivity from equation (3–29). Then integrating yields

Hemispherical total reflectivity (in terms of hemispherical spectral reflectivity) $\equiv \rho$

$$=\frac{\int_0^\infty \rho_\lambda(\lambda) d^2Q_{\lambda,i}(\lambda)}{dQ_i} \qquad (3\text{–}43\text{b})$$

3.5.3 Summary of Restrictions on Reciprocity Relations Between Reflectivities

In table 3–III, a summary is presented of the restrictive conditions

TABLE 3–III. – SUMMARY OF RECIPROCITY RELATIONS BETWEEN REFLECTIVITIES

Type of quantity	Equality	Restrictions
A. Bidirectional spectral (eq. (3–22))	$\rho_\lambda''(\lambda, \beta, \theta, \beta_r, \theta_r)$ $=\rho_\lambda''(\lambda, \beta_r, \theta_r, \beta, \theta)$	None
B. Directional spectral (eq. (3–28))	$\rho_\lambda'(\lambda, \beta, \theta)=\rho_\lambda'(\lambda, \beta_r, \theta_r)$ where $\beta=\beta_r$ and $\theta=\theta_r$	$\rho_\lambda'(\lambda, \beta_r, \theta_r)$ is for uniform incident intensity *or* $\rho_\lambda''(\lambda)$ independent of β, θ, β_r, and θ_r
C. Bidirectional total (eq. (3–40))	$\rho''(\beta, \theta, \beta_r, \theta_r)$ $=\rho''(\beta_r, \theta_r, \beta, \theta)$	$i_{\lambda,i}'(\lambda, \beta, \theta)=Ci_{\lambda,i}'(\lambda, \beta_r, \theta_r)$ *or* $\rho_\lambda''(\beta, \theta, \beta_r, \theta_r)$ independent of wavelength
D. Directional total (eq. (3–42))	$\rho'(\beta, \theta)=\rho'(\beta_r, \theta_r)$ where $\beta=\beta_r$ and $\theta=\theta_r$	One restriction from both B and C

necessary for application of the various reciprocity relations for reflectivities.

3.6 RELATIONS AMONG REFLECTIVITY, ABSORPTIVITY, AND EMISSIVITY

From the definitions of absorptivity and reflectivity as fractions of incident energy absorbed or reflected, it is evident that for an opaque body (no radiation transmitted through the body) some simple relations exist between these surface properties. By using Kirchhoff's law (see section 3.4.7) and taking note of the restrictions involved, further relations can be found in certain cases between the emissivity and the reflectivity.

Because the spectral energy per unit time $d^3Q'_{\lambda,i}$ incident upon dA of an opaque body from a solid angle $d\omega$ is either absorbed or reflected, it is evident that

$$d^3Q'_{\lambda,i}(\lambda, \beta, \theta) = d^3Q'_{\lambda,a}(\lambda, \beta, \theta, T_A) + d^3Q'_{\lambda,r}(\lambda, \beta, \theta, T_A)$$

or

$$\frac{d^3Q'_{\lambda,a}(\lambda,\beta,\theta,T_A)}{d^3Q'_{\lambda,i}(\lambda,\beta,\theta)} + \frac{d^3Q'_{\lambda,r}(\lambda,\beta,\theta,T_A)}{d^3Q'_{\lambda,i}(\lambda,\beta,\theta)} = 1 \tag{3-44}$$

Since the energy is incident from the direction (β, θ), the two energy ratios of equation (3–44) are the directional spectral absorptivity (eq. (3–10a)) and the directional-hemispherical spectral reflectivity (eq. (3–24)), respectively. Substituting gives

$$\alpha'_\lambda(\lambda,\beta,\theta,T_A) + \rho'_\lambda(\lambda,\beta,\theta,T_A) = 1 \tag{3-45}$$

Kirchhoff's law (eq. (3–12)) can then be applied without restriction to yield

$$\epsilon'_\lambda(\lambda,\beta,\theta,T_A) + \rho'_\lambda(\lambda,\beta,\theta,T_A) = 1 \tag{3-46}$$

When the total energy arriving at dA from a given direction is considered, equation (3–44) becomes

$$\frac{d^2Q'_a(\beta, \theta, T_A)}{d^2Q'_i(\beta, \theta)} + \frac{d^2Q'_r(\beta, \theta, T_A)}{d^2Q'_i(\beta, \theta)} = 1 \tag{3-47}$$

Substituting equation (3–14a) and (3–41a) for the energy ratios results in

$$\alpha'(\beta, \theta, T_A)+\rho'(\beta, \theta, T_A)=1 \tag{3–48}$$

The absorptivity is the directional total value, and the reflectivity is the directional-hemispherical total value.

Kirchhoff's law for directional total properties (section 3.4.4) can then be applied to give

$$\epsilon'(\beta, \theta, T_A)+\rho'(\beta, \theta, T_A)=1 \tag{3–49}$$

under the restrictions that the incident radiation obeys the relation $i'_{\lambda,i}(\lambda, \beta, \theta)=C(\beta, \theta)i'_{\lambda b}(\lambda, T_A)$ *or* the surface is directional gray.

If the incident spectral energy is assumed to be arriving at dA from all directions over the hemisphere, equation (3–44) gives

$$\frac{d^2Q_{\lambda,a}(\lambda, T_A)}{d^2Q_{\lambda,i}(\lambda)}+\frac{d^2Q_{\lambda,r}(\lambda, T_A)}{d^2Q_{\lambda,i}(\lambda)}=1 \tag{3–50}$$

Equation (3–50) can then be written as

$$\alpha_\lambda(\lambda, T_A)+\rho_\lambda(\lambda, T_A)=1 \tag{3–51}$$

where the radiative properties are hemispherical spectral values from equations (3–16) and (3–29). Substitution of the hemispherical spectral emissivity $\epsilon_\lambda(\lambda, T_A)$ for $\alpha_\lambda(\lambda, T_A)$ in this relation is valid *only* if the intensity of incident radiation is independent of incident angle, that is, it is uniform over all incident directions, or if the α_λ and ϵ_λ do not depend on angle (see section 3.4.7). Under these restrictions, equation (3–51) becomes

$$\epsilon_\lambda(\lambda, T_A)+\rho_\lambda(\lambda, T_A)=1 \tag{3–52}$$

If the incident energy on dA is summed over all wavelengths and directions, equation (3–44) becomes

$$\frac{dQ_a(T_A)}{dQ_i}+\frac{dQ_r(T_A)}{dQ_i}=1 \tag{3–53}$$

The energy ratios are now the hemispherical total values of absorptivity and reflectivity (eqs. (3–18) and (3–43a), respectively), and equation (3–53) becomes

$$\alpha(T_A)+\rho(T_A)=1 \tag{3–54}$$

Again, certain restrictions apply if $\epsilon(T_A)$ is substituted for $\alpha(T_A)$ to obtain

$$\epsilon(T_A)+\rho(T_A)=1 \tag{3-55}$$

The principal restrictions on the validity of this relation are that the incident spectral intensity is proportional to the emitted spectral intensity of a blackbody at T_A *and* the incident intensity is uniform over all incident angles; that is, $i'_{\lambda,i}(\lambda)=Ci'_{\lambda b}(\lambda, T_A)$. Other special cases where the substitution $\alpha(T_A)=\epsilon(T_A)$ can be made are listed in section 3.4.7.

When the body is not opaque so that some radiation is transmitted entirely through it, a transmitted fraction must be introduced. This topic is more properly discussed in connection with radiation in absorbing media.

EXAMPLE 3–5: Radiation from the Sun is incident on a surface in orbit above the Earth's atmosphere. The surface is at 1800° R, and the directional total emissivity is given in figure 3–3. If the incident energy is at an angle 25° from the normal to the surface, what is the reflected energy flux?

From figure 3–3 $\epsilon'(25°, 1800° \text{ R})=0.8$. The spectrum of radiation from the Sun is similar to that of a blackbody. Section 3.4.7 shows that $\alpha'(25°, 1800° \text{ R})=\epsilon'(25°, 1800° \text{ R})=0.8$, only when the incident spectrum is proportional to that emitted by a blackbody at $T_A=1800°$ R. This is not the case here since the Sun acts like a blackbody at 10 000° R. Hence, $\alpha' \neq 0.8$, and without α' we cannot determine ρ'; the emissivity data given are insufficient to work the problem.

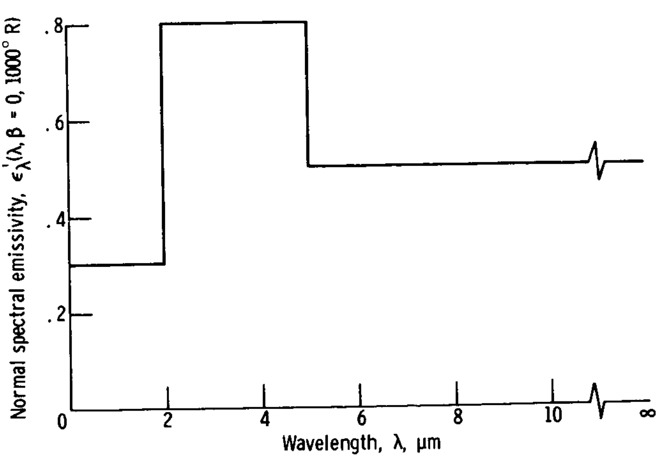

FIGURE 3–6.—Directional spectral emissivity in normal direction for example 3–6.

EXAMPLE 3–6: A surface at $T_A = 1000°$ R has a spectral emissivity in the normal direction that can be approximated as shown in figure 3–6. This surface is maintained at 1000° R by cooling water and is then enclosed by a black hemisphere heated to $T_i = 3000°$ R. What will the reflected intensity be into the direction normal to the surface?

From equation (3–46)

$$\rho'_\lambda(\lambda, \beta=0°, T_A) = 1 - \epsilon'_\lambda(\lambda, \beta=0°, T_A)$$

which is the reflectivity into the hemisphere for radiation arriving from the normal direction. From reciprocity, for uniform incident intensity over the hemisphere,

$$\rho'_\lambda(\lambda, \beta_r=0°, T_A) = \rho'_\lambda(\lambda, \beta=0°, T_A)$$

Hence, the reflectivity into the normal direction resulting from the incident radiation from the hemisphere is (by use of fig. 3–6)

$$\rho'_\lambda(0 \leq \lambda < 2, \beta_r=0°, T_A) = 0.7$$

$$\rho'_\lambda(2 \leq \lambda < 5, \beta_r=0°, T_A) = 0.2$$

$$\rho'_\lambda(5 \leq \lambda \leq \infty, \beta_r=0°, T_A) = 0.5$$

The incident intensity is $i'_{\lambda,i}(\lambda, T_i) = i'_{\lambda b}(\lambda, 3000° \text{ R})$. From the relation preceding equation (3–41b), the reflected intensity is

$$i'_r(\beta_r=0°) = \int_0^\infty i'_{\lambda b}(\lambda, T_i)\rho'_\lambda(\lambda, \beta_r=0°, T_A)\, d\lambda$$

$$= \frac{\sigma T_i^4}{\pi} \int_0^\infty \left[\frac{e_{\lambda b}(\lambda, T_i)}{\sigma T_i^5} \rho'_\lambda(\lambda, \beta_r=0°, T_A)\, d(\lambda T_i)\right]$$

From equation (2–27) this becomes

$$i'_r(\beta_r=0°) = \frac{\sigma T_i^4}{\pi} (0.7F_{0-2T_i} + 0.2F_{2T_i-5T_i} + 0.5_{5T_i-\infty})$$

$$= \frac{0.1712}{\pi} (30)^4 [0.7(0.347) + 0.2(0.869 - 0.347) + 0.5(1 - 0.869)]$$

$$= 18\,200 \text{ Btu/(hr) (sq ft) } (\mu\text{m}) \text{ (sr)}$$

3.7 CONCLUDING REMARKS

In this chapter, a precise system of nomenclature has been introduced, and careful definitions of the radiative properties have been given. The defining equations are summarized in table 3–I for convenience, along with the symbols used here.

By using these definitions, it was possible to examine the restrictions on the various forms of Kirchhoff's law relating emissivity to absorptivity. These restrictions are sometimes a source of confusion, and it is hoped that the summary given (table 3–II, section 3.4.7) will make clear the conditions when α can be set equal to ϵ. These restrictions are also invoked when deriving the relation $\epsilon+\rho=1$ from the general relation $\alpha+\rho=1$ for opaque bodies.

The detailed definitions given made it possible to derive the reciprocal relations for reflectivities and examine the restrictions involved. These restrictions are listed in a convenient summary in table 3–III, section 3.5.3.

REFERENCE

1. BRANDENBERG, W. M.: The Reflectivity of Solids at Grazing Angles. Measurement of Thermal Radiation Properties of Solids. Joseph C. Richmond, ed. NASA SP–31, 1963, pp. 75–82.

Chapter 4. Prediction of Radiative Properties by Classical Electromagnetic Theory

4.1 INTRODUCTION

James Clerk Maxwell, in 1864, published an article defining what is generally conceded to be the crowning achievement of classical physics: the relation between electrical and magnetic fields and the realization that electromagnetic waves propagate with the speed of light, indicating strongly that light itself is in the form of an electromagnetic wave (ref. 1). Although quantum effects have since been shown to be the controlling phenomena in electromagnetic energy propagation, it is possible and indeed necessary to describe many of the properties of light and radiant heat by the classical wave approach.

It will be demonstrated in this chapter that the reflectivity, emissivity, and absorptivity of materials can in certain cases be calculated from the optical and electrical properties of the materials. The relations between the radiative properties of a material and its optical and electrical properties are found by considering the interaction that occurs when an electromagnetic wave traveling through one medium is incident on the surface of another medium.

The analysis will be based on the assumption that there is an ideal interaction between the incident waves and the surface. Physically this means that the results are for optically smooth, clean surfaces that reflect in a specular fashion. The wave propagation and surface interaction will be investigated here in a somewhat simplified fashion by using Maxwell's fundamental equations relating electric and magnetic fields. For ideal surface conditions, it is possible to perform more accurate property computations by using theory that is more rigorous than the wave analysis presented here. However, the labor involved is generally not justified, because neither the simplified nor the more sophisticated approach can account for the effects of surface preparation. The departures of real materials from the ideal materials assumed in the theory are often responsible for introducing large variations of measured property values from theoretical predictions. These departures are caused by factors such as impurities, surface roughness, surface contamination, and crystal structure modification by surface working.

Although in practice there can be large effects of surface condition, the theory presented here does serve a number of useful purposes. It provides an understanding of why there are basic differences in the radiative properties of insulators and electrical conductors, and reveals general trends that help unify the presentation of experimental data. These trends are also useful when it is required for engineering calculations to extrapolate limited experimental data into another range. The theory has utility in the theoretical understanding of the angular behavior of the directional reflectivity, absorptivity, and emissivity. Since the electromagnetic theory applies for pure substances with ideally smooth surfaces, it provides a means by which one limit of attainable properties can be computed; for example, the maximum reflectivity or minimum emissivity of a metallic surface can be determined.

The derivation of radiative property relations from classical theory is carried out in some detail in sections 4.3 through 4.5. The results are then gathered and their use demonstrated in section 4.6. Those readers interested only in the use of the results for property predictions are invited to pass over the derivation portions to section 4.6.

4.2 SYMBOLS

C_1, C_2	constants in Planck spectral energy distribution
c	speed of electromagnetic wave
c_o	speed of electromagnetic wave in vacuum
E	amplitude of electric intensity wave
e	emissive power
H	amplitude of magnetic intensity wave
K	dielectric constant, γ/γ_o
n	refractive index
$\vec{n}$	complex refractive index, $n-i\kappa$
r_e	electrical resistivity
$\underline{S}$	instantaneous rate of energy transport per unit area
$\vec{S}$	Poynting vector, eq. (4–24)
T	absolute temperature
t	time
x, y, z	coordinates in Cartesian system referenced to interface between media (fig. 4–1)
x', y', z'	coordinates in Cartesian system referenced to wave propagating in a medium (fig. 4–1)
β	angle measured from normal of surface; cone angle
γ	permittivity
ϵ	emissivity
θ	circumferential angle
κ	extinction coefficient
λ	wavelength

μ	magnetic permeability
ν	frequency
ρ	reflectivity
χ	angle of refraction
ω	angular frequency
$\int_{\Omega}$	integration over solid angle of entire enclosing hemisphere

Subscripts:

A	property of body or surface A
b	black
i	incident
M	maximum value
n	normal
o	in a vacuum
r	reflected
s	specular
t	transmitted
x, y, z	components in x, y, or z direction
x', y', z'	components in x', y', or z' direction
λ	spectral
1, 2	medium 1 or 2
$\perp$	perpendicular component
$\parallel$	parallel component

Superscript:

	directional quantity

4.3 FUNDAMENTAL EQUATIONS OF ELECTROMAGNETIC THEORY

Maxwell's equations can be used to describe the interaction of electric and magnetic fields within any isotropic medium, including a vacuum, under the condition of no accumulation of static charge. With these restrictions the equations are, in mks units,

$$\nabla \times \vec{H} = \gamma \frac{\partial \vec{E}}{\partial t} + \frac{\vec{E}}{r_e} \tag{4-1}$$

$$\nabla \times \vec{E} = -\mu \frac{\partial \vec{H}}{\partial t} \tag{4-2}$$

$$\nabla \cdot \vec{E} = 0 \tag{4-3}$$

$$\nabla \cdot \vec{H} = 0 \tag{4-4}$$

TABLE 4-I.—QUANTITIES FOR USE IN ELECTROMAGNETIC EQUATIONS IN MKS UNITS

Symbol	Quantity	Units	Value
c	Speed of electromagnetic wave propagation.	m/sec	....
c_0	Speed of electromagnetic wave propagation in vacuum.	m/sec	2.9979×10^8
E	Electric intensity........	N/C (newtons/coulomb)	....
H	Magnetic intensity........	C/(m) (sec)	....
K	Dielectric constant, γ/γ_0........	....	....
r_e	Electrical resistivity........	(ohm)(m), $(N)(m^2)(sec)/C^2$	....
S	Instantaneous rate of energy transport per unit area.	$(N)(m)/(sec)(m^2)$	....
x, y, z; x', y', z'	Cartesian coordinate position.	m	....
γ	Electrical permittivity........	$C^2/(N)(m^2)$	....
γ_0	Electrical permittivity of vacuum.	$C^2/(N)(m^2)$	$\frac{1}{4\pi \times 8.9875} \times 10^{-9}$
μ	Magnetic permeability........	$(N)(sec^2)/C^2$	....
μ_0	Magnetic permeability of vacuum.	$(N)(sec^2)/C^2$	$4\pi \times 10^{-7}$

where $\vec{H}$ *and* $\vec{E}$ *are the magnetic and electric intensities, respectively,* γ *is the permittivity,* r_e *is the electrical resistivity, and* μ *is the magnetic permeability of the medium.* The mks units for these quantities are shown in table 4-I. Zero subscripts denote quantities evaluated in a vacuum.

The solutions to these equations will reveal how radiation waves travel within a material and what the interaction is between the electric and magnetic fields. By knowing how the waves move in each of two adjacent media and applying coupling relations at the interface between the media, the relations governing reflection and absorption will be formulated.

4.4 RADIATIVE WAVE PROPAGATION

The derivation of radiative wave propagation for perfect dielectrics will be considered in section 4.4.1, and then media of finite electrical conductivity will be analyzed in section 4.4.2.

4.4.1 Propagation in Perfect Dielectric Media

For simplicity, the situation will first be considered where the medium is a vacuum or other insulator having an electrical resistivity so large that the last term in equation (4–1), $\vec{E}/r_e$, can be neglected. With this simplification, equations (4–1) and (4–2) can be written out in Cartesian coordinates to provide two sets of three equations relating the x, y, and z components of the electric and magnetic intensities, that is,

$$\frac{\partial H_z}{\partial y}-\frac{\partial H_y}{\partial z}=\gamma\frac{\partial E_x}{\partial t} \tag{4–5a}$$

$$\frac{\partial H_x}{\partial z}-\frac{\partial H_z}{\partial x}=\gamma\frac{\partial E_y}{\partial t} \tag{4–5b}$$

$$\frac{\partial H_y}{\partial x}-\frac{\partial H_x}{\partial y}=\gamma\frac{\partial E_z}{\partial t} \tag{4–5c}$$

$$\frac{\partial E_z}{\partial y}-\frac{\partial E_y}{\partial z}=-\mu\frac{\partial H_x}{\partial t} \tag{4–6a}$$

$$\frac{\partial E_x}{\partial z}-\frac{\partial E_z}{\partial x}=-\mu\frac{\partial H_y}{\partial t} \tag{4–6b}$$

$$\frac{\partial E_y}{\partial x}-\frac{\partial E_x}{\partial y}=-\mu\frac{\partial H_z}{\partial t} \tag{4–6c}$$

From equations (4–3) and (4–4), we get

$$\frac{\partial E_x}{\partial x}+\frac{\partial E_y}{\partial y}+\frac{\partial E_z}{\partial z}=0 \tag{4–7}$$

and

$$\frac{\partial H_x}{\partial x}+\frac{\partial H_y}{\partial y}+\frac{\partial H_z}{\partial z}=0 \tag{4–8}$$

The interaction of a wave of incident electromagnetic radiation with a material will be considered. The coordinate system x, y, z will be fixed to the material with the x direction normal to the surface. A second coordinate system x', y', z' is fixed to the path of the incident wave (fig. 4–1).

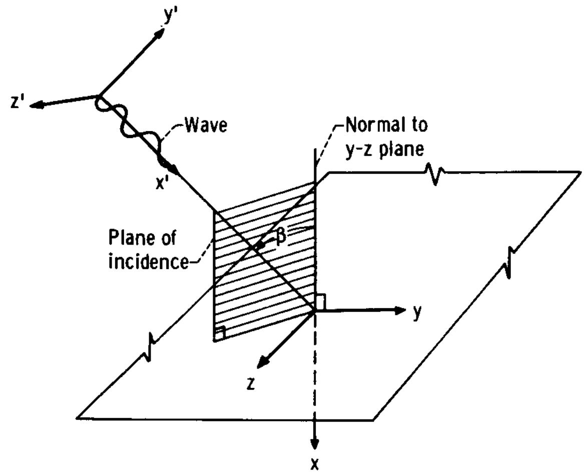

FIGURE 4–1.—Definition of coordinate systems.

For simplicity, a plane wave of incident radiation is considered that is propagating in the x' direction. From the definition of a plane wave, this wave has all quantities concerned with it constant over any $y'-z'$ plane at any given time. Hence $\partial/\partial y' = \partial/\partial z' = 0$. For these conditions, equations (4–5) to (4–8) reduce to the following:

$$0=\gamma\frac{\partial E_{x'}}{\partial t} \tag{4–9a}$$

$$-\frac{\partial H_{z'}}{\partial x'}=\gamma\frac{\partial E_{y'}}{\partial t} \tag{4–9b}$$

$$\frac{\partial H_{y'}}{\partial x'}=\gamma\frac{\partial E_{z'}}{\partial t} \tag{4–9c}$$

$$0=-\mu\frac{\partial H_{x'}}{\partial t} \tag{4–10a}$$

$$-\frac{\partial E_{z'}}{\partial x'}=-\mu\frac{\partial H_{y'}}{\partial t} \tag{4–10b}$$

$$\frac{\partial E_{y'}}{\partial x'}=-\mu\frac{\partial H_{z'}}{\partial t} \tag{4–10c}$$

$$\frac{\partial E_{x'}}{\partial x'}=0 \tag{4–11}$$

$$\frac{\partial H_{x'}}{\partial x'}=0 \tag{4-12}$$

The H components are then eliminated by differentiating equations (4–9b) and (4–9c) with respect to t and equations (4–10b) and (4–10c) with respect to x' to obtain

$$-\frac{\partial^2 H_{z'}}{\partial t \partial x'}=\gamma \frac{\partial^2 E_{y'}}{\partial t^2} \tag{4-13a}$$

$$\frac{\partial^2 H_{y'}}{\partial t \partial x'}=\gamma \frac{\partial^2 E_{z'}}{\partial t^2} \tag{4-13b}$$

$$-\frac{\partial^2 E_{z'}}{\partial x'^2}=-\mu \frac{\partial^2 H_{y'}}{\partial x' \partial t} \tag{4-14a}$$

$$\frac{\partial^2 E_{y'}}{\partial x'^2}=-\mu \frac{\partial^2 H_{z'}}{\partial x' \partial t} \tag{4-14b}$$

Equations (4–13a) and (4–14b) are then combined to eliminate $H_{z'}$ and similarly (4–13b) and (4–14a) to eliminate $H_{y'}$. This provides the following two equations:

$$\mu\gamma \frac{\partial^2 E_{y'}}{\partial t^2}=\frac{\partial^2 E_{y'}}{\partial x'^2} \tag{4-15a}$$

and

$$\mu\gamma \frac{\partial^2 E_{z'}}{\partial t^2}=\frac{\partial^2 E_{z'}}{\partial x'^2} \tag{4-15b}$$

These wave equations govern the propagation of the y' and z' components of the electric intensity in the x' direction. For simplicity in the remainder of the derivation, it will be assumed that the electromagnetic waves are polarized such that the vector $\vec{E}$ is contained only within the x'-y' plane (see fig. 4–2). . Then $E_{z'}$ and its derivatives are zero and equation (4–15b) need not be considered. The vector $\vec{E}$ will have only x' and y' components.

With regard to the x' components of $\vec{E}$ and $\vec{H}$, from equations (4–9a), (4–10a), (4–11), and (4–12), $\partial E_{x'}/\partial t=\partial E_{x'}/\partial x'=\partial H_{x'}/\partial t=\partial H_{x'}/\partial x'=0$. Hence, the electric and magnetic intensity components in the direction of propagation are both steady and independent of the propagation direction, x'. Consequently, the only time-varying component of $\vec{E}$ is $E_{y'}$ as governed by equation (4–15a). Since this component is normal to x', the direction of propagation, the wave is a transverse wave.

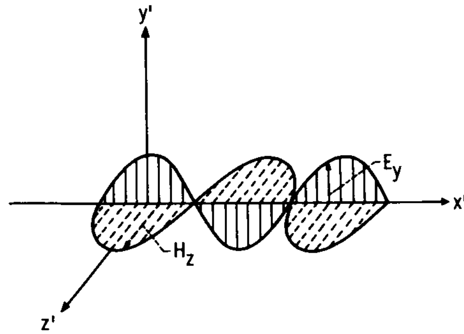

FIGURE 4–2.—Electric field wave polarized in x'-y' plane, traveling in x' direction with companion magnetic field wave.

Equation (4–15a) is recognized as the *wave equation* that describes the propagation of the wave component $E_{y'}$ in the x' direction. The general solution of this equation is

$$E_{y'}=f\left(x'-\frac{t}{\sqrt{\mu\gamma}}\right)+g\left(x'+\frac{t}{\sqrt{\mu\gamma}}\right) \tag{4–16a}$$

where f and g are *any* differentiable functions. The f function provides propagation in the positive x' direction, while the g function accounts for propagation in the negative x' direction. Since the present discussion deals with a wave moving in the positive direction, only the f function will be present in the analysis.

To obtain the wave propagation speed, consider an observer moving along with the wave; the observer will always be at a fixed value of $E_{y'}$. The x' location of the observer must then vary with time such that the argument of f, $x'-(t/\sqrt{\mu\gamma})$ is also fixed. Hence, $dx'/dt=1/\sqrt{\mu\gamma}$. The relation

$$E_{y'}=f\left(x'-\frac{t}{\sqrt{\mu\gamma}}\right) \tag{4–16b}$$

thus represents a wave with y' component $E_{y'}$ propagating in the positive x' direction with speed $1/\sqrt{\mu\gamma}$. In free space, the propagation speed of the wave is c_o, *the speed of electromagnetic radiation in vacuum*, so that there is the relation $c_o=\sqrt{1/\mu_o\gamma_o}$.[11]

[11] Independent measurements of μ_o, γ_o, and c_o validate the result. The fact that Maxwell's equations predict that all electromagnetic radiation propagates in vacuum with speed c_o was considered convincing evidence that light is a form of electromagnetic radiation, and was one of the early triumphs of the electromagnetic theory.

Accompanying the $E_{y'}$ wave component is a companion wave component of the magnetic field. If equation (4–9b) is differentiated with respect to x' and equation (4–10c) with respect to t, the results can be combined to yield

$$\mu\gamma \frac{\partial^2 H_{z'}}{\partial t^2} = \frac{\partial^2 H_{z'}}{\partial x'^2} \tag{4–17}$$

Equation (4–17) is the same wave equation as equation (4–15a). Hence, the $H_{z'}$ component of the magnetic field propagates along with $E_{y'}$ as shown in figure 4–2.

Any propagating waveform as designated by the f function in equation (4–16b) can be represented using Fourier series as a superposition of waves, each wave having a different fixed wavelength. Let us then consider only one such monochromatic wave, and note that any waveform could then be built up from a number of monochromatic components. For convenience in later portions of the analysis, the wave component will be given in complex form.

Suppose that at the origin ($x'=0$) the waveform variation with time is

$$E_{y'} = E_{y'M} \exp (i\omega t)$$

A position on the wave that leaves the origin ($x'=0$) at time t_1 arrives at location x' after a time interval x'/c, where c is the wave speed in the medium. A wave traveling in the positive x' direction is then given by

$$E_{y'} = E_{y'M} \exp \left[i\omega \left(t - \frac{x'}{c} \right) \right]$$

or

$$E_{y'} = E_{y'M} \exp \left[i\omega \left(t - \sqrt{\mu\gamma}\, x' \right) \right] \tag{4–18a}$$

This is a solution to the governing wave equation (eq. 4–15a) as shown by comparison with equation (4–16b). If desired, other forms of the solution can be obtained by using the relations $\omega = 2\pi\nu = 2\pi c/\lambda = 2\pi c_o/\lambda_o$, where λ and λ_o are the wavelengths in the medium and in a vacuum, respectively.

The simple refractive index n is defined as the ratio of the wave speed in vacuum c_o to the speed in the medium $c = 1/\sqrt{\mu\gamma}$. Hence,

$$n = \frac{c_o}{c} = c_o\sqrt{\mu\gamma} = \sqrt{\frac{\mu\gamma}{\mu_o\gamma_o}}$$

and equation (4–18a) can be written as

$$E_{y'} = E_{y'M}\exp\left[i\omega\left(t - \frac{n}{c_o}x'\right)\right] \tag{4–18b}$$

As shown by equation (4–18), the wave propagates with undiminished amplitude through the medium. This is a consequence of the assumption that the medium can be regarded as a perfect dielectric, that is, one with zero conductivity. In many real materials the conductivity is significant and the last term on the right in equation (4–1) cannot be neglected. As will now be shown, the inclusion of this term will lead to an attenuation of the wave.

4.4.2 Propagation in Isotropic Media of Finite Conductivity

For simplicity, a single plane wave is again considered as described by equations (4–18). If an exponential attenuation with distance is introduced (it will be shown by equations (4–21) to (4–23) that this obeys Maxwell's equations), the wave takes the form

$$E_{y'} = E_{y'M}\exp\left[i\omega\left(t - \frac{n}{c_o}x'\right)\right]\exp\left(-\frac{\omega}{c_o}\kappa x'\right) \tag{4–19a}$$

where κ *is termed the extinction coefficient for the medium.* The attenuation term indicates an absorption of the energy of the wave as it travels through the medium. The present form of the attenuation exponent was chosen so that the exponential terms could be combined into the relation

$$E_{y'} = E_{y'M}\exp\left\{i\omega\left[t - (n - i\kappa)\frac{x'}{c_o}\right]\right\} \tag{4–19b}$$

Using complex number relations, equation (4–19b) can be written for later reference as

$$E_{y'} = E_{y'M}\left(\cos\left\{\omega\left[t - (n - i\kappa)\frac{x'}{c_o}\right]\right\} + i\sin\left\{\omega\left[t - (n - i\kappa)\frac{x'}{c_o}\right]\right\}\right) \tag{4–19c}$$

A comparison of equation (4–19b) with equation (4–18b) shows that the simple refractive index n has been replaced by a complex term that will be termed the *complex refractive index* $\bar{n}$. Thus,

$$\bar{n}=n-i\kappa \tag{4–20}$$

It remains to be shown that equation (4–19b) constitutes a solution of the governing equations with the last term on the right of equation (4–1) included. With this term retained, equation (4–15a) takes the form

$$\mu\gamma\frac{\partial^2 E_{y'}}{\partial t^2}=\frac{\partial^2 E_{y'}}{\partial x'^2}-\frac{\mu}{r_e}\frac{\partial E_{y'}}{\partial t} \tag{4–21}$$

The waveform of equation (4–19b) is substituted into equation (4–21) and the following equality results:

$$c_o^2\mu\gamma=(n-i\kappa)^2+\frac{i\mu\lambda_o c_o}{2\pi r_e} \tag{4–22a}$$

where λ_o is the wavelength in a vacuum. Equation (4–22a) provides the relation between the wavelength and the properties of the medium necessary for the wave to satisfy Maxwell's equations. Equating the real and imaginary parts of equation (4–22a) yields

$$n^2-\kappa^2=\mu\gamma c_o^2 \tag{4–22b}$$

and

$$n\kappa=\frac{\mu\lambda_o c_o}{4\pi r_e} \tag{4–22c}$$

These equations may be solved for the components of the complex refractive index, n and κ, in terms of μ, γ, λ_o, c_o, and r_e to yield

$$n^2=\frac{\mu\gamma c_o^2}{2}\left[1+\sqrt{1+\left(\frac{\lambda_o}{2\pi c_o r_e\gamma}\right)^2}\right] \tag{4–23a}$$

and

$$\kappa^2=\frac{\mu\gamma c_o^2}{2}\left[-1+\sqrt{1+\left(\frac{\lambda_o}{2\pi c_o r_e\gamma}\right)^2}\right] \tag{4–23b}$$

In the solutions, positive signs were chosen in front of the square roots since n and κ must physically be positive real quantities.

Comparison of equation (4–18b), the solution to the wave equation for dielectric media, with equation (4–19b), the solution of the wave equation for conducting media, shows the solutions to be identical with one exception: The simple refractive index n appearing in the dielectric solution is replaced for conductors by the complex refractive index $(n-i\kappa)$. This is a most important observation. It means that any general relations that we derive for dielectrics will also hold for conductors provided that we substitute the complex index $(n-i\kappa)$ for the simple refractive index n. Extensive use will be made of this analogy in succeeding sections.

4.4.3 Energy of an Electromagnetic Wave

The instantaneous energy carried per unit time and per unit area by an electromagnetic wave is given by the cross product of the electric and magnetic intensity vectors. This product is called the Poynting vector $\vec{S}$ where

$$\vec{S}=\vec{E}\times\vec{H}$$

and according to the properties of the cross product, $\vec{S}$ is a vector propagating at right angles to the $\vec{E}$ and $\vec{H}$ vectors in a direction defined by the right-hand rule. For the plane wave under consideration as shown in figure 4–2, the propagation is in the positive x' direction. The magnitude of $\vec{S}$ is given for the plane wave by

$$|\vec{S}|=E_{y'}H_{z'} \tag{4–24}$$

If $E_{y'}$ is given by equation (4–19b), then equation (4–10c), which holds for conductors as well as dielectrics, can be used to find $H_{z'}$ as follows:

$$-\mu\frac{\partial H_{z'}}{\partial t}=\frac{\partial E_{y'}}{\partial x'}=\frac{-i\omega}{c_o}(n-i\kappa)E_{y'}=-\frac{i\omega\bar{n}}{c_o}E_{y'}$$

Then noting the t dependence of $E_{y'}$ in equation (4–19b) and integrating yield the following relation between electric and magnetic intensities:

$$H_{z'}=\frac{\bar{n}}{\mu c_o}E_{y'} \tag{4–25}$$

The constant of integration has been taken to be zero. It would correspond to the presence of a steady magnetic intensity in addition to that induced by $E_{y'}$ and is zero for the conditions of the present discussion.

When $H_{z'}$ is substituted in equation (4–24), the magnitude of the Poynting vector becomes

$$|\vec{S}| = \frac{\bar{n}}{\mu c_o} E_{y'}^2 \qquad (4\text{–}26)$$

Thus, the instantaneous energy per unit time and area carried by the wave is proportional to the square of the amplitude of the electric intensity.

Because $|\vec{S}|$ is a monochromatic property, it is seen by examination of its definition to be proportional to the quantity we have called spectral radiant intensity. For radiation passing through a medium, the exponential decay factor in the radiant intensity must then be, by virtue of equation (4–26), equal to the square of the decay term in $E_{y'}$. Thus, from equation (4–19a) the intensity decay factor is $\exp(-2\omega\kappa x'/c_o)$ or $\exp(-4\pi\kappa x'/\lambda_o)$.

4.5 LAWS OF REFLECTION AND REFRACTION

In the previous derivations, the wave nature of the propagating radiation has been revealed and the characteristics of movement through an isotropic medium have been found. The analysis provided a complex refractive index which is related to the velocity of propagation and the wave attenuation as it moves through a medium. Now the interaction of the electromagnetic wave with the interface between two media will be considered. This will provide laws of reflection and refraction in terms of the complex refractive indices which are in turn related to the electric and magnetic properties of the media by means of equations (4–23).

For simplicity throughout this discussion a simple cosine wave will be utilized as obtained by retaining only the cosine term in equation (4–19c). This wave is moving in the x' direction and strikes the interface between two media as shown in figure 4–3. The plane containing both the normal to the interface and the incident direction x' is defined as the *plane of incidence* (fig. 4–1). In figure 4–3 the coordinate system has been drawn so that the y' direction is in the plane of incidence. The interaction of the wave with the interface depends on the wave orientation relative to the plane of incidence. For example, if the amplitude vector of the incident wave is in the plane of incidence (amplitude vector in the y' direction), the amplitude vector is at an angle to the interface. If the amplitude vector is normal to the plane of incidence (amplitude vector in z' direction), the incident wave vector is parallel to the interface.

Figure 4–3 shows a plane transverse wave front propagating in the x' direction. Although the wave will in general bend as it moves across

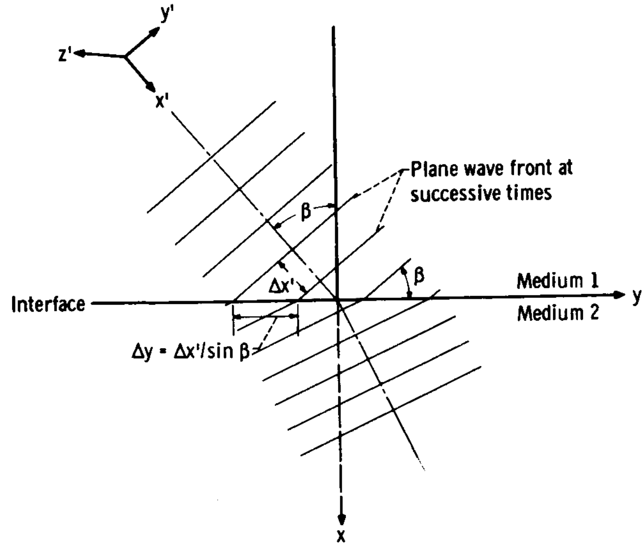

FIGURE 4–3.—Plane wave incident upon interface between two media.

the interface because of the difference in propagation velocity in the two media, the wave will be continuous, so that the velocity component tangent to the interface (y component) is the same in both media at the interface. This continuity relation will be used in deriving the laws of reflection.

Consider now an incident wave $E_{\|,i}$ polarized so that it has amplitude only in the $x'-y'$ plane (fig. 4–4) and, hence, is parallel to the plane of incidence. From equation (4–19c), retaining only the cosine term for simplicity, the wave is characterized by

$$E_{\|,i}=E_{M\|,i}\cos\left(\omega t-\frac{\bar{n}\omega x'}{c_o}\right) \tag{4–27}$$

From figure 4–4(a), the components of the incident wave in the x, y, z coordinate system are (components are taken to be positive in the positive coordinate directions)

$$E_{x,i}=-E_{\|,i}\sin\beta \tag{4–28a}$$

$$E_{y,i}=E_{\|,i}\cos\beta \tag{4–28b}$$

$$E_z=0 \tag{4–28c}$$

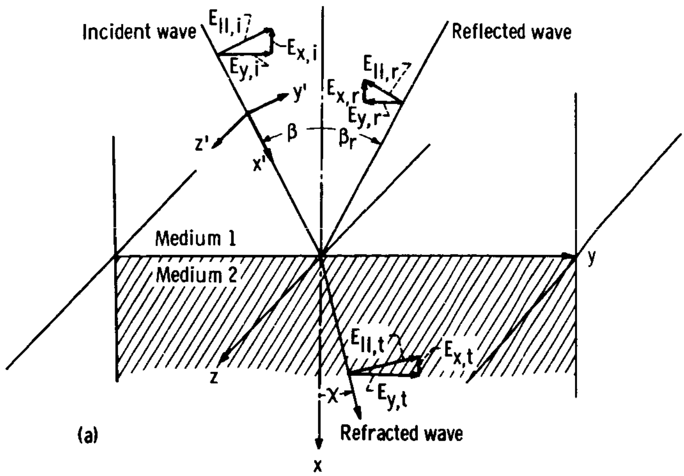

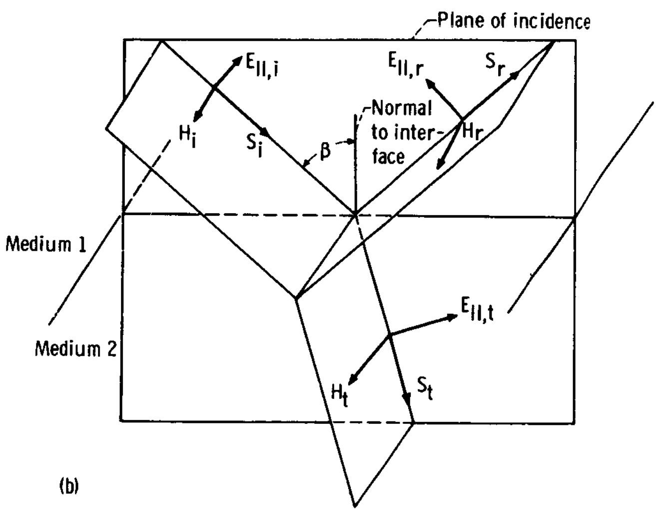

(a) Plane electric field wave polarized in x-y plane striking intersection of two media.
(b) Electric intensity, magnetic intensity, and Poynting vectors for incident wave polarized in plane of incidence.

FIGURE 4–4. — Interaction of electromagnetic wave with boundary between two media.

Substituting equation (4–27) into equations (4–28) and noting that x', the distance the wave front travels in a given time, is related to the y distance the front travels along the interface by

$$x' = y \sin \beta \tag{4-29}$$

as can be seen from figure 4–3, we obtain for the incident components

$$E_{x,i} = -E_{M\|,i} \sin \beta \cos \left[\omega \left(t - \frac{\bar{n}_1 y \sin \beta}{c_o}\right)\right] \tag{4-30a}$$

$$E_{y,i} = E_{M\|,i} \cos \beta \cos \left[\omega \left(t - \frac{\bar{n}_1 y \sin \beta}{c_o}\right)\right] \tag{4-30b}$$

$$E_{z,i} = 0 \tag{4-30c}$$

Upon striking the bounding $y-z$ plane between medium 1 and medium 2, the incident wave separates into a portion $E_{\|,r}$ reflected at angle β_r and a portion $E_{\|,t}$ refracted at angle χ and transmitted into medium 2. From the geometry shown in figure 4–4, the components in the positive coordinate directions of the reflected ray evaluated at the interface are

$$E_{x,r} = -E_{M\|,r} \sin \beta_r \cos \left[\omega \left(t - \frac{\bar{n}_1 y \sin \beta_r}{c_o}\right)\right] \tag{4-31a}$$

$$E_{y,r} = -E_{M\|,r} \cos \beta_r \cos \left[\omega \left(t - \frac{\bar{n}_1 y \sin \beta_r}{c_o}\right)\right] \tag{4-31b}$$

$$E_{z,r} = 0 \tag{4-31c}$$

The direction of $E_{\|,r}$ was drawn such that $E_{\|,r}$, H_r, and S_r would be consistent with the right-hand rule connecting the Poynting vector with the E and H fields. In a similar fashion from figure 4–4, the components of the refracted portion of the wave are

$$E_{x,t} = -E_{M\|,t} \sin \chi \cos \left[\omega \left(t - \frac{\bar{n}_2 y \sin \chi}{c_o}\right)\right] \tag{4-32a}$$

$$E_{y,t} = E_{M\|,t} \cos \chi \cos \left[\omega \left(t - \frac{\bar{n}_2 y \sin \chi}{c_o}\right)\right] \tag{4-32b}$$

$$E_{z,t} = 0 \tag{4-32c}$$

Certain boundary conditions must be followed by the waves at the interface of the two media. The sum of the components, parallel to the interface, of the electric intensities of the reflected and incident waves must be equal to the intensity of the refracted wave in the same plane. This is because the intensity in medium 1 is the superposition of the incident and reflected intensities. For the polarized wave considered here, this condition gives the following for the equality of the y components (parallel to interface) in the two media:

$$\left\{E_{M\|,i} \cos \beta \cos \left[\omega\left(t-\frac{\bar{n}_1 y \sin \beta}{c_o}\right)\right]\right.$$

$$-E_{M\|,r} \cos \beta_r \cos \left[\omega\left(t-\frac{\bar{n}_1 y \sin \beta_r}{c_o}\right)\right]$$

$$\left.=E_{M\|,t} \cos \chi \cos \left[\omega\left(t-\frac{\bar{n}_2 y \sin \chi}{c_o}\right)\right]\right\}_{x=0} \qquad (4\text{–}33)$$

Since equation (4–33) must hold for arbitrary t and y and the angles β, β_r, and χ are independent of t and y, the cosine terms involving time must be equal. This can only be true if

$$\bar{n}_1 \sin \beta=\bar{n}_1 \sin \beta_r=\bar{n}_2 \sin \chi \qquad (4\text{–}34)$$

which provides that

$$\beta=\beta_r \qquad (4\text{–}35)$$

The angle of reflection of an electromagnetic wave is thus equal to its angle of incidence (rotated about the normal to the interface through a circumferential angle of $\theta=\pi$). These are the relations that define mirrorlike or specular reflections as discussed in section 3.5.1.6.2.

Equation (4–34) also yields the following relation between β and χ:

$$\frac{\sin \chi}{\sin \beta}=\frac{\bar{n}_1}{\bar{n}_2}=\frac{n_1-i\kappa_1}{n_2-i\kappa_2} \qquad (4\text{–}36)$$

where the definition of $\bar{n}$ has been substituted from equation (4–20).

For the general case where κ_1 and κ_2 are not zero, equation (4–36) shows that $\sin \chi$ must be complex since $\bar{n}_1$ and $\bar{n}_2$ are complex quantities. This complex ratio of angles can be interpreted to mean that the interaction of the incident wave with the interface will result in both phase and amplitude changes for the refracted wave.

With the cosine terms involving time equal and by using equation (4–35), there also follows from equation (4–33)

$$(E_{M\|,i} \cos \beta-E_{M\|,r} \cos \beta=E_{M\|,t} \cos \chi)_{x=0} \qquad (4\text{–}37)$$

This can be used to find how the reflected electric intensity is related to the incident value. The refracted component $E_{M\|,t}$ must be eliminated and to accomplish this the magnetic intensities must be considered.

The magnetic intensity parallel to the boundary must be continuous at the boundary plane. The magnetic intensity vector is perpendicular to the electric intensity; since the electric intensity being considered is in the plane of incidence, the magnetic intensity will then be parallel to the boundary. Continuity at the boundary provides that

$$(H_i + H_r = H_t)_{x=0} \tag{4-38}$$

The relation between electric and magnetic components was shown in equation (4–25). Although for simplicity this relation was derived for only the specific components $H_{z'}$ and $E_{y'}$, it is true more generally so that the magnitudes of the $\vec{E}$ and $\vec{H}$ vectors are related by

$$|\vec{H}| = \frac{\bar{n}}{\mu c_o} |\vec{E}| \tag{4-39}$$

For both dielectrics and metals the magnetic permeability is very close to that of a vacuum so that $\mu \approx \mu_o$. Then equation (4–38) can be written as

$$(\bar{n}_1 E_{M\|,i} + \bar{n}_1 E_{M\|,r} = \bar{n}_2 E_{M\|,t})_{x=0} \tag{4-40}$$

Equations (4–37) and (4–40) are combined to eliminate $E_{M\|,t}$ and give the reflected electric intensity in terms of the incident intensity

$$\frac{E_{M\|,r}}{E_{M\|,i}} = \frac{\dfrac{\cos\beta}{\cos\chi} - \dfrac{\bar{n}_1}{\bar{n}_2}}{\dfrac{\cos\beta}{\cos\chi} + \dfrac{\bar{n}_1}{\bar{n}_2}} \tag{4-41}$$

If the preceding derivation is repeated for an incident plane electric wave polarized perpendicular to the incident plane, the relation between reflected and incident components is

$$\frac{E_{M\perp,r}}{E_{M\perp,i}} = -\frac{\dfrac{\cos\chi}{\cos\beta} - \dfrac{\bar{n}_1}{\bar{n}_2}}{\dfrac{\cos\chi}{\cos\beta} + \dfrac{\bar{n}_1}{\bar{n}_2}} \tag{4-42}$$

The general relations in this section will now be interpreted for the specific cases of dielectrics and metals.

4.5.1 Incidence and Reflection of a Wave from Dielectric or Transparent Media (κ Negligible Compared to n)

When each of the media either is dielectric or transparent, then $\kappa_1 = \kappa_2 \to 0$ and equation (4–36) reduces to

$$\frac{\sin \chi}{\sin \beta} = \frac{n_1}{n_2} \tag{4–43}$$

This relates the angle of refraction to the angle of incidence by means of the refractive indices. Equation (4–43) is known as *Snell's law*. For the often encountered case when the incident wave is in air ($n_1 \approx 1$), then $n_2 = \sin \beta / \sin \chi$.

For dielectric media, equation (4–41) reduces to

$$\frac{E_{M\|,r}}{E_{M\|,i}} = \frac{\dfrac{\cos \beta}{\cos \chi} - \dfrac{n_1}{n_2}}{\dfrac{\cos \beta}{\cos \chi} + \dfrac{n_1}{n_2}} \tag{4–44}$$

Then equation (4–43) can be used to eliminate n_1/n_2 in terms of $\sin \chi / \sin \beta$. With some manipulation using trigonometric identities, the resulting expression can be cast into the form

$$\frac{E_{M\|,r}}{E_{M\|,i}} = \frac{\tan (\beta - \chi)}{\tan (\beta + \chi)} \tag{4–45}$$

Similarly from equation (4–42)

$$\frac{E_{M\perp,r}}{E_{M\perp,i}} = -\frac{\dfrac{\cos \chi}{\cos \beta} - \dfrac{n_1}{n_2}}{\dfrac{\cos \chi}{\cos \beta} + \dfrac{n_1}{n_2}} = -\frac{\sin (\beta - \chi)}{\sin (\beta + \chi)} \tag{4–46}$$

The energy carried by a wave is proportional to the square of the amplitude of the wave as shown by equation (4–26). Squaring the ratio $E_{M,r}/E_{M,i}$ therefore gives the ratio of the energy reflected from a surface to the energy incident upon the surface from a given direction. This ratio was defined in section 3.5.1.3 as the directional-hemispherical reflectivity. Because electromagnetic radiation for the ideal conditions examined here was shown by equation (4–35) to reflect specularly and because the electromagnetic theory relations are based on monochromatic waves, the energy ratio more exactly gives the directional-hemispherical spectral specular reflectivity as discussed in section 3.5.1.6.2. The spectral dependence arises from the variation of the optical constants with wavelength.

The values of $\rho_s'(\lambda, \beta, \theta)$ for incident parallel and perpendicular polarized components are then obtained as

$$\left.\begin{aligned} \rho_{\|,s}'(\lambda, \beta, \theta) &= \left(\frac{E_{M\|,r}}{E_{M\|,i}}\right)^2 \\ \rho_{\lambda\perp,s}'(\lambda, \beta, \theta) &= \left(\frac{E_{M\perp,r}}{E_{M\perp,i}}\right)^2 \end{aligned}\right\} \tag{4-47}$$

The subscript s denotes a specular reflectivity, and the notation is that used in section 3.5.1.6.2. Because *all* reflectivities predicted by electromagnetic theory are specular, the subscript s will not be carried from this point on in order to simplify an already complicated notation. Further, because of the assumption of isotropic behavior at the surface for the ideal surfaces considered, there is no dependence on the angle θ; hence, this variable will no longer be retained.

For unpolarized incident radiation the electric field has no definite orientation relative to the incident plane and can be resolved into parallel and perpendicular components that are equal. Then the directional-hemispherical spectral specular reflectivity is the average of $\rho_{\lambda\|}'(\lambda, \beta)$ and $\rho_{\lambda\perp}'(\lambda, \beta)$. By using equations (4–45) to (4–47), the result is

$$\begin{aligned} \rho_\lambda'(\lambda, \beta) &= \frac{\rho_{\lambda\|}'(\lambda, \beta)+\rho_{\lambda\perp}'(\lambda, \beta)}{2} \\ &= \frac{1}{2}\left[\frac{\tan^2(\beta-\chi)}{\tan^2(\beta+\chi)}+\frac{\sin^2(\beta-\chi)}{\sin^2(\beta+\chi)}\right] = \frac{1}{2}\frac{\sin^2(\beta-\chi)}{\sin^2(\beta+\chi)}\left[1+\frac{\cos^2(\beta+\chi)}{\cos^2(\beta-\chi)}\right] \end{aligned} \tag{4-48}$$

Equation (4–48) is known as *Fresnel's equation*, and it gives the directional-hemispherical spectral reflectivity for an unpolarized ray incident upon a dielectric medium. The relation between χ and β is given by equation (4–43).

In the special case when the incident radiation is normal to the interface between the two media, $\cos\beta=\cos\chi=1$ and equations (4–44) and (4–46) yield

$$\left|\frac{E_{M\|,r}}{E_{M\|,i}}\right| = \left|\frac{E_{M\perp,r}}{E_{M\perp,i}}\right| = \frac{1-\dfrac{n_1}{n_2}}{1+\dfrac{n_1}{n_2}} = \frac{n_2-n_1}{n_2+n_1} \tag{4-49}$$

The normal directional-hemispherical spectral specular reflectivity is then

$$\rho'_{\lambda,n}(\lambda)=\rho'_{\lambda}(\lambda,\ \beta=\beta_r=0)=\left(\frac{n_2-n_1}{n_2+n_1}\right)^2 \tag{4-50}$$

For a wave entering the dielectric from air ($n_1 \approx 1$),

$$\rho'_{\lambda,n}(\lambda)=\left(\frac{n_2-1}{n_2+1}\right)^2 \tag{4-51}$$

The foregoing reflectivities are spectral quantities because n_1 and n_2 are functions of λ.

4.5.2 **Incidence on an Absorbing Medium**

When the media have significant κ values, the theoretical relations are of the same form as the dielectric case except that the complex dielectric constant $\bar{n}$ is retained. The angles β and χ are related by equation (4–36), and the relations between reflected and incident wave amplitudes given by equations (4–41) and (4–42) can be used for the wave interaction at the interface between two metals or between an absorbing dielectric and a metal.

For a ray incident normal to the interface, equations (4–41) and (4–42) yield, in an analogous fashion to equation (4–50),

$$\rho'_{\lambda,n}(\lambda)=\left[\frac{(n_2-i\kappa_2)-(n_1-i\kappa_1)}{(n_2-i\kappa_2)+(n_1-i\kappa_1)}\right]^2 \tag{4-52}$$

This is a complex quantity and can be interpreted as giving both the magnitude and phase change of the reflected wave. The ratio of the magnitude of the reflected energy to that of the incident energy is obtained by multiplying by the complex conjugate of equation (4–52) to give

$$\rho'_{\lambda,n}(\lambda)=\frac{(n_2-n_1)^2+(\kappa_2-\kappa_1)^2}{(n_2+n_1)^2+(\kappa_2+\kappa_1)^2} \tag{4-53}$$

For an incident ray in air ($n_1=1$, $\kappa_1\approx 0$) striking an absorbing material (n_2, κ_2), equation (4–53) reduces to

$$\rho'_{\lambda,n}(\lambda)=\frac{(n_2-1)^2+\kappa_2^2}{(n_2+1)^2+\kappa_2^2} \tag{4-54}$$

When the material is transparent ($\kappa_2 \to 0$), equation (4–54) reduces to equation (4–51).

For oblique incidence the directional-hemispherical reflectivity can be obtained from equations (4–41) and (4–42). For an incident ray polarized parallel to the plane at incidence, equation (4–41) gives the complex ratio

$$\frac{E_{M\|,r}}{E_{M\|,i}}=\frac{\dfrac{\cos\beta}{\cos\chi}-\left(\dfrac{n_1-i\kappa_1}{n_2-i\kappa_2}\right)}{\dfrac{\cos\beta}{\cos\chi}+\left(\dfrac{n_1-i\kappa_1}{n_2-i\kappa_2}\right)} \tag{4–55}$$

The reflectivity is obtained as the square of the ratio of the reflected magnitude to the incident magnitude, which is found by multiplying equation (4–55) by its complex conjugate. This yields

$$\rho'_{\lambda\|}(\lambda,\beta)=\frac{(n_2\cos\beta-n_1\cos\chi)^2+(\kappa_2\cos\beta-\kappa_1\cos\chi)^2}{(n_2\cos\beta+n_1\cos\chi)^2+(\kappa_2\cos\beta+\kappa_1\cos\chi)^2} \tag{4–56}$$

Similarly for the polarized component perpendicular to the incident plane

$$\rho'_{\lambda\perp}(\lambda,\beta)=\frac{(n_2\cos\chi-n_1\cos\beta)^2+(\kappa_2\cos\chi-\kappa_1\cos\beta)^2}{(n_2\cos\chi+n_1\cos\beta)^2+(\kappa_2\cos\chi+\kappa_1\cos\beta)^2} \tag{4–57}$$

As before, if the incident beam has no specific polarization, the reflectivity is an average of the parallel and perpendicular components as in equation (4–48).

To this point in this chapter, the wave nature of radiation has been shown from a consideration of Maxwell's equations. Then the interaction of these waves with nonabsorbing and absorbing media has been discussed in terms of the refractive index n and the complex refractive index $\bar{n}$. Now the results will be applied more specifically to a discussion of some actual radiative properties.

4.6 APPLICATION OF ELECTROMAGNETIC THEORY RELATIONS TO RADIATIVE PROPERTY PREDICTIONS

The electromagnetic theory as applied here to radiative property prediction has a number of drawbacks that limit its usefulness for practical calculations. Aside from the many assumptions used in the derivations, the theory itself becomes invalid when the frequencies being considered become of the order of molecular vibrational frequencies.

These qualifications restrict the equations used here to wavelengths longer than in the visible spectrum.

The theory completely neglects the effects of surface conditions on the radiative properties. This is its most serious limitation, since perfectly clean optically smooth interfaces are rarely encountered in practice. The greatest usefulness of the theory is probably in providing a means for intelligent extrapolation when only limited experimental data are available. In the following sections, the equations of electromagnetic theory that are useful for the prediction of properties will be examined and the assumptions inherent in their derivation discussed.

4.6.1 Radiative Properties of Dielectric ($\kappa \to 0$)

The equations to be examined in this section all contain these assumptions: (1) The medium is isotropic; that is, its electrical and internal optical properties are independent of direction. (2) The magnetic permeability of the medium is equal to that of a vacuum. (3) There is no accumulation of static electrical charge. (4) No externally produced electrical conduction currents are present.

The measured index of refraction of the medium is, in general, a function of wavelength, and thus any calculated radiative properties will be wavelength dependent. If, however, the refractive index is calculated from the permittivity γ or the *dielectric constant* K (where $K=\gamma/\gamma_o$), which are not generally given as functions of wavelength, the spectral dependency is lost. Because of these considerations, no notation is used in the following equations to signify spectral dependence, but the reader should be aware that such dependence can be included if the optical or electromagnetic properties are known as a function of wavelength.

The surfaces are further assumed to be "optically smooth," that is, smooth in comparison with the wavelength of the incident radiation so that specular reflections result.

4.6.1.1 *Reflectivity.*—Under the aforementioned restrictions, the directional-hemispherical specular reflectivity of a wave incident on a surface at angle β and polarized parallel to the plane of incidence may be obtained from equations (4–47) and (4–45) as

$$\rho'_{\parallel}(\beta)=\left[\frac{\tan(\beta-\chi)}{\tan(\beta+\chi)}\right]^2 \tag{4–58}$$

Similarly, from equations (4–47) and (4–46), for a wave polarized perpendicular to the incidence plane

$$\rho'_{\perp}(\beta) = \left[\frac{\sin(\beta-\chi)}{\sin(\beta+\chi)}\right]^2 \tag{4–59}$$

where χ is the angle of refraction in the medium on which the ray impinges. For a given incident angle β, the angle χ can be determined from equation (4–43) as

$$\frac{\sin\chi}{\sin\beta} = \frac{n_1}{n_2} = \frac{\sqrt{\gamma_1}}{\sqrt{\gamma_2}} = \frac{\sqrt{K_1}}{\sqrt{K_2}} \tag{4–60}$$

where γ is the permittivity, K is the dielectric constant, and n is the refractive index; the n, γ, and K are assumed not to have any angular dependence.

The reflectivity for unpolarized radiation was shown in equation (4–48) (Fresnel's equation) to be given by

$$\rho'(\beta) = \frac{1}{2}\frac{\sin^2(\beta-\chi)}{\sin^2(\beta+\chi)}\left[1+\frac{\cos^2(\beta+\chi)}{\cos^2(\beta-\chi)}\right] \tag{4–61}$$

EXAMPLE 4–1: An unpolarized beam of radiation is incident at angle $\beta = 30°$ from the normal on a dielectric surface (medium 2) in air (medium 1). The surface is of a material where $\kappa_2 \approx 0$ and whose index of refraction is $n_2 = 3.0$. Find the directional-hemispherical reflectivity for the polarized components and the unpolarized beam.

Because the incident beam is in air, $n_1 - i\kappa_1 \approx 1$, and from equation (4–60), $n_1/n_2 = 1/3.0 = \sin\chi/\sin 30°$; therefore, $\chi = 9.6°$. The reflectivity for the parallel component is, from equation (4–58),

$$\rho'_{\parallel}(\beta=30°) = \{[\tan(20.4°)]/[\tan(39.6°)]\}^2 = 0.202$$

and that for the perpendicular component is, from equation (4–59),

$$\rho'_{\perp}(\beta=30°) = \{[\sin(20.4°)]/[\sin(39.6°)]\}^2 = 0.301$$

The reflectivity for the unpolarized beam obtained from equation (4–61) or, more simply here, from the average of the components is

$$\rho'(\beta=30°) = (0.202+0.301)/2 = 0.252$$

By performing the type of calculation shown in example 4–1 for various incidence angles and ratios of the indices of refraction, the reflectivity can be tabulated or presented graphically. This is a directional-hemispherical reflectivity in that it provides all the reflected energy resulting from an incident beam from one direction. It is a spectral quantity in the sense that the indices of refraction can correspond to a particular wavelength if the details of the wavelength dependency are available. Finally, it is a specular quantity in that it obeys the constraints of equation (4–35).

4.6.1.2 *Emissivity.*—After the reflectivity has been evaluated, the directional spectral emissivity can be found from equation (3–37) as

$$\epsilon'(\beta) = 1 - \rho'(\beta)$$

where the body is opaque.

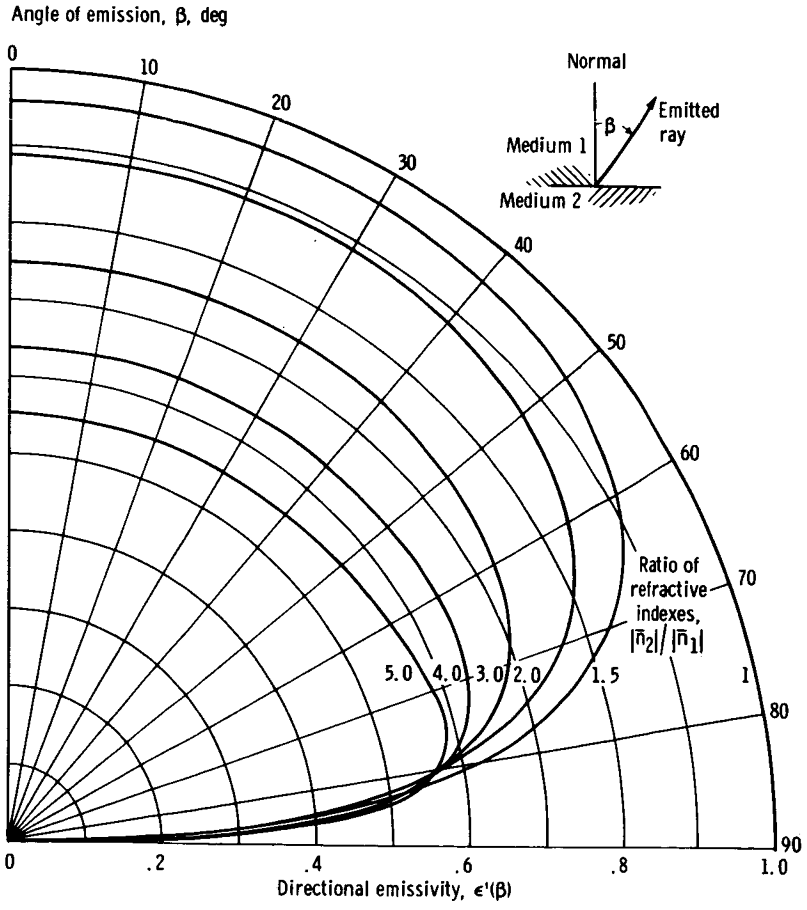

FIGURE 4–5.—Directional emissivity as predicted from electromagnetic theory.

A graph of the directional emissivity is shown in figure 4–5 for various ratios of $|\bar{n}_2|/|\bar{n}_1|$, which is a more general ratio than n_2/n_1 as it includes the cases where κ_1 and κ_2 are not zero. For an incident beam in air ($|\bar{n}_1| \approx 1$), the ratio reduces to the absolute magnitude of the complex refractive index for the material on which the beam is incident. For an insulating material where $\kappa \ll n$, as is being discussed in this section, figure 4–5 can be regarded as giving the emissivity of a dielectric into air when the value for the parameter $|\bar{n}_2|/|\bar{n}_1|$ is set equal to the simple refractive index n of the dielectric material. In the following discussion, figure 4–5 will be interpreted in this sense.

For $n=1$, the emissivity becomes unity (blackbody case), and the curve for this value on figure 4–5 is circular with a radius of unity. As n increases, the curves remain circular up to about $\beta=70°$ and then begin to decrease rapidly to a zero value at $\beta=90°$. Thus, dielectric materials emit poorly at large angles from the normal direction. For angles of less than 70°, the emissivities are quite high so that, in a hemispherical sense, dielectrics are good emitters. It should be emphasized again that the assumptions used for the present interpretation of Maxwell's equations restrict these findings to wavelengths longer than the visible spectrum, as borne out by comparisons with experimental measurements.

From the directional spectral emissivity, the hemispherical spectral emissivity can be computed from equation (3–5) to be

$$\epsilon_\lambda(\lambda, T_A) = \frac{1}{\pi} \int_\cap \epsilon'_\lambda(\lambda, \beta, \theta, T_A) \cos \beta \, d\omega$$

Then an integration can be performed over all wavelengths to obtain the hemispherical total emissivity as given by equation (3–6a). Since the optical properties are generally not known in sufficient detail so that a wavelength integration of theoretical ϵ_λ can be made, in the theory spectral ϵ_λ values are used for total ϵ values for lack of anything better.

The integration of $\epsilon'(\beta)$ to evaluate ϵ is complicated by the implicit relation between χ and β, and, hence, the integration is performed numerically. The normal emissivity provides a convenient value to which the hemispherical value may be referenced. The normal emissivity can be computed from equation (4–51) as

$$\epsilon'_n = 1 - \left(\frac{n_2 - 1}{n_2 + 1}\right)^2 \tag{4–62}$$

for emission from a dielectric (medium 2) into air. The ϵ'_n is shown as a function of n in figure 4–6(a). Note that normal emissivities less than about 0.50 correspond to $n > 6$. Such large n values are not common

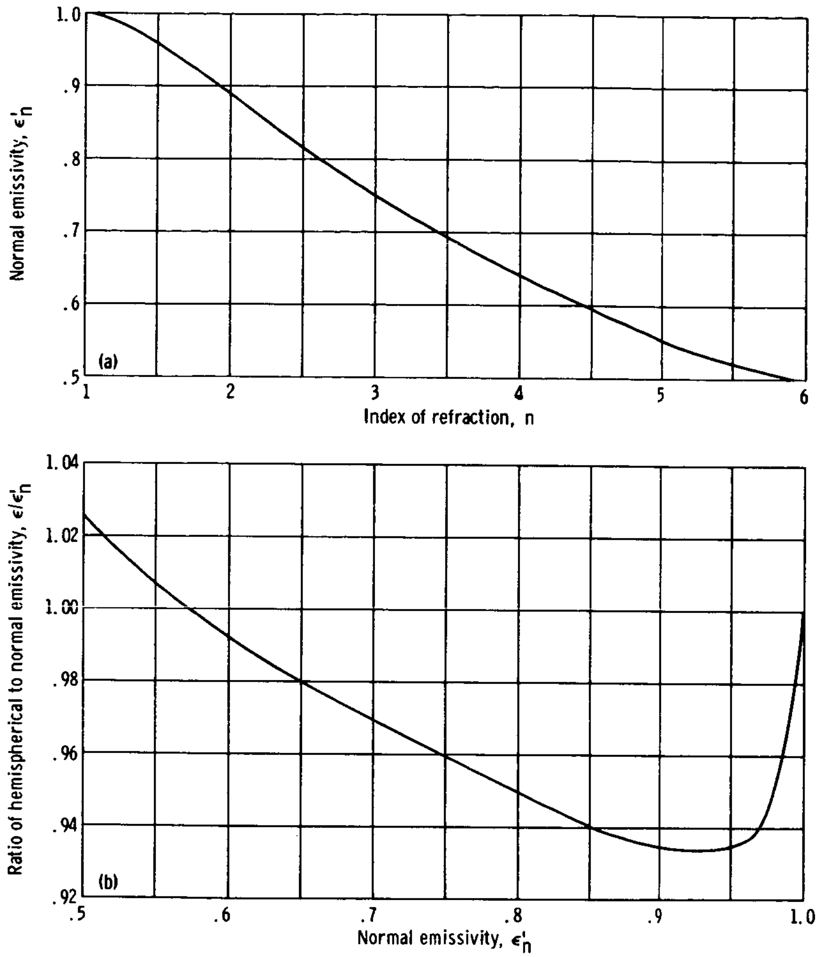

(a) Normal emissivity as function of refractive index.
(b) Relation between normal and hemispherical emissivity.

FIGURE 4–6.—Predicted emissivities of dielectric materials .

for dielectrics, so that the curve is not extended to smaller ϵ'_n. The ratio of hemispherical to normal emissivity for dielectrics is provided as a function of normal emissivity in figure 4–6(b).

EXAMPLE 4–2: A dielectric has a refractive index of 1.41. What is its hemispherical emissivity into air at the wavelength where the refractive index was measured?

From equation (4–62) the normal emissivity is

$$\epsilon'_n = 1 - (0.41/2.41)^2 = 0.97$$

From figure 4–6(b), $\epsilon/\epsilon_n'=0.94$ and the hemispherical emissivity is $\epsilon=0.97\times0.94=0.91$.

For a large n the ϵ_n' values are relatively low, and with increasing n the curves shown in figure 4–5 depart more and more from the circular form of the curve corresponding to $n=1$. Figure 4–6(b) reveals that the flattening of the curves of figure 4–5 in the region near the normal causes the hemispherical emissivity to exceed the normal value at large n. For n near unity (ϵ_n' near 1), the hemispherical value is lower than the normal value because of the poor emission at large β as shown in figure 4–5.

4.6.2 Radiative Properties of the Metals

The properties of metals were shown to be given by relations of the same form as for insulating materials. For electrical conductors, however, the extinction factor κ cannot be neglected with respect to the refractive index n. As will be shown, there are certain simplifying assumptions that lead to more useful equations than the general results from the theory. The main difficulty in application of the theoretical results is that the optical properties for use in these equations are difficult to obtain; when measured values are available, they are often inaccurate because of the experimental problems involved in their measurement.

4.6.2.1 *Reflectivity and emissivity relations using optical constants.*— For most metals, the simple index of refraction n and the extinction coefficient κ are quite large at wavelengths longer than those in the visible region. Because of this fact, the angle of refraction χ is quite small and cos χ will be close to unity for incidence from a dielectric having n near unity. This is shown as follows:

For a metal, the absolute magnitude of the complex refractive index ratio relating χ and β can be obtained by multiplying by the complex conjugate of equation (4–36). This gives, for $|\bar{n}_1|\approx1$ (incidence through dielectric or air (medium 1) onto a metal (medium 2)),

$$|\bar{n}_2|=|n_2-i\kappa_2|=\sqrt{n_2^2+\kappa_2^2}=\frac{\sin\beta}{\sin\chi} \tag{4–63a}$$

The maximum value of sin β is unity; hence, for a given n_2 and κ_2 the maximum value of sin χ is

$$\sin\chi=\frac{1}{\sqrt{n_2^2+\kappa_2^2}} \tag{4–63b}$$

For the large n_2 and κ_2 typical of metals (this will be demonstrated later by table 4–II), χ will have a small value. If $\sqrt{n_2^2+\kappa_2^2}$ has a value greater than about 3.3, χ will be less than 18°. However, cos 18° is about 0.95. Thus, *if* $\sqrt{n_2^2+\kappa_2^2} > 3.3$, *cos* χ *can be set equal to unity with an error of less than 5 percent.*

This fact allows us as a good approximation to set cos χ in equations (4–41) and (4–42) equal to unity; these equations then reduce to, for incidence through a dielectric,

$$\frac{E_{M\|,r}}{E_{M\|,i}}=\frac{\cos\beta-\dfrac{n_1}{\bar{n}_2}}{\cos\beta+\dfrac{n_1}{\bar{n}_2}} \tag{4–64a}$$

and

$$\frac{E_{M\perp,r}}{E_{M\perp,i}}=-\frac{\dfrac{1}{\cos\beta}-\dfrac{n_1}{\bar{n}_2}}{\dfrac{1}{\cos\beta}+\dfrac{n_1}{\bar{n}_2}} \tag{4–64b}$$

where n_1 is close to unity.

Equations (4–56) and (4–57) give the general reflectivity relations. For the incident beam from a transparent or dielectric medium, the reflectivity components for the metal (cos $\chi=1$) become

$$\rho_{\|}'(\beta)=\frac{\left(n_2-\dfrac{n_1}{\cos\beta}\right)^2+\kappa_2^2}{\left(n_2+\dfrac{n_1}{\cos\beta}\right)^2+\kappa_2^2} \tag{4–65}$$

and

$$\rho_{\perp}'(\beta)=\frac{(n_2-n_1\cos\beta)^2+\kappa_2^2}{(n_2+n_1\cos\beta)^2+\kappa_2^2} \tag{4–66}$$

These expressions are the squares of the real parts of equations (4–64).

For a beam incident through air on a metal with complex refractive index $n_2-i\kappa_2$, these equations reduce to (since the refractive index for air is $n_1=1$ as a very good approximation)

$$\rho_{\|}'(\beta)=\frac{(n_2\cos\beta-1)^2+(\kappa_2\cos\beta)^2}{(n_2\cos\beta+1)^2+(\kappa_2\cos\beta)^2} \tag{4–67}$$

and

$$\rho'_{\perp}(\beta)=\frac{(n_2-\cos\beta)^2+\kappa_2^2}{(n_2+\cos\beta)^2+\kappa_2^2} \tag{4-68}$$

For an unpolarized beam,

$$\rho'(\beta)=\frac{\rho'_{\perp}(\beta)+\rho'_{\parallel}(\beta)}{2} \tag{4-69}$$

The corresponding emissivity values are found from $\epsilon'(\beta)=1-\rho'(\beta)$, and these simplify to

$$\epsilon'_{\parallel}(\beta)=\frac{4n_2\cos\beta}{(n_2^2+\kappa_2^2)\cos^2\beta+2n_2\cos\beta+1} \tag{4-70}$$

$$\epsilon'_{\perp}(\beta)=\frac{4n_2\cos\beta}{\cos^2\beta+2n_2\cos\beta+n_2^2+\kappa_2^2} \tag{4-71}$$

For an unpolarized beam,

$$\epsilon'(\beta)=\frac{\epsilon'_{\perp}(\beta)+\epsilon'_{\parallel}(\beta)}{2} \tag{4-72}$$

The use of these emissivity relations is demonstrated in figure 4-7 for a pure smooth platinum surface at a wavelength of 2 μm, and it is evident by comparison with the experimental data that, although the general shape of the curve predicted by equation (4-72) is correct, the magnitude is in error. The data for n and κ for platinum, taken from the Handbook of Chemistry and Physics, 44th Edition (ref. 2), are $n=5.7$ and $\kappa=9.7$.[12] A comment as to the difficulty of the measurement of the optical properties of metals, perhaps because of the large influence of metal purity and the ease of contamination, is that the 35th edition of the Handbook lists values for platinum from an older measurement for identical conditions as $n=0.70$ and $\kappa=3.5$. The newer measurements thus differ by a factor of 8 in refractive index and 2.8 in the extinction factor.

Although the inaccuracy of the optical constants presents a difficulty in the precise evaluation of radiative property values, the theory does provide an understanding of the directional behavior of the properties.

---

[12] The reader should be aware that the complex refractive index can be defined in other ways than $\bar{n}=n-i\kappa$ as used here. It is also commonly given as $\bar{n}=n-in\kappa$ and occasionally with a positive sign in front of the extinction factor. When consulting data references, care should be taken in determining what definition is used so that conversion to the system used in this report can be carried out if necessary.

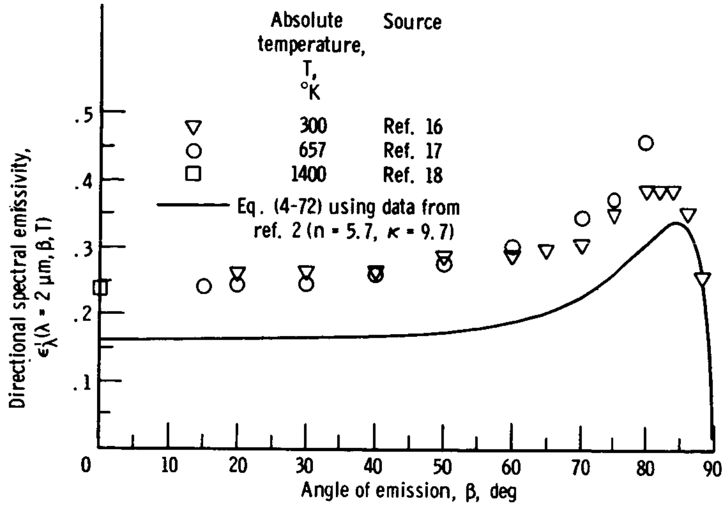

FIGURE 4–7.—Directional spectral emissivity of platinum at wavelength $\lambda = 2\ \mu m$.

For metals, as illustrated by the results for platinum in figure 4–7, the emissivity is essentially constant for about 40° away from the normal and then it increases to a maximum located within a few degrees of the tangent to the surface. This angular dependence for emission from metals is in contrast to the behavior for dielectrics for which the emission decreases substantially as the angle from the normal becomes larger than about 60°.

In table 4–II, the prediction of normal spectral emissivity by using equation (4–72) with $\beta = 0$ is compared with measured values. All data are taken from reference 2. A wavelength of $\lambda = 0.589\ \mu m$ is used for some of the comparisons because of the wealth of data available. This is because of the ease with which a sodium vapor lamp, which emits at this wavelength, can be employed as an intense monochromatic energy source in the laboratory. Since this wavelength is in the visible range, it is in the borderline short wavelength region where the electromagnetic theory becomes inaccurate.

Comparison of the values in the table 4–II shows the agreement between predicted and measured $\epsilon'_{\lambda,n}$ to be good, for example, for nickel and tungsten, but a factor of 4 in error for magnesium. For the cases of poor agreement, it is difficult to ascribe the error specifically to the optical constants, the measured emissivity, or the theory itself. Any or all could contribute to the discrepancy. Most probably the optical constants are somewhat in error, and the experimental samples do not meet the standards of perfection in surface preparation demanded by the theory.

TABLE 4-II. – COMPARISON OF SPECTRAL NORMAL EMISSIVITY PREDICTIONS FROM ELECTROMAGNETIC THEORY WITH EXPERIMENT

[Data from ref. 2]

Metal	Wavelength, λ, μm	Refractive index, n	Extinction coefficient, κ	Spectral normal emissivity, $\epsilon'_{\lambda,n}(\lambda)$	
				Experimental	Calculated from equation (4–72)
Copper	0.650 2.25 4.00	0.44 1.03 1.87	3.26 11.7 21.3	0.20 .041 .027	0.140 .029 .014
Gold	0.589 2.00	0.47 .47	2.83 12.5	0.176 .032	0.184 .012
Iron	0.589	1.51	1.63	0.43	0.674
Magnesium	0.589	0.37	4.42	0.27	0.070
Nickel	0.589 2.25	1.79 3.95	3.33 9.20	0.355 .152	0.381 .145
Silver	0.589 2.25 4.50	0.18 .77 4.49	3.64 15.4 33.3	0.074 .021 .015	0.049 .013 .014
Tungsten	0.589	3.46	3.25	0.49	0.455

The hemispherical emissivity for a metal (having complex refractive index $n-i\kappa$) in air or vacuum is found by substituting equation (4–72) into equation (3–5). After carrying out the integration, this yields

$$\epsilon = 4n - 4n^2 \log_e \left(\frac{1+2n+n^2+\kappa^2}{n^2+\kappa^2}\right) + \frac{4n(n^2-\kappa^2)}{\kappa} \tan^{-1}\left(\frac{\kappa}{n+n^2+\kappa^2}\right)$$
$$+ \frac{4n}{n^2+\kappa^2} - \frac{4n^2}{(n^2+\kappa^2)^2} \log_e (1+2n+n^2+\kappa^2)$$
$$- \frac{4n(\kappa^2-n^2)}{\kappa(n^2+\kappa^2)^2} \tan^{-1} \frac{\kappa}{1+n} \tag{4-73}$$

Evaluation of equation (4–73) is difficult because it involves small dif-

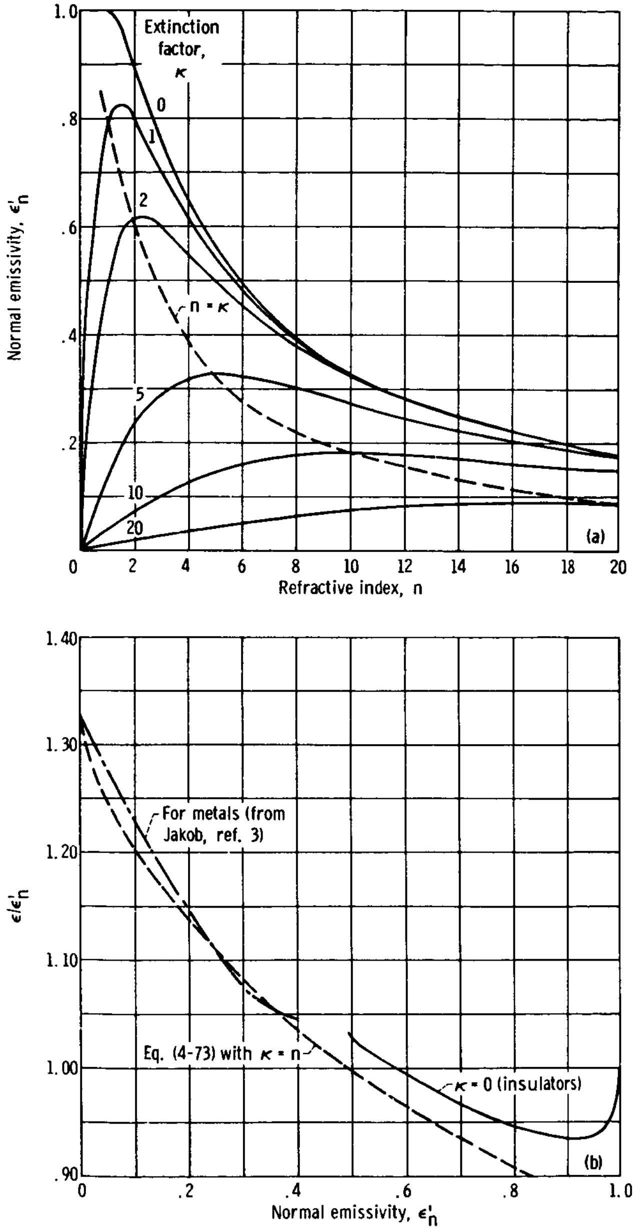

(a) Normal emissivity of attenuating media emitting into air.
(b) Ratio of hemispherical to normal emissivity.

FIGURE 4-8.—Emissivity of metals as computed from electromagnetic theory.

ferences of large numbers, and many significant figures must be carried in the calculations.

From equation (4–72), the normal emissivity from a metal into air can be computed by letting $\beta=0$, and this is shown in figure 4–8(a) as a function of n and κ. Note that, because the velocity of the waves in the medium must be less than c_o, the curve for $\kappa=0$ cannot extend below $n=1$.

It is of interest to compare the hemispherical emissivity with the normal value. The practical use for this comparison arises from the fact that it is often the normal emissivity that is measured experimentally because of the relative simplicity of placing a radiation detector in this one orientation. With regard to the total amount of heat dissipation, however, it is the hemispherical emissivity that is desired.

Figure 4–8(b) shows the ratio of hemispherical to normal emissivity as a function of the normal value. Equation (4–73) divided by ϵ_n' has been plotted for the case where $\kappa=n$. This is valid at large wavelengths for many metals as shown in the next section. The curve is seen to be close to that presented by Jakob (ref. 3) for metals as derived from approximate equations and to lie somewhat below the curve for insulators (as taken from fig. 4–6(b)) at high normal emissivities.

For polished metals when ϵ_n' is less than about 0.5, the hemispherical emissivity is larger than the normal value because of the increase in emissivity in the direction near tangency to the surface as was pointed out in figure 4–7. Hence, in a table listing emissivity values for polished metals, if the ϵ_n' is given, it should be multiplied by a factor larger than unity such as obtained from figure 4–8(b) to estimate the hemispherical value. Real surfaces that have roughness or may be slightly oxidized often tend to have a directional emissivity that is more diffuse than for polished specimens. For a practical case, therefore, the emissivity ratio may be closer to unity than indicated by figure 4–8(b).

4.6.2.2 *Relation between emissive and electrical properties.*—The wave solutions to Maxwell's equations provide a means for determining n and κ from the electric and magnetic properties of a material. The relations for n and κ are given by equations (4–23). For metals where r_e is small, and for relatively long wavelengths, say $\lambda_o > \sim 5$ μm, the term $\lambda_o/(2\pi c_o r_e \gamma)$ becomes dominating, and equations (4–23) then reduce to (the magnetic permeability is taken equal to μ_o)

$$n=\kappa=\sqrt{\frac{\lambda_o \mu_o c_o}{4\pi r_e}}=\sqrt{\frac{30\lambda_o}{r_e}} \tag{4–74}$$

for all quantities in mks units. If λ_o is taken in microns and r_e has the units of ohm-centimeters (rather than ohm-meters), equation (4–74) becomes

$$n=\kappa=\sqrt{\frac{0.003\lambda_o}{r_e}} \tag{4–75}$$

This is known as the Hagen-Rubens equation (ref. 4). Predictions of n and κ from this equation can be greatly in error, as shown in table 4–III. Nevertheless, some useful results will eventually be obtained.

With the simplification that $n=\kappa$, an equation such as equation (4–54) reduces to the following expression for a material with refractive index n radiating in the normal direction into air or vacuum:

$$\epsilon'_{\lambda,n}(\lambda)=1-\left(\frac{2n^2-2n+1}{2n^2+2n+1}\right) \tag{4–76a}$$

TABLE 4–III. — COMPARISON OF MEASURED OPTICAL CONSTANTS WITH ELECTROMAGNETIC THEORY PREDICTIONS

Metal	Wave-length, λ_o, μm	Measured values			$n=\kappa$ calculated from equation (4–75)	Spectral normal emissivity, $\epsilon'_{\lambda,n}(\lambda)$	
		Electrical resistivity (at 20° C), r_e, (ohm) (cm) ([a])	Refractive index, n	Extinction coefficient, κ		Measured	Calculated from equation (4–77)
Aluminum.	12	2.82×10^{-6}	[b] 33.6	[b] 76.4	113	[a] 0.02	0.018
Copper.....	4.20	1.72×10^{-6}	[b] 1.92	[b] 22.8	86	[a,c] 0.027	......
	4.20	1.72	[b] 1.92	[b] 22.8	86	[d] .015	0.023
	5.50	1.72	[a] 3.16	[a] 28.4	98	[d] .012	.020
Gold........	5.00	2.44×10^{-6}	[a] 1.81	[a] 32.8	78	[a,c] 0.031	0.026
Platinum..	5.00	10×10^{-6}	[a] 11.5	[a] 15.7	39	[d] 0.050	0.051
Silver.......	4.50	1.63×10^{-6}	[a] 4.49	[a] 33.3	91	[a,c] 0.015	0.022
	4.37	1.63	[b] 4.34	[b] 32.6	90	[a,c] .015	.022

[a] Data from ref. 2.
[b] Data from ref. 14.
[c] Measured at 4 μm.
[d] Data from ref. 15.

Although there is no difficulty in evaluating equation (4–76a), a further simplification is often made by expanding in a series to give

$$\epsilon'_{\lambda,n}(\lambda) = 1-\left(1-\frac{2}{n}+\frac{2}{n^2}-\frac{1}{n^3}+\frac{1}{2n^5}-\frac{1}{2n^6}+\cdot\cdot\cdot\right) \qquad \text{(4–76b)}$$

Because the index of refraction of metals as predicted from equation (4–75) is generally large at the long wavelengths being considered here, $\lambda_o > \sim 5$ μm (see table 4–III, column 6), only the first two terms of the series often are retained, and the normal spectral emissivity is then given by substituting equation (4–75) to obtain the *Hagen-Rubens emissivity relation*

$$\epsilon'_{\lambda,n}(\lambda) = 1-\rho'_{\lambda,n}(\lambda) \approx 1-\left(1-\frac{2}{n}\right) = \frac{2}{\sqrt{\dfrac{0.003\lambda_o}{r_e}}} \qquad \text{(4–77)}$$

Data for polished nickel are shown in figure 4–9, and the extrapolation to long wavelengths by equation (4–77) appears reasonable. The predictions of normal spectral emissivity at long wavelengths as presented in table 4–III are much better than the prediction of attendant optical constants.

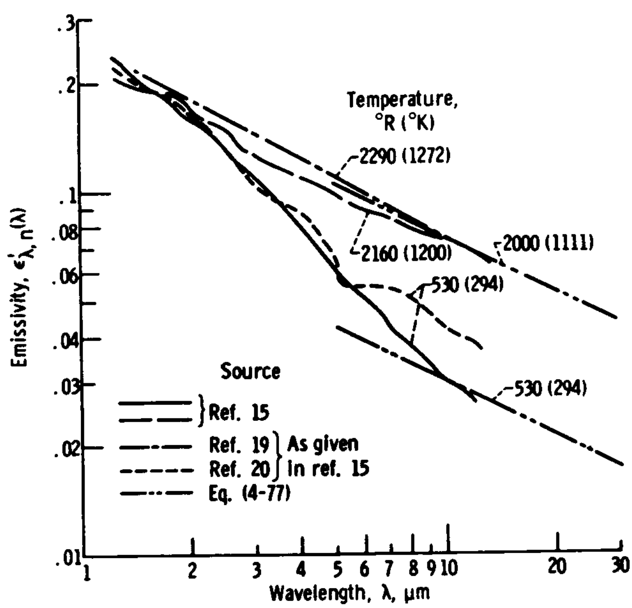

FIGURE 4–9.—Comparison of measured values with theoretical predictions for spectral normal emissivity of polished nickel.

The normal spectral emissivity given in equation (4–77) can be integrated with respect to wavelength to yield a normal total emissivity. The integration relating spectral and total quantities is given by equation (3–3b) (modified for a normal emissivity so that $\beta=0$):

$$\epsilon_n'(T)=\frac{\pi\int_0^\infty \epsilon_{\lambda,n}'(\lambda,T)\,i_{\lambda b}'(\lambda,T)\,d\lambda}{\sigma T^4}$$

Equation (4–77) is only valid for $\lambda_o > \sim 5\ \mu m$, so that in performing the integration starting from $\lambda=0$, the condition is being imposed that the metal temperature is such that the energy radiated from $\lambda_o=0$ to $5\ \mu m$ is small compared with that at wavelengths longer than $5\ \mu m$. Then substituting equation (4–77) and equation (2–11a) for $i_{\lambda b}'$ into the integral provides

$$\epsilon_n'(T)\cong\frac{\pi\int_0^\infty 2\left(\frac{r_e}{0.003\lambda_o}\right)^{1/2}\frac{2C_1}{\lambda_o^5(e^{C_2/\lambda_o T}-1)}\,d\lambda_o}{\sigma T^4}$$

$$=\frac{4\pi C_1(Tr_e)^{1/2}}{(0.003)^{1/2}\sigma C_2^{4.5}}\int_0^\infty\frac{\zeta^{3.5}}{e^\zeta-1}\,d\zeta \qquad (4\text{–}78)$$

where $\zeta=C_2/\lambda_o T$ as was used in conjunction with equation (2–19). The integration is carried out by use of Γ functions to yield

$$\epsilon_n'(T)\cong\frac{4\pi C_1(Tr_e)^{1/2}}{(0.003)^{1/2}\sigma C_2^{4.5}}\ (12.27) \qquad (4\text{–}79)$$

For pure metals, r_e is approximately described near room temperature by

$$r_e\cong r_{e,\,492}\left(\frac{T}{492}\right) \qquad (4\text{–}80)$$

where $r_{e,\,492}$ is the electrical resistivity, still in ohm-centimeters, evaluated at 492° R (0° C). Substituting equation (4–80) into equation (4–79) gives the result

$$\epsilon_n'(T)\cong\frac{4\pi C_1(12.27)}{(0.003)^{1/2}\sigma C_2^{4.5}}\sqrt{\frac{r_{e,\,492}}{492}}\,T \qquad (4\text{–}81a)$$

or simply

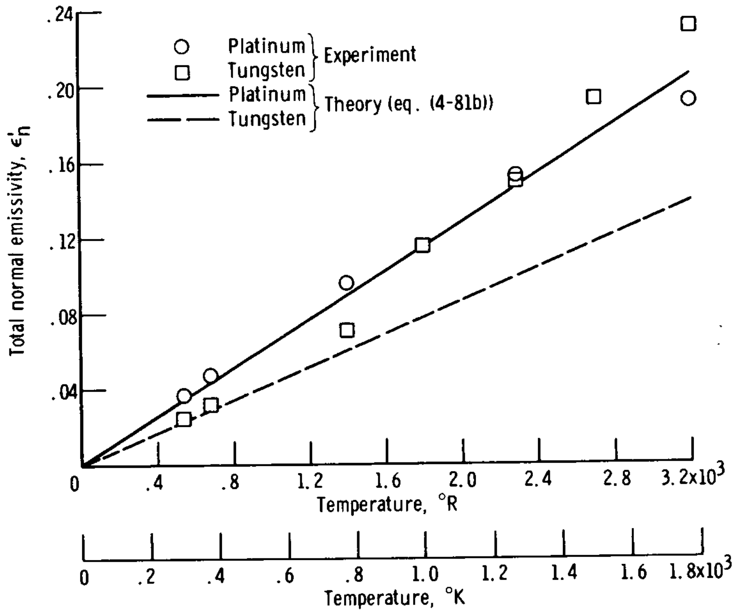

FIGURE 4–10.—Temperature dependence of total normal emissivity of polished metals.

$$\epsilon_n'(T) \cong 0.0193 \sqrt{r_{e,\,492}}\, T \tag{4–81b}$$

where T is in °R. This indicates that, for long wavelengths ($\lambda_0 > \sim 5$ μm), the total emissivity of pure metals should be directly proportional to temperature. This result was originally derived by Aschkinass (ref. 5) in 1905. In some cases it holds to unexpectedly high temperatures where considerable radiation is in the short wavelength region (for platinum, to near 3200° R), but, in general, applies only below about 1000° R. This is illustrated in figure 4–10 for platinum and tungsten (data from ref. 2).

In figure 4–11, a comparison is made at 100° C of the total normal emissivity from experiment and from equation (4–81b) for a variety of polished surfaces of pure metals. Agreement is generally satisfactory. The experimental values are the minimum values of results available in three standard compilations (refs. 2, 6, and 7).

By using the emissivity from equation (4–81), the total intensity in the normal direction emitted by a metal is given by

$$i'_{n,\,\mathrm{metals}} = \epsilon'_{n,\,\mathrm{metals}} \left(\frac{\sigma T^4}{\pi}\right) \propto T^5 \tag{4–82}$$

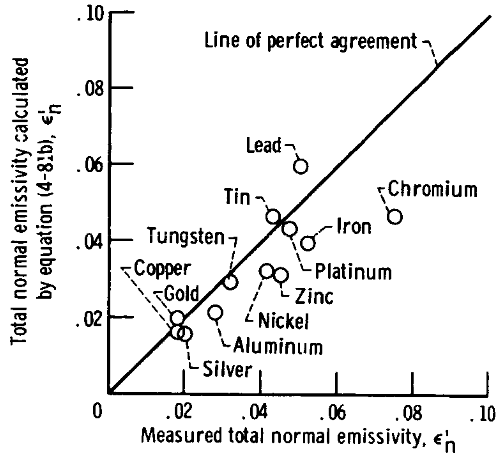

FIGURE 4–11.—Comparison of data with calculated total normal emissivity for polished metals at 100° C.

This indicates that the normal total intensity is proportional to the *fifth* power of absolute temperature rather than the fourth power as with a blackbody. Again it must be emphasized that many assumptions were made to obtain this simplified result. If for example more than two terms had been retained from the series in equation (4–76b), it would be found that the exact proportionality between normal total intensity and T^5 no longer holds, although the exponent would still be greater than 4.

The results of a more detailed computation are given in reference 3, and these include an integration over all directions to provide hemispherical quantities. The following approximate equations for the hemispherical total emissive power fit the results in two ranges:

$$e(T) = \sigma T^4 (0.751\sqrt{r_e T} - 0.396 r_e T); \qquad 0 < r_e T < 0.2 \qquad \text{(4–83a)}$$

and

$$e(T) = \sigma T^4 (0.698\sqrt{r_e T} - 0.266 r_e T); \qquad 0.2 < r_e T < 0.5 \qquad \text{(4–83b)}$$

where the numerical factors in the parentheses and those used in specifying the ranges of validity apply for T in °K and r_e in ohm-centimeters. The resistivity r_e depends on T to the first power so that the first term inside the parentheses of each of these equations provides the T^5 dependency discussed earlier.

4.6.3 Summary of Prediction Equations

A summary of equations for property predictions by use of electromagnetic theory is given in table 4–IV.

EXAMPLE 4–3: A polished platinum surface is maintained at temperature $T_A=400°$ R. Energy is incident upon the surface from a black enclosure at temperature $T_i=800°$ R that encloses the surface. What is the hemispherical-directional total reflectivity into the direction normal to the surface?

Equation (3–48) shows that the directional-hemispherical total reflectivity can be found from

$$\rho_n'(T_A=400°\text{ R})=1-\alpha_n'(T_A=400°\text{ R})$$

TABLE 4–IV.—SUMMARY OF EQUATIONS FOR PROPERTY PREDICTION BY ELECTROMAGNETIC THEORY

Property	Equation	Conditions
	Dielectrics ($\kappa=0$)	
Directional reflectivity	(4–58), (4–60)	Polarized in plane parallel to plane of incidence.
Directional reflectivity	(4–59), (4–60)	Polarized in plane perpendicular to plane of incidence.
Directional reflectivity	(4–61), (4–60)	Unpolarized.
Normal reflectivity	(4–50)	Polarized or unpolarized.
Hemispherical emissivity	([a])	Emission into medium having $n=1$.
	Metals (in contact with transparent medium of unity refractive index)	
Directional reflectivity	(4–67)	Parallel polarized component.
Directional reflectivity	(4–68)	Perpendicular polarized component.
Directional reflectivity	(4–69)	Unpolarized.
Directional emissivity	(4–72)	Unpolarized.
Hemispherical emissivity	(4–73)	Unpolarized.
Normal spectral emissivity.	(4–76a), (4–77)	Polarized or unpolarized $\lambda>\sim 5\ \mu$m.
Normal total emissivity	(4–81b)	$T<\sim 1000°$ R.

[a] See fig. 4–6.

where $\alpha_n'(T_A=400°\ \mathrm{R})$ is the normal total absorptivity of a surface at 400° R for incident black radiation at 800° R, that is,

$$\alpha_n'(T_A=400°\ \mathrm{R})=\frac{\int_0^\infty \alpha_{\lambda,n}'(\lambda, T_A=400°\ \mathrm{R})i_{\lambda b}'(\lambda, 800°\ \mathrm{R})\,d\lambda}{\int_0^\infty i_{\lambda b}'(\lambda, 800°\ \mathrm{R})\,d\lambda}$$

For spectral quantities $\alpha_{\lambda,n}'(\lambda,\ T_A=400°\ \mathrm{R})=\epsilon_{\lambda,n}'(\lambda,\ T_A=400°\ \mathrm{R})$. From equation (4–77) the variation of r_e with temperature provides the emissivity variation $\epsilon_{\lambda,n}'(\lambda,\ T_A)\propto T_A^{1/2}$. Then $\epsilon_{\lambda,n}'(\lambda,\ T_A=400°\ \mathrm{R})=\epsilon_{\lambda,n}'(\lambda,\ T_A=800°\ \mathrm{R})\ (400/800)^{1/2}$ and we obtain

$$\alpha_n'(T_A=400°\ \mathrm{R})=\frac{\sqrt{\frac{1}{2}}\int_0^\infty \epsilon_{\lambda,n}'(\lambda, T_A=800°\ \mathrm{R})i_{\lambda b}'(\lambda, 800°\ \mathrm{R})\,d\lambda}{\int_0^\infty i_{\lambda b}'(\lambda, 800°\ \mathrm{R})\,d\lambda}$$

$$=\frac{\epsilon_n'(T_A=800°\ \mathrm{R})}{\sqrt{2}}$$

where the last equality is obtained by examination of the emissivity definition, equation (3–36). The normal total emissivity of platinum at 800° R is given by equation (4–81b) as plotted in figure 4–10 as

$$\epsilon_n'(T_A=800°\ \mathrm{R})=0.0193\sqrt{r_{e,\,492}}\times 800=0.051$$

Note that equation (4–81b) is only to be used when temperatures are such that most of the energy involved is at wavelengths greater than 5 μm. Examination of the blackbody functions, table V of the appendix, shows that for a temperature of 800° R, about 10 percent of the energy is at less than 5 μm so that possibly a small error is introduced.

The reciprocity relation of equation (3–28) for uniform incident intensity can now be employed to give the final result for the hemispherical-directional total reflectivity,

$$\rho_n'(T_A=400°\ \mathrm{R})=1-\alpha_n'(T_A=400°\ \mathrm{R})\approx 1-\frac{\epsilon_n'}{\sqrt{2}}(T_A=800°\ \mathrm{R})$$

$$=1-\frac{0.051}{\sqrt{2}}=0.964$$

4.7 EXTENSIONS OF THE THEORY OF RADIATIVE PROPERTIES

Much work has been expended in improving the theory of the radiative properties of materials, using both classical wave theory and quantum theory. A number of authors have successfully removed some restrictions which are present in the classical development presented here. Notable are the contributions of Davisson and Weeks (ref. 8), Foote (ref. 9), Schmidt and Eckert (ref. 10), and Parker and Abbott (ref. 11), who all extended the emissivity relations for metals to shorter wavelengths and higher temperatures, and of Mott and Zener (ref. 12), who derived relations for metal emissivity at very short wavelengths on the basis of quantum relations.

None of these treatments, however, accounts for surface effects. Because of the difficulty of specifying surface conditions and controlling surface preparation, it is found that comparison of the theory with experiment is not always adequate for even the refined theories. In fact, comparison to the less exact but simpler relations given here is often better. For even the purest materials given the most meticulous preparation, the elementary relations are often more accurate because the errors in the simpler theory are in the direction which cause compensation for surface working.

Polarization effects entered into the mathematical description of electromagnetic waves and wave reflections. A detailed discussion of these effects is beyond the intent of this publication. A comprehensive discussion of the analytical methods and technology of polarization phenomena is given in reference 13.

REFERENCES

1. Maxwell, James Clerk: A Dynamical Theory of the Electromagnetic Field. Vol. 1 of The Scientific Papers of James Clerk Maxwell. W. D. Niven, ed., Cambridge University Press, 1890.
2. Weast, Robert C., ed.: Handbook of Chemistry and Physics. 44th ed., Chemical Rubber Co., 1962.
3. Jakob, Max: Heat Transfer. John Wiley and Sons, Inc., 1949.
4. Hagen, E.; and Rubens, H.: Metallic Reflection. Ann. d. Physik, vol. 1, no. 2, Feb. 1900, pp. 352–375. (See also Hagen, E.; and Rubens, H.: Emissivity and Electrical Conductivity of Alloys. Deutsch. Phys. Gesell. Verh., vol. 6, no. 4, Feb. 29, 1904, pp. 128–136.)
5. Aschkinass, E.: Heat Radiation of Metals. Ann. d. Physik, vol. 17, no. 5, Sept. 26, 1905, pp. 960–976.
6. Hottel, H. C.: Radiant Heat Transmission. Heat Transmission. William H. McAdams, Third ed., McGraw-Hill Book Co., Inc., 1954, pp. 55–125.
7. Eckert, E. R. G.; and Drake, R. M., Jr.: Heat and Mass Transfer. Second ed., McGraw-Hill Book Co., Inc., 1959.
8. Davisson, C.; and Weeks, J. R., Jr.: The Relation Between the Total Thermal Emissive Power of a Metal and Its Electrical Resistivity. Opt. Soc. Am. J., vol. 8, no. 5, May 1924, pp. 581–605.

9. FOOTE, PAUL D.: The Emissivity of Metals and Oxides. III. The Total Emissivity of Platinum and the Relation Between Total Emissivity and Resistivity. NBS Bulletin, vol. 11, no. 4, 1915, pp. 607–612.
10. SCHMIDT, E.; AND ECKERT, E. R. G.: Ueber die Richtungsverteilung der Waermestrahlung von Oberflaechen. Forschung. Geb. Ing.-Wes., vol. 6, no. 4, July–Aug. 1935, pp. 175–183.
11. PARKER, W. J.; AND ABBOTT, G. L.: Theoretical and Experimental Studies of the Total Emittance of Metals. Symposium on Thermal Radiation of Solids. NASA SP–55, 1964, pp. 11–28.
12. MOTT, N. F.; AND ZENER, C.: The Optical Properties of Metals. Cambridge Phil. Soc. Proc., vol. 30, pt. II, 1934, pp. 249–270.
13. SHURCLIFF, W. A.: Polarized Light, Production and Use. Harvard University Press, 1962.
14. GARBUNY, M.: Optical Physics. Academic Press, 1965.
15. SEBAN, R. A.: Thermal Radiation Properties of Materials, Part III. (WADD–TR–60–370, Pt. III), California University, Aug. 1963.
16. BRANDENBERG, W. M.: The Reflectivity of Solids at Grazing Angles. Measurement of Thermal Radiation Properties of Solids. Joseph C. Richmond, ed. NASA SP–31, 1963, pp. 75–82.
17. BRANDENBERG, W. M.; AND CLAUSEN, O. W.: The Directional Spectral Emittance of Surfaces Between 200° and 600° C. Symposium on Thermal Radiation of Solids. NASA SP–55, 1964, pp. 313–320.
18. PRICE, DEREK, J.: The Emissivity of Hot Metals in the Infra-Red. Phys. Soc. (London) Proc., Sec. A, vol. 59, pt. 1, Jan. 1947, pp. 118–131.
19. HURST, C.: The Emission Constants of Metals in the Near Infra-Red. Roy. Soc. Proc., Ser. A, vol. 142, no. 847, Nov. 1, 1933, pp. 466–490.
20. PEPPERHOFF, W.: Temperaturstrahlung. D. Steinkopf (Darmstadt, Germany), 1956.

Chapter 5. Radiative Properties of Real Materials

5.1 INTRODUCTION

In this chapter, the general characteristics of the radiative properties of real materials will be examined. These properties can vary considerably from the idealized cases presented in chapter 4 for "optically smooth" materials as predicted by electromagnetic theory. The analytical predictions yield useful trends and provide a unifying basis to help explain various radiation phenomena. However, the analyses are inadequate in the sense that the engineer is generally dealing with surfaces coated in varying degrees with contaminants, oxide, paint, etc., and having a surface roughness that is difficult to specify completely. Examples of some typical variations of radiative properties as a function of these and other parameters will be presented in this chapter to illustrate the types of property variations that can occur. This will provide the reader with an appreciation of how sensitive the radiative performance is to the surface condition. In addition to the typical properties presented, a number of atypical examples will be given in order to demonstrate that a careful examination of individual properties must be made to properly select the property values to be used in radiative exchange calculations.

The discussion in this chapter will be limited to opaque solids, where opaque is defined to mean that no transmission of radiant energy occurs through the entire thickness of the body. A composite body such as a thin coating on a substrate of a different material can have partial transmission through the coating, but it is assumed for the present discussion that none of the transmitted radiation will pass entirely through the substrate. No attempt to compile comprehensive property data will be made. Extensive but by no means complete tabulations and graphs of radiative properties have been gathered in references 1 to 6.

As discussed in chapter 4, there are basic differences in the radiative behavior of metals and dielectrics that are evident from electromagnetic theory. For this reason the first two sections in this chapter will deal with these two classes of materials, with metals being discussed first. Then some special surfaces will be discussed that have specific desirable variations of properties with wavelength and direction.

5.2 SYMBOLS

A area

c_0	speed of electromagnetic radiation in vacuum
e	emissive power
$F_{0-\lambda}$	fraction of blackbody energy in spectral range $0-\lambda$
p	probability function
Q	energy rate, energy per unit time
q	energy flux, energy per unit time per unit area
r_e	electrical resistivity
T	absolute temperature
z	height of surface roughness
α	absorptivity
β	angle measured from normal of surface
γ	electrical permittivity
ϵ	emissivity
θ	circumferential angle
λ	wavelength
μ	magnetic permeability
ρ	reflectivity
σ	Stefan-Boltzmann constant (table IV of the appendix)
σ_0	root-mean-square height of surface roughness

Subscripts:

A	of surface A
a	absorber
b	blackbody condition
c	evaluated at cutoff wavelength
e	emitted
eq	at equilibrium
i	incident
max	maximum value
n	normal direction
R	radiator
r	reflected
s	specular
λ	spectrally dependent
$0-\lambda$	in wavelength range $0-\lambda$

Superscripts:

$'$	directional
$''$	bidirectional

5.3 RADIATIVE PROPERTIES OF METALS

Pure, smooth metals are often characterized by low values of emissivity and absorptivity, and therefore comparatively high values of reflectivity. Figure 4–11 of the preceding chapter demonstrates that the emissivity in the direction normal to the surface is quite low for a variety of polished metals. However, low emissivity values are not an absolute rule for metals; in some of the examples that will be given, the spectral emissivity rises to 0.5 or larger as the wavelength becomes short, or the total emissivity becomes large as the temperature is elevated.

5.3.1 Directional Variations

A behavior typical of polished metals is that the directional emissivity tends to increase with increasing angle of emission β (where β is the angle measured with respect to the surface normal). This is predicted by electromagnetic theory and was shown to be true for platinum in figure 4–7. At wavelengths shorter than the range for which the simple electromagnetic theory of chapter 4 applies, a deviation from this behavior might be expected. To illustrate this deviation, the directional spectral emissivity of polished titanium is shown in figure 5–1.

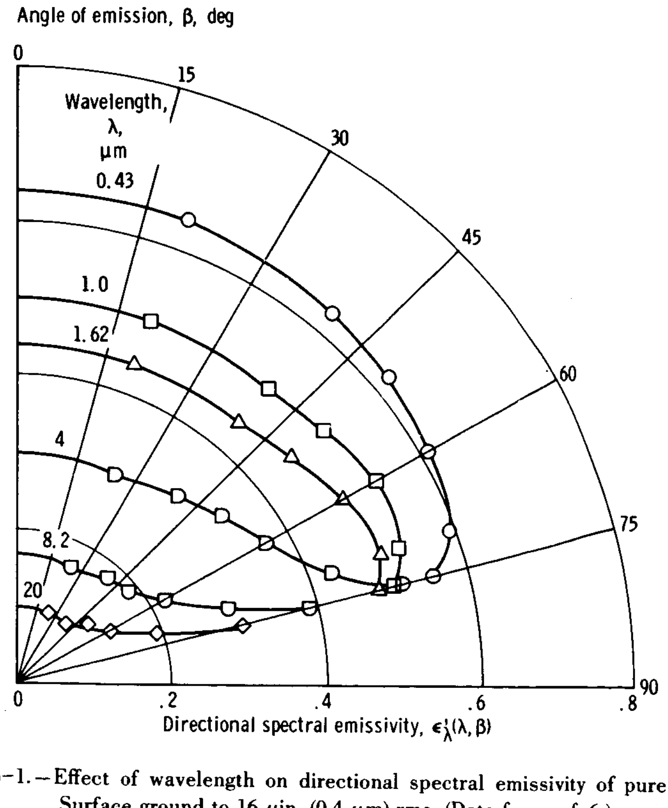

FIGURE 5–1.—Effect of wavelength on directional spectral emissivity of pure titanium. Surface ground to 16 μin. (0.4 μm) rms. (Data from ref. 6.)

At wavelengths greater than about 1 μm, the directional spectral emissivity of titanium does indeed tend to increase with increasing β over most of the β range. The increase with β becomes smaller as wavelength decreases; finally, at wavelengths less than about 1 μm, the directional spectral emissivity actually decreases with increasing β over the entire range of β. Hence, for polished metals, the typical behavior of increased emission for directions nearly tangent to the surface can be violated at short wavelengths.

5.3.2 Effect of Wavelength

In the infrared region, it was shown in chapter 4 that the spectral emissivity of metals tends to increase with decreasing wavelength. This trend remains true over a large span of wavelength as illustrated for several metals in figure 5–2 which gives the spectral emissivity in the normal direction. For other directions, the same effect is illustrated in figure 5–1 except at large angles from the normal where curves for various wavelengths may cross. The curve for copper in figure 5–2 provides an exception as the emissivity remains relatively constant with wavelength.

At very short wavelengths, the assumptions upon which the simplified electromagnetic theory of chapter 4 are based become invalid.

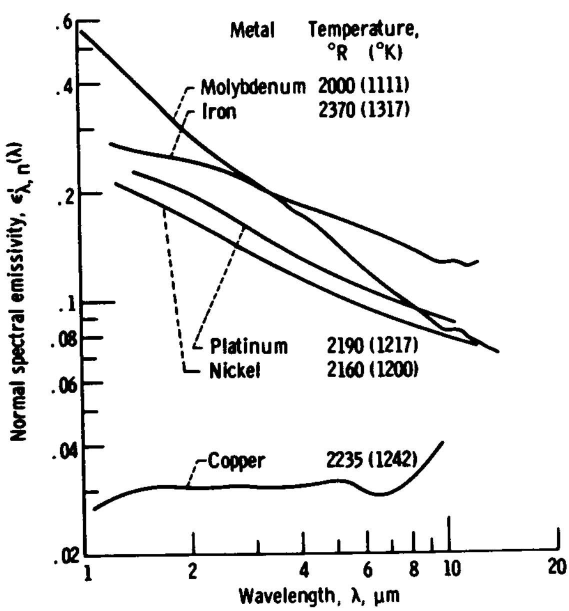

FIGURE 5–2.—Variation with wavelength of normal spectral emissivity for polished metals. (Data from Seban (ref. 15).)

Indeed, most metals exhibit a peak emissivity somewhere near the visible region, and the emissivity then decreases rapidly with further decrease in wavelength. This is illustrated by the behavior of tungsten in figure 5–3.

5.3.3 Effect of Surface Temperature

The Hagen-Rubens relation (eq. (4–77)) showed that, for wavelengths that are not too short ($\lambda > \sim 5$ μm), the spectral emissivity of a metal is proportional to the resistivity of the metal to the one-half power. Hence, we can expect the spectral emissivity of pure metals to increase with temperature as does the resistivity, and this is found to be the case in most instances. Figure 5–3 is an example for the hemispherical spectral emissivity of tungsten. The expected trend is observed for $\lambda > 1.27$ μm. Figure 5–3 also illustrates a phenomenon characteristic of many metals as discussed in reference 7. At short wavelengths (in the case of tungsten $\lambda < 1.27$ μm), the temperature effect is reversed and the spectral emissivity decreases as temperature is increased.

The observed increase of spectral emissivity with decreasing wavelength for metals in the infrared radiation region (wavelengths longer than visible region) as discussed in section 5.3.2 accounts for the increase in total emissivity with temperature. With increased temperature, the peak of the blackbody radiation curve (fig. 2–6) moves toward shorter wavelengths. Consequently, as the surface temperature is increased, proportionately more radiation is emitted in the region of higher spectral emissivity, which results in an increased total emis-

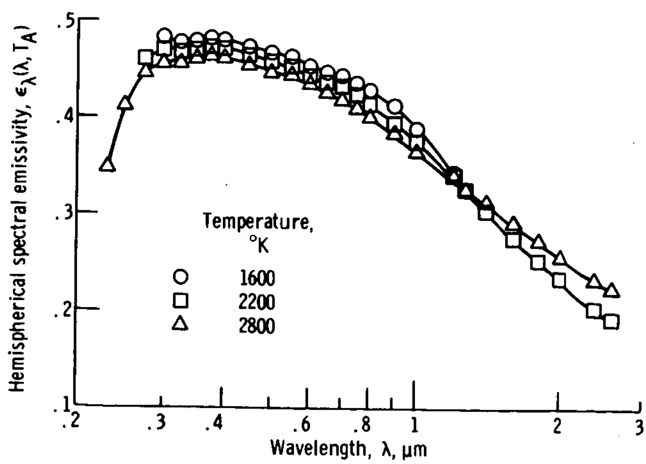

FIGURE 5–3.—Effect of wavelength and surface temperature on hemispherical spectral emissivity of tungsten (ref. 16).

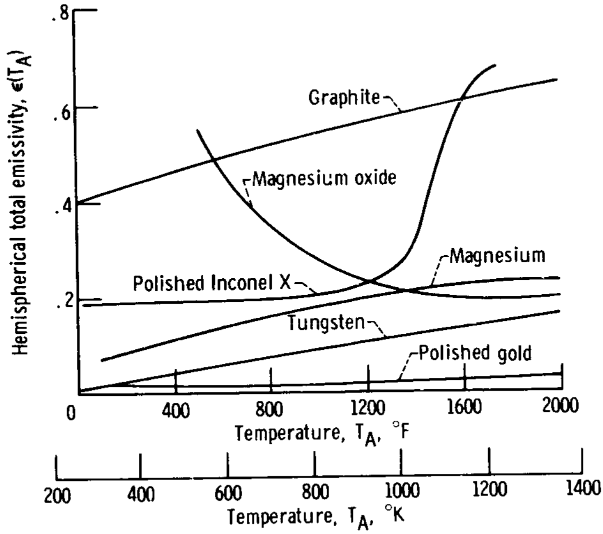

FIGURE 5–4.—Effect of temperature on hemispherical total emissivity of several metals and one dielectric. (Data from Gubareff et al. (ref. 1).)

sivity. Some examples are shown in figure 5–4. Here the behavior of metals is contrasted with that of a dielectric, magnesium oxide, for which the emissivity decreases with increasing temperatures.

The next two factors to be discussed are surface roughness and surface impurities or coatings. These can cause major deviations from the electromagnetic theory predictions of chapter 4.

5.3.4 Effect of Surface Roughness

If the surface imperfections present on a material are much smaller than the wavelength of the radiation being considered, the material is said to be *optically smooth*. A material that is optically smooth for long wavelengths may be comparatively quite rough at short wavelengths. The radiative properties of optically smooth materials can be predicted within the limitations of electromagnetic theory as discussed in chapter 4.

For wavelengths that are very short in comparison with the degree of roughness, the directional distribution of emitted or reflected energy is governed chiefly by the roughness. If the orientation and constitution of the roughness is specified, it is possible in certain cases to predict analytically these directional distributions. Such a case for parallel grooves will be noted in section 5.5.2.

Various attempts at predicting the effect of surface roughness on the radiative properties of metals have been made. All must be viewed as preliminary probings of an extremely complex subject, and none are satisfactory over the entire range of variables encountered for engineering surfaces.

A chief stumbling block is in the precise definition of surface characteristics for use in an analysis. Perhaps the most common way of characterizing surface roughness is by the method of preparation (lapping, grinding, etching, etc.) plus a specification of root-mean-square (rms) roughness. The latter is usually obtained by means of a profilometer, which is an instrument that traverses a sharp stylus over the surface and reads out the vertical perturbations of the stylus in terms of a rms value. It does not account for the horizontal spacing of the roughness and gives no indication of the *distribution* of the size of roughness around the rms value. At present, there is no generally accepted method of accurately specifying surface characteristics, and none of those mentioned in this paragraph are adequate for prediction of radiative properties.

A few of the analytical approaches taken in the face of the aforementioned difficulty will now be mentioned. Davies (ref. 8) has examined the reflecting properties of a surface with roughness that is assumed to be distributed according to a Gaussian (normal) probability distribution, specified as a probability $p(z)$ of having a roughness of height z given by

$$p(z) = \frac{1}{\sigma_0\sqrt{2\pi}} \exp\left(-\frac{z^2}{2\sigma_0^2}\right)$$

where σ_0 is the rms roughness. Using this distribution and the assumptions that the individual surface irregularities are of sufficiently small slope that shadowing can be neglected, that the material is a perfect electrical conductor, and that σ_0 is very much smaller than the wavelength of incident radiation λ, Davies was able to derive relations that predicted the distribution of reflected intensity. The reflected distribution was found to consist of a specular component and a component distributed about the specular peak.

A similar derivation, with σ_0 assumed much larger than λ, again yielded a distribution of reflected intensity about the specular peak, this time of larger angular spread than for the case of $\sigma_0 \ll \lambda$. This would be expected since the surface should behave increasingly like an ideal specular reflector as the roughness becomes very small compared with the wavelength of the incident radiation. Davies' treatment is found to be very inaccurate at near grazing angles because of the neglect of shadowing.

Porteus (ref. 9) extended Davies' approach by removing the restrictions on the relation between σ_0 and λ and including more parameters for specification of the surface roughness characteristics. Some success in predicting the roughness characteristics of prepared samples from measured reflectivity data was obtained, but certain types of surface roughness led to poor agreement. Measurements were mainly at normal incidence, and the neglect of shadowing makes the results of doubtful value at near grazing angles.

A more satisfactory treatment has been given by Beckmann and Spizzichino (ref. 10). Their method includes the autocorrelation distance of the roughness in the prescription of the surface. This is a measure of the spacing of the characteristic roughness peaks on the surface. The method gives somewhat better data correlation than the earlier analyses.

Some observed effects of surface roughness are shown in figures 5–5 and 5–6. The former shows the directional emissivity of titanium at a wavelength of 2 μm for three surface roughnesses, the maximum roughness being 16 microinches (μin.). Since 2 μm is equal to 78.7 μin., the

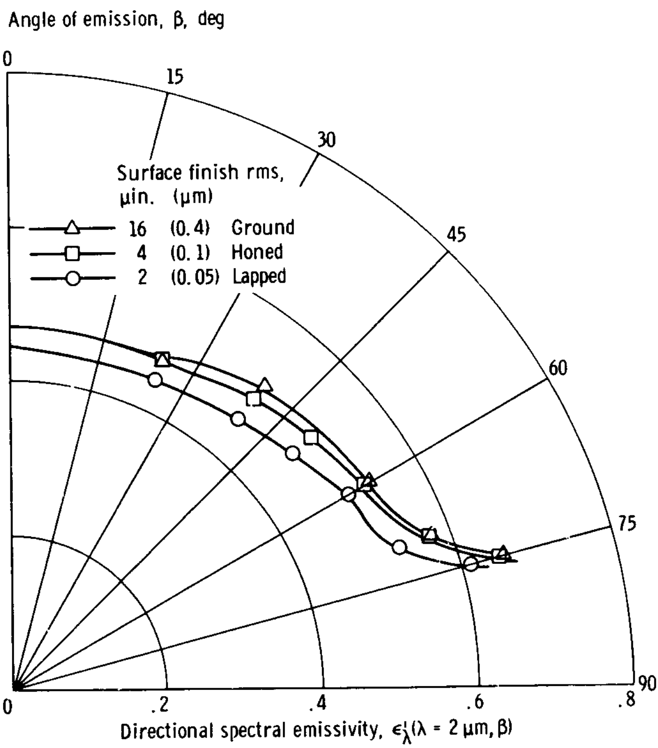

FIGURE 5–5.—Effect of surface finish on directional spectral emissivity of pure titanium. Wavelength, 2 μm (78.7 μin.). (Data from ref. 6.)

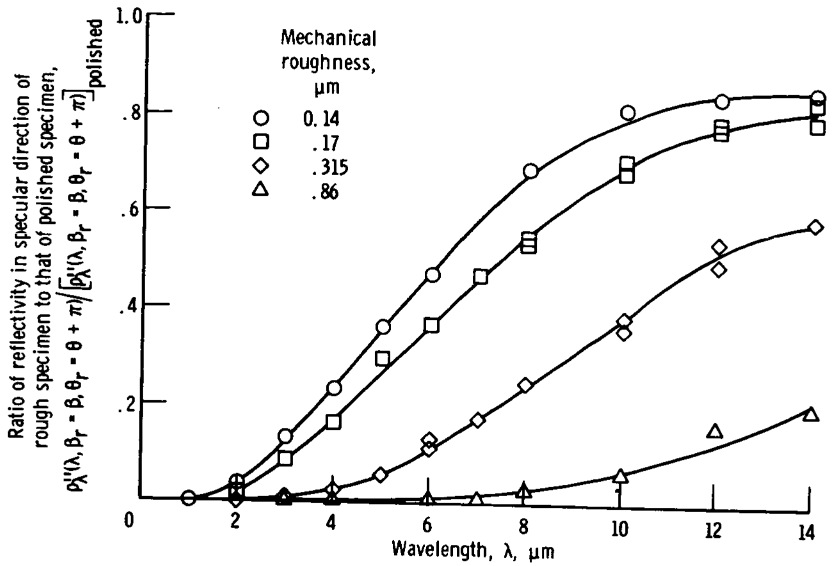

FIGURE 5-6.—Effect of roughness on reflectivity in specular direction for ground nickel specimens. Mechanical roughness for polished specimen, 0.015 μm. (Data from ref. 17.)

wavelength of the radiation is significantly larger than the surface roughnesses. Hence, relative to this wavelength the specimens are smooth. As a result, the emissivity changes only a small amount as the roughness varies from 2 to 16 μin.

Figure 5-6 provides the reflectivity of nickel for energy reflected into the specular direction from a beam incident at an angle 10° from the normal. In this figure, the reflectivities of the rough specimens are expressed as a ratio to the reflectivity of a polished surface in order to exhibit the effect of roughness. The polished surface used for comparison had a roughness about 10 times less than that of the rough specimens. A high value of the ordinate thus means that the specimen is behaving more like a polished surface. Data are shown for ground nickel specimens with four different roughnesses. The reflectivity rises as wavelength is increased because for a given roughness the surface is more smooth relative to the incident radiation. As expected, for a fixed wavelength the reflectivity for the specular direction decreased as the roughness was increased.

5.3.5 Effect of Surface Impurities

Impurities in this context include contaminants of any type which cause deviations of the surface properties from those of an optically

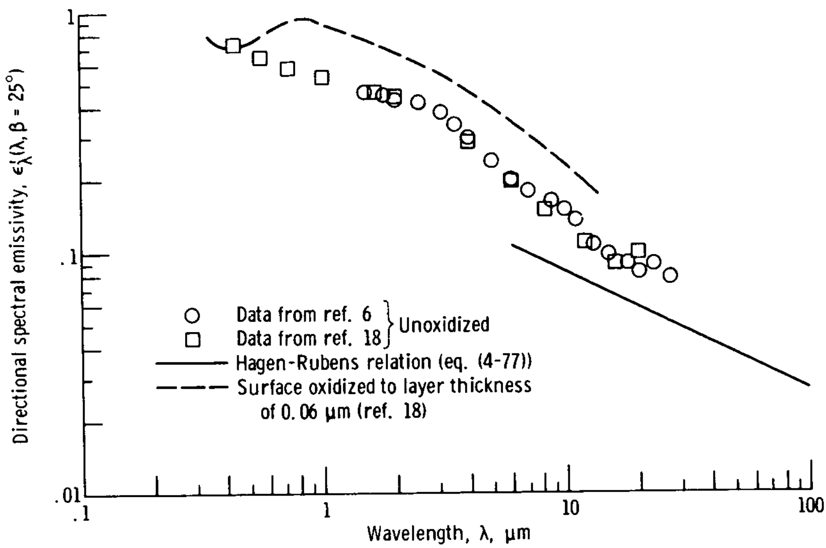

FIGURE 5-7.—Effect of oxide layer on directional spectral emissivity of titanium. Emission angle, 25°; surface lapped to 2 μin. (0.05 μm) rms; temperature, 530° R (294° K).

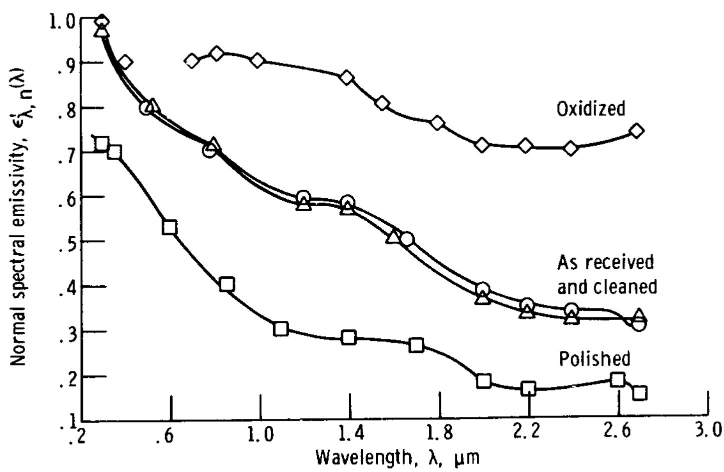

FIGURE 5-8.—Effect of oxidation on normal spectral emissivity of Inconel X. (Data from ref. 5.)

smooth pure metal. The most common contaminants are thin layers of foreign materials deposited either by adsorption, such as in the case of water vapor, or by chemical reaction. The common example of the latter is the presence of a thin layer of an oxide on the metal. Because dielectrics, as will be discussed in section 5.4, have generally high values of emissivity, an oxide or other nonmetallic contaminant layer will usually increase the emissivity of an otherwise ideal metallic body.

Figure 5–7 shows the directional spectral emissivity of titanium at an angle of 25° to the surface normal. The data points are for the unoxidized metal, and the solid line is the ideal emissivity predicted from electromagnetic theory. The dashed curve shown above the data points is the observed emissivity when an oxide layer only 0.06 μm in thickness is present. The emissivity is seen to be increased by a factor of almost 2 from that of the pure material over much of the wavelength range. Figure 5–8 shows a similar large increase in the normal spectral emissivity of Inconel X for an oxidized surface as compared with that for the polished metal.

Figures 5–9 and 5–10 illustrate the effect of an oxide coating on the hemispherical total emissivity of copper and the normal total emissivity of stainless steel. The details of the oxide coatings are not specified, but the large effect of surface oxidation is apparent. A more precise indication of oxide coating effect is shown in figure 5–11 where the hemispherical total emissivity of aluminum is given. An oxide thickness of a few ten-thousandths of an inch provides a very substantial emissivity increase.

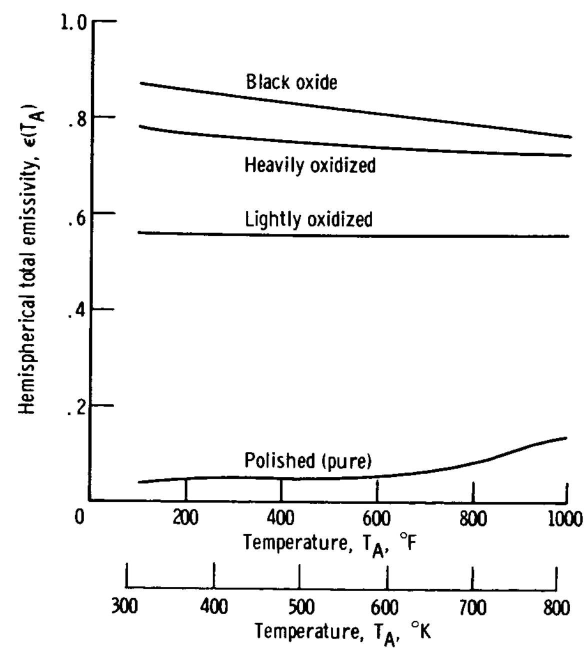

FIGURE 5–9. – Effect of oxide coating on hemispherical total emissivity of copper. (Data from Gubareff et al. (ref. 1).)

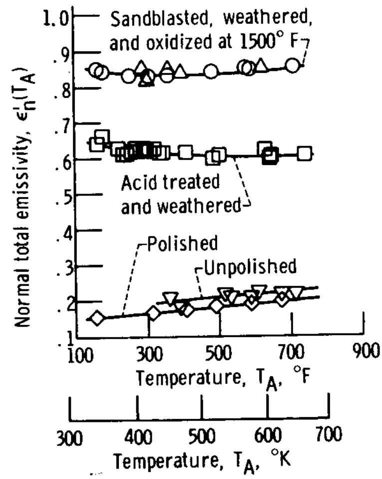

FIGURE 5-10.—Effect of surface condition and oxidation on normal total emissivity of stainless steel type 18-8. (Data from ref. 5.)

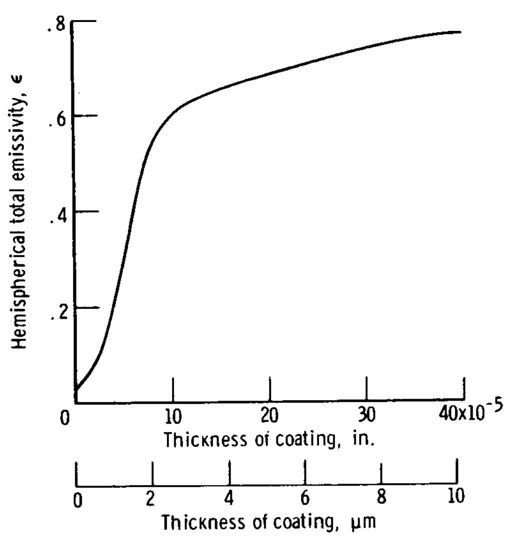

FIGURE 5-11.—Typical curve illustrating effect of electrolytically produced oxide thickness on hemispherical total emissivity of aluminum. Temperature, 100° F. (Data from Gubareff et al. (ref. 1).)

Figure 5-12 shows approximately the directional total absorptivity of an anodized aluminum surface for radiation incident from various β directions and originating from sources at various temperatures. The quantity $\rho_s'(\beta)$ is the fraction of the incident energy that is reflected into

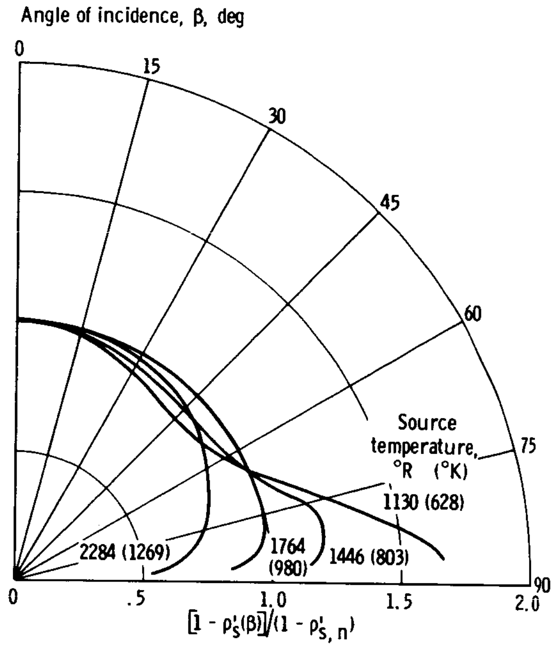

FIGURE 5–12.—Approximate directional total absorptivity of anodized aluminum at room temperature relative to value for normal incidence. (Redrawn from data of Munch (ref. 19).)

the specular direction; hence, $1-\rho_s'(\beta)$ is the fraction of the incident energy that is absorbed plus the fraction of the incident energy reflected into directions other than the specular direction. For the specimens tested, only a few percent of the energy was reflected into directions other than the specular direction. Thus, in figure 5–12, the quantity $1-\rho_s'(\beta)$ can be regarded as a good approximation to the directional total absorptivity. The curves have all been normalized to pass through unity at $\beta=0$; hence, it is the shapes of the curves that are significant. At low source temperatures, the incident radiation is predominantly in the long wavelength region. This incident radiation is barely influenced by the thin oxide film on the anodized surface; consequently, the specimen acts like a bare metal and has large absorptivities at large angles from the normal. At high source temperatures where the incident radiation is predominantly at shorter wavelengths, the thin oxide film has a significant effect and the surface behaves as a nonmetal where the absorptivity decreases with increasing β.

The structure of the surface coating can also have a substantial effect on the radiative behavior. Figure 5–13 shows the hemispherical spectral reflectivity of aluminum coated with lead sulfide. The mass of

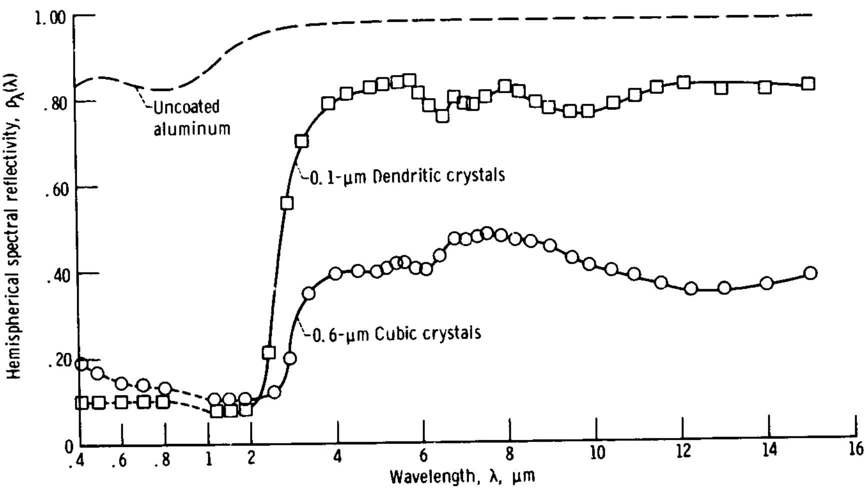

FIGURE 5–13.—Hemispherical spectral reflectivity for normal incident beam on aluminum coated with lead sulfide. Coating mass per unit surface area, 0.68 mg/cm^2. (Data from ref. 20.)

the coating per unit area of surface is the same for both sets of data shown. The difference in crystal structure and size causes the reflectivity of the coated specimens to differ by a factor of 2 at wavelengths longer than about 3 μm.

5.4 RADIATIVE PROPERTIES OF OPAQUE NONMETALS

Roughly speaking, nonmetals are characterized by large values of total hemispherical emissivity and absorptivity at moderate temperatures and, therefore, generally small values of reflectivity in comparison with metals. For a clean optically smooth surface, several results were arrived at in chapter 4 by use of the simplified electromagnetic theory presented there. These provide the following generalizations (bearing in mind the rather stringent assumptions of the theory): the directional emissivity will decrease with increasing angle from the surface normal; wavelength dependence is often weak, as it enters the predicted properties through the refractive index which varies slowly with wavelength for many nonmetals; finally, the temperature dependence of the properties of nonmetals will also be small, since temperature also enters the prediction only through the refractive index which is usually a weak function of temperature.

The difficulty with these generalizations is that most nonmetals cannot be polished to the degree necessary to allow their surfaces to be considered ideal, although some common exceptions exist such as glass, large crystals of various types, gem stones, and some plastics (some of these are not opaque materials like those being discussed here). As a result of having such nonideal surface finishes, many nonmetals, in practice, deviate radically from the behavior predicted by electromagnetic theory.

Available property measurements for nonmetals are much less detailed than for metals. Specifications of the surface composition, texture, and so forth, are often lacking. Table 5–I (taken from ref. 1) illustrates this, as the type of wood, texture of the brick, and composition of the oil paint are unspecified. This table does reveal the large emissivity values that many of the nonmetal materials have at room temperature.

TABLE 5–I.—NORMAL TOTAL EMISSIVITY OF NONMETALS AT ROOM TEMPERATURE (68° F)

[Data from Gubareff et al. (ref. 1)]

Material	ϵ_n'
Brick	0.94
Lampsoot	.95
Oil paint	.89 to .97
Roofing paper	.91
Hard rubber	.92
Wood	.8 to .9

An effect which complicates the interpretation of the measured properties of nonmetals is that radiation passing into such a material may penetrate quite far (this is evident for visible wavelengths in glass as an example) before being absorbed. A specimen must be of sufficient thickness to absorb essentially all the radiation that enters it; if it does not, it cannot be considered opaque and transmitted radiation must be accounted for. Often, samples of nonmetals such as paints are sprayed onto a metallic or other opaque base (substrate), and then the properties of the composite are measured. If in such a case it is desired to have the surface behave completely as the coating material, the thickness of the nonmetal coating must be sufficient to assure that no significant radiation is transmitted through the coating. Otherwise, when making a reflectivity measurement, some of the incident radiation will be reflected from the substrate and then transmitted again through the coating to reappear as energy measured by the instruments. The measured data will then be a function of both the coating material and the substrate.

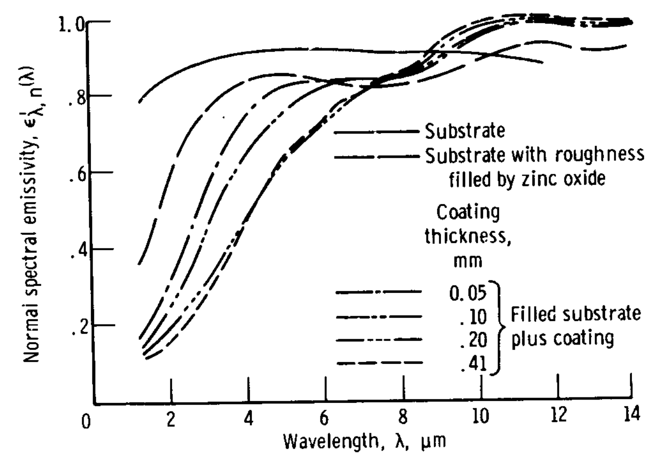

FIGURE 5–14.—Emissivity of zinc oxide coatings on oxidized stainless steel substrate. Surface temperature, 880±8° K. (Data from ref. 11.)

In emissivity measurements of a coating material, the coating must be thick enough that no emitted energy from the substrate penetrates the coating. A good illustration is given by Liebert (ref. 11). He examined the spectral emissivity of zinc oxide on a variety of substrates, using various oxide thicknesses. The effect of coating thickness on the emissivity of the composite formed by the zinc oxide coating and a substrate of approximately constant normal spectral emissivity is shown in figure 5–14. The effect of increasing the coating thickness becomes small in the range of 0.2- to 0.4-millimeter (mm) thickness, indicating that the emissivity of the zinc oxide alone is being approached.

We will now examine the effects of wavelength, temperature, and surface roughness on the radiative properties of dielectrics and then briefly examine the radiative properties of semiconductors.

5.4.1 Spectral Measurements

Compared with metals, there are relatively few detailed spectral measurements for dielectrics. Figure 5–15 shows the hemispherical-normal spectral reflectivity for three paint coatings on steel. From Kirchhoff's law and the reflectivity reciprocity relations, we can regard the difference between unity and these reflectivity values as the normal spectral emissivity. The three paints shown all exhibit somewhat different characteristics. White paint has a high reflectivity (low emissivity) at short wavelengths, and the reflectivity decreases at longer wavelengths. Black paint, on the other hand, has a relatively low reflectivity over the entire wavelength region shown. Using aluminum powder

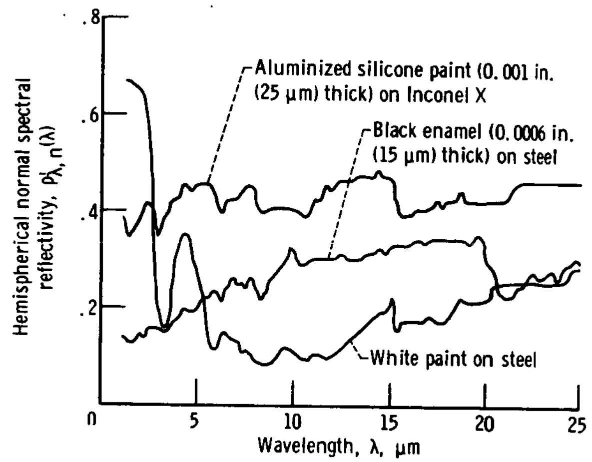

FIGURE 5–15.—Spectral reflectivity of paint coatings. Specimens at room temperature. (Data from ref. 21.)

in a silicone base as a paint increases the reflectivity as would be expected for the more metallic coating. This particular specimen of aluminized paint acts approximately as a "gray" surface since the properties are reasonably independent of wavelength. Because of the large variation in spectral emissivity at short wavelengths, the gray approximation would be poor for the white paint unless very little of the participating radiation were at the shorter wavelengths.

Figure 5–16 illustrates that at the short wavelengths in the visible range the reflectivity for some nonmetals may decrease substantially.

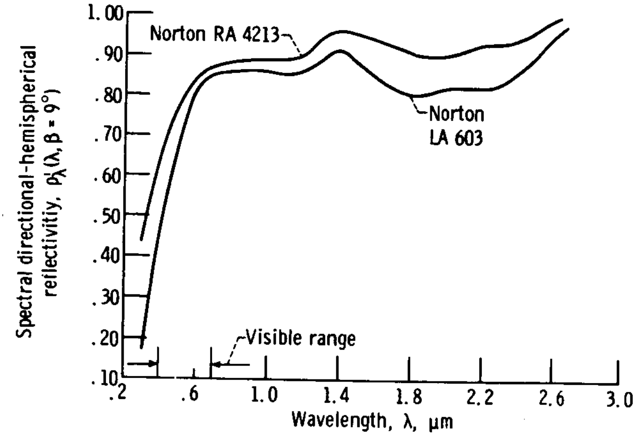

FIGURE 5–16.—Spectral directional-hemispherical reflectivity of aluminum oxide. Incident angle, 9°; specimens at room temperature. (Data from ref. 5.)

This behavior is very important when considering the suitability of a specific nonmetallic coating for reflecting radiation from a high temperature source where much of the energy will be at short wavelengths.

5.4.2 Variation of Total Properties With Temperature

The effect of surface temperature on the total emissivity of several nonmetallic materials is shown in figures 5–17 to 5–19. Both increasing

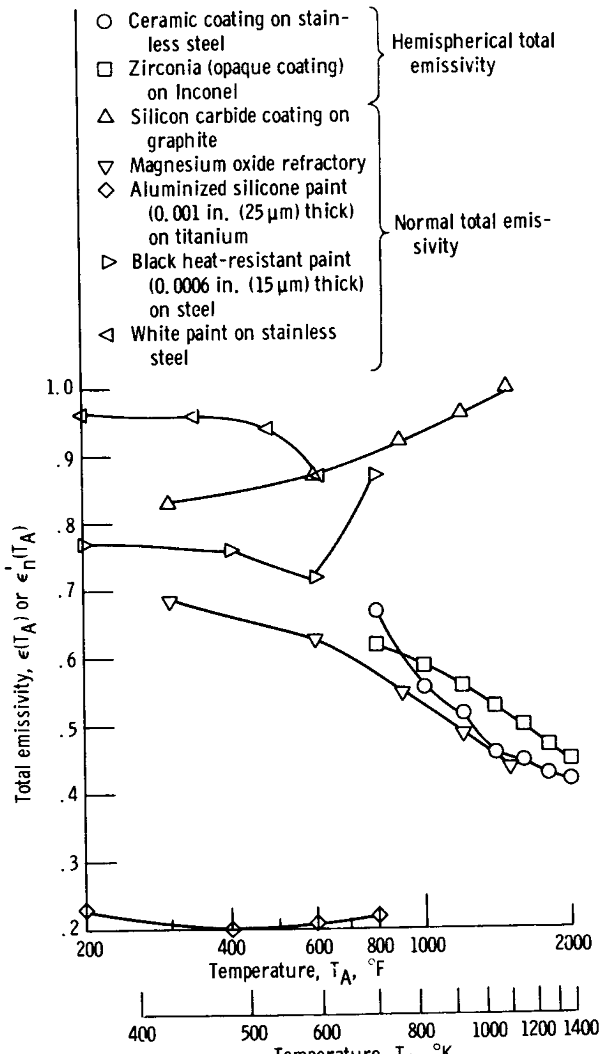

FIGURE 5–17.—Effect of surface temperature on emissivity of dielectrics. (Data from Gubareff et al. (ref. 1).)

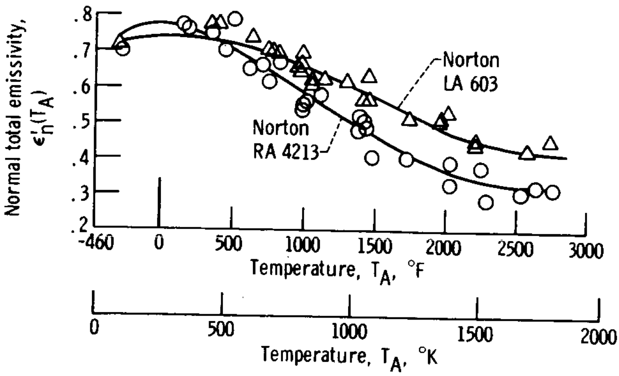

FIGURE 5–18.—Effect of surface temperature on normal total emissivity of aluminum oxide. (Data from ref. 5.)

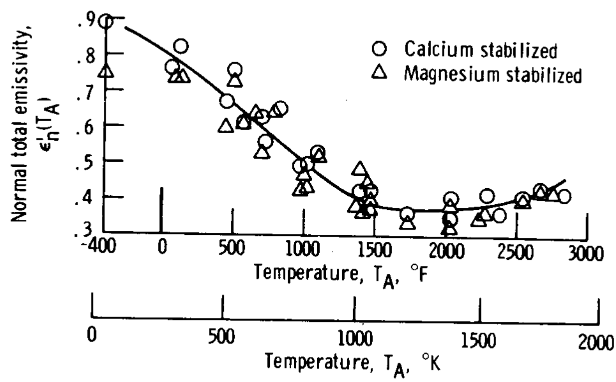

FIGURE 5–19.—Effect of surface temperature on normal total emissivity of zirconium oxide. (Data from ref. 5.)

and decreasing emissivity trends with temperature are observed. Some of these effects may be caused by the fact that the dielectric coating is rather thin; hence, the properties are influenced by the temperature and spectral characteristics of the underlying material (substrate). For example, as shown in figure 5–17, magnesium oxide refractory exhibits a significant emissivity decrease with increasing temperature. For a silicon carbide coating on graphite, however, the emissivity increases with temperature; this may be partly caused by the emissive behavior of the graphite substrate, which was shown in figure 5–4 to increase with temperature.

White and black paint both have high emissivities for the temperature range shown as is typical for ordinary oil-base paint. Aluminized paint is considerably lower in emissive ability since it behaves partly like a metal.

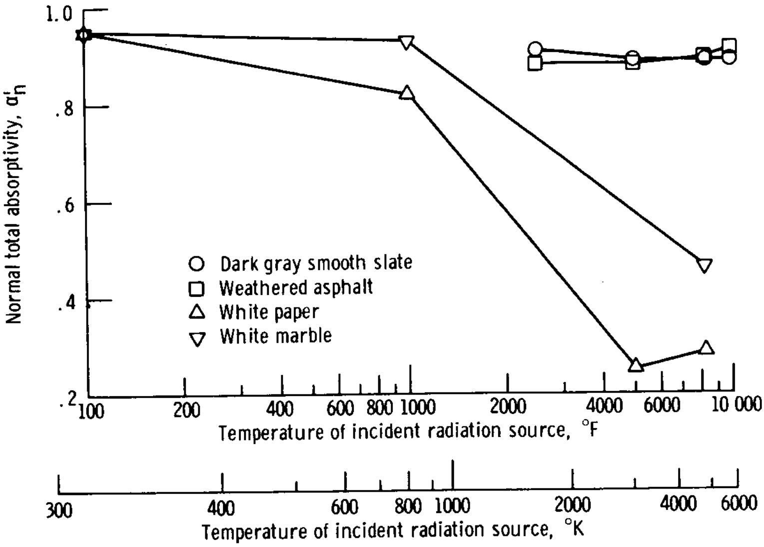

FIGURE 5–20.—Normal total absorptivity of nonmetals at room temperature for incident black radiation from source at indicated temperatures. (Data from Gubareff et al. (ref. 1).)

Note that the emissivity for aluminized paint in figure 5–17 is about one-half that in figure 5–15. This further emphasizes the wide variation in properties that can be found for samples having the same general description. For applications where the property values are critical, it may often be necessary to make radiation measurements for the specific materials being used.

Figure 5–20 gives the normal total absorptivity of a few materials for blackbody radiation incident from sources at various temperatures. White paper is shown to be a good absorber for radiation emitted at low temperatures but is a poor absorber for the spectrum emitted at temperatures of several thousand degrees Fahrenheit. It is thus a reasonably good reflector of energy incident from the Sun. An asphalt pavement or a gray slate roof, on the other hand, absorbs energy from the Sun very well.

5.4.3 Effect of Surface Roughness

In figure 5–21 the bidirectional total reflectivity of typewriter paper is shown for three different angles of incidence. For an ideal (polished, smooth) surface, a specular peak would be expected with the angle of reflection and the angle of incidence symmetric about the normal; obviously, the surface finish of typewriter paper is not ideal, since the reflected intensity occupies a rather large angular envelope around the direction of specular reflection.

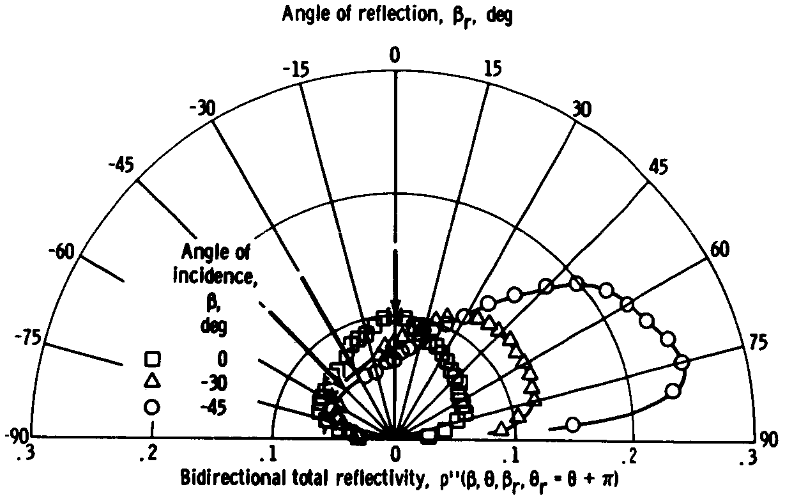

FIGURE 5–21.—Bidirectional total reflectivity of typewriter paper in plane of incidence. Source temperature, 2120° R (1178° K). (Replotted from data of Munch (ref. 19).)

The type of curves shown in figure 5–21 has suggested characterizing reflected energy as a combination of a purely diffuse plus a purely specular component. This type of approximation has merit in some cases and results in a simplification of radiant interchange calculations in comparison with the use of exact directional properties (refs. 12 and 13); in other cases, however, the approximation would fail completely. An example is shown in figure 5–22. This figure shows the observed bidirectional total reflectivity for visible light reflected from the surface of the Moon. These particular curves are for the mountainous regions, but very similar curves are obtained for other areas. The interesting feature of these curves is that the peak of the reflected radiation is back into the direction of the incident radiation. This peak is located at a circumferential angle θ of 180° away from where a specular peak would occur.

A moment's thought will confirm that curves of this type must characterize the lunar reflectivity. At full moon, which occurs when the Sun, Earth, and Moon are almost (but not quite) in a straight line (fig. 5–23), the Moon appears equally bright across its face. For this to be true, it follows that an observer on Earth sees equal intensities from all points on the Moon. However, the solar energy incident upon a unit area of the lunar surface varies as the cosine of the angle β between the Sun and the normal to the lunar surface. The angle β varies from 0° to 90°, as the position of the incident energy varies from the center to the edge of the lunar disk. To reflect a constant intensity to an observer on Earth from all observable points on the lunar surface therefore requires that the

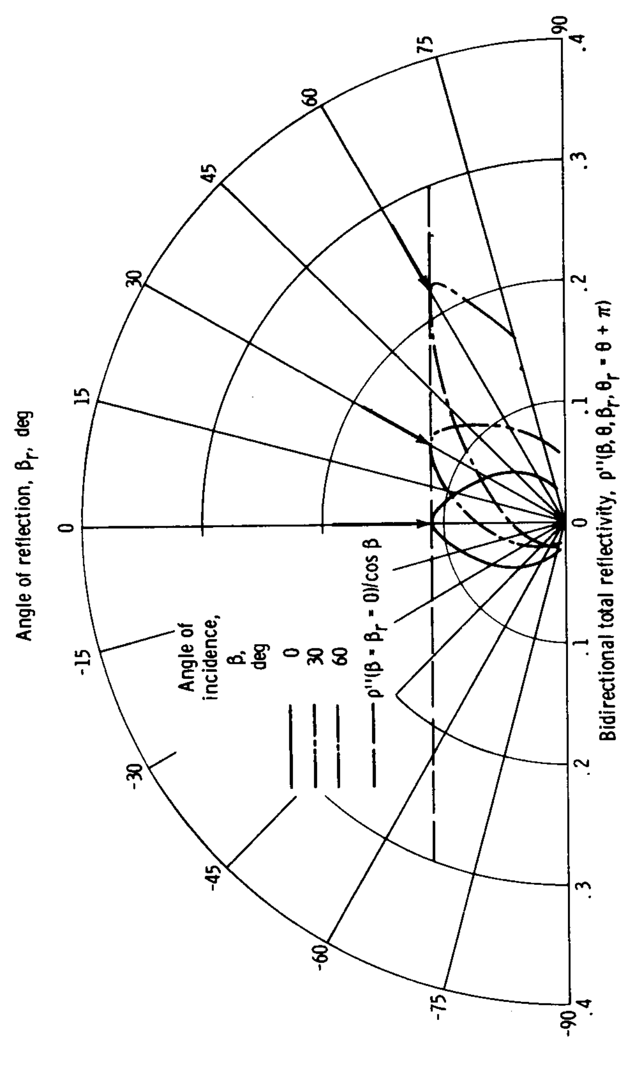

FIGURE 5–22.—Bidirectional total reflectivity in plane of incidence ($\theta_r=\theta+\pi$) for mountainous regions of lunar surface (after Orlova (ref. 22)).

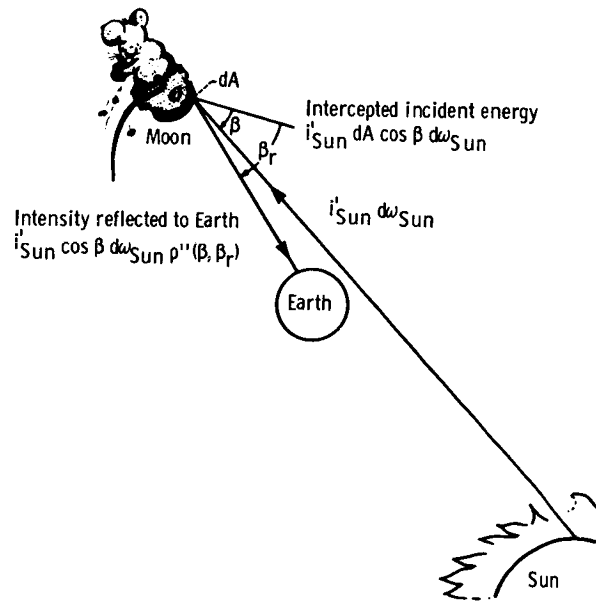

FIGURE 5–23. – Reflected energy at full moon.

product $\rho''(\beta, \beta_r) \cos \beta$ be constant. Consequently, the value of the bidirectional reflectivity in the direction of incidence must increase approximately in proportion to $1/\cos \beta$ (shown by the dashed line in fig. 5–22) as the angle of incidence increases. This change in reflectivity with angle of incidence will compensate for the reduced energy incident per unit area on the Moon at the large angles. The reflectivity behavior is confirmed by the curves in figure 5–22. Hence, the fact that the Moon appears uniformly bright does not imply that it is a diffuse reflector. If the Moon were diffuse, it would appear bright at the center and dark at the edges.

5.4.4 **Semiconductors**

Semiconductors are arbitrarily considered here along with the nonmetals, but they behave partly as metals. Liebert (ref. 14) has shown that their radiative properties can be determined through electromagnetic theory by treating semiconductors as metals with high resistivity. In figure 5–24, the normal spectral emissivity of a silicon semiconductor is shown. The Hagen-Rubens relation shown for comparison is based on the dc resistivity measured for the same sample, one of the few cases where such comparable emissive and electrical data are available. Agreement does not become good until wavelengths are reached that are much

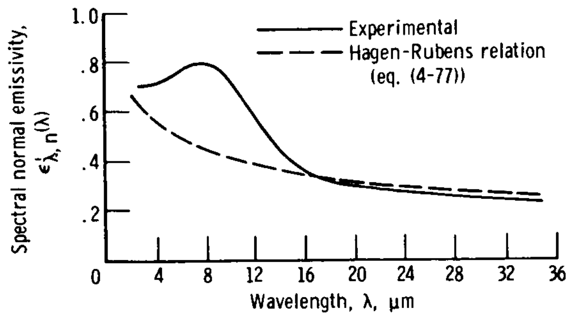

FIGURE 5–24.—Normal spectral emissivity of a highly doped silicon semiconductor at room temperature. (Data from ref. 14.)

greater than those giving agreement for metals. This difference in range of agreement can be traced to the following assumption used in deriving the Hagen-Rubens equation (see section 4.6.2.2):

$$\left(\frac{\lambda_o}{2\pi c_o r_e \gamma}\right)^2 \gg 1$$

For semiconductors, where the resistivity is larger than it is for metals, this inequality cannot hold until a range of wavelengths larger than those for metals is reached.

The shape of the curve measured for silicon (fig. 5–24) resembles what would be expected for a polished metal (see, for example, the tungsten data in fig. 5–3). The emissivity increases with decreasing wavelength over much of the measured spectrum, with a peak occurring at shorter wavelengths. However, most of the features of the semiconductor curve occur at longer wavelengths than for a metal; the peak emissivity, for example, is well outside the visible region.

Liebert (ref. 14) was also able to show excellent agreement between the measured emissivity and predictions from electromagnetic theory which included the effects of free electrons and was more sophisticated than that discussed in chapter 4. The theoretical equations were evaluated by using required physical properties that were measured from the specific samples on which the emissivity measurements were made.

5.5 SPECIAL SURFACES

For engineering purposes, it is often desirable to tailor the radiative properties of surfaces to increase or decrease their natural ability to absorb, emit, or reflect radiant energy. This can be done to provide two general types of behavior, a desired spectral performance or desired directional characteristics.

5.5.1 Modification of Spectral Characteristics

In applications of surfaces for use in the collection of radiant energy, such as in solar distillation units, solar furnaces, or solar collectors for energy conversion, it is desirable to maximize the energy absorbed by a surface while minimizing the amount lost by emission. In solar thermionic or thermoelectric devices, it is desirable to maintain the highest possible equilibrium temperature on the surface exposed to the Sun. Here again a maximum-collection, minimum-loss performance is needed. Later in this section the condition will be discussed where it is desirable to keep a surface cool when it is exposed to the Sun. In the latter case, it is desirable to have a maximum solar reflection accompanied by a maximum radiative emission from the surface.

For purposes of solar energy collection, a black surface will, of course, maximize the absorption of incident solar energy; unhappily, it also maximizes the emissive losses. However, if a surface could be manufactured that had an absorptivity large in the spectral region of short wavelengths about the peak solar energy, yet small in the spectral region of longer wavelengths where the peak emission would occur, it might be possible to absorb nearly as well as a blackbody while emitting very little energy. Such surfaces are called "spectrally selective." One method of manufacture is to coat a thin, nonmetallic layer onto a metallic substrate. For radiation with large wavelengths, the thin coating is essentially transparent, and the surface behaves as a metal yielding low values

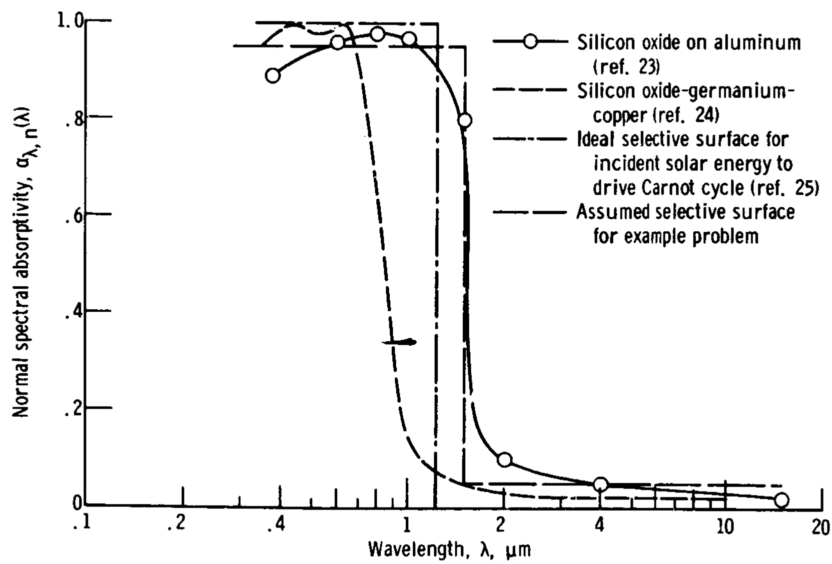

FIGURE 5–25.—Characteristics of some spectrally selective surfaces.

for the spectral absorptivity and emissivity. At short wavelengths, however, the radiation characteristics approach those of the nonmetallic coating so that the spectral emissivity and absorptivity are relatively large. Some examples of material behavior of this type are shown in figure 5–25.

An *ideal* solar selective surface would absorb a maximum solar energy while emitting a minimum amount of energy. The surface would thus have an absorptivity of unity over the range of short wavelengths where the incident solar energy has a large intensity. At longer wavelengths, the absorptivity should drop sharply to zero. The wavelength λ_c at which this sharp drop occurs is termed the cutoff wavelength.

EXAMPLE 5–1: An *ideal* selective surface is exposed to a normally incident flux of radiation corresponding to the average solar constant q_i, where $q_i = 442$ Btu/(hr)(sq ft). The only means of heat transfer to or from the surface is by radiation. Determine the maximum equilibrium temperature T_{eq} corresponding to a cutoff wavelength of $\lambda_c = 1$ μm. (Note that the energy arriving from the Sun can be assumed to have a spectral distribution proportional to that of a blackbody at 10 000° R.)

Since the only means of heat transfer is by radiation, the radiant energy absorbed must be equal to that emitted. Since we have specified an ideal selective absorber, the hemispherical emissivity and absorptivity are given by

$$\epsilon_\lambda(\lambda) = \alpha_\lambda(\lambda) = 1, \; 0 \leq \lambda < \lambda_c$$

and

$$\epsilon_\lambda(\lambda) = \alpha_\lambda(\lambda) = 0, \; \lambda_c \leq \lambda < \infty$$

The energy absorbed by the surface per unit time is

$$Q_a = (1) F_{0-\lambda_c}(T_R) q_i A$$

where $F_{0-\lambda_c}(T_R)$ is the fraction of blackbody energy in the range of wavelengths between zero and the cutoff value, for a radiating source at temperature T_R. In this case, T_R is the effective solar radiating temperature of about 10 000° R. Similarly, the energy emitted by the selective surface is

$$Q_e = (1) F_{0-\lambda_c}(T_{eq}) \sigma T_{eq}^4 A$$

Equating Q_e and Q_a yields

$$T_{eq}^4 F_{0-\lambda_c}(T_{eq}) = \frac{q_i F_{0-\lambda_c}(T_R)}{\sigma}$$

For the chosen value for λ_c, all terms on the right are known, and we can solve for T_{eq} by trial and error. The equilibrium temperature for $\lambda_c = 1$ μm, as specified in the problem, is 2400° R. Values of T_{eq} corresponding to other values of λ_c are given in the following table:

Cutoff wavelength, λ_c, μm	Equilibrium temperature, T_{eq}, °R
0.6	3250
.8	2750
1.0	2400
1.2	2150
1.5	1890
$\to \infty$	712

For a blackbody ($\lambda_c \to \infty$), the equilibrium temperature is 712° R; this is the equilibrium temperature of the surface of a black object in space near the Earth's orbit when exposed to solar radiation and with all other surfaces of the object perfectly insulated. The same equilibrium temperature is reached by a gray body, since a gray emissivity would cancel out of the energy balance equation.

As smaller values of λ_c are taken, T_{eq} continues to increase even though less energy is absorbed, because it becomes relatively more difficult to emit energy as λ_c is decreased.

A common measure of the performance of a given selective surface is the ratio of the directional total absorptivity $\alpha'(\beta, \theta, T_A)$ of the surface for incident solar energy to the hemispherical total emissivity of the surface $\epsilon(T_A)$. The ratio α'/ϵ for the condition of incident solar energy is a measure of the theoretical maximum temperature that an otherwise insulated surface can attain when exposed to solar radiation. The significance of α'/ϵ is shown as follows.

The energy absorbed per unit time by any surface when exposed to a directional incident intensity is given by

$$dQ'_a(\beta, \theta, T_A) = \alpha'(\beta, \theta, T_A) dQ'_i(\beta, \theta) \tag{5-1}$$

For the case of solar energy with a flux of $q_i = 442$ Btu/(hr)(sq ft), incident from direction (β, θ) on a surface element dA, this can be written as

$$dQ'_a(\beta, \theta, T_A) = \alpha'(\beta, \theta, T_A) q_i dA \cos\beta \tag{5-2}$$

The total energy emitted per unit time by the surface element is given by

$$dQ_e = e(T_A) dA = \epsilon(T_A) \sigma T_A^4 \, dA \tag{5-3}$$

If the only energy absorbed by the surface in question is that given by equation (5–2) and the surface only loses energy by radiation, the emitted and absorbed energies as given by equations (5–3) and (5–2), respectively, may be equated to give

$$\frac{\alpha'(\beta, \theta, T_{eq})}{\epsilon(T_{eq})} = \frac{\sigma T_{eq}^4}{q_i \cos\beta} \tag{5-4}$$

where T_{eq} is the equilibrium temperature that is achieved. Thus, the ratio $\alpha'(\beta, \theta, T_A)/\epsilon(T_A)$ is a measure of the equilibrium temperature of the element. Note also that the temperature at which the properties α' and ϵ are selected must be the equilibrium temperature that the body attains. In practice, temperature dependence of the properties is often assumed small so that this restriction can be somewhat relaxed.

The most common case considered is when the solar radiation is incident in the direction normal to the surface. Equation (5–4) becomes

$$\frac{\alpha'_n(T_{eq})}{\epsilon(T_{eq})} = \frac{\sigma T_{eq}^4}{q_i} \tag{5-5}$$

Equation (5–5) shows that the smaller the value of α'_n/ϵ that can be reached, the smaller will be the equilibrium temperature. For a cryogenic storage tank in space, α'_n/ϵ should be as small as possible. In practice, values of α'_n/ϵ in the range 0.20 to 0.25 can be obtained.

To attain high equilibrium temperatures, α'_n/ϵ should be as large as possible. Polished metals attain α'_n/ϵ values of 5 to 7, while specially manufactured surfaces have values of α'_n/ϵ approaching 20.

The upper limit of α'_n/ϵ is established by the thermodynamic argument that the equilibrium temperature of the selective surface cannot exceed the effective solar temperature of about 10 000° R. Substituting this solar temperature value into equation (5–5) gives

$$\left.\frac{\alpha'_n(T_{eq})}{\epsilon(T_{eq})}\right|_{\max} = \frac{\sigma(10\ 000)^4}{442} = 3.87 \times 10^4 \tag{5-6}$$

Attaining anything even close to this value of α_n'/ϵ is far beyond the present state of the art.

EXAMPLE 5–2: The properties of a real SiO-Al selective surface can be approximated by the long-dashed curve of figure 5–25. (It is assumed that the long-dashed curve can be extrapolated toward $\lambda = 0$ and $\lambda = \infty$.) What is the equilibrium temperature of the surface for normally incident solar radiation when the only heat transfer is by radiation? What is α_n'/ϵ for the surface? Describe the spectra of the absorbed and emitted energy at the surface. (Assume normal and hemispherical emissivities are equal.)

As in the derivation of equation (5–5), we equate the absorbed and emitted energies. The emissivity has nonzero values on both sides of the cutoff wavelength, so that

$$Q_a = \epsilon_{0-\lambda_c} F_{0-\lambda_c}(T_R) q_i A + \epsilon_{\lambda_c-\infty} F_{\lambda_c-\infty}(T_R) q_i A = \alpha_n' q_i A$$

and

$$Q_e = \epsilon_{0-\lambda_c} F_{0-\lambda_c}(T_{eq}) \sigma T_{eq}^4 A + \epsilon_{\lambda_c-\infty} F_{\lambda_c-\infty}(T_{eq}) \sigma T_{eq}^4 A = \epsilon \sigma T_{eq}^4 A$$

Equating Q_e and Q_a gives

$$\{0.95 F_{0-\lambda_c}(T_R) + 0.05[1 - F_{0-\lambda_c}(T_R)]\} q_i = \{0.95 F_{0-\lambda_c}(T_{eq}) + 0.05[1 - F_{0-\lambda_c}(T_{eq})]\} \sigma T_{eq}^4$$

Solving by trial and error as in example 5–1, we obtain for $\lambda_c = 1.5\ \mu m$, $T_{eq} = 1430°$ R. For $q_i = 442$ Btu/(hr)(sq ft), equation (5–5) gives $\alpha_n'/\epsilon = \sigma(1430)^4/442 = 16.2$. The small difference in properties in this example from the properties of an ideal selective surface produced a significant change in T_{eq}, which from the previous example was 1890° R for an ideal selective surface having the same cutoff wavelength. The spectral curves of absorbed and emitted energy are shown in figure 5–26. The spectral curve of incident solar energy is given by

$$e_{\lambda,i}(\lambda, T_R) \propto e_{\lambda b}(\lambda, T_R)$$

It has the shape of the blackbody curve at the solar temperature, but it is reduced in magnitude so that the integral of $e_{\lambda,i}$ over all λ is equal to q_i, the total incident solar energy per unit area. Multiplying this curve by the spectral absorptivity of the selective surface gives the spectrum of the absorbed energy. The spectrum of emitted energy

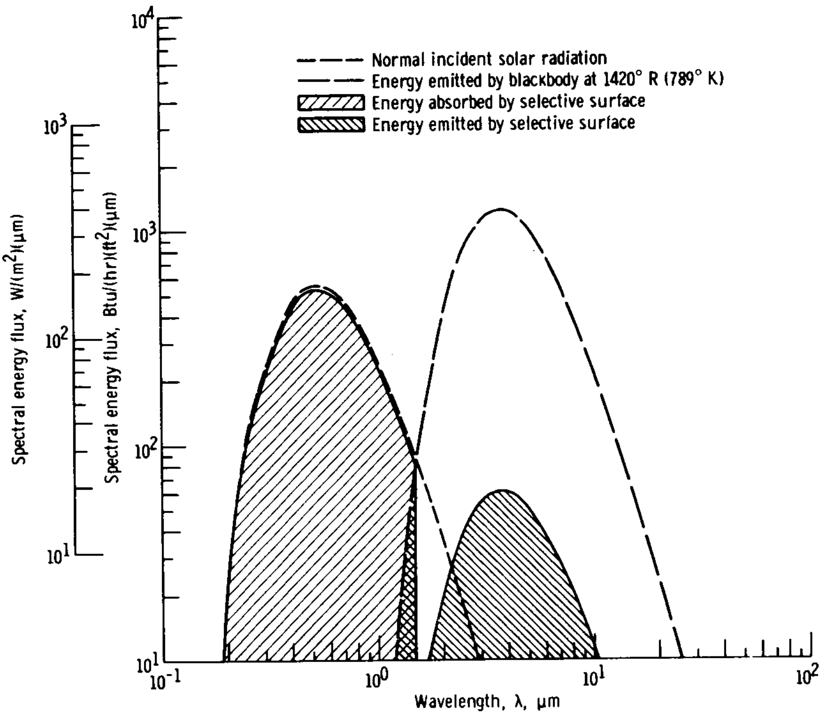

FIGURE 5–26. — Spectral distribution of energy absorbed and emitted by example selective absorber.

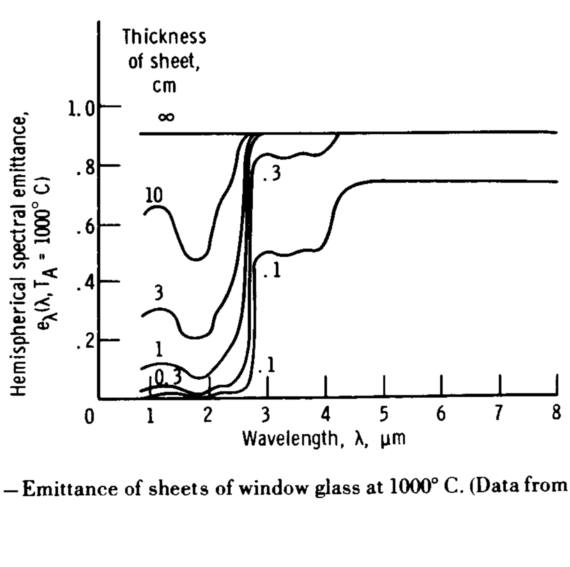

FIGURE 5–27. — Emittance of sheets of window glass at 1000° C. (Data from Gardon (ref. 26).)

is that of a blackbody at 1420° R multiplied by the spectral emissivity of the selective surface. The integrated energy under the spectral curves of absorbed and emitted energy are equal, although this is not obvious from the log-log plot.

EXAMPLE 5–3: A selective surface having spectral characteristics as given in the previous example is to be used as a solar energy absorber. The surface is to be maintained at a temperature of $T_A = 712°$ R by extracting energy to be used in a power generating cycle. If the absorber is placed in orbit around the Sun at the same radius as the Earth, how much net energy will a square foot of the surface provide? How does this energy compare with that supplied by a black surface at the same temperature?

The net energy extracted from the surface is the difference between that absorbed and that emitted. The absorbed energy flux is as in example 5–2

$$q_a = \{0.95F_{0-\lambda_c}(T_R) + 0.05[1 - F_{0-\lambda_c}(T_R)]\}q_i$$

$$= [0.95(0.869) + 0.05(1 - 0.869)]442$$

$$= 368 \frac{\text{Btu}}{(\text{hr})(\text{sq ft})}$$

The emitted flux is

$$q_e = \{0.95F_{0-\lambda_c}(T_A) + 0.05[1 - F_{0-\lambda_c}(T_A)]\}\sigma T_A^4$$

$$= \{0.95 \times (\sim 0) + 0.05[1 - (\sim 0)]\}0.1712 \times 10^{-8} \times (712)^4$$

$$= 22.0 \frac{\text{Btu}}{(\text{hr})(\text{sq ft})}$$

and the net energy that can be used for power generation is $(368 - 22) = 346$ Btu/(hr)(sq ft). For a black or gray body, the equilibrium temperature was found in example 5–1 as 712° R, so that the net useful energy that could be removed from such a surface would be zero.

Although it is partly a transmission effect, it is worth mentioning the characteristic ability of a glass enclosure, such as a greenhouse, to trap solar energy. A glass plate can also be used to cover a surface in order to increase the efficiency of the surface as a solar absorber. The reason for this is that many types of glass are spectrally selective with regard to their transmission of radiation. Figure 5–27 shows the emittance (being an extensive property) of window glass sheets of various thicknesses, and the form of the curves with regard to variation with wavelength is opposite to that in figure 5–25. The cutoff wavelength is about 2.7 μm; this means that the glass has a low absorptance for solar radiation which is primarily at the short wavelengths, and consequently incident solar radiation passes readily into a glass enclosure. The emission from objects at ambient temperature inside the enclosure is at long wavelengths and is trapped because of the high absorptance (poor transmission) of the glass in this spectral region.

Another application in which spectrally selective surfaces can be employed to advantage is where it is desirable to cool an object that is exposed to incident radiation from a high-temperature source. The most common situation would be objects exposed to the Sun, such as a gasoline storage tank, a cryogenic fuel tank in space, or the roof of a building. A highly reflecting coating could be utilized, such as a polished metal. This would reflect much of the incident energy, but would be poor for radiating away any energy that was absorbed or generated within the enclosure (e.g., an enclosure filled with electronic equipment). Also, some metals have a tendency toward lower reflectivity at the shorter wavelengths; this is shown, for example, for uncoated aluminum in figure 5–13. For some applications, it may be advantageous to use a material that is spectrally selective; white paint as shown in figure 5–28

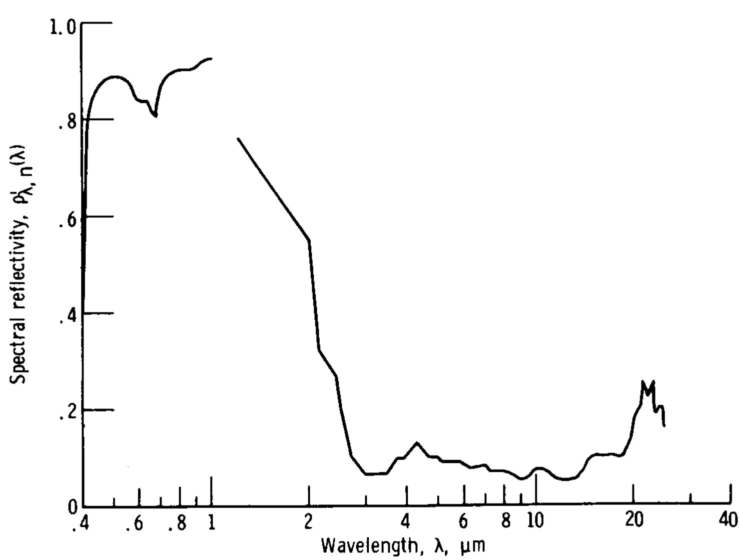

FIGURE 5–28.—Reflectivity of white paint coating on aluminum. (Replotted from Dunkle (ref. 27).)

is an example. This will not only reflect the incident radiation which is predominantly at short wavelengths but will also radiate well at the longer wavelengths characteristic of the relatively low temperature of the body.

5.5.2 Modification of Directional Characteristics

As discussed in previous sections of this chapter, the roughness of a surface can have profound effects on the radiative properties and will indeed become a controlling factor when the roughness is large in comparison with the wavelength of the energy being considered. This leads to the concept of controlling the roughness in order to tailor the directional characteristics of a surface.

If the surface is used as an emitter, the surface might be roughened or designed in such a way as to emit strongly in preferred directions, while reducing emission into unwanted directions. Commercial radiant area heating equipment would operate more efficiently using such surfaces by directing energy to the areas where it is most needed. The most common device for controlling the directional distribution of electromagnetic radiation in the visible region is called a "lamp shade."

If the directional surface were primarily used as an absorber, then, using a solar absorber as an example, we might make it strongly absorbing in the direction of incident solar radiation but as close as possible to nonabsorbing in other directions. The surface would, because of Kirchhoff's law for directional properties, emit strongly toward the Sun, but weakly in other directions. The surface would absorb the same energy as a nondirectional absorber since the incident energy is only from the direction of the Sun but would emit less energy than a surface that emits well into all directions.

The characteristics of one such surface are shown in figure 5–29. The surface has very long grooves of angle 18.2° running parallel to each other. A highly reflecting specular coating is placed on the side walls of each groove, and a black surface is placed at the base of each groove. The solid line gives the behavior predicted by analysis of such an ideal surface, while the data points show experimental results for an actual surface. It is seen that the directional total emissivity is very high for angles of emission less than about 30° from the surface normal. It then drops rapidly as the angle becomes larger. Many other such surface configurations exhibit similar characteristics.

EXAMPLE 5–4: Suppose that a directional surface has a directional total emissivity given by

$$\epsilon(\beta)=1 \qquad 0 \leqslant \beta \leqslant 30^\circ$$

$$\epsilon(\beta)=0 \qquad \beta > 30^\circ$$

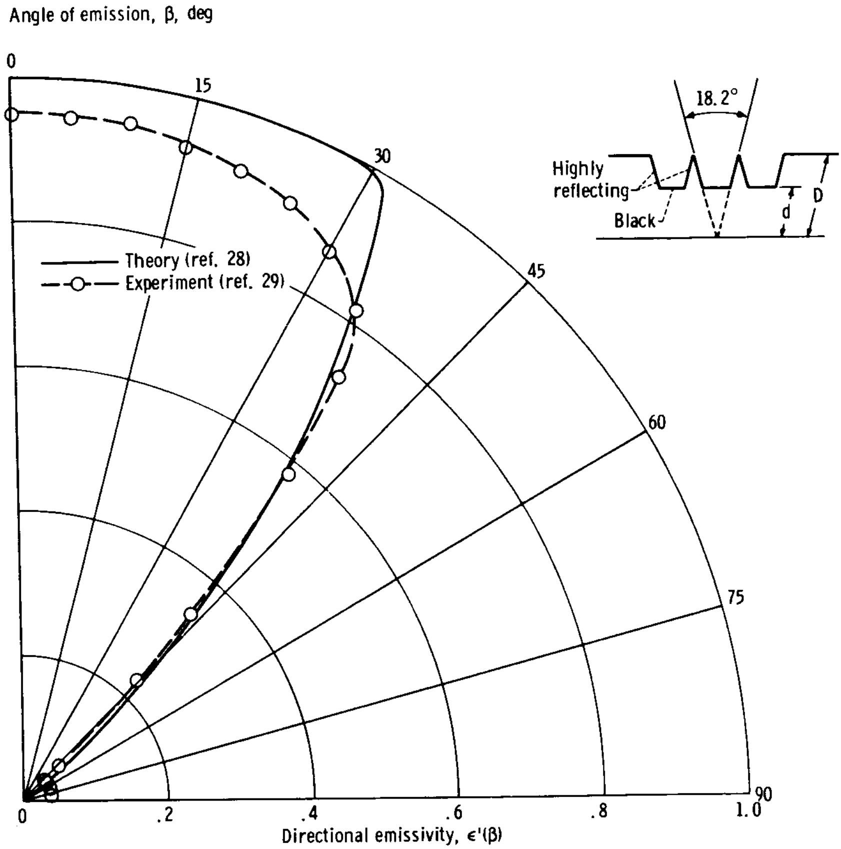

FIGURE 5-29.—Directional emissivity of grooved surface with highly reflecting specular side walls and highly absorbing base; $d/D = 0.649$.

For solar radiation incident normally on such a surface on Earth with no other heat exchange except by radiation from the directional surface, what is the equilibrium temperature of the surface? How does this temperature compare with that achieved by a black surface?

The absorptivity of this surface for normal incident radiation is unity. Therefore, the absorbed energy per unit time is

$$Q_a = (1) q_i A$$

where q_i is again the solar constant for an object at a distance equal to the mean radius of the Earth's orbit from the Sun ($q_i = 442$ Btu/(hr)(sq ft)).

The energy emitted by the body when it is at thermal equilibrium is

$$Q_e = \epsilon\sigma T_{eq}^4 A$$

where ϵ is the hemispherical total emissivity given by equation (3–6b) as

$$\epsilon(T_e) = \frac{1}{\pi}\int_{\Omega} \epsilon'(\beta, \theta, T_{eq}) \cos\beta \, d\omega$$

For this problem, ϵ becomes

$$\epsilon = \frac{2\pi}{\pi}\int_{\beta=0}^{30^\circ} \sin\beta \cos\beta \, d\beta = 0.25$$

Equating Q_a and Q_e for radiative equilibrium gives

$$T_{eq} = \left(\frac{q_i}{\epsilon\sigma}\right)^{1/4} = \left(\frac{442}{0.25\times 0.1712\times 10^{-8}}\right)^{1/4} = 1005^\circ \text{ R}$$

This is larger than the equilibrium temperature of a black or gray diffuse body of 712° R as shown in example 5–1.

Note that equation (5–5) can be used for the α_n'/ϵ of directional as well as spectrally selective surfaces. For the surface used in this example, $\alpha_n'/\epsilon = 4.0$. Combining selective and directional effects would be a way for obtaining considerably increased values of α_n'/ϵ for a given surface.

It should not be inferred that the directional distribution of emissivity assumed in this example corresponds to that of the parallel grooved surface in figure 5–29. In the case of figure 5–29, there is a strong dependence on the angle θ, which has been ignored in this example.

5.6 CONCLUDING REMARKS

The radiative property examples discussed in the present chapter have illustrated a number of the features that may be encountered when dealing with real surfaces. Certain broad generalizations could be attempted. For example, the total emissivities of dielectrics at moderate temperatures are larger than those for metals, and the spectral emissivity of metals increases with temperature over a broad range of wavelengths. However, these types of rules can be misleading because of the large property variations that can occur as a result of surface roughness, contamination, oxide coating, grain structure, and so forth. The presently available analytical procedures cannot account for all these factors so that it is not possible to predict radiation property values directly except for surfaces that approach ideal conditions of composition and finish. By coupling analytical trends with observations of experimental trends, it is possible to gain some insight into what classes of surfaces would be expected to be suitable for specific applications and how surfaces may be fabricated to obtain certain types of radiative behavior. The latter includes spectrally selective surfaces which are of great value in a number of practical applications such as the collection of solar energy.

Some other factors affecting radiative properties that evade prediction are outside the range of interest in this work, but they should be mentioned. For example, it is well known that exposure to ultraviolet radiation; cosmic rays; neutron, gamma, and proton bombardment; and the solar wind can all cause significant changes in radiative properties. For design of spacecraft, these effects are of major concern.

Finally, some comment on the measurement of radiative properties should be given. It has been noted that few precise measurements of directional spectral properties have been made. The reason for this lies in one of the many practical difficulties involved. This is that for a directional measurement the energy available for detection at a small solid angle centered about a given direction is itself small. If only the portion of this small energy that lies within a wavelength band is then measured to obtain directional spectral values, an even smaller energy is available for detection. Minor absolute errors in the measurement of the energy can then lead to large percentage errors in the directional properties being determined. Further, the sheer magnitude of the amount of data generated for such combined directional spectral properties precludes its gathering unless a very specific problem requires it. These and similar practical problems make the field of thermal radiation property measurement a most exacting and difficult one.

REFERENCES

1. GUBAREFF, G. G.; JANSSEN, J. E.; AND TORBERG, R. H.: Thermal Radiation Properties Survey. Second ed., Honeywell Research Center, 1960.
2. SVET, DARIĬ IAKOVLEVICH: Thermal Radiation; Metals, Semiconductors, Ceramics, Partly Transparent Bodies, and Films. Consultants Bureau, 1965.
3. GOLDSMITH, ALEXANDER; AND WATERMAN, THOMAS E.: Thermophysical Properties of Solid Materials. (WADC TR 58–476), Armour Research Foundation, Jan. 1959.
4. HOTTEL, H. C.: Radiant Heat Transmission. Heat Transmission. William H. McAdams, Third ed., McGraw-Hill Book Co., Inc., 1954, pp. 472–479.
5. WOOD, W. D.; DEEM, H. W.; AND LUCKS, C. F.: Thermal Radiative Properties. Plenum Press, 1964.
6. EDWARDS, D. K.; AND CATTON, IVAN: Radiation Characteristics of Rough and Oxidized Metals. Advances in Thermophysical Properties at Extreme Temperatures and Pressures. Serge Gratch, ed., ASME, 1965, pp. 189–199.
7. SADYKOV, B. S.: Temperature Dependence of the Radiating Power of Metals. High Temp., vol. 3, no. 3, May–June 1965, pp. 352–356.

8. DAVIES, H.: The Reflection of Electromagnetic Waves from a Rough Surface. Inst. Elect. Engrs. Proc., IV, vol. 101, Aug. 1954, pp. 209–214.
9. PORTEUS, J. O.: Relation Between the Height Distribution of a Rough Surface and the Reflectance at Normal Incidence. Opt. Soc. Am. J., vol. 53, no. 12, Dec. 1963, pp. 1394–1402.
10. BECKMANN, P.; AND SPIZZICHINO, A.: The Scattering of Electromagnetic Waves From Rough Surfaces. The Macmillan Company, 1963.
11. LIEBERT, CURT H.: Spectral Emittance of Aluminum Oxide and Zinc Oxide on Opaque Substrates. NASA TN D–3115, 1965.
12. SAROFIM, A. F.; AND HOTTEL, H. C.: Radiative Exchange Among Non-Lambert Surfaces. J. Heat Transfer, vol. 88, no. 1, Feb. 1966, pp. 37–44.
13. SPARROW, E. M.; AND LIN, S. L.: Radiation Heat Transfer at a Surface Having Both Specular and Diffuse Reflectance Components. Intl. J. Heat Mass Transfer, vol. 8, May 1965, pp. 769–779.
14. LIEBERT CURT H.: Spectral Emissivity of Highly Doped Silicon. Paper No. 67–302, AIAA, Apr. 1967.
15. SEBAN, R. A.: Thermal Radiation Properties of Materials. Part III. (WADD TR–60–370, Pt. III), California Univ. (Berkeley), Aug. 1963.
16. DEVOS, J. C.: A New Determination of the Emissivity of Tungsten Ribbon. Physica, vol. 20, 1954, pp. 690–714.
17. BIRKEBAK, R. C.; AND ECKERT, E. R. G.: Effects of Roughness of Metal Surfaces on Angular Distribution of Monochromatic Reflected Radiation. J. Heat Transfer, vol. 87, no. 1, Feb. 1965, pp. 85–94.
18. EDWARDS, D. K.; AND DEVOLO, N. BAYARD: Useful Approximations for the Spectral and Total Emissivity of Smooth Bare Metals. Advances in Thermophysical Properties at Extreme Temperatures and Pressures. Serge Gratch, ed., ASME, 1965, pp. 174–188.
19. MUNCH, B.: Directional Distribution in the Reflection of Heat Radiation and its Effect in Heat Transfer. Ph. D. thesis, Swiss Technical College of Zurich, 1955.
20. WILLIAMS, D. A.; LAPPIN, T. A.; AND DUFFIE, J. A.: Selective Radiation Properties of Particulate Coatings. J. Eng. Power, vol. 85, no. 3, July 1963, pp. 213–220.
21. OHLSEN, P. E.; AND ETAMAD, G. A.: Spectral and Total Radiation Data of Various Aircraft Materials. Rep. No. NA57–330, North American Aviation, July 23, 1957.
22. ORLOVA, N. S.: Photometric Relief of the Lunar Surface. Astron. Zhur., vol. 33, no. 1, Jan./Feb. 1956, pp. 93–100.
23. LONG, R. L.: A Review of Recent Air Force Research on Selective Solar Absorbers. J. Eng. Power, vol. 87, no. 3, July 1965, pp. 277–280.
24. HIBBARD, R. R.: Equilibrium Temperatures of Ideal Spectrally Selective Surfaces. Solar Energy, vol. 5, no. 4, Oct.–Dec. 1961, pp. 129–132.
25. SHAFFER, L. H.: Wavelength-Dependent (Selective) Processes for the Utilization of Solar Energy. J. Solar Energy Science Eng., vol. 2, no. 3–4, July–Oct. 1958, pp. 21–26.
26. GARDON, ROBERT: The Emissivity of Transparent Materials. Am. Ceramic Soc. J., vol. 39, no. 8, Aug. 1956, pp. 278–287.
27. DUNKLE, R. V.: Thermal Radiation Characteristics of Surfaces. Theory and Fundamental Research in Heat Transfer. J. A. Clark, ed., Pergamon Press, 1963, pp. 1–31.
28. PERLMUTTER, MORRIS; AND HOWELL, JOHN R.: A Strongly Directional Emitting and Absorbing Surface. J. Heat Transfer, vol. 85, no. 3, Aug. 1963, pp. 282–283.
29. BRANDENBERG, W. M.; AND CLAUSEN, O. W.: The Directional Spectral Emittance of Surfaces Between 200° and 600° C. Symposium on Thermal Radiation of Solids, S. Katzoff, ed., NASA SP–55 (AFML–TDR–64–159), 1965.

295–763 OL–68—12

Appendix

Tables of conversion factors between the mks and other common systems of units are given in tables I to III of this appendix. In table IV, accurate values of the various radiation constants are given in both mks units and the common English engineering units. Finally, table V lists various blackbody properties as functions of the variable λT, again in both mks and English engineering units.

With regard to table V, Pivovonsky and Nagel (ref. 3) and Wiebelt (ref. 4) have presented polynomial curves fitted to the function $F_{0-\lambda T}$. These curve fits can be quite useful for computer solutions of various types of radiation problems. Wiebelt recommends use of the following polynomials:

$$F_{0-\lambda T}=\frac{15}{\pi^4}\sum_{m=1,2,\ldots}\frac{e^{-mv}}{m^4}\{[(mv+3)mv+6]mv+6\},\ v\geq 2$$

$$F_{0-\lambda T}=1-\frac{15}{\pi^4}v^3\left(\frac{1}{3}-\frac{v}{8}+\frac{v^2}{60}-\frac{v^4}{5040}+\frac{v^6}{272160}-\frac{v^8}{13305600}\right),\ v<2$$

where

$$v=\frac{C_2}{\lambda T}$$

and C_2 is given in table IV. The series is carried out to a sufficient number of terms to gain the desired accuracy.

REFERENCES

1. MECHTLY, E. A.: The International System of Units. Physical Constants and Conversion Factors. NASA SP-7012, 1964.
2. GUBAREFF, G. G.; JANSSEN, J. E.; AND TORBERG, R. H.: Thermal Radiation Properties Survey. Second ed., Honeywell Research Center, 1960.
3. PIVOVONSKY, MARK; AND NAGEL, MAX R.: Tables of Blackbody Radiation Functions. Macmillan Book Co., 1961.
4. WIEBELT, JOHN A.: Engineering Radiation Heat Transfer. Holt, Rinehart & Winston, 1966.

TABLE I. – CONVERSION FACTORS FOR LENGTHS

	Mile (mi)	Kilometer (km)	Meter (m)	Foot (ft)	Inch (in.)	Centimeter (cm)	Millimeter (mm)	Micron (μm)	Millimicron (mμm)	Angstrom (Å)
1 mile = ...	1	1.609	1609	5280	6.336×10^{4}	1.609×10^{5}	1.609×10^{6}	1.609×10^{9}	1.609×10^{12}	1.609×10^{13}
1 kilometer = ...	0.6214	1	10^{3}	3.281×10^{3}	3.937×10^{4}	10^{5}	10^{6}	10^{9}	10^{12}	10^{13}
1 meter = ...	6.214×10^{-4}	10^{-3}	1	3.281	39.37	10^{2}	10^{3}	10^{6}	10^{9}	10^{10}
1 foot = ...	1.894×10^{-4}	3.048×10^{-4}	0.3048	1	12	30.48	3.048×10^{2}	3.048×10^{5}	3.048×10^{8}	3.048×10^{9}
1 inch = ...	1.578×10^{-5}	2.540×10^{-5}	2.540×10^{-2}	8.333×10^{-2}	1	2.540	25.40	2.540×10^{4}	10^{7}	10^{8}
1 centimeter = ..	6.214×10^{-6}	10^{-5}	10^{-2}	3.281×10^{-2}	0.3937	1	10	10^{4}	10^{7}	10^{8}
1 millimeter = ...	6.214×10^{-7}	10^{-6}	10^{-3}	3.281×10^{-3}	.03937	10^{-1}	1	10^{3}	10^{6}	10^{7}
1 micron = ...	6.214×10^{-10}	10^{-9}	10^{-6}	3.281×10^{-6}	3.937×10^{-5}	10^{-4}	10^{-3}	1	10^{3}	10^{4}
1 millimicron (nanometer) = .	6.214×10^{-13}	10^{-12}	10^{-9}	3.281×10^{-9}	3.937×10^{-8}	10^{-7}	10^{-6}	10^{-3}	1	10
1 angstrom = ...	6.214×10^{-14}	10^{-13}	10^{-10}	3.281×10^{-10}	3.937×10^{-9}	10^{-8}	10^{-7}	10^{-4}	10^{-1}	1

TABLE II. – CONVERSION FACTORS FOR ENERGY UNITS[a]

	Kilowatt-hour (kW-hr)	British thermal unit (Btu)	Gram-calorie (g-cal)	Joule (J)	Erg	Electron volt (eV)
1 kilowatt-hour =	1	3412	8.598×10^{5}	3.600×10^{6}	3.600×10^{13}	2.247×10^{25}
1 British thermal unit[b] =	2.931×10^{-4}	1	252.0	1055	1.055×10^{10}	6.585×10^{21}
1 gram-calorie[b] =	1.163×10^{-6}	3.968×10^{-3}	1	4.187	4.187×10^{7}	2.614×10^{19}
1 joule (W-sec) =	2.778×10^{-7}	9.479×10^{-4}	0.2388	1	10^{7}	6.242×10^{18}
1 erg (dyne-cm) =	2.778×10^{-14}	9.479×10^{-11}	2.388×10^{-8}	10^{-7}	1	6.242×10^{11}
1 electron volt =	4.450×10^{-26}	1.519×10^{-22}	3.826×10^{-20}	1.602×10^{-19}	1.602×10^{-12}	1

[a] Values are taken from ref. 1.
[b] Based on International Steam Table.

TABLE III. — CONVERSION FACTORS FOR ENERGY FLUX

	cal/(sec)(cm²)	Btu/(hr)(ft²)	W/m²	erg/(sec)(cm²)
1 cal/(sec)(cm²)[a] =	1	1.329×10^{4}	4.187×10^{4}	4.187×10^{7}
1 Btu/(hr)(ft²) =	7.525×10^{-5}	1	3.152	3.152×10^{3}
1 W/m² =	2.388×10^{-5}	0.3174	1	10^{3}
1 erg/(sec)(cm²) =	2.388×10^{-8}	3.174×10^{-4}	10^{-3}	1

[a] Based on International Steam Table.

TABLE IV. — RADIATION CONSTANTS [a]

Symbol	Definition	Value
C_1	Constant in Planck's spectral energy distribution, (Btu)(μm⁴)/(hr)(ft²); W/cm²	0.18892×10^{8}; 0.59544×10^{-12}
C_2	Constant in Planck's spectral energy distribution, (μm)(°R); (cm)(°K)	25898; 1.4388
C_3	Constant in Wien's displacement law (μm)(°R); (cm)(°K)	5216.0; 0.28978
$\sigma_{calculated}$	Calculated Stefan-Boltzmann constant, Btu/(hr)(ft²)(°R⁴); W/(cm²)(°K⁴)	0.1712×10^{-8}; 5.6693×10^{-12}
$\sigma_{experimental}$	Experimental Stefan-Boltzmann constant, Btu/(hr)(ft²)(°R⁴); W/(cm²)(°K⁴)	0.173×10^{-8}; 5.729×10^{-12}

[a] Recommended values from ref. 2.

TABLE V.—BLACKBODY FUNCTIONS

Wavelength-temperature product, λT		Blackbody hemispherical spectral emissive power divided by fifth power of temperature, $e_{\lambda b}/T^5$		Blackbody fraction, $F_{0-\lambda T}$	Difference between successive $F_{0-\lambda T}$ values, ΔF
(μm)(°R)	(μm)(°K)	$\frac{\text{Btu}}{(\text{hr})(\text{sq ft})(\mu\text{m})(°\text{R}^5)}$	$\frac{\text{W}}{(\text{cm}^2)(\mu\text{m})(°\text{K}^5)}$		
1000	555.6	0.000671×10^{-15}	0.400×10^{-20}	0.170×10^{-7}	0
1100	611.1	.00439	$.261 \times 10^{-19}$	$.136 \times 10^{-6}$	$.119 \times 10^{-6}$
1200	666.7	.0202	$.120 \times 10^{-18}$	$.756 \times 10^{-6}$	$.620 \times 10^{-6}$
1300	722.2	.0713	$.424 \times 10^{-18}$	$.317 \times 10^{-5}$	$.241 \times 10^{-5}$
1400	777.8	.204	$.00122 \times 10^{-15}$	$.106 \times 10^{-4}$	$.748 \times 10^{-5}$
1500	833.3	$.496 \times 10^{-15}$	$.00296 \times 10^{-15}$	$.301 \times 10^{-4}$	$.194 \times 10^{-4}$
1600	888.9	1.057	.00630	$.738 \times 10^{-4}$	$.437 \times 10^{-4}$
1700	944.4	2.023	.01205	$.161 \times 10^{-3}$	$.876 \times 10^{-4}$
1800	1000.0	3.544	.02111	$.321 \times 10^{-3}$	.00016
1900	1055.6	5.767	.03434	$.589 \times 10^{-3}$	.00027
2000	1111.1	8.822×10^{-15}	$.05254 \times 10^{-15}$	.00101	.00042
2100	1166.7	12.805	.07626	.00164	.00063
2200	1222.2	17.776	.10587	.00252	.00089
2300	1277.8	23.746	.14142	.00373	.00121
2400	1333.3	30.686	.18275	.00531	.00158
2500	1388.9	38.526×10^{-15}	$.22945 \times 10^{-15}$	.00733	.00202
2600	1444.4	47.167	.28091	.00983	.00250
2700	1500.0	56.483	.33639	.01285	.00302
2800	1555.6	66.334	.39505	.01643	.00358
2900	1611.1	76.571	.45602	.02060	.00417
3000	1666.7	87.047×10^{-15}	$.51841 \times 10^{-15}$	.02537	.00477
3100	1722.2	97.615	.58135	.03076	.00539
3200	1777.8	108.14	.64404	.03677	.00600
3300	1833.3	118.50	.70573	.04338	.00661
3400	1888.9	128.58	.76578	.05059	.00721
3500	1944.4	138.29×10^{-15}	$.82362 \times 10^{-15}$	.05838	.00779
3600	2000.0	147.56	.87878	.06672	.00834
3700	2055.6	156.30	.93088	.07559	.00887
3800	2111.1	164.49	.97963	.08496	.00936
3900	2166.7	172.08	1.0248	.09478	.00982
4000	2222.2	179.04×10^{-15}	1.0663×10^{-15}	.10503	.01025
4100	2277.8	185.36	1.1039	.11567	.01064
4200	2333.3	191.05	1.1378	.12665	.01099
4300	2388.9	196.09	1.1678	.13795	.01130
4400	2444.4	200.51	1.1942	.14953	.01158

TABLE V.—BLACKBODY FUNCTIONS—Continued

Wavelength-temperature product, λT		Blackbody hemispherical spectral emissive power divided by fifth power of temperature, $e_{\lambda b}/T^5$		Blackbody fraction, $F_{0-\lambda T}$	Difference between successive $F_{0-\lambda T}$ values, ΔF
(μm)(°R)	(μm)(°K)	$\frac{\text{Btu}}{(\text{hr})(\text{sq ft})(\mu\text{m})(°\text{R}^5)}$	$\frac{\text{W}}{(\text{cm}^2)(\mu\text{m})(°\text{K}^5)}$		
4500	2500.0	204.32×10^{-15}	1.2169×10^{-15}	0.16135	0.01182
4600	2555.6	207.55	1.2361	.17337	.01202
4700	2611.1	210.20	1.2519	.18556	.01219
4800	2666.7	212.32	1.2645	.19789	.01233
4900	2722.2	213.93	1.2741	.21033	.01244
5000	2777.8	215.06×10^{-15}	1.2808×10^{-15}	.22285	.01252
5100	2833.3	215.74	1.2848	.23543	.01257
5200	2888.9	216.00	1.2864	.24803	.01260
5300	2944.4	215.87	1.2856	.26063	.01260
5400	3000.0	215.39	1.2827	.27322	.01259
5500	3055.6	214.57×10^{-15}	1.2779×10^{-15}	.28576	.01255
5600	3111.1	213.46	1.2713	.29825	.01249
5700	3166.7	212.07	1.2630	.31067	.01242
5800	3222.2	210.43	1.2532	.32300	.01233
5900	3277.8	208.57	1.2422	.33523	.01223
6000	3333.3	206.51×10^{-15}	1.2299×10^{-15}	.34734	.01211
6100	3388.9	204.28	1.2166	.35933	.01199
6200	3444.4	201.88	1.2023	.37118	.01185
6300	3500.0	199.35	1.1872	.38289	.01171
6400	3555.6	196.69	1.1714	.39445	.01156
6500	3611.1	193.94×10^{-15}	1.1550×10^{-15}	.40585	.01140
6600	3666.7	191.09	1.1380	.41708	.01124
6700	3722.2	188.17	1.1206	.42815	.01107
6800	3777.8	185.18	1.1029	.43905	.01089
6900	3833.3	182.15	1.0848	.44977	.01072
7000	3888.9	179.08×10^{-15}	1.0665×10^{-15}	.46031	.01054
7100	3944.4	175.98	1.0481	.47067	.01036
7200	4000.0	172.86	1.0295	.48085	.01018
7300	4055.6	169.74	1.0109	.49084	.01000
7400	4111.1	166.60	0.99221	.50066	.00981
7500	4166.7	163.47×10^{-15}	$.97357\times10^{-15}$	.51029	.00963
7600	4222.2	160.35	.95499	.51974	.00945
7700	4277.8	157.25	.93650	.52901	.00927
7800	4333.3	154.16	.91813	.53809	.00909
7900	4388.9	151.10	.89990	.54700	.00891

TABLE V. — BLACKBODY FUNCTIONS — Continued

Wavelength-temperature product, λT		Blackbody hemispherical spectral emissive power divided by fifth power of temperature, $e_{\lambda b}/T^5$		Blackbody fraction, $F_{0-\lambda T}$	Difference between successive $F_{0-\lambda T}$ values, ΔF
(μm)(°R)	(μm)(°K)	$\frac{\text{Btu}}{(\text{hr})(\text{sq ft})(\mu\text{m})(°\text{R}^5)}$	$\frac{\text{W}}{(\text{cm}^2)(\mu\text{m})(°\text{K}^5)}$		
8000	4444.4	148.07×10^{-15}	0.88184×10^{-15}	0.55573	0.00873
8100	4500.0	145.07	.86396	.56429	.00855
8200	4555.6	142.10	.84629	.57267	.00838
8300	4611.1	139.17	.82884	.58087	.00821
8400	4666.7	136.28	.81163	.58891	.00804
8500	4722.2	133.43×10^{-15}	$.79467 \times 10^{-15}$	.59678	.00787
8600	4777.8	130.63	.77796	.60449	.00771
8700	4833.3	127.87	.76151	.61203	.00754
8800	4888.9	125.15	.74534	.61941	.00738
8900	4944.4	122.48	.72944	.62664	.00723
9000	5000.0	119.86×10^{-15}	$.71383 \times 10^{-15}$	.63371	.00707
9100	5055.6	117.29	.69850	.64063	.00692
9200	5111.1	114.76	.68346	.64740	.00677
9300	5166.7	112.28	.66870	.65402	.00662
9400	5222.2	109.85	.65423	.66051	.00648
9500	5277.8	107.47×10^{-15}	$.64006 \times 10^{-15}$	.66685	.00634
9600	5333.3	105.14	.62617	.67305	.00620
9700	5388.9	102.86	.61257	.67912	.00607
9800	5444.4	100.62	.59925	.68506	.00594
9900	5500.0	98.431	.58621	.69087	.00581
10000	5555.6	96.289×10^{-15}	$.57346 \times 10^{-15}$	.69655	.00568
10100	5611.1	94.194	.56098	.70211	.00556
10200	5666.7	92.145	.54877	.70754	.00544
10300	5722.2	90.141	.53684	.71286	.00532
10400	5777.8	88.181	.52517	.71806	.00520
10500	5833.3	86.266×10^{-15}	$.51376 \times 10^{-15}$	.72315	.00509
10600	5888.9	84.394	.50261	.72813	.00498
10700	5944.4	82.565	.49172	.73301	.00487
10800	6000.0	80.777	.48107	.73777	.00477
10900	6055.6	79.031	.47067	.74244	.00466
11000	6111.1	77.325×10^{-15}	$.46051 \times 10^{-15}$	.74700	.00456
11100	6166.7	75.658	.45059	.75146	.00446
11200	6222.2	74.031	.44089	.75583	.00437
11300	6277.8	72.441	.43143	.76010	.00427
11400	6333.3	70.889	.42218	.76429	.00418

TABLE V.—BLACKBODY FUNCTIONS—Continued

Wavelength-temperature product, λT		Blackbody hemispherical spectral emissive power divided by fifth power of temperature, $e_{\lambda b}/T^5$		Blackbody fraction, $F_{0-\lambda T}$	Difference between successive $F_{0-\lambda T}$ values, ΔF
(μm)(°R)	(μm)(°K)	Btu / (hr)(sq ft)(μm)(°R^5)	W / (cm^2)(μm)(°K^5)		
11500	6388.9	69.373×10^{-15}	0.41315×10^{-15}	0.76838	0.00409
11600	6444.4	67.892	.40434	.77238	.00401
11700	6500.0	66.447	.39573	.77630	.00392
11800	6555.6	65.036	.38732	.78014	.00384
11900	6611.1	63.658	.37912	.78390	.00376
12000	6666.7	62.313×10^{-15}	$.37111 \times 10^{-15}$	.78757	.00368
12100	6722.2	60.999	.36328	.79117	.00360
12200	6777.8	59.717	.35565	.79469	.00352
12300	6833.3	58.465	.34819	.79814	.00345
12400	6888.9	57.242	.34091	.80152	.00338
12500	6944.4	56.049×10^{-15}	$.33380 \times 10^{-15}$	.80482	.00331
12600	7000.0	54.884	.32687	.80806	.00324
12700	7055.6	53.747	.32009	.81123	.00317
12800	7111.1	52.636	.31348	.81433	.00310
12900	7166.7	51.552	.30702	.81737	.00304
13000	7222.2	50.493×10^{-15}	$.30071 \times 10^{-15}$	.82035	.00298
13100	7277.8	49.459	.29456	.82327	.00292
13200	7333.3	48.450	.28855	.82612	.00286
13300	7388.9	47.465	.28268	.82892	.00280
13400	7444.4	46.502	.27695	.83166	.00274
13500	7500.0	45.563×10^{-15}	$.27135 \times 10^{-15}$	.83435	.00269
13600	7555.6	44.645	.26589	.83698	.00263
13700	7611.1	43.749	.26055	.83956	.00258
13800	7666.7	42.874	.25534	.84209	.00253
13900	7722.2	42.019	.25024	.84457	.00248
14000	7777.8	41.184×10^{-15}	$.24527 \times 10^{-15}$	.84699	.00243
14100	7833.3	40.368	.24042	.84937	.00238
14200	7888.9	39.572	.23567	.85171	.00233
14300	7944.4	38.794	.23104	.85399	.00229
14400	8000.0	38.033	.22651	.85624	.00224
14500	8055.6	37.291×10^{-15}	$.22209 \times 10^{-15}$	.85843	.00220
14600	8111.1	36.565	.21777	.86059	.00216
14700	8166.7	35.856	.21354	.86270	.00211
14800	8222.2	35.163	.20942	.86477	.00207
14900	8277.8	34.487	.20539	.86681	.00203

TABLE V.—BLACKBODY FUNCTIONS—Continued

Wavelength-temperature product, λT		Blackbody hemispherical spectral emissive power divided by fifth power of temperature, $e_{\lambda b}/T^5$		Blackbody fraction, $F_{0-\lambda T}$	Difference between successive $F_{0-\lambda T}$ values, ΔF
(μm)(°R)	(μm)(°K)	$\frac{\text{Btu}}{(\text{hr})(\text{sq ft})(\mu\text{m})(°\text{R}^5)}$	$\frac{\text{W}}{(\text{cm}^2)(\mu\text{m})(°\text{K}^5)}$		
15000	8333.3	33.825×10^{-15}	0.20145×10^{-15}	0.86880	0.00199
15100	8388.9	33.179	.19760	.87075	.00196
15200	8444.4	32.547	.19383	.87267	.00192
15300	8500.0	31.929	.19016	.87455	.00188
15400	8555.6	31.326	.18656	.87640	.00185
15500	8611.1	30.736×10^{-15}	$.18305 \times 10^{-15}$	.87821	.00181
15600	8666.7	30.159	.17961	.87999	.00178
15700	8722.2	29.595	.17625	.88173	.00174
15800	8777.8	29.043	.17297	.88344	.00171
15900	8833.3	28.504	.16976	.88512	.00168
16000	8888.9	27.977×10^{-15}	$.16662 \times 10^{-15}$	.88677	.00165
16100	8944.4	27.462	.16355	.88839	.00162
16200	9000.0	26.957	.16055	.88997	.00159
16300	9055.6	26.464	.15761	.89153	.00156
16400	9111.1	25.982	.15474	.89306	.00153
16500	9166.7	25.510×10^{-15}	$.15193 \times 10^{-15}$	.89457	.00150
16600	9222.2	25.049	.14918	.89604	.00148
16700	9277.8	24.597	.14649	.89749	.00145
16800	9333.3	24.156	.14386	.89891	.00142
16900	9388.9	23.723	.14129	.90031	.00140
17000	9444.4	23.301×10^{-15}	$.13877 \times 10^{-15}$	.90168	.00137
17100	9500.0	22.887	.13630	.90303	.00135
17200	9555.6	22.482	.13389	.90435	.00132
17300	9611.1	22.085	.13153	.90565	.00130
17400	9666.7	21.697	.12922	.90693	.00128
17500	9722.2	21.318×10^{-15}	$.12696 \times 10^{-15}$	.90819	.00126
17600	9777.8	20.946	.12475	.90942	.00123
17700	9833.3	20.582	.12258	.91063	.00121
17800	9888.9	20.226	.12046	.91182	.00119
17900	9944.4	19.877	.11838	.91299	.00117
18000	10000.0	19.536×10^{-15}	$.11635 \times 10^{-15}$	.91414	.00115
18100	10055.6	19.201	.11435	.91527	.00113
18200	10111.1	18.874	.11240	.91638	.00111
18300	10166.7	18.553	.11049	.91748	.00109
18400	10222.2	18.239	.10862	.91855	.00107

TABLE V. – BLACKBODY FUNCTIONS – Continued

Wavelength-temperature product, λT		Blackbody hemispherical spectral emissive power divided by fifth power of temperature, $e_{\lambda b}/T^5$		Blackbody fraction, $F_{0-\lambda T}$	Difference between successive $F_{0-\lambda T}$ values, ΔF
(μm)(°R)	(μm)(°K)	$\frac{\text{Btu}}{(\text{hr})(\text{sq ft})(\mu\text{m})(°\text{R}^5)}$	$\frac{\text{W}}{(\text{cm}^2)(\mu\text{m})(°\text{K}^5)}$		
18500	10277.8	17.931×10^{-15}	0.10679×10^{-15}	0.91961	0.00106
18600	10333.3	17.630	.10500	.92064	.00104
18700	10388.9	17.335	.10324	.92166	.00102
18800	10444.4	17.045	.10151	.92267	.00100
18900	10500.0	16.762	.09983	.92365	.00099
19000	10555.6	16.484×10^{-15}	$.09817 \times 10^{-15}$	.92462	.00097
19100	10611.1	16.212	.09655	.92558	.00095
19200	10666.7	15.945	.09496	.92652	.00094
19300	10722.2	15.684	.09341	.92744	.00092
19400	10777.8	15.428	.09188	.92835	.00091
19500	10833.3	15.177×10^{-15}	$.09039 \times 10^{-15}$	.92924	.00089
19600	10888.9	14.931	.08892	.93012	.00088
19700	10944.4	14.690	.08749	.93098	.00086
19800	11000.0	14.453	.08608	.93183	.00085
19900	11055.6	14.221	.08470	.93267	.00084
20000	11111.1	13.994×10^{-15}	$.08334 \times 10^{-15}$	.93349	.00082
20200	11222.2	13.553	.08071	.93510	.00161
20400	11333.3	13.128	.07819	.93666	.00156
20600	11444.4	12.720	.07575	.93816	.00151
20800	11555.6	12.327	.07341	.93963	.00146
21000	11666.7	11.949×10^{-15}	$.07116 \times 10^{-15}$	.94104	.00142
21200	11777.8	11.585	.06899	.94242	.00137
21400	11888.9	11.234	.06691	.94375	.00133
21600	12000.0	10.897	.06490	.94504	.00129
21800	12111.1	10.572	.06296	.94629	.00125
22000	12222.2	10.258×10^{-15}	$.06109 \times 10^{-15}$	.94751	.00122
22200	12333.3	9.956	.05930	.94869	.00118
22400	12444.4	9.665	.05756	.94983	.00115
22600	12555.6	9.384	.05589	.95094	.00111
22800	12666.7	9.114	.05428	.95202	.00108
23000	12777.8	8.852×10^{-15}	$.05272 \times 10^{-15}$	.95307	.00105
23200	12888.9	8.600	.05122	.95409	.00102
23400	13000.0	8.357	.04977	.95508	.00099
23600	13111.1	8.122	.04837	.95604	.00096
23800	13222.2	7.895	.04702	.95698	.00093

TABLE V.—BLACKBODY FUNCTIONS—Continued

Wavelength-temperature product, λT		Blackbody hemispherical spectral emissive power divided by fifth power of temperature, $e_{\lambda b}/T^5$		Blackbody fraction, $F_{0-\lambda T}$	Difference between successive $F_{0-\lambda T}$ values, ΔF
(μm)(°R)	(μm)(°K)	$\frac{\text{Btu}}{(\text{hr})(\text{sq ft})(\mu\text{m})(°\text{R}^5)}$	$\frac{\text{W}}{(\text{cm}^2)(\mu\text{m})(°\text{K}^5)}$		
24000	13333.3	7.676×10^{-15}	0.04572×10^{-15}	0.95788	0.00091
24200	13444.4	7.465	.04446	.95877	.00088
24400	13555.6	7.260	.04324	.95963	.00086
24600	13666.7	7.063	.04206	.96046	.00084
24800	13777.8	6.872	.04092	.96128	.00081
25000	13888.9	6.687×10^{-15}	$.03982 \times 10^{-15}$	.96207	.00079
25200	14000.0	6.508	.03876	.96284	.00077
25400	14111.1	6.336	.03773	.96359	.00075
25600	14222.2	6.169	.03674	.96432	.00073
25800	14333.3	6.007	.03577	.96503	.00071
26000	14444.4	5.850×10^{-15}	$.03484 \times 10^{-15}$	.96572	.00069
26200	14555.6	5.699	.03394	.96639	.00067
26400	14666.7	5.552	.03307	.96705	.00066
26600	14777.8	5.410	.03222	.96769	.00064
26800	14888.9	5.273	.03140	.96831	.00062
27000	15000.0	5.139×10^{-15}	$.03061 \times 10^{-15}$	.96892	.00061
27200	15111.1	5.010	.02984	.96951	.00059
27400	15222.2	4.885	.02909	.97009	.00058
27600	15333.3	4.764	.02837	.97065	.00056
27800	15444.4	4.646	.02767	.97120	.00055
28000	15555.6	4.532×10^{-15}	$.02699 \times 10^{-15}$	.97174	.00054
28200	15666.7	4.422	.02633	.97226	.00052
28400	15777.8	4.315	.02570	.97277	.00051
28600	15888.9	4.211	.02508	.97327	.00050
28800	16000.0	4.110	.02448	.97375	.00049
29000	16111.1	4.012×10^{-15}	$.02389 \times 10^{-15}$	.97423	.00047
29200	16222.2	3.917	.02333	.97469	.00046
29400	16333.3	3.824	.02278	.97514	.00045
29600	16444.4	3.735	.02224	.97558	.00044
29800	16555.6	3.648	.02172	.97601	.00043
30000	16666.7	3.563×10^{-15}	$.02122 \times 10^{-15}$	.97644	.00042
30200	16777.8	3.481	.02073	.97685	.00041
30400	16888.9	3.401	.02026	.97725	.00040
30600	17000.0	3.324	.01979	.97764	.00039
30800	17111.1	3.248	.01935	.97802	.00038

TABLE V. – BLACKBODY FUNCTIONS – Continued

Wavelength-temperature product, λT		Blackbody hemispherical spectral emissive power divided by fifth power of temperature, $e_{\lambda b}/T^5$		Blackbody fraction, $F_{0-\lambda T}$	Difference between successive $F_{0-\lambda T}$ values, ΔF
(μm)(°R)	(μm)(°K)	$\frac{\text{Btu}}{(\text{hr})(\text{sq ft})(\mu\text{m})(°\text{R}^5)}$	$\frac{\text{W}}{(\text{cm}^2)(\mu\text{m})(°\text{K}^5)}$		
31000	17222.2	3.175×10^{-15}	0.01891×10^{-15}	0.97840	0.00037
31200	17333.3	3.104	.01849	.97877	.00037
31400	17444.4	3.035	.01807	.97912	.00036
31600	17555.6	2.967	.01767	.97947	.00035
31800	17666.7	2.902	.01728	.97982	.00034
32000	17777.8	2.838×10^{-15}	$.01690 \times 10^{-15}$	.98015	.00033
32200	17888.9	2.776	.01653	.98048	.00033
32400	18000.0	2.716	.01618	.98080	.00032
32600	18111.1	2.657	.01583	.98111	.00031
32800	18222.2	2.600	.01549	.98142	.00031
33000	18333.3	2.545×10^{-15}	$.01515 \times 10^{-15}$	.98172	.00030
33200	18444.4	2.490	.01483	.98201	.00029
33400	18555.6	2.438	.01452	.98230	.00029
33600	18666.7	2.386	.01421	.98258	.00028
33800	18777.8	2.336	.01392	.98286	.00028
34000	18888.9	2.288×10^{-15}	$.01363 \times 10^{-15}$	.98313	.00027
34200	19000.0	2.240	.01334	.98339	.00026
34400	19111.1	2.194	.01307	.98365	.00026
34600	19222.2	2.149	.01280	.98390	.00025
34800	19333.3	2.105	.01254	.98415	.00025
35000	19444.4	2.062×10^{-15}	$.01228 \times 10^{-15}$	.98440	.00024
35200	19555.6	2.021	.01203	.98463	.00024
35400	19666.7	1.980	.01179	.98487	.00023
35600	19777.8	1.940	.01156	.98510	.00023
35800	19888.9	1.902	.01133	.98532	.00022
36000	20000.0	1.864×10^{-15}	$.01110 \times 10^{-15}$	.98554	.00022
36200	20111.1	1.827	.01088	.98576	.00022
36400	20222.2	1.791	.01067	.98597	.00021
36600	20333.3	1.756	.01046	.98617	.00021
36800	20444.4	1.722	.01026	.98638	.00020
37000	20555.6	1.689×10^{-15}	$.01006 \times 10^{-15}$	.98658	.00020
37200	20666.7	1.656	.00986	.98677	.00020
37400	20777.8	1.624	.00967	.98696	.00019
37600	20888.9	1.593	.00949	.98715	.00019
37800	21000.0	1.563	.00931	.98734	.00018

TABLE V.—BLACKBODY FUNCTIONS—Continued

Wavelength-temperature product, λT		Blackbody hemispherical spectral emissive power divided by fifth power of temperature, $e_{\lambda b}/T^5$		Blackbody fraction, $F_{0-\lambda T}$	Difference between successive $F_{0-\lambda T}$ values, ΔF
(μm)(°R)	(μm)(°K)	Btu / (hr)(sq ft)(μm)(°R^5)	W / (cm^2)(μm)(°K^5)		
38000	21111.1	1.533×10^{-15}	0.00913×10^{-15}	0.98752	0.00018
38200	21222.2	1.505	.00896	.98769	.00018
38400	21333.3	1.476	.00879	.98787	.00017
38600	21444.4	1.449	.00863	.98804	.00017
38800	21555.6	1.422	.00847	.98821	.00017
39000	21666.7	1.396×10^{-15}	$.00831\times10^{-15}$	.98837	.00016
39200	21777.8	1.370	.00816	.98853	.00016
39400	21888.9	1.345	.00801	.98869	.00016
39600	22000.0	1.320	.00786	.98885	.00016
39800	22111.1	1.296	.00772	.98900	.00015
40000	22222.2	1.273×10^{-15}	$.00758\times10^{-15}$	.98915	.00015
42000	23333.3	1.065	.00634	.99051	.00136
44000	24444.4	.898	.00535	.99165	.00114
46000	25555.6	.762	.00454	.99262	.00097
48000	26666.7	.651	.00388	.99344	.00082
50000	27777.8	$.560\times10^{-15}$	$.00333\times10^{-15}$	.99414	.00071
52000	28888.9	.484	.00288	.99475	.00061
54000	30000.0	.420	.00250	.99528	.00053
56000	31111.1	.367	.00218	.99574	.00046
58000	32222.2	.321	.00191	.99614	.00040
60000	33333.3	$.283\times10^{-15}$	$.00168\times10^{-15}$	.99649	.00035
62000	34444.4	.250	.00149	.99680	.00031
64000	35555.6	.222	.00132	.99707	.00027
66000	36666.7	.197	.00117	.99732	.00024
68000	37777.8	.176	.00105	.99754	.00022
70000	38888.9	$.158\times10^{-15}$	$.940\times10^{-18}$	.99773	.00019
72000	40000.0	.142	.844	.99791	.00017
74000	41111.1	.128	.760	.99806	.00016
76000	42222.2	.115	.687	.99820	.00014
78000	43333.3	.104	.622	.99833	.00013
80000	44444.4	$.0948\times10^{-15}$	$.564\times10^{-18}$	.99845	.00012
82000	45555.6	.0862	.513	.99855	.00010
84000	46666.7	.0786	.468	.99865	.00010
86000	47777.8	.0718	.428	.99874	.00009
88000	48888.9	.0657	.391	.99882	.00008

TABLE V.—BLACKBODY FUNCTIONS—Concluded

Wavelength-temperature product, λT		Blackbody hemispherical spectral emissive power divided by fifth power of temperature, $e_{\lambda b}/T^5$		Blackbody fraction, $F_{0-\lambda T}$	Difference between successive $F_{0-\lambda T}$ values, ΔF
(μm)(°R)	(μm)(°K)	$\frac{\text{Btu}}{(\text{hr})(\text{sq ft})(\mu\text{m})(°\text{R}^5)}$	$\frac{\text{W}}{(\text{cm}^2)(\mu\text{m})(°\text{K}^5)}$		
90000	50000.0	0.0603×10^{-15}	0.359×10^{-18}	0.99889	0.00007
92000	51111.1	.0554	.330	.99896	.00007
94000	52222.2	.0510	.304	.99902	.00006
96000	53333.3	.0470	.280	.99908	.00006
98000	54444.4	.0434	.259	.99913	.00005
100000	55555.6	$.0402 \times 10^{-15}$	$.239 \times 10^{-18}$	.99918	.00005

Index

U.S. GOVERNMENT PRINTING OFFICE : 1968 OL—295-763